CR-86164

RCA

December, 1968
Final Report

Navigation | Traffic Control Satellite Mission Study

Contract No. NAS 12-596

Volume III

Selected Navigation | Traffic Control Satellite System Analysis and Equipment Definition

RCA

Prepared for
Electronics Research Center
National Aeronautics and
Space Administration
Cambridge, Massachusetts

RCA | Defense Electronic Products | System Engineering, Evaluation & Research | Moorestown, New Jersey

RCA

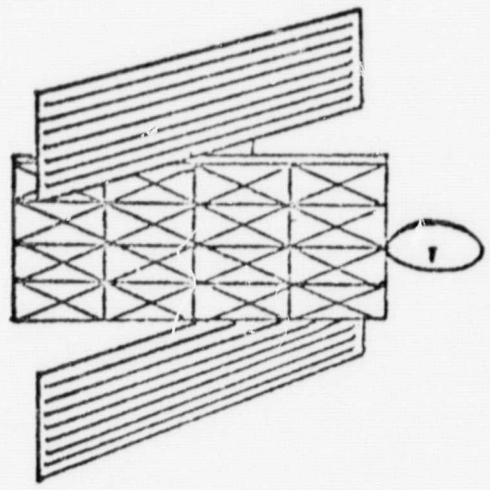

December, 1968
Final Report

Navigation|Traffic Control Satellite Mission Study

Contract No. NAS 12-596

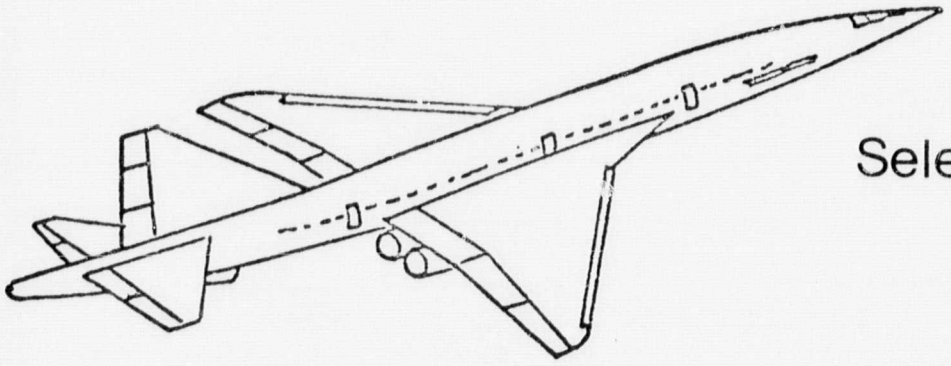

Volume III
Selected Navigation|Traffic Control Satellite System Analysis and Equipment Definition

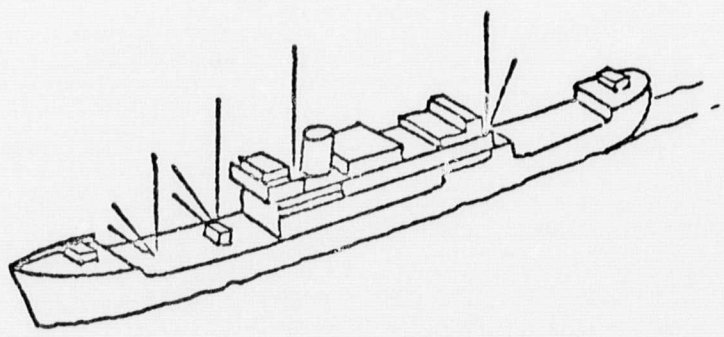

Prepared for
Electronics Research Center
National Aeronautics and
Space Administration
Cambridge, Massachusetts

RCA|Defense Electronic Products|System Engineering, Evaluation & Research|Moorestown, New Jersey

PREFACE

The objective of this study is to identify the technological and economic factors involved in the implementation of a navigation/traffic control satellite system that would provide for efficient and safe operation of aircraft and ships over ocean areas by 1975.

Organization of Final Report

The final report of the Navigation/Traffic Control Satellite Mission Study prepared by RCA is comprised of four volumes.

Volume I is a summary of the study and presents in concise form the objectives and results of the overall effort.

Volume II describes the candidate navigation/traffic control satellite systems which were investigated and compared, and documents the performance and cost analyses which were conducted in order to select a preferred system concept.

Volume III presents the mechanization of the preferred system after detailed trade-off analyses of various alternatives for the major elements and subsystems. Preliminary designs of the user equipments, spacecraft, and ground stations are described. The results of a performance analysis of the selected system, and cost estimates of an operational system configuration are tabulated.

Volume IV describes (1) the critical technology areas requiring further development, (2) a recommended experimental spacecraft and program for demonstrating the feasibility of the system concept in an operational environment, (3) the economic factors for developing and implementing the system for the North Atlantic and Globally, (4) the expanded coverage and growth capabilities of the system, and (5) the additional applications for which the system can be used.

Contributors to the Study

This report represents a concerted effort by RCA personnel from (1) the Systems Engineering, Evaluation and Research (SEER) group, who led the technical effort and performed the overall system's analyses; (2) the Astro-Electronics Division (AED), who analyzed and designed the spacecraft and (3) the Aerospace Systems Division (ASD), who analyzed and designed the user equipments.

The principal RCA participants in this study were Michael W. Mitchell, Program Manager and Technical Director; Harry Rose and Leroy Tangradi, RF Design and Communications; Brian Stockwell, Space System Design and Integration; Carl Heldwein and Gerald Zerfas, User Equipments; William Lindorfer, Spacecraft Systems; Sajjad Durrani, Phased Arrays; Frank Taylor, Space Communications; Alfred Smith, Signal Processing; Morris Levinson, Error Analysis; and Jerome Barnla and Jack Breckman, Consultants.

Grateful acknowledgement is made for the suggestions and critiques of Mr. Ernest Steele, NASA-ERC Technical Monitor, and Mr. Eugene Ehrlich of NASA, Headquarters.

PRECEDING PAGE BLANK NOT FILMED.

CONTENTS

VOLUME III

Section

ILLUSTRATIONS

VOLUME III

TABLES

VOLUME III

Section 1

INTRODUCTION AND SUMMARY

The Phase I Study resulted in the selection of the ranging technique as that best suited to the Navigation/Traffic Control (Nav/TC) position location requirements within the North Atlantic Region. The purpose of the Phase II Study was to define the necessary communications services that are also needed by the user field, to integrate these with the position location functions (in both active and passive modes), and to define in outline the resulting system.

In fact, in the course of the study, two total systems have been considered in some detail:

- The first version has an L-band navigation/traffic surveillance/data relay capability, and in addition includes VHF voice communications for aviation and marine users.
- The second version has the same L-band navigation/traffic surveillance/data relay capability, but utilizes L-band voice communications for aviation and marine users.

After detailed trade-off analyses were performed, the second version was favored and recommended for development to meet the post-1975 requirements for North Atlantic and global service. The former or VHF voice system, although reflecting favorable transmitter power tradeoffs for the satellite to aircraft links and possible utilization of available aircraft equipment, was limited by RF bandwidth availability and required relatively large antennas.

With the proposed two-satellite range-range system, it is possible to combine both position location via ground surveillance and self-navigation in a single system without any extra equipment burden. The service is indicated schematically in Figure 1-1. The up-link from Ground Control at frequency f_2 to satellite 2 and then at frequency f_4 to the active user (and to the whole field) carries the cooperative user address and interrogation call. The active user replies on frequency f_5 to satellites 1 and 2, and these replies are relayed to Ground Control at frequencies f_7 and f_6 respectively. The so-far unused up-link to satellite 1 at frequency f_1 is shifted to frequency f_3 and is employed (in combination with f_2 shifted to f_4) so as to provide a navigation field signal to passive users. In this latter case any data broadcast is carried on the $f_1 \rightarrow f_3$ link. The equipment requirement is common to both spacecraft.

The voice channel requirements are of paramount importance to sizing of the space system, and considerable attention has been given to the identification of channel needs elsewhere in this report.

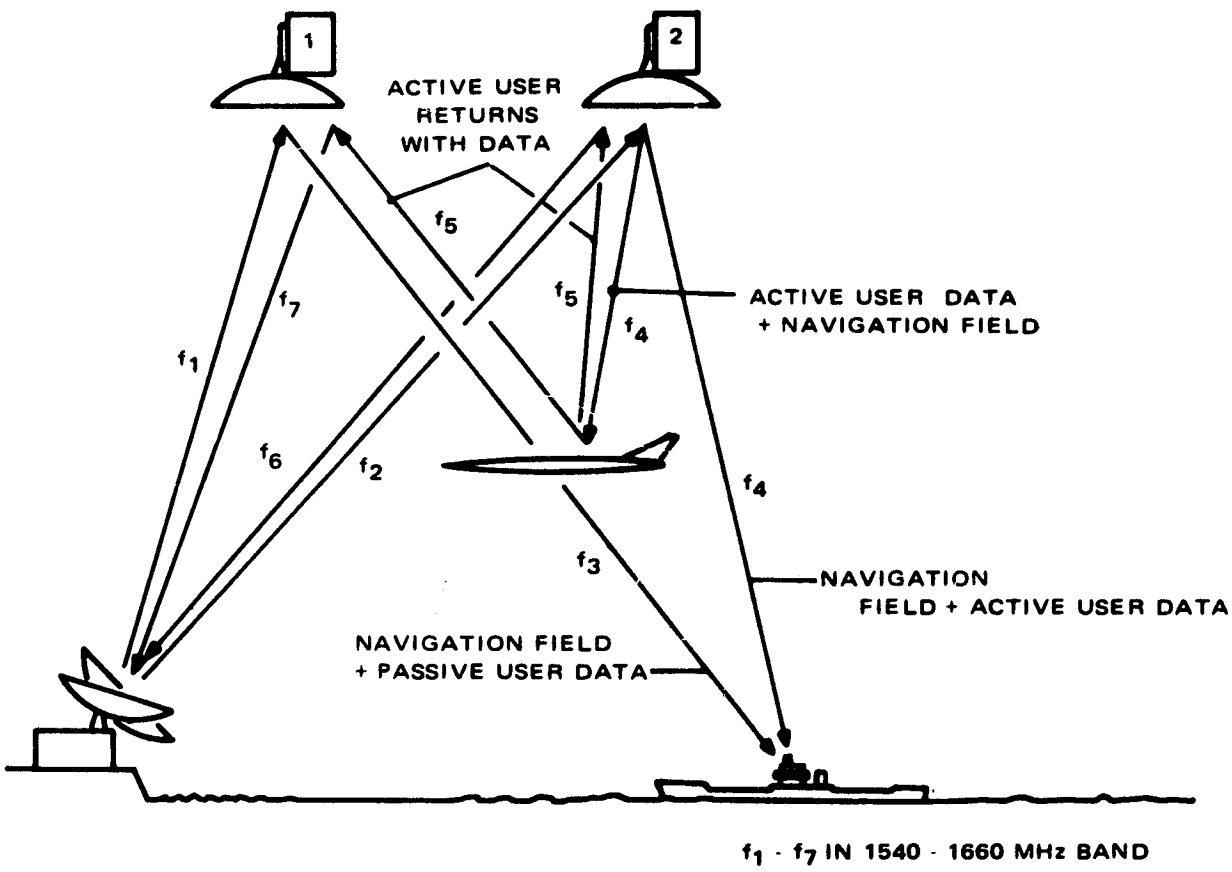

Figure 1-1. Position Determination and Data Transfer

ICAO data indicates that the North Atlantic 1975 "Busy Hour" flight count could approach 300, this number being obtained by interpretation of the largest of the hourly flows averaged for each day of the week separately during July and August.

This is a high estimate, and a lower "peak" bound is set by assumption of an in-the-air count of 170 subsonic and 20 supersonic aircraft, as laid down for the study.

Now, present practice is for situation reporting at every 10° of longitude, as a minimum (and when technically possible) so that a flight count of 190 implies about 460 calls per hour in the North Atlantic (about 60° N. latitude). This is for aviation alone of course.

Present experience is that a typical call lasts about 3 minutes (and is about 33% efficient in terms of transfer of useful information) so that it is immediately seen that even with an unrealistic 100% channel efficiency about 23 voice channels would be required to fill 1975 estimated "needs". More realistically, the mean call duration might be reduced to 1 minute by rigid discipline (and noting that with existing systems in many cases no communications are possible), whence at a mean waiting time of around 30 seconds nine channels might suffice.

Going one step further and postulating the presence of a digitized link for routine status and meteorological data reporting, plus automatic position reporting via the position

location system, then the average flight might well get away with three 1-minute voice messages, viz:

1. Some time after entry to the oceanic area, corresponding to exit from direct ground surveillance.
2. At the mid-flight point.
3. Some time prior to re-entry into ground surveillance.

The corresponding average call frequencies, based upon typical flight times, are about once every two hours for subsonic aircraft and once every hour for supersonic aircraft. Under these assumptions, the estimated 1975 traffic load across the North Atlantic could be borne by three voice channels, at a mean waiting time of about 15 seconds, and even the higher estimated traffic load (ICAO model) by five channels.

The addition of a clear emergency channel is thus seen to lead to a minimum total requirement for four aviation voice channels, with a six channel total provision being easily justified. The former is associated in this report with the VHF (FM) voice system, and the latter with the L-band (FM) voice system--the selection being based on the premise that a VHF system has more immediate application (1972) and the L-band system is preferred as the growth version for 1975 and beyond.

With regard to the field of potential Maritime users for voice channels, statistics for the mid-1970's indicate a requirement for about 240 calls per hour. This is excluding fishing vessels and allows in general one call per vessel per day (survey vessels get four per day). With one minute message duration, it is clear that somewhat more than four channels are required, even without specific provision for an emergency channel, and while the VHF system considered has been held to four marine channels the L-band system has been given six.

The various voice channels have been arranged in frequency so that (in a single channel) all space-to-earth transmissions are at one frequency and all earth-to-space transmissions at another. In this way a potential user can hear any traffic on a selected channel and thus knows immediately if it is clear. The VHF arrangement is indicated in Figure 1-2 and the channels are listed in Table 1-1, while the L-band system is depicted in Figure 1-3 in somewhat less detail since UHF allocations are tentative.

Examination of the bit load associated with the necessarily digitized transfer of meteorological and other routine data indicates that this load can easily be carried by both the backward and forward links of the position location system, via PSK modulation of the coarse tone.

The typical data package to be transmitted to or from an active user can be compressed into about 200 bits. The package might contain three 7-bit words for synchronization (as confirmation in part of the position location determination) and 14 words for position and altitude reporting, 7 words for meteorological data and 3 or 4 words for other advisory information. In this active mode, the various users are addressed repetitively so that advisory information could be accumulated. But, in any event, since a 2-second interrogation is proposed for the position location function, a transfer rate as low as 100 bits per second (bps) will suffice. Furthermore, at 1800 fixes per hour (corresponding to two seconds of interrogation) and a peak traffic count of 190 the

TABLE 1-1. CHANNEL ALLOCATIONS

Function	Channel		
	Designation	Use	Frequency* (MHz)
Ground Control Transmission	f1	Navigation field plus data for passive user	L-Band, (1550)
	f2	Navigation field plus data for active user	L-Band, (1550)
	f9	Maritime voice (channel 5)	156-157, (157)
	f11	Maritime voice (channel 6)	156-157, (157)
	f13	Aviation voice (channel 1)	120-125, (124)
	f15	Aviation voice (channel 2)	120-125, (124)
	f17	Maritime voice (channel 7)	156-157, (157)
	f19	Maritime voice (channel 8)	156-157, (157)
	f21	Aviation voice (channel 3)	120-125, (124)
	f23	Aviation voice (channel 4)	120-125, (124)
Ground Control Reception	f6	Return from Active user, with data	L-Band, (1631)
	f7	Return from Active user, with data	L-Band, (1631)
	f10	Maritime voice (channel 5)	160-162, (161)
	f12	Maritime voice (channel 6)	160-162, (161)
	f14	Aviation voice (channel 1)	130-135, (131)
	f16	Aviation voice (channel 2)	130-135, (131)
	f18	Maritime voice (channel 7)	160-162, (161)
	f20	Maritime voice (channel 8)	160-162, (161)
	f22	Aviation voice (channel 3)	130-135, (131)
	f24	Aviation voice (channel 4)	130-135, (131)
Active User Transmission	f5	Position location return with data	L-Band, (1551)
	f13	Voice (channel 1)	Listed previously in this table
	f15	Voice (channel 2)	
	f21	Voice (channel 3)	
	f23	Voice (channel 4)	
Active User Reception	f4	Ground Control address and data	L-Band, (1630)
	f14	Voice channel 1	Listed previously
	f16	Voice channel 2	
	f22	Voice channel 3	
	f24	Voice channel 4	
Passive User Transmission	f9	Voice channel 5	Listed previously
	f11	Voice channel 6	
	f17	Voice channel 7	
	f19	Voice channel 8	
Passive User Reception	f3	Nav. field and data	L-Band, (1630)
	f4	Nav. field	
	f10	Voice channel 5	Listed previously
	f12	Voice channel 6	
	f18	Voice channel 7	
	f20	Voice channel 8	

*Selected frequency in parentheses.

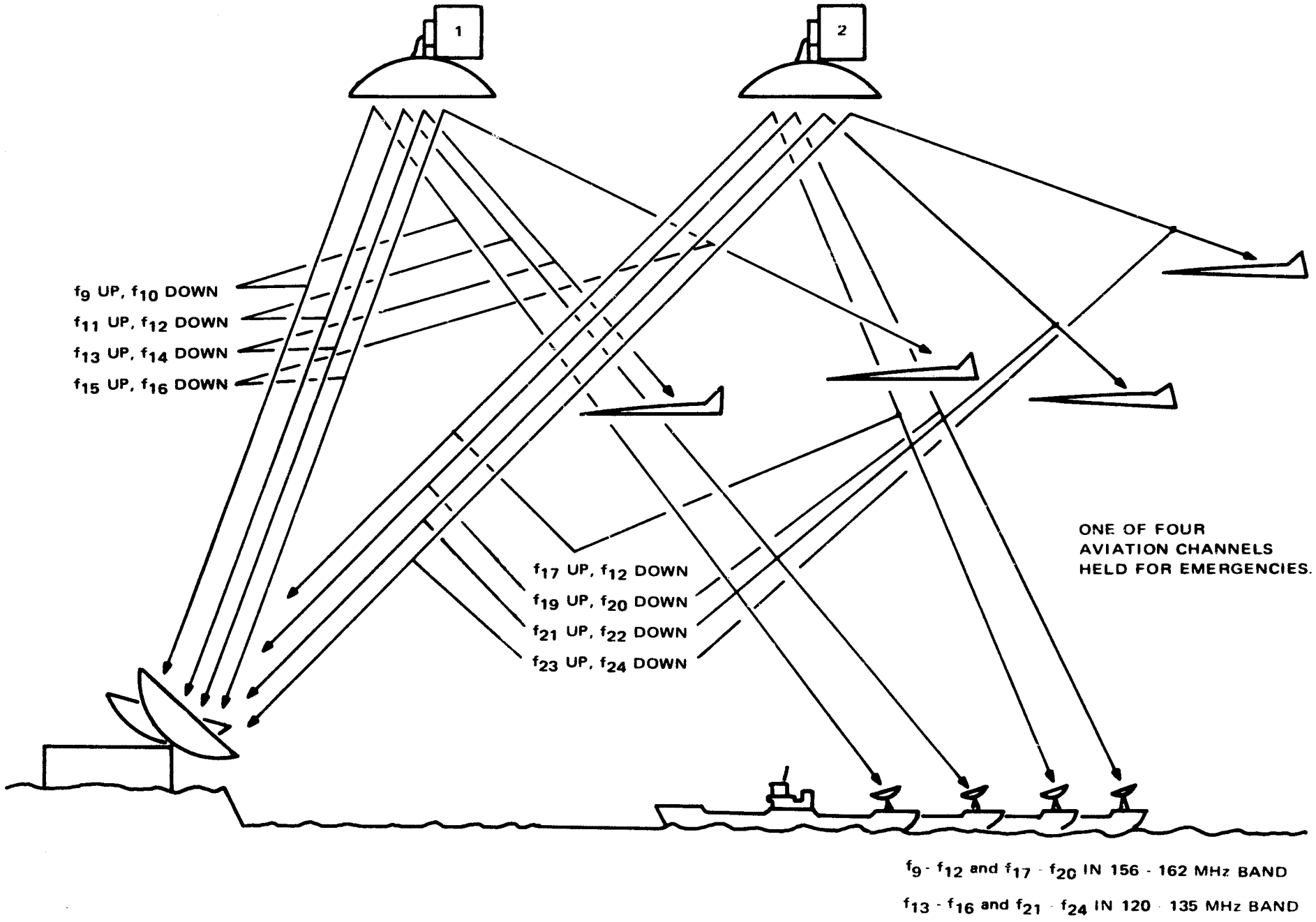

Figure 1-2. VHF Voice Communications

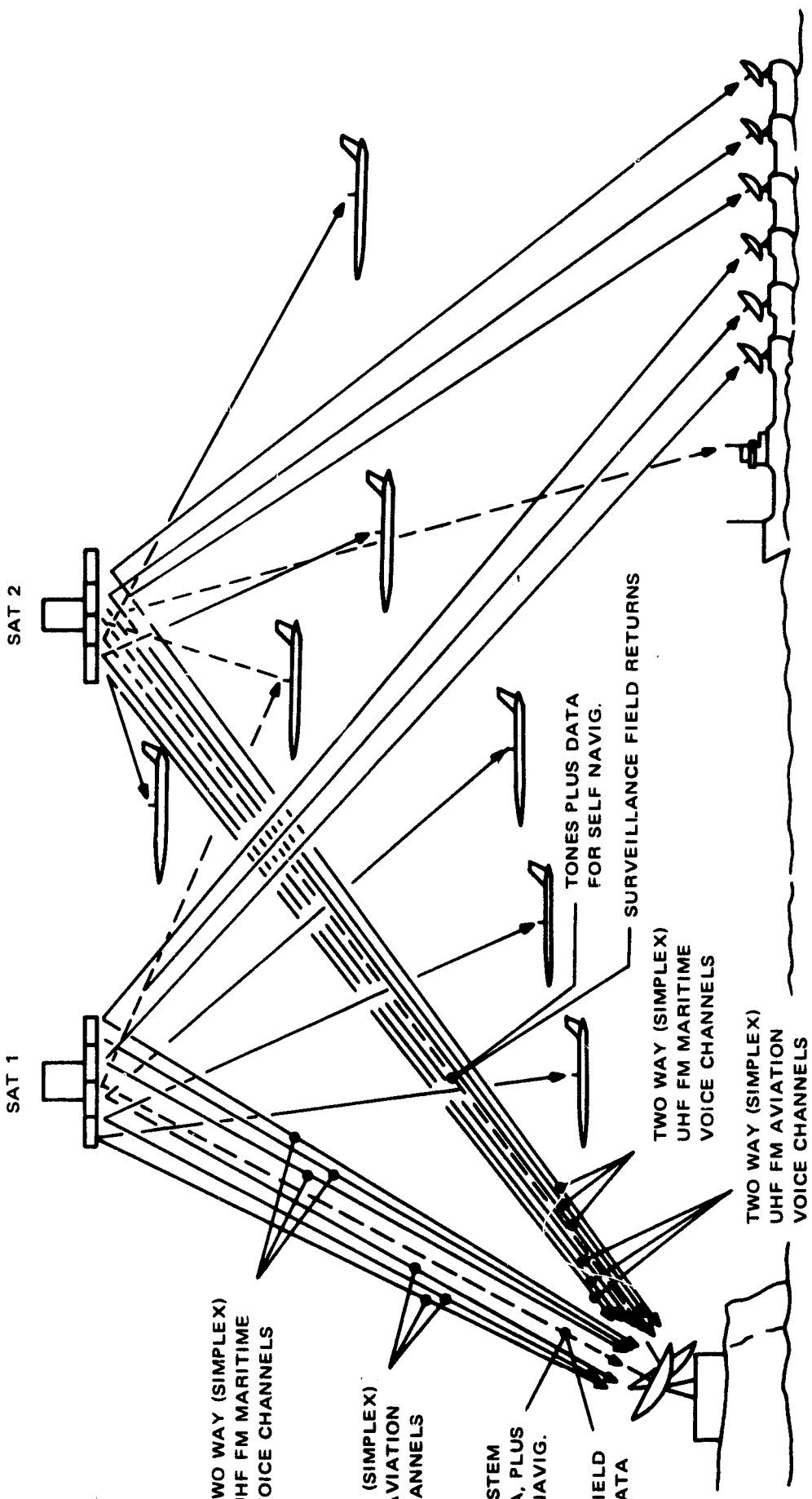

Figure 1-3. L-band Total System Scenario

sampling frequency is far greater than would be necessary from the point of view of routine message transfer.

The data transfer proposed for the passive user is "outward" only and so is not subject to restriction upon message length limitations. The 100-bps transfer rate is therefore more than adequate in this case.

It should be noted that in the self-navigation mode, the range determinations are made at the user, and are dependent upon a knowledge at the user of Ground Control time (or more precisely, phase). Over periods of a day or so off-the-shelf, temperature-controlled crystal oscillators can provide sufficient accuracy, but over longer periods the user has to tie in to the surveillance network say once per day and at a quiet time so as to effect recalibration.

Also, the voice link power problem turns out to be sufficiently severe to demand help from the user where possible so that in the maritime case (where occasional antenna pointing is not objectionable) 10 dB of gain has been assumed.

In both the VHF (voice) and the L-band systems the total capacity has been split equally between the two spacecraft in terms of "voice" as well as of the position location function. The vehicles are thus identical, thus facilitating system production and repair.

The various satellite and user RF characteristics for both the voice systems that have been considered in detail are summarized in Tables 1-2 and 1-3. Both systems employ navigation/traffic control by tone ranging, and the navigation link carries a 100 bps two-way data stream in the "active" mode and a 100 bps one-way stream in the passive case. Link powers for this service will be defined subsequently.

A sketch of the total VHF system is shown in Figure 1-4, while the UHF system is depicted in Figure 1-5.

TABLE 1-2. VHF SYSTEM CHARACTERISTICS

NAV/TC VHF VOICE COMMUNICATIONS	AIRCRAFT USERS
Satellite	User (Aircraft)
1. Hard Limiting Repeater (FM)	1. Antenna: 0 dB gain for elevation angles above 10°.
2. Frequencies (tentative): Transmit: 130-135 MHz Receive: 120-125 MHz	2. Transmitter: 150 watts (RF) (includes 7 dB margin and corresponds to present airline planning)
3. Power: 30 Watts (RF), each of two channels per satellite	
4. Antenna: Earth coverage (28.5 ft dia.)	

NAV/TC VHF VOICE COMMUNICATIONS	MARITIME USERS
Satellite	User (Ships)
1. Hard Limiting Repeater (FM)	1. Antenna: 10 dB gain
2. Frequencies: Transmit: 160-162 MHz Receive: 156-157 MHz	2. Transmitter: 20 watts (RF)
3. Power: 3 Watts (RF), each of two channels per satellite.	
4. Antenna: As above	

TABLE 1-3. UHF SYSTEM CHARACTERISTICS

NAV/TC UHF VOICE COMMUNICATIONS	AIRCRAFT USERS
Satellite	**User (Aircraft)**
1. Hard Limiting Repeater (FM)	1. Antenna: 0 dB net gain for elevation angles above 5°.
2. Frequencies:* Transmit: 1540-1560 MHz Receive: 1640-1660 MHz	2. Transmitter: 20 watts (RF) pilot, 17 watts (RF) transmission required (34 watts suggested for extra margin)
3. Power: 17 watts net (RF) each of 3 channels per satellite	
4. Antenna: Earth coverage scan, 30 dB retro-array	

NAV/TC UHF VOICE COMMUNICATIONS	MARITIME USERS
Satellite	**User (Ships)**
1. Hard Limiting Repeater (FM)	1. Antenna: 10 dB net gain
2. Frequencies: Transmit: 1540-1560 MHz Receive: 1640-1660 MHz	2. Transmitter: 2 watts (RF) pilot, 2 watts (RF) transmission required (4 watts suggested for extra margin)
3. Power: 2 watts net (RF), each of 3 channels per satellite	
4. Antenna: Earth coverage scan 30 dB retro-array	

* These frequency allocations are tentative. There would be some separation between the Aviation and Maritime assignments.

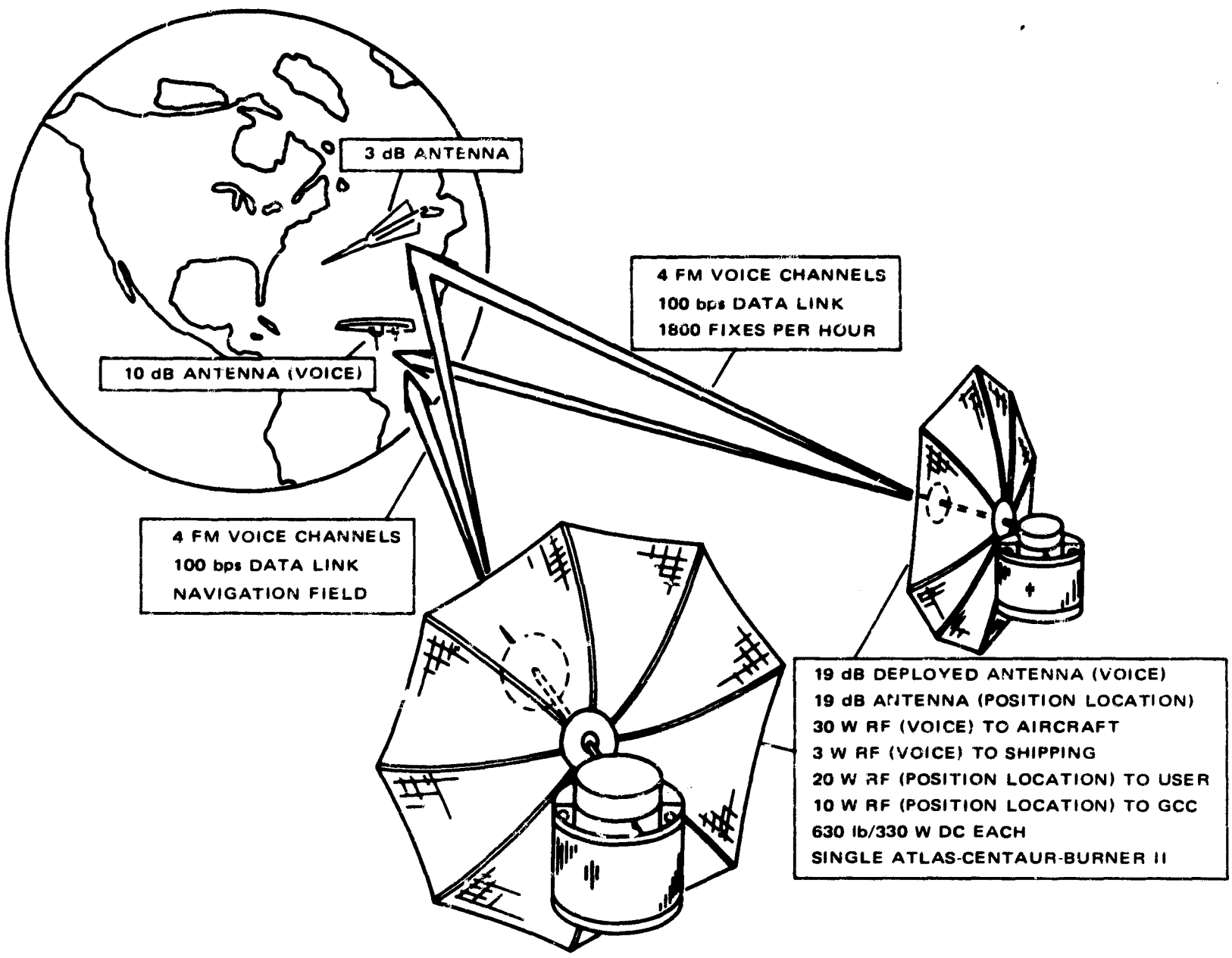

Figure 1-4. VHF Voice/L-Band Position Location System Capability

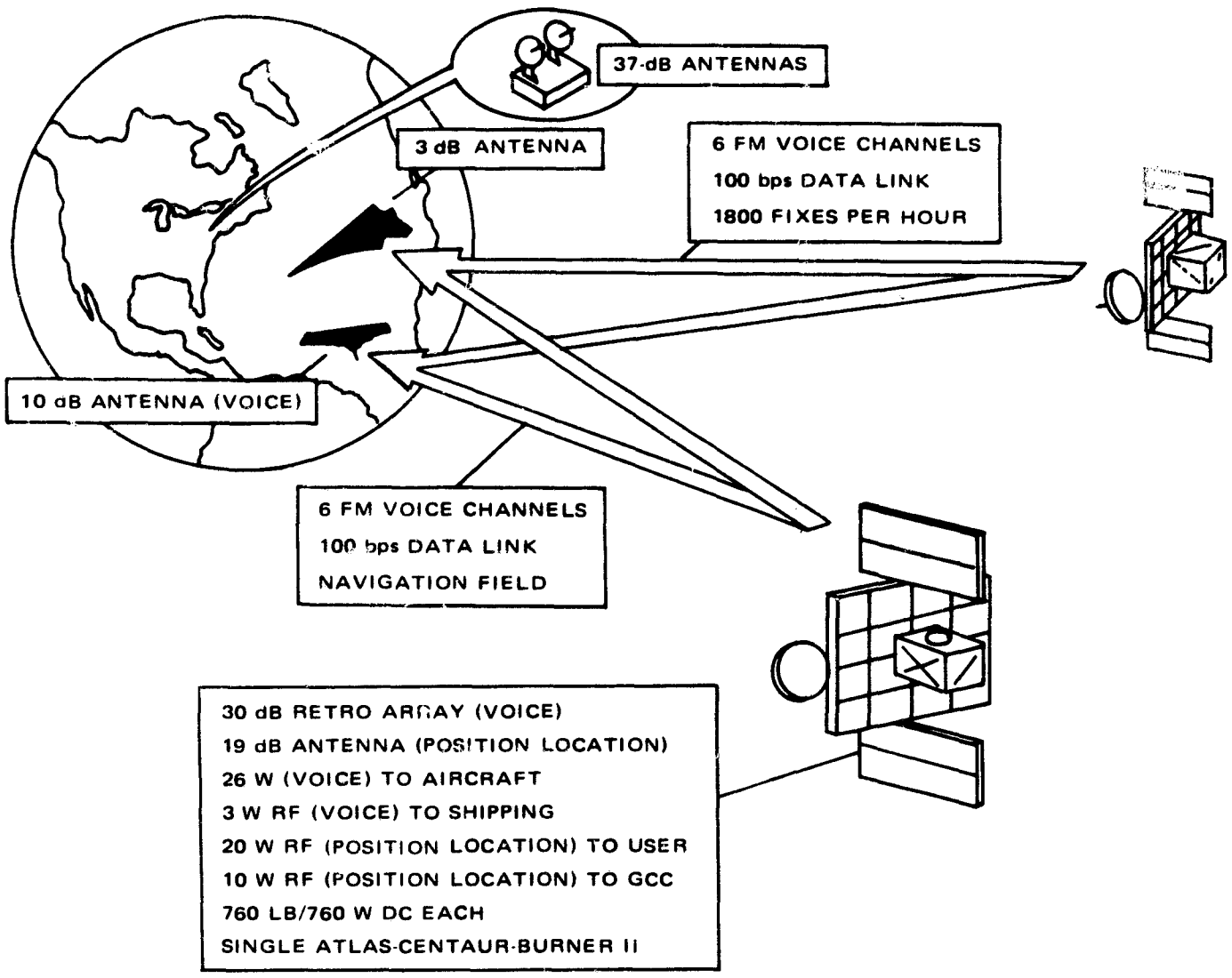

Figure 1-5. UHF Operational System Capability

SECTION 2

SYSTEM TRADEOFFS

2.1 RF FREQUENCY SELECTION

The principal advantage of a satellite navigation system is the extremely large coverage area which lies within line of sight of satellites, particularly at synchronous altitude. RF signals transmitted or relayed by satellites to the surface of the earth can operate at higher frequencies and be less affected by atmospheric and ionospheric environments than ground based navigation systems.

Table 2-1 summarizes the RF characteristics of four radio bands which have some promising features for Nav/TC satellite systems. The three principal functions analyzed were the position location (navigation) field signal, a narrow band data link and a two-way voice link. The information bandwidths give some indication of the processing gain which is possible at the receiver terminals. Thus, the position location signal bandwidth of 1 Hz offers much higher processing gain potential than the voice bandwidth of 2.7 kHz.

The RF bandwidths shown in Table 2-1 are the sum of the IF bandwidths and the equipment and doppler frequency variations. Although these bandwidths increase at higher carrier frequencies, more RF spectrum is available at the higher RF bands.

The significance of the data in Table 2-1 is not apparent until Table 2-2 is examined. The critical or most demanding RF links in all cases were those between the satellites and users. The VHF band would be preferable in terms of offering the lowest transmitter power requirements. However, the range measurement errors associated with ionospheric refraction appear excessive for a precision navigation system. The "L" band offers a good compromise between range accuracy and power for the position location signal. Specifically, the navigation band at 1540 to 1660 MHz presents a good choice from the viewpoint of international regulatory agency preferences also.

For the voice channel, RF power requirements for all bands above VHF appear high for the satellite-user link. On the other hand, the satellite antenna size of 28.5 feet diameter presented a penalty for VHF compared to an L-band antenna of 2.3 feet diameter for earth coverage at synchronous equatorial orbit. Of greater significance is the comparison of antenna sizes for the aviation user. A circularly polarized hemispherical beam antenna would measure approximately 40-60 inches in diameter at VHF and about 5-8 inches in diameter at L-band.

The tradeoffs between VHF and L-band revolve around the satellite and user power and antenna requirements. The results of extensive analysis indicated that although VHF voice links were preferable for immediate implementation, an L-band voice communication system employing a high-gain, retrodirective satellite antenna (phase conjugating array with pilot tones for steering) would serve the post-1975 era better. This L-band system would have more channel capacity, have modest power needs for the user and satellite, and require a relatively small antenna for aircraft users.

TABLE 2-1. RADIO FREQUENCY CHARACTERISTICS FOR NAV/TC SATELLITE SYSTEM

	RF Band			
	VHF	L	C	X
Nominal Freq. (MHz)	150	1600	4000	8000
Freq. Instabilities & Doppler:				
Equipments (1×10^{-5} Osc. Instab.) (kHz)	±1.5	±16	±40	±80
Doppler (Max. A/C Vel. of Mach 3) (kHz)	±0.45	±4.8	±12	±24
Sum Freq. Errors (kHz)	3.9	41.6	104	208
Nav/TC Field Signal (Position Location):				
Inform Bandwidth (Hz)	1.0	1.0	1.0	1.0
IF Bandwidth for 8 kHz Tone System (kHz) (1.0 mile accuracy)	16.0	16.0	16.0	16.0
RF Bandwidth for 8 kHz Tone System (kHz)	19.9	57.6	120	224
IF Bandwidth for 64 kHz Tone System (kHz) (0.1 mile accuracy)	128.0	128.0	128.0	128.0
RF Bandwidth for 64 kHz Tone System (kHz)	132	170	232	336
Narrow Band Data Link (100 bps)				
Inform Bandwidth (Hz)	75	75	75	75
IF Bandwidth (Hz)	150	150	150	150
RF Bandwidth (kHz)	4.0	41.7	104	208
Voice Link (FM - 12 dB Clipping Mod. Index 1.8)				
Inform Bandwidth (kHz)	2.7	2.7	2.7	2.7
IF Bandwidth (kHz)	18.1	18.1	18.1	18.1
RF Bandwidth (kHz)	22.0	59.7	122	226

TABLE 2-2. RF POWER AND REFRACTION RANGE ERRORS FOR VARIOUS RF BAND SELECTIONS

	RF Band			
	VHF	L	C	X
Nominal Frequency (MHz)	150	1600	4000	8000
SAT USER LINK ATTENUATION FACTORS:				
Space Loss (dB)	164	190	198	204
Atmospheric (dB)	.4	.5	.6	.7
Rain (dB)	-	-	1.5	6.0
Total (dB)	164.4	190.5	200.1	210.7
*SAT USER LINK TRANSMITTER POWER REQUIREMENTS:				
Nav/TC Field Signal and Narrow Band Data Link - W/O Rain (W)	.5	20	125	600
With Rain (W)	.5	20	180	2400
Voice** - W/O Rain (kW)	.030	.550	2.2	8.8
Voice** - With Rain (kW)	.030	.550	2.2	35.2
TRANSMITTER EFFICIENCY				
TWT (%)	-	30	35	35
Solid State Ampl. (%)	50	30	-	-
NAV/TC REFRACTION RANGE ERRORS AT 10° ELEV.:				
Ionosphere, in m (ft)	550(1800)	4.9(16)	.8(2.6)	.2(.6)
Troposphere, in m (ft)	12(40)	12(40)	12(40)	12(40)

*Earth Coverage Satellite Antenna and Hemispherical User Antenna
**FM - 12 dB Clipping

In summary then, the effects of ionospheric refraction and absorption, extraterrestrial noise, space loss and RF equipment state-of-the-art led to the selection of the following nominal RF frequencies:

Nav/TC Signals	L-band
Narrow Band Data Links	L-band
Voice Links	L-band

2.2 NAV/TC SIGNAL MODULATION ANALYSIS

2.2.1 INTRODUCTION

In this section two types of range measuring modulation techniques are compared. The first, a pulsed carrier system, is exemplified by a periodic pulse train that turns on a

high-power L-band transmitter for a specific time duration. The peak power of the transmitter is quite high although the average power is modest. The receiving equipment is quite simple in that a non-coherent envelope detector can be used for demodulation, similar to pulsed radars. A false alarm threshold is set to a predetermined level, at the detector output, and when this level is exceeded by the received signal (and noise) a time measurement is made. The penalty paid for the simple receiver is a high-peak-power transmitter. One method of reducing this high peak power requirement is to use "pulse compression" modulation.

To observe the benefits of pulse compression, two link analyses are performed on the pulse system, one without and one with pulse compression. Finally, the link analysis of the pulse compression method is extended to the case of an overall ground position accuracy of 0.1 nmi, which is found to require extremely high RF power in the satellite.

The second modulation technique is a CW system in which a periodic waveform, such as a set of sine waves or a digital pulse train, phase-modulates an L-band transmitter. In this case the receiver is more complex in that coherent demodulation is required to avoid the "weak signal suppression" effect. Offsetting the more complex receiver (as compared to the pulse system) is a simple transmitter. Power requirements for various transmitters in the link are quite modest (less than 50 watts) so that solid state devices may be utilized as power amplifiers. Finally, a comparison of the two CW systems (i.e., the tone modulated system and the digital pulse train system) was made in order to select the better modulation technique. The selection criteria included lock-up time, data link modulation implementation and the impact of increasing the overall ground position accuracy from 1.0 to 0.1 nmi.

2.2.2 LINK ANALYSIS OF PULSED SYSTEMS

2.2.2.1 NON-PROCESSED PULSE, L-BAND SYSTEM

In this case a non-processed pulse originates at the control center, is received by the user via a satellite, and is returned to the control center via two satellites. The arrival times of both signals are then processed to obtain the round trip times of both signals. These times result in two range-to-the-user measurements resulting in a fix (the user altitude is known).

The link calculations shown in Table 2-3 are based on typical values of various parameters, like power, antenna gains, bandwidths, noise figures, etc.* The satellite, user, and ground control center are assumed to have bandwidths of 130 kHz, 160 kHz and 200 kHz respectively, resulting in an effective system noise bandwidth of 74 kHz for a two-way trip of the signal (from ground to user and back) without demodulation at satellite or user.

*In the interest of brevity, a detailed explanation of the link analysis (with justification for the choice of each parameter) is omitted here, but several parameters are the same as those used in the CW system and discussed more fully in Section 2.2.3.2.

TABLE 2-3. LINK CALCULATIONS FOR A TYPICAL PULSE SYSTEM (RANGE-RANGE NAVIGATION)

Forward Path - Values for forward-path parameters are tabulated below:

	Value
CONTROL CENTER	
Transmitter frequency (MHz)	1660
Transmitter power (64W) (dBW)	18.0
Antenna coupling loss (dB)	1.5
Antenna gain (dB)	37.0
Rain and snow attenuation (dB)	0.2
Effective radiated power, ERP (dBW)	53.3
PROPAGATION	
Path loss for 26000 miles (dB)	190.0
Atmosphere and ionosphere attenuation (dB)	0.5
SATELLITE	
Antenna gain (dB) (-3db beam edge)	16.5
Antenna polarization loss (dB)	0.5
Antenna coupling loss (dB)	1.0
Received RF power (dBW)	-122.2
SATELLITE NOISE POWER	
Receiver noise figure (dB)	5.0
Receiver noise temperature (°K)	680.0
Effective sun temperature (°K)	0.0
Total galactic noise temperature (°K)	2.0
Effective earth temperature (°K)	115.0
Total noise temperature (°K)	797.0
System noise figure (dB)	4.4
Noise density (dBW/Hz)	-199.6
Satellite noise bandwidth (KHz)	130.0
Satellite noise power (dBW)	-148.5
RF power/noise (dB)	26.3
Transmitter power (14.2KW) (dBW)	41.5
Antenna coupling loss (dB)	1.0
Antenna gain (dB) (-3db beam edge)	16.5
ERP (dBW)	57.0
Effective radiated noise, ERN, (dBW)	30.7
PROPAGATION	
Path loss (dB)	190.0
Atmospheric and ionospheric attenuation (dB)	0.5

TABLE 2-3. LINK CALCULATIONS FOR A TYPICAL PULSE SYSTEM (RANGE-RANGE NAVIGATION) (Continued)

Forward Path - Values for forward-path parameters are tabulated below:	
	Value
USER	
Antenna gain (dB)	2.0
Antenna polarization loss (dB)	1.5
Antenna coupling loss (dB)	2.0
Received RF power (dB)	-135.0
USER NOISE POWER	
Receiver noise figure (dB)	5.0
Receiver noise temperature (°K)	917.0
Total galactic noise temperature (°K)	2.0
Effective sun temperature (°K)	2.0
Total noise temperature (°K)	921.0
System noise figure (dB)	5.0
Noise density (dBW/Hz)	-199.0
Received noise from satellite (dBW)	-161.3
Received noise denisty (dBW/Hz)	-212.4
Total noise density (dBW/Hz)	-198.8
Predetection noise bandwidth (KHz)	160.0
Predetection noise power (dBW)	-146.8
RF power/noise (dB)	11.8
Return Path - Values for the return-path parameters are tabulated below:	
USER	
Transmitter power (44.0 KW) (dBW)	46.4
Antenna gain (dB)	2.0
Antenna coupling losses (dB)	2.0
ERP (dBW)	46.1
Effective radiated noise ERN (dBW)	34.3
PROPAGATION	
Path loss (dB)	190.0
Atmospheric and Ionospheric attenuation (dB)	0.5
SATELLITE	
Antenna gain (dB) (-3 db beam edge)	16.5
Antenna polarization loss (dB)	1.5
Antenna coupling loss (dB)	1.0
Received RF power (dBW)	-130.4

TABLE 2-3. LINK CALCULATIONS FOR A TYPICAL PULSE SYSTEM (RANGE-RANGE NAVIGATION) (Continued)

Return Path - Values for the return-path parameters are tabulated below:

	Value	
SATELLITE NOISE POWER		
Noise density (same as forward path) (dBW/Hz)	-199.6	
Received noise density from user (dBW/Hz)	-194.2	
Combined noise density (dBW/Hz)	-193.1	
Satellite noise bandwidth (KHz)	130.0	
Effective noise power (dBW)	-142.0	
Received RF power/noise (dB)	11.6	
Transmitter power (66W) (dBW)	18.2	
Antenna coupling losses (dB)	1.0	
Antenna gain (dB) (-3 db beam edge)	16.5	
ERP (dBW)	33.4	
ERN (dBW)	21.8	
PROPAGATION		
Path loss (dB)	190.0	
Atmospheric and ionospheric attenuation (dB)	0.5	
CONTROL CENTER		
Antenna gain (dB)	37.0	
Antenna polarization loss (dB)	0.5	
Antenna coupling loss (dB)	1.0	
Received RF power (dBW)	-121.6	
***CONTROL CENTER NOISE POWER**		
System noise figure (dB)	3.3	
System noise density (dBW/Hz)	-200.7	
Received noise density from satellite (dBW/Hz)	-184.3	
Total noise density (dBW/Hz)	-184.3	
RF Power/total noise density (dB-Hz)	62.7	= S/N_o
Predetection noise bandwidth (KHz)	200.0	
Carrier/noise (dB)	9.7	
**Effective system noise bandwidth (KHz)	74.0	= B_{ef}

*This section excludes the effect of the control center antenna pointing directly at the sun which occurs at the spring and fall equinoxes for about a 7-day period with the maximum duration of 8 minutes during any one day.

**See Appendix 2.2.21-A.

TABLE 2-3. LINK CALCULATIONS FOR A TYPICAL PULSE SYSTEM (RANGE-RANGE NAVIGATION) (Continued)

Return Path - Values for the return-path parameters are tabulated below:		
	Value	
EFFECT OF SUN		
Receiver noise figure (dB)	4.0	
Receiver noise temperature (K)	624.0	
Solar noise temperature (K)	3600.0	
System noise figure	10.9	
Total noise density (dBW/Hz)	-183.8	
Increase in noise due to sun (dB)	0.5	
RF power/total noise density (dB-Hz)	62.2	= S/N_O
Carrier/noise (dB)	9.2	

The link parameters are chosen with the objective of obtaining a satisfactory value of S/N_O (i.e. signal power/noise power density per Hz) for the return signal received at the ground. To obtain an overall accuracy of 1 nmi, and leaving an allowance for various factors like propagation errors, a position accuracy about 0.7 nmi is necessary due to S/N considerations. Using values of Table 2-3 (i.e., S/N_O = 62.2 dB-Hz and effective noise bandwidth

B_{ef} = 74 kHz, the range error is*

$$\delta_R = \frac{C}{2} \left(\frac{1}{4\, B_{ef}\, S/N_o} \right)^{1/2}$$

$$= 0.116 \text{ nmi}$$

where C = speed of light = 162,000 nmi/sec. Now the system uses two satellites, each producing this RMS error, so that the resultant error is $\sqrt{2}\ \delta R$. Assuming a GDOP factor of 3, the resultant error in ground position is

$$\sigma_R = 3\sqrt{2}\ \delta R = 0.49 \text{ nmi}$$

which is within the permissible value of 0.7 nmi noted above.

*M.I. Skolnik, "Introduction to Radar Systems", McGraw-Hill, 1962, eq 10.35.

Although the link has a satisfactory value of S/N_O, it requires very high powers to achieve it. Thus (from Table 2-3), the satellite needs 14.2 kW for the link to user and 66 W for the link to ground, and the user needs 44.0 kW. These values are unrealistic and lead to the consideration of pulse-compression techniques, which result in power saving.

2.2.2.2 PULSE-COMPRESSION, L-BAND SYSTEM

The following link analysis is for a pulse compression pulsed L-band carrier system. Essentially, it is identical to the range-pulse analysis of Candidate System I, discussed in volume II. It will be repeated in the following analysis for the sake of completeness. It is to be noted that the 500-μs pulsed carrier is compressed (by a factor of 20) to 25 μs at the user receiver and at the control center receiver; elsewhere it is the full 500 μs long.

Details of the link calculation are shown in Table 2-4. The satellite bandwidth is assumed to be 100 KHz, while the effective bandwidth at both user and ground control center is 40 KHz for this pulse format. The worst E/N_O (i.e. signal energy/noise power density per Hz) at the ground station is 14.1 dB.

Following Skolnik's analysis*, with B = 40 KHz, E/N_O = 14.1 dB and C = 162,000 nmi/sec, the range error is

$$\delta_R = \frac{\sqrt{3}}{\pi B \left(2 \frac{E}{N_o}\right)^{1/2}} \frac{C}{2}$$

$$= 0.156 \text{ nmi}$$

For a system using two satellites and having a GDOP factor of 3, the ground position accuracy is

$$\sigma_R = 3\sqrt{2}\, \delta_R = 0.662 \text{ nmi}$$

This satisfactory operation is obtained with RF powers of 3.2W at the ground, 710 W and 3.3 W at the satellite for the links to user and ground, respectively, and 2.2 KW (peak) at the user. These are reasonable values and are much lower than those of Table 2-3.

---

*M.I. Skilnik, "Introduction to Radar Systems", McGraw Hill, 1962, equation 10.102.

TABLE 2-4. TYPICAL LINK CALCULATIONS: PULSE COMPRESSION SYSTEM (RANGE-RANGE NAVIGATION)

Forward Path - Values for forward-path parameters are tabulated below:

	Value
CONTROL CENTER	
Frequency	1660 MHz
Transmitter power (3.2 W, peak) (dB W)	5.0
Antenna coupling losses (dB)	1.5
Antenna gain (dB)	37.0
Rain and snow attenuation (dB)	0.2
Effective radiated power, ERP (dB W)	40.3
PROPAGATION	
Path loss (26000 miles) (dB)	190.0
Atmosphere and ionosphere attenuation (dB)	0.5
SATELLITE	
Antenna gain (dB) (-3 dB beam edge)	16.5
Antenna polarization loss (dB)	0.5
Antenna coupling loss (dB)	1.0
Received RF power (dB)	-135.2
SATELLITE NOISE POWER	
Receiver noise figure (dB)	5.0
Receiver noise temperature (°K)	680.0
Effective sun temperature (°K)	0.0
Total galactic noise temperature (°K)	2.0
Effective earth temperature (°K)	118.0
Total noise temperature (°K)	800.0
System noise figure (dB)	4.3
Noise density (dB W/Hz)	-199.7
Satellite noise bandwidth (KHz)	100.0
Satellite noise power (dB W)	-149.7
RF power/noise (dB)	14.5
Transmitter power (710 W) (dB W)	28.5
Antenna coupling loss (dB)	1.0
Antenna gain (dB)	16.5
ERP (dB W)	44.0
Effective radiated noise, ERN (dB W)	29.5
PROPAGATION	
Path loss (dB)	190.0
Atmospheric and ionospheric attenuation (dB)	0.5

TABLE 2-4. TYPICAL LINK CALCULATIONS: PULSE - COMPRESSION SYSTEM (RANGE-RANGE NAVIGATION) (Continued)

Forward Path - Values for forward-path parameters are tabulated below:	
	Value
USER	
Antenna gain (dB)	2.0
Antenna polarization loss (dB)	1.5
Antenna coupling loss (dB)	2.0
Received RF power (dB)	-148.0
USER NOISE POWER	
Receiver noise figure (dB)	5.0
Receiver noise temperature (°K)	917.0
Total galactic noise temperature (°K)	2.0
Effective sun temperature (°K)	2.0
Total noise temperature (°K)	921.0
System noise figure (dB)	5.0
Noise density (dB W/Hz)	-199.0
Received noise from satellite (dB W)	-162.5
Received noise density (dB W/Hz)	-212.5
Total noise density (dB W/Hz)	-199.0
Precompression Signal/noise density (dB W/Hz)	51.0
Precompression pulse width (microseconds)	500.0
Pulse compression ratio (dB)	13.0
Post compression signal/noise density (S/N_O)	64.0
Post compression pulse width (microsecond) T	25.0
Effective filter bandwidth B = 1/T (KHz)	40.0
Filter insertion loss (dB)	0.8
Post detection signal/noise (dB)	19.2
Signal Energy/noise density E/N_O (dB)	18.0
Return path - Values for return-path parameters are tabulated below:	
USER	
Transmitter power (2.2 KW peak) (dB W)	33.4
Antenna gain (dB)	2.0
Antenna coupling losses (dB)	2.0
ERP (dB W)	29.4
PROPAGATION	
Path loss (dB)	190.0
Atmospheric and ionospheric attenuation (dB)	0.5

TABLE 2-4. TYPICAL LINK CALCULATIONS: PULSE - COMPRESSION SYSTEM (RANGE-RANGE NAVIGATION) (Continued)

Return path - Values for return-path parameters are tabulated below:

	Value
SATELLITE	
Antenna gain (dB)	16.5
Antenna polarization loss (dB)	1.5
Antenna coupling loss (dB)	1.0
Received RF power (dB W)	-147.1
SATELLITE NOISE POWER	
Noise density (same as forward path) (dB W/Hz)	-199.7
Satellite noise bandwidth (KHz)	100.0
Effective noise power (dB W)	-149.7
Received RF power/noise (dB)	2.6
Transmitter power (3.3 W) (dB W)	5.2
Antenna coupling losses (dB)	1.0
Antenna gain (B)	16.5
ERP (dB W)	18.8
ERN (dB W)	16.3
PROPAGATION	
Path Loss (dB)	190.0
Atmospheric and ionospheric attenuation (dB)	0.5
CONTROL CENTER	
Antenna gain (dB)	37.0
Antenna polarization loss (dB)	0.5
Antenna coupling loss (dB)	1.0
Received RF power (dB W)	-136.2
***CONTROL CENTER NOISE POWER**	
System noise figure (dB)	3.3
System noise density (dB W/Hz)	-200.7
Received noise density from satellite (dB W/Hz)	-188.7
Total noise density (dB W/Hz)	-188.3
Precompression Signal/total noise density (dB Hz)	52.1
Precompression pulse width (microseconds)	500.0
Pulse compression ratio (dB)	13.0
Post compression pulse width (microsecond) T	25.0

*This section excludes the effect of the control center antenna pointing directly at the sun which occurs at the spring and fall equinoxes for about a 7-day period with the maximum duration of 8 minutes during any one day.

TABLE 2-4. TYPICAL LINK CALCULATIONS: PULSE - COMPRESSION SYSTEM (RANGE-RANGE NAVIGATION) (Continued)

Return path - Values for return-path parameters are tabulated below:	
	Value
CONTROL CENTER NOISE POWER (Cont.)	
Effective filter bandwidth, kHz	40.0 = B
Filter loss (dB)	0.8
**Post compression signal/total noise density (dB Hz)	61.0
Signal energy/noise density, E/N_o (dB)	15.0 = E/N_o
EFFECT OF SUN	
Receiver noise figure (dB)	4.0
Receiver noise temperature (°K)	624.0
Solar noise temperature (°K)	3600.0
System noise figure (dB)	10.9
Received noise density from satellite (dB W/Hz)	-188.7
Total noise density (dB W/Hz)	-187.4
Increase in noise due to sun (dB)	0.9
Signal energy/noise density, E/N_o (dB)	14.1 = E/N_o
Note that the ranging pulse will be placed at the end of the data message as discussed below.	

2.2.2.3 DATA LINK ANALYSIS

The data link message structure and signal waveform is described in some detail in Section 4.1.2 of Volume II. It is a pulsed on/off carrier with "on" being the mark and "off" being the space as shown in Figure 2-1.

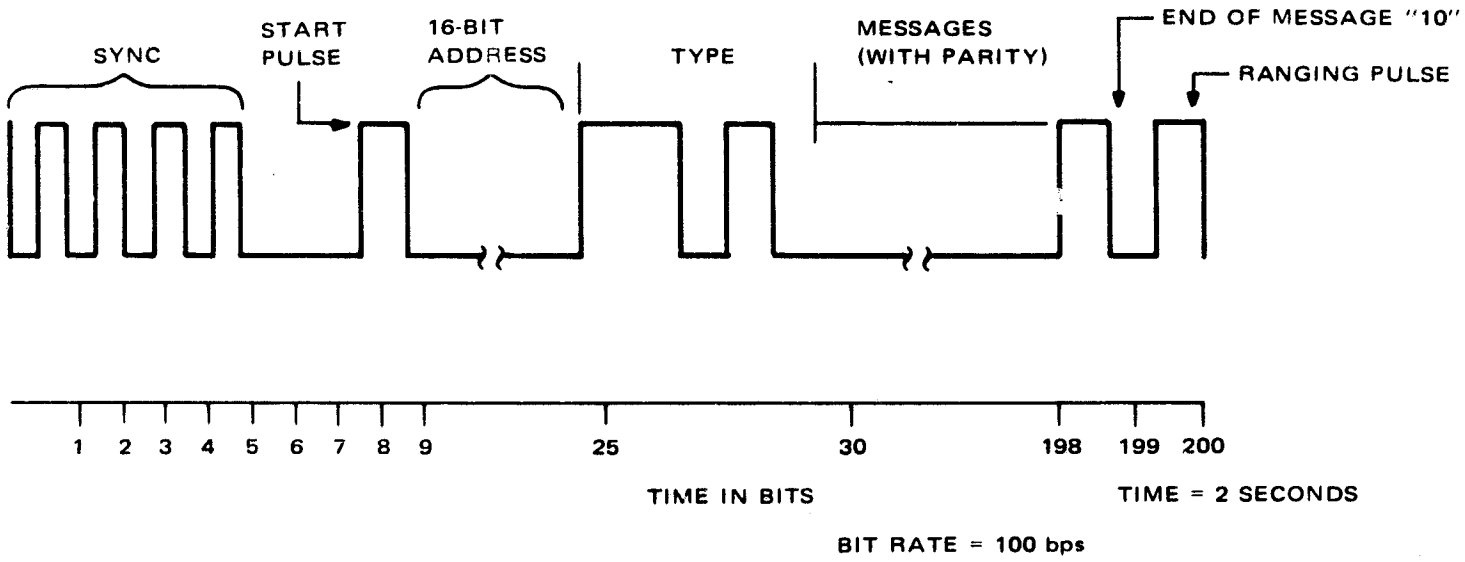

Figure 2-1. Typical ATC Data-Message Format

**Value derives from user S/N_o (64.0 dB) and control center S/N_o (64.3 dB)

Bit-error probabilities for the user and control center are found as follows:

a. User bit error: From the link analysis of Table 2-4 the signal energy to noise spectral density, E/N_0 at the user is 18.0 dB. By extrapolation of Lawton's* Figure 2, the bit error probability is less than 10^{-9}. At a bit rate of 100 bits/seconds, the mean time to error is $\frac{1}{100} \times \frac{1}{10^{-9}} = 10^7$ seconds = approx 115 days. This error is quite small and could be considered negligible.

b. Control Center bit error: From Table 2-4, the E/N_0 at the control center is 14.1 dB (worst case with antenna looking into the sun).

Again using Lawton's Figure 2, the bit error probability is about 10^{-6}. For a bit rate of 100 bits/second the mean time to error is $\frac{1}{100} \times \frac{1}{10^{-6}} = 10^4$ seconds = 2.78 hours.

Note that 10^4 seconds represents 5000 messages (since a message is sent every 2 seconds in the roll call mode). The probability of 1 bit being in error in 5000 messages is quite acceptable.

The above level of performance is obtained by using the parameters shown in Table 2-4.

2.2.2.4 PROJECTION TO 0.1 NAUTICAL MILE

From section 2.2.2.2, we see that the link analysis yields a ground range error, σ_R, of 0.662 nmi for the specified E/N_0 (= 14.1 dB) at the gound control center. For a σ_R of 0.10 nmi, it is necessary that the $B(2E/N_0)^{1/2}$ product be increased by a factor of 6.62. Actually the increase should be ten-fold if the previous allowance for propagation and other errors is maintained.) In order to obtain this with a reasonable E/N_0, it is necessary to increase B. Now if the pulse compression ratio, $B\tau$, is increased from 20 to 50 (a practical upper limit for a one-way pulse), then $(2E/N_0)^{1/2}$ would have to be increased by a factor of 2.65 times, i.e. E/N_0 must be increased by 8.4 dB. The resulting E/N_0 would be 22.5 dB. The corresponding increase of 8.4 dB in satellite transmitter power will result in an RF requirement of 5000 watts (instead of 710 W). Space qualified devices capable of supplying this power do not now exist and probably will not be around until the late 1970's or early 1980's.

Likewise, the user power in the return direction will also have to be increased by a factor of 8.4 dB, increasing the required RF power from 2.2 kW to 15.4 kW.

Both these increases lead to a rejection of the pulse modulation system when projected to 0.1 nmi accuracy.

2.2.3 CONTINUOUS-WAVE (CW) MODULATION TECHNIQUES

2.2.3.1 INTRODUCTION: CHOICE OF TONE FREQUENCIES

2.2.3.1.1 Ranging Signal Modulation - Because of the extremely large path loss encountered for synchronous satellites, the predetection signal-to-noise ratio of the

*J. G. Lawton, "Comparison of Binary Data Transmission Systems, 1958 Conference Proceedings on Military Electronics, IRE.

received signal is much less than unity. Under this condition, wideband cannot be used because of the inherent wideband threshold effect.[1]

For low-index angle modulation, Rowe[2] has shown that the analysis is quite similar to the analysis of amplitude modulation; however, angle modulation (constant amplitude) is favored because the satellite is peak power limited.

2.2.3.1.2 Ranging Signal Demodulation - The predetection signal-to-noise ratio is low because of the relatively low satellite transmitter power, the high path loss due to the slant range, and the large IF bandwidth required (on the order of 100 KHz). In order to prevent a degradation of the signal-to-noise because of the "weak signal suppression effect" of a square-law detector[3], coherent detection must be performed on the signal. In order to provide a coherent reference for the received signal, a highly stable voltage controlled crystal oscillator (VCXO) is phase-locked to the weak carrier. The noise bandwidth of the loop is narrow enough to ensure a carrier-to-noise ratio of at least 7 dB, and wide enough to maintain carrier lock during high vehicle-to-satellite accelerations.

Once carrier lock is obtained, the ranging signals are demodulated by multiplying the composite IF signal with the restored carrier. This multiplication occurs in the ranging demodulator. Since the signal-to-noise ratio at the output of this demodulator is approximately the same as that at the input (quite low), additional filtering of the signals is required. The degree of filtering will result in a ranging signal-to-noise ratio of at least 20 dB.

2.2.3.1.3 Ranging Signal Design

Tone Signal[4] Requirements - In both the Air-Traffic Control mode and in the self-Navigation mode, the end result is a phase measurement made on a ranging tone. The tone frequency must be high enough to ensure desired resolution, yet low enough to resolve the ambiguity about which cycle is received. If the tone was received in a noiseless environment and the phase measured with instruments of unlimited resolution, one tone would suffice. To overcome the limitations imposed by a finite signal-to-noise ratio and finite phase resolution, two or more tones are recommended.

---

(1) In order to keep the scope of effort to a reasonable level, wideband techniques that required the modulation to be periodically turned off were not considered.

(2) Rowe, "Signals and Noise in Communication Systems," D. Van Nostrand Company, 1965, pp 104 and 105.

(3) Davenport and Root, "Random Signals and Noise," McGraw-Hill, 1958, pp 266 and 267.

(4) Tone signal is construed to mean either a sine wave or a rectangular wave.

Minimum Signal-to-Noise Requirements - Baghdady[5] has shown that the practical threshold for phase demodulation (comparison) occurs when the signal-to-noise ratio of the tone, at the input to the phase resolver, is at least 7 dB. In order to prevent non-linear degradation of the phase measurement a 3-dB margin was added thus requiring the minimum signal-to-noise power ratio to be 10 dB.

Fine-Tone Frequency - It is shown in Section 2.5 that to achieve an overall user position accuracy of 1 nmi, the user position precision due to the signal-to-noise only should be 3/4 of a mile. If the rms phase error due to the signal-to-noise is allowed to be no greater than 5° the fine-tone (or square wave) frequency will be approximately 8 kHz. See Figures 2-2 and 2-3 for other values of phase jitter and tone frequencies.

Coarse-Tone Frequency - Consider a Mach-3 SST that is interrogated by the control center every 3 minutes; the distance covered is thus 100 nautical miles. This distance represents the minimum lane width for the air traffic control mode.

The frequency corresponding to this distance is 720 hertz. See Figure 2-4 for a plot of lane width vs tone frequency. In order to insure that a lane would not be missed if the interrogation-time is longer than 3 minutes or if the speed were greater than Mach-3 (because of the jetstream, for example), a frequency of 500 hertz was used for the lane-resolution tone. This results in a fine tone to coarse tone ratio of 16 to 1. (It is to be noted that 16 is a power of 2, which is compatible with binary-type ranging signals.) It is to be noted that geometric effects expand the real lane widths.

2.2.3.2 CW SYSTEM PERFORMANCE PARAMETERS

The system performance is affected by several parameters, e.g. path loss, noise levels, system losses, and antenna characteristics. These parameters are discussed at some length in this section, because they apply to both the modulation techniques (sine wave and digital code) considered later.

2.2.3.2.1 Free Space Path Attenuation

The free space path attenuation, in dB, is

$$\alpha = 37 + 20 \log f + 20 \log d$$

where f is in MHz with a range of 1540 MHz to 1660 MHz, and d is the distance in miles which varies from 22,300 miles (overhead satellite) to 26,250 miles (satellite on horizon). With these parameters, the minimum and maximum values of α are:

$$\alpha_{min} = 187.7 \approx \underline{188 \text{ dB}}$$

and

$$\alpha_{max} = 189.8 \quad 190 \text{ dB}$$

---

(5) Baghdady, "On the Noise Threshold of Conventional FM and PM Demodulators", Proceedings of the IEEE, Sept. 1963, pp 1260 and 1261.

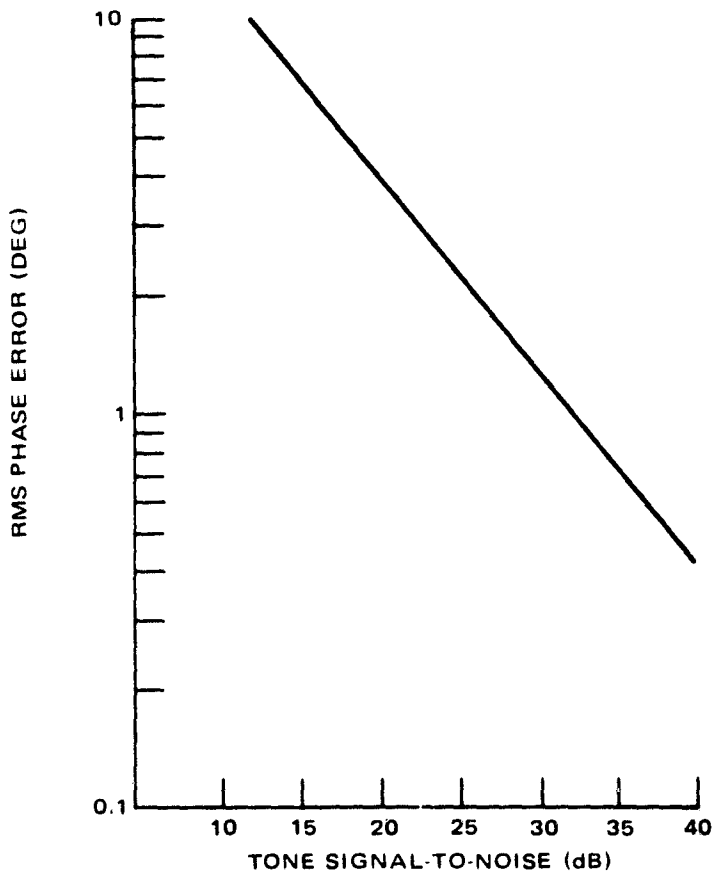

Figure 2-2. RMS Phase Error Vs. Tone Signal/Noise

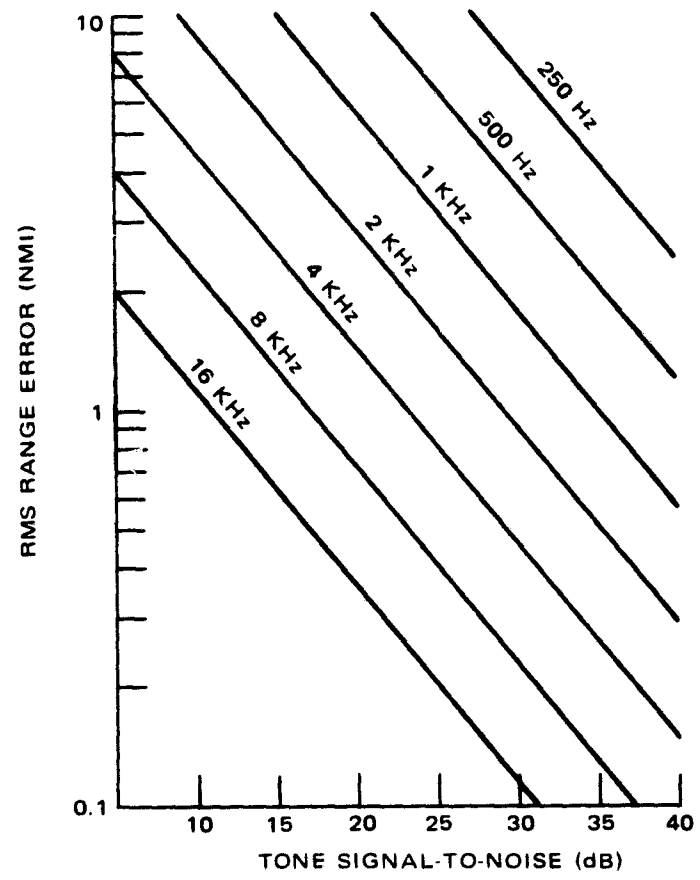

Figure 2-3. RMS Range Error Vs. Signal/Noise

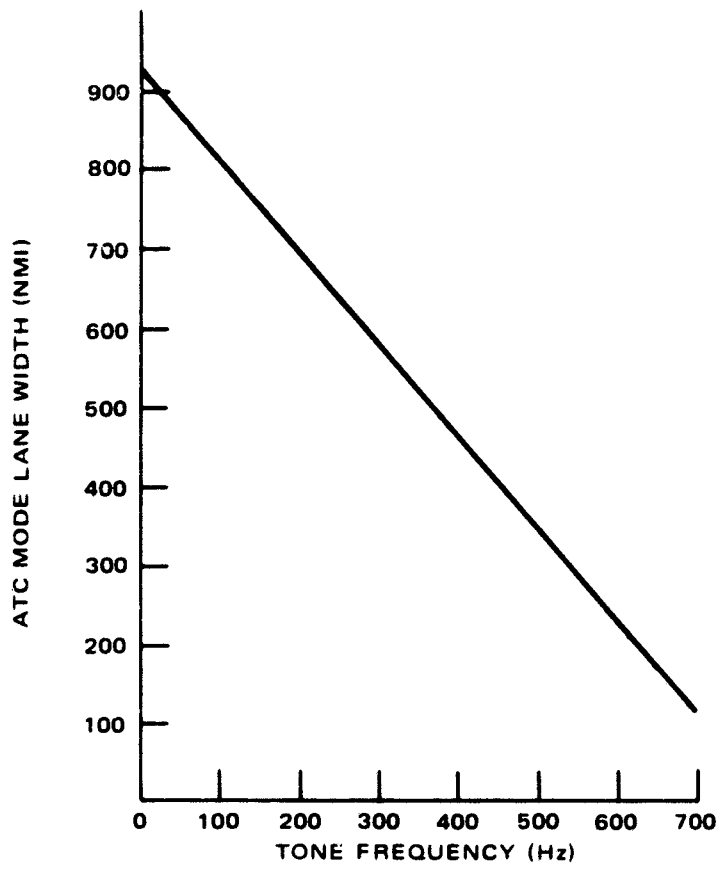

Figure 2-4. ATC Lane Width Vs. Tone Frequency

The variation of free space path loss due to the range variation is only 2 dB. For the purposes of the analysis, we will assume the worst case attenuation applies, i.e., = α_{max} = 190 dB.

2.2.3.2.2 Noise Sources

2.2.3.2.2.1 Receiver Noise

The equivalent input noise temperature T_e of a receiver including the effects of all losses between the antenna terminals and the input amplifier is given by:

$$T_e = (L-1)\ T_L + L\ (F-1)\ x\ 290$$

where: L is the power loss of the lossy section(s),

T_L is the temperature of the lossy section, and

F is the noise figure of the basic receiver

The assumed noise figures for all the various receivers in the system, i.e. at the control center, satellite (both directions) and the user, are shown in Table 2-5, which also shows the effective T_e and the corresponding equivalent noise figure F_e at these locations.

TABLE 2-5. EQUIVALENT INPUT NOISE TEMPERATURE

Location	L (dB)	F (dB)	T_L (°K)	T_e (°K)	F_e (dB)
Satellite	1	5	60	808.5	4.4
User	2	5	290	1171.7	6.1
Control Center	1	4	290	623.5	3.3
$F_e = 10 \log (T_e/290)$					

2.2.3.2.2.2 Non-Terrestial Noise Sources

2.2.3.2.2.2.1 Sun Noise Temperature

The sun noise temperature[1], T_s, is given by [2]

$$\frac{T_s}{290} = \frac{675}{f_{GHz}} \left[1 + \frac{1}{2.3} \sin 2\pi \frac{\log_{10} 6 (f - 0.01 \text{ GHz})}{2.3} \right]$$

For f = 1.54 GHz this leads to

$$T_s = 1.54 \times 10^5 \text{ °K}$$

Since the sun subtends an angle of approximately .5° at the surface of the earth, antennas with a beamwidth of .5° or less (ideal antenna with infinite cutoff at beam edge) will effectively see the full 1.54×10^5 K° temperature. For beamwidths of greater than .5° the antenna temperature is decreased by the square of the beamwidth[3] with respect to the sun's diameter, i.e.,

$$T_a = T_s \left(\frac{0.5}{\theta} \right)^2$$

where θ = plane angle beamwidth of antenna in degrees. Table 2-6 illustrates the effect of the antenna beamwidth on system noise figure, F_{db}, for a receiver noise figure, F_{cc}, of 5 dB. In the table, T_e (°K) is the sum of the antenna and the receiver noise temperatures T_a and T_{cc}, and ΔF_{db} is the increase of the system noise figure over the receiver noise figure of 5 dB.

---

[1] David C. Hogg & W. W. Humford of Bell Telephone Labs, The Microwave Journal, March 1960, pp 80-84

[2] Ibid. Equation (10)

[3] Ibid Equation (11a)

TABLE 2-6. SYSTEM NOISE FIGURE (F_{cc} = 5dB AND T_{cc} = 627 °K)

(deg)	T_a (°K)	T_e (°K) = $T_a + T_{cc}$	F-1 = $T_e/290$	F	F_{dB}	ΔF_{dB}
0.5	1.54×10^5	1.55×10^5	534	535	27.3	22.3
1.0	3.85×10^4	3.91×10^4	135	136	21.3	16.3
1.5	1.71×10^4	1.77×10^4	61.0	62.0	17.9	12.9
2.0	9.63×10^3	10.26×10^3	35.4	36.4	15.6	10.6
2.5	6.16×10^3	6.79×10^3	23.4	24.4	13.9	8.9
3.0	4.28×10^3	4.91×10^3	16.9	17.9	12.5	7.5
5	1.54×10^3	2.17×10^3	7.48	8.48	9.3	4.3
10	385	1012	3.48	4.48	6.5	1.5
15	171	798	2.75	3.75	5.7	0.7
20	96.3	723.3	2.49	3.49	5.4	0.4
25	61.3	688.3	2.39	3.39	5.3	0.3
50	15.4	642.4	2.21	3.21	5.1	0.1

2.2.3.2.2.2.2 Extra-Solar System Noise Sources

Galactic Center[1] - Calculated and observed antenna noise temperatures due to radiation from the galactic center are listed below. (The values are for 1200 MHz, but also hold approximately for the 1600 MHz band.)

Antenna Beamwidth (deg)	Calculated (°K)	Observed (°K)
2.8°	18.7	17
Infinitely Narrow	34	—

[1]David C. Hogg & W.W. Humford of Bell Telephone Labs, The Microwave Journal, March 1960, pp. 80-84.

Isotropic Component (Background Noise)[1]

T_{ISO} = 1 K° at 1200 MHz

Approximately the same value holds at 1600 MHz also.

Discrete Galactic Noise Sources[2]

A few of the more intense discrete galactic noise sources and their intensities are shown in Table 2-7. The values for 1500 MHz are interpolated from the other data.

TABLE 2-7. INTENSITY OF NOISE SOURCES ($W/ft^2/Hz$) AT FOUR FREQUENCIES

Source	200 MHz	1000 MHz	3000 MHz	1500 MHz
Cassiopeia A	10^{-23}	3×10^{-24}	10^{-24}	2×10^{-24}
Cygnus A	10^{-23}	10^{-24}	7×10^{-25}	9×10^{-25}
Tarus A	10^{-24}	10^{-24}	10^{-24}	10^{-24}
Virgo A	10^{-24}	3×10^{-25}	10^{-25}	2×10^{-25}

The noise power density of a discrete source is given by $P_d = SA_e$ where

P_d = Discrete source noise power density (W/Hz)

S = Discrete source intensity (W/area/Hz)

A_e = Effective area of the antenna in square feet; for a 20-foot diameter antenna, A_e = 314 square feet.

The discrete source noise power density, P_d, is converted to an effective antenna temperature, T_{ad}, by the formula:

$$T_{ad} = \frac{P_d}{k}, \text{ where k = Boltzman's Const. } = 1.38 \times 10^{-23} \text{ joules/°K}$$

The effective antenna temperatures for the discrete galactic noise sources shown in Table 2-7 for 1500 MHz are shown in Table 2-8 (for a 20-foot diameter antenna).

[1] David C. Hogg & W. W. Humford of Bell Telephone Labs, The Microwave Journal, March 1960, pp. 80-84.

[2] RFI in Satellite Communications Systems, C. M. Salati, Electronic Industries, April 1960, Table 1

TABLE 2-8. EFFECTIVE ANTENNA (20-ft diam) TEMPERATURES FOR DISCRETE SOURCES

Source	Intensity, S ($W/ft^2/Hz$)	Power Density, P_d (W/Hz)	$T_{ad}(^{o}K)$
Cassiopeia A	2×10^{-24}	6.28×10^{-22}	45.5
Cygnus A	9×10^{-25}	2.83×10^{-22}	20.5
Tarus A	10^{-24}	3.14×10^{-22}	22.8
Virgo A	2×10^{-25}	6.28×10^{-23}	4.55

It is to be noted that all the above extra-solar system noise sources have a negligible contribution to the total system noise and they can be ignored.

2.2.3.2.2.2.3 Terrestial Noise Sources: Antenna Minor Lobes - The increase in effective antenna noise temperature, due to minor lobe pickup, is directly related to the gain of the minor lobe as compared to the main lobe and the temperature of the medium in which the lobe is directed.

The relationship is:[6]

$$T_{\text{minor lobes}} = \sum_{k=1}^{n} \gamma_k \delta_k T_k$$

where

γ_k = total fractional attenuation of the kth minor lobe compared with the main lobe.

δ_k = total fractional absorption of the reflected, scattered, and transmitted minor lobe in a medium whose temperature is T_k.

For example, if the minor lobe is looking at the earth, i.e.

T_k = 290°K, and the $\gamma_k \times \delta_k$ is -10 dB, then $T_{\text{minor lobe}}$ = 29°K.

2.2.3.2.3 System Loss Sources

Antenna Polarization Loss - Because of the geometry involved (satellite-to-earth or earth-to-satellite), the maximum polarization loss (assuming all antennas are circularly polarized with the correct sense) will be 3 dB. This occurs when one field of the linear polarizations (e.g., horizontal or vertical) is reduced to near zero, e.g., when the satellite is low on the horizon.

[6]Baghdady, "Lectures on Communication System Theory," McGraw-Hill, 1961, Chapter 15, pp. 387 and 388; equation (47).

Transmission Line and Coupler Losses - The insertion of any passive networks such as transmission lines, antenna couplers, preselectors, etc., attenuates the signal by the magnitude of the loss. The combined transmission line and coupler losses are expected to be less than 2.0 dB, at the user and less than 1 dB at the control center and at the satellite.

Attenuation of Signal Due to Snow and/or Rain on Radome - It is desired to determine the degradation of the received signal during a period of heavy rain and/or snow. Furthermore, it is desired to determine the additional degradation that a radome over the antenna will contribute.

Experimental data[7] taken at Andover, Maine by Bell Telephone Laboratory and Communications Satellite Corporation personnel on transmissions received from the Early Bird satellite, transmitting at a frequency of approximately 4000 MHz, indicate that the carrier-to-noise degradation during a heavy rain can exceed 6 dB. Further measurements taken by Bell Telephone Laboratory personnel on the radio source Cassiopeia A, at a frequency of 4000 MHz indicated transmission degradations as high as 8 dB.

Using an analysis similar to Bievis[9] (who utilized equations developed by Leaderman and Turner[10]) in conjunction with rainfall data[11] and the value of the dielectric constant of water[12] at UHF, the average expected attenuation due to rainfall will be 0.5 dB; there is a 1% probability that the attenuation will exceed 2.5 dB during any five-minute period during the next 25 years. The above values of attenuation are for rainfall rates of 1 inch/hour, and 12 inch/hour on a 30-foot radome, the radome covering a 20-foot antenna. Without a radome, the worst case attenuation would be less than 0.5 dB.

At this writing, it is felt that the only equipment that would be affected by the rain-radome consideration would be at the ground control center. The reasoning is as follows: boats, ships, trucks, and for general field use, a radome will not be required. High performance aircraft, SST and conventional jets will, in general, fly above the rain. Low performance aircraft will generally have small antennas, say, less than two feet in diameter, and hence, small radomes (for a radome 3 feet in diameter, the worst case attentuation as described above will be 0.6 dB — quite small).

---

[7]"Experimental Performance of the Early Bird Communications System," L. F. Gray, AIAA Communications Satellite Systems Conference, Washington, D. C., May 2-4, 1966, AIAA Paper No. 66-246.

[8]"4-Gc Transmission Degradation Due to Rain at the Andover, Maine, Satellite Station," A. J. Giger, Bell System Technical Journal, September 1965, pp. 1528-1533.

[9]B. C. Blevis, "Losses Due to Rain on Radomes and Antenna Reflecting Surfaces," IEEE Transactions on Antennas and Propagation, January 1965, pp. 175 and 176.

[10]H. Leaderman and L. A. Turner, "Theory of the Reflection and Transmission of Electromagnetic Waves by Dielectric Materials, Radar Scanners and Radomes," Vol. 26, Rad. Lab. Series, McGraw Hill, 1948, Chapter 12.

[11]"Climatic Extremes and a 500 Foot Radome," Aerospace Instr. Lab. AFCRL (technical report).

[12]E. H. Grant, et al., "Dielectric Behavior of Water at Microwave Frequencies," The Journal of Chemical Physics, Vol. 26, No. 1, January 1957, pp. 156-161.

2.2.3.2.4 Satellite Antenna Parameters

Beamwidth, θ - The beamwidth θ of a satellite antenna located at synchronous altitude (19,500 nmi) and covering the earth (radius 3430 nmi) is found from

$$\frac{\theta}{2} = \text{Arctan } \frac{3430}{22,930} = 8.6^\circ$$

or $\theta = 17.2^\circ$

Antenna Gain - A parabolic antenna with an illumination factor of 0.54 and a beamwidth of θ degrees has a power gain G that is expressed by the formula

$$G = (44.3 - 20 \log \theta) \text{ dB}$$

Therefore $G = 19.5$ dB, for $\theta = 17.2^\circ$

In the link analyses we will consider the case where the user and/or the control center is at the -3 dB beam edge of the satellite antenna, i.e. the effective satellite gain is 19.5 - 3.0 = 16.5 dB. This is the number that will be used in the link analyses for both the sine-wave and digital-code modulations.

2.2.3.3 SINE WAVE MODULATION (2-TONE)

2.2.3.3.1 Description

Coarse Tone Signal-to-Noise - Consider the case in which only 2-tones are used as the ranging signals. If we are to resolve which cycle of the fine tone is the correct one when observing a specific segment of the coarse tone, and resolve the fine tone with a 3σ (99.7%) accuracy, the signal-to-noise ratio of the coarse tone must be at least 22.7 dB for a 16 to 1 tones ratio, as shown in Appendix 2.2.3.3-A. This value of 22.7 dB takes into account an instrumentation error of 3.0° RMS.

Fine Tone Signal-to-Noise - As stated previously and shown in Section 2.5, the RMS phase jitter on the fine tone is to be no greater than 5° in order to obtain the overall ground accuracy of 1 nautical mile. In order to obtain the 5° RMS phase jitter the signal-to-noise must be at least 18.3 dB as shown in Figure 2-2.

Carrier Signal-to-Noise - As shown in Appendix 2.2.3.3-B, a signal-to-noise ratio of 7 dB will insure that the mean time to unlock is quite large and in fact is 1.6 days.

A block diagram of the carrier extraction and tone demodulation instrumentation used in both the user and control center receiving equipment is shown in Figure 2-5. In this figure a word of explanation is required to clarify the use of the block labeled "CARRIER N.B. FILT."

The purpose of this filter is to pass the carrier to the carrier phase detector while at the same time rejecting the modulation sidebands. This filter must be compensated sufficiently for any carrier frequency shift due to user doppler and for all other frequency errors. For a Mach 3 user aircraft with a nominal received signal at 1660 MH_Z, the doppler is about ±5 kHz. Also for a typical oscillator drift of 1.5 parts in

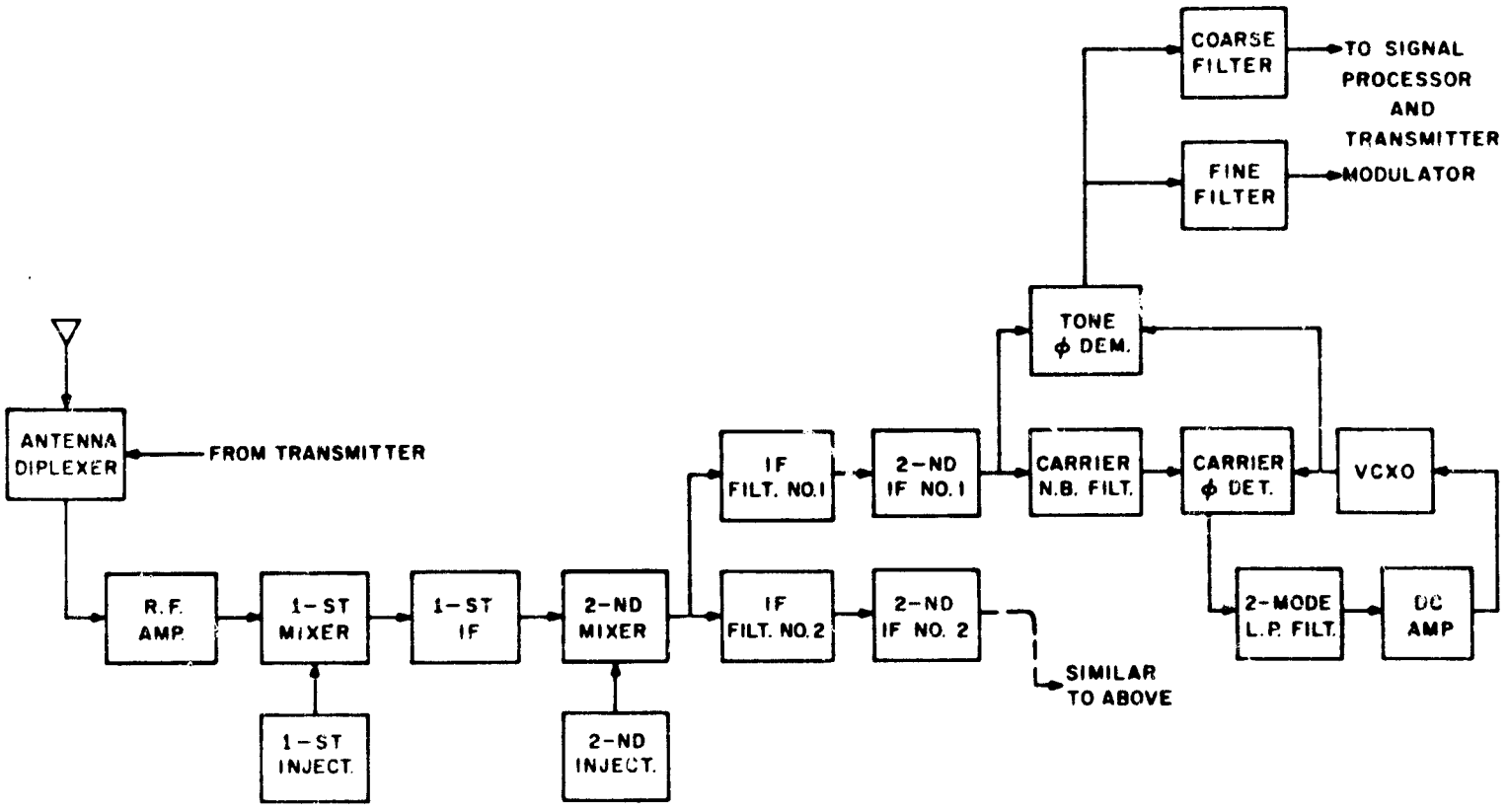

Figure 2-5. Receiver (Functional Block Diagram)

10^9 per hour, the maximum frequency error is ±600 Hz, provided the first injection setting is calibrated once every 10 days. Therefore, the filter has to be at least 11.2 kHz wide (i.e., have a half-bandwidth of 5.6 kHz); it should be narrow enough to reject the first-order sidebands of the fine tone modulation which are separated by 8.0 kHz. It is only necessary to reject one of the fine tone sidebands in order to have a negative signal-to-noise of the remaining sideband in the carrier loop.

The shape-factor requirements are rather modest in that a 3-pole filter is all that is required to reject these first-order sidebands by 20 dB. The peak-to-valley ripple of the filter is about 0.1 dB. These requirements are easily met with a simple crystal filter.

Note that the coarse tone does not present any discrete sideband components about the carrier since it is modulated by the data signal.

Modulation Indices & Signal-to-Noise Density Ratios - A discussion of the phase-modulation index for 2-tone ranging (Appendix 2.2.3.3-C) shows that near-optimum performance occurs with a coarse-tone phase modulation index of 1.4 and a fine-tone phase modulation index of 0.65. The resulting carrier power is 5.9 dB down from the total RF power level, while the coarse-tone and the fine-tone power levels are down 3.2 dB and 12.1 dB respectively. The principal reason for the larger modulation index on the coarse-tone as compared to the fine-tone is due to the requirement for a low bit-error probability on the data modulating the coarse tone, as described in Section 2.2.3.3.3 which follows. A discussion of the bit-error probability can be found in Appendix 2.2.3.3-D, where it is shown that the error rate corresponds to a word error rate of one word in 10,000 messages.

The two appendixes (2.2.3.3-C and -D) also state the signal-to-noise density ratios needed for the desired performance in terms of ranging accuracy and data errors. Specifically, C/N_O = 27 dB-Hz for the carrier, S/N_O = 29.5 dB-Hz for the coarse tone, and S/N_O = 20.3 dB-Hz for the fine tone. These values are achieved in the link analysis described later.

2.2.3.3.2 Sine Wave Link Analysis and Conclusions

The parameters discussed above are used to prepare the link analysis for a sine wave modulation, as shown in Table 2-8. The results indicate that the required position accuracy of 1 nmi can be obtained by modulating the L-band carrier with an 8 kHz fine tone sine wave. Furthermore, a 500 Hz coarse-tone sine wave will insure a lanewidth of greater than 100 nmi, the distance a Mach-3 SST travels in 3 minutes.

One-way navigation (passive) is possible with power levels of 5 watts at the control center (and a modest 20 feet diameter parabolic dish), 20 watts at the satellite (and an earth coverage antenna of less than two feet in diameter), and an upper hemisphere user antenna. Two-way navigation (active - ATC mode) is accomplished by the incorporation of (1) a diplexer and 20-watt user transmitter and (2) a diplexer and 10-watt transmitter at the satellite.

The predetection bandwidth, at all three places, of 100 kHz (quite modest) is a good compromise between signal phase stability and signal-to-noise ratio requirements. A post detection bandwidth of 142 Hz at the user and 205 Hz at the ground control station insures a C/N of 7 dB for carrier detection. The controlling parameter for carrier detection is 7 dB so that the bandwidth will be adjusted to conform to this value throughout.

Receiver noise figures of 5 dB are quite adequate at the satellite and the user while that at the control center can be as poor as 14 dB before any increase in system noise would be noted.

A phase modulation index of 1.4 for the coarse tone insures a high probability (99.7%) of resolving the proper cycle of fine tone in the coarse tone, and data word-error rate of one word in 10,000 messages, corresponding to S/N_O of 29.5 dB-Hz in the coarse tone or C/N_O of 27 dB-Hz for the carrier, as discussed in Appendixes 2.3.3.3-C and -D. This modulation index also insures that ample carrier is present for coherent detection and signal modulation. A phase modulation index of 0.65 on the fine-tone provides ample signal-to-noise so that the ground position error is less than 1 nmi.

2.2.3.3.3 Data Link - Air Traffic Control

Data Modulation Method - The proposed method of adding binary data to the ranging signal is to shift the phase of the coarse tone by a factor of 0° or 180° depending upon the composition of the data message (see Figure 2-6). The binary system selected is Differentially Coherent Phase Shift Keying (DCPSK). This method of data transmission is less than 1 dB away from the optimum method of binary modulation, coherent PSK. However, with coherent PSK an absolute phase standard must be used for demodulation, which adds greatly to the system complexity and cost. Because of the near randomness of the message the subcarrier component (i.e. the coarse tone) is either non-existent or very much reduced in power level from what it would be if no data modulation were present.

TABLE 2-8. LINK CALCULATIONS FOR SINE WAVE MODULATION

Forward Path - Values for forward-path parameters are tabulated below:

	Value
CONTROL CENTER	
Transmitter power (5 W) (dBW)	7
Antenna coupling losses (dB)	1.5
Antenna gain (dB)	37.0
Rain and snow attenuation (dB)	0.2
Effective radiated power, ERP (dBW)	42.8
PROPAGATION	
Path loss (dB)	190.0
Atmosphere and ionosphere attenuation (dB)	0.5
SATELLITE	
Antenna gain (-3 dB) (dB)	16.5
Antenna polarization loss (dB)	0.5
Antenna coupling loss (dB)	1.0
Received RF power (dB)	-133.2
SATELLITE NOISE POWER	
Receiver noise figure (dB)	5.0
Receiver noise temperature (°K)	809.0
Effective sun temperature (°K)	0
Total galactic noise temperature (°K)	2
Effective earth temperature (°K)	105
Total noise temperature (°K)	916
System noise figure (dB)	5.0
Noise density (dBW/Hz)	-199.0
Satellite noise bandwidth (kHz)	100
Satellite noise power (dBW)	-149.0
RF power/noise (dB)	15.8
Transmitter power (20 W) (dBW)	13.0
Antenna coupling loss (dB)	1.0
Antenna gain (dB)	16.5
ERP (dBW)	28.5
Effective radiated noise, ERN, (dBW)	12.7
PROPAGATION	
Path loss (dB)	190.0
Atmospheric and ionospheric attenuation (dB)	0.5

TABLE 2-8. LINK CALCULATIONS FOR SINE WAVE MODULATION (Continued)

Forward Path - Values for forward-path parameters are tabulated below:

	Value
USER	
Antenna gain (dB)	2.0
Antenna polarization loss (dB)	1.5
Antenna coupling loss (dB)	2.0
Received RF power (dB)	-163.5
USER NOISE POWER	
Receiver noise figure (dB)	5.0
Receiver noise temperature (°K)	1172
Total galactic noise temperature (°K)	2
Effective sun temperature (°K)	2
Total noise temperature (°K)	1176
System noise figure (dB)	6.1
Noise density (dBW/Hz)	-197.9
Received noise from satellite (dBW)	-179.3
Received noise density (dBW/Hz)	-229.3
Total noise density (dBW/Hz)	-197.9
Predetection noise bandwidth (kHz)	100
Predetection noise power (dBW)	-147.9
RF power/noise (dB)	- 15.6
Carrier/noise at (Mod. Loss = 5.9 dB) (dB)	- 21.5
Postdetection carrier noise bandwidth (Hz)	142
Reference carrier/noise (dB)	7.0
Tone noise bandwidth (Fine) (Hz)	10.0
Tone signal/noise (Fine) (Mod. Loss = 12.1 dB) (dB)	12.3
SELF-NAVIGATION MODE	
*Tone noise bandwidth (Fine) (Hz)	1.0
Tone signal/noise (dB)	22.3

Return Path - Values for return-path parameters are tabulated below:

	Value
USER	
Transmitter power (20 W) (dBW)	13.0
Antenna gain (dB)	2.0

*In active mode, user tone-bandwidth is much larger (10-times) than control center tone-bandwidth so that the integration time (reciprocal of the tone-bandwidth) is predominantly determined by the control center. In the case where the user wants his position (either in the active or passive mode), the effective bandwidth of the user's navigation equipment is 1 Hz.

TABLE 2-8. LINK CALCULATIONS FOR SINE WAVE MODULATION (Continued)

Return Path - Values for return-path parameters are tabulated below:	
	Value
USER (Cont.)	
Antenna coupling losses (dB)	2.0
ERP (dBW)	13.0
*Effective radiated noise density (dBW/Hz)	- 21.4
PROPAGATION	
Path loss (dB)	190.0
Atmospheric and Ionospheric attenuation (dB)	0.5
SATELLITE	
Antenna gain (dB)	16.5
Antenna polarization loss (dB)	1.5
Antenna coupling loss (dB)	1.0
Received RF power (dBW)	-163.0
SATELLITE NOISE POWER	
Noise density (same as forward path) (dBW/Hz)	-199.0
**Received noise density from user (dBW/Hz)	-197.4
Combined noise density (dBW/Hz)	-195.1
Effective noise power (dBW)	-149.0
Received RF power/noise (dB)	- 14.0
Transmitter power (10 W) (dBW)	10.0
Antenna coupling losses (dB)	1.0
Antenna gain (dB)	16.5
ERP (dBW)	11.4
ERN (dBW)	25.4
PROPAGATION	
Path loss (dB)	190.0
Atmospheric and ionospheric attenuation (dB)	0.5
CONTROL CENTER	
Antenna gain (dB)	37.0
Antenna polarization loss (dB)	0.5
Antenna coupling loss (dB)	1.0
Received RF power (dBW)	-143.4

*Retransmitted noise in a ±1 Hz bandwidth about each tone.

**Only affects the demodulated signal at the control center, since the noise is narrowbanded.

Note: The user generates a new carrier rather than turn-around tne received carrier.

TABLE 2-8. LINK CALCULATIONS FOR SINE WAVE MODULATION (Continued)

Return Path - Values for return-path parameters are tabulated below:

	Value
*CONTROL CENTER NOISE POWER	
System noise figure (dB)	3.3
System noise density (dBW/Hz)	-200.7
**Received noise density from satellite (dBW/Hz)	-175.5
Total noise density (dBW/Hz)	-175.5
RF Power/total noise density (dBw-Hz)	32.1
Postdetection carrier noise bandwidth (Hz)	204
Reference carrier/noise (Mod Loss = 5.9 dB) (dB)	7
Tone noise bandwidth (Fine) (Hz)	1.0
Tone signal/noise (Fine) (Mod. Loss = 12.1 dB) (dB)	20.0
Excess signal/noise (fine tone) (dB)	2.7
EFFECT OF SUN	
Receiver noise figure (dB)	4.0
Receiver noise temperature (°K)	624
Solar noise temperature (°K)	3600
System Noise Density (dBW/Hz)	194.4
Received Noise Density from Satellite (dBW/Hz)	-175.5
Total Noise Density (dBW/Hz)	-175.5
Increase in noise due to sun (dB)	0.0
RF Power/total noise density (dBW-Hz)	32.1
Demodulated carrier/noise (dB)	7.0
Fine Tone signal/noise (dB)	20.0
Excess signal/noise (fine tone) (dB)	2.7

*This section excludes the effect of the control center antenna pointing directly at the sun which occurs at the spring and fall equinoxes for about a 7-day period with the maximum duration during any one day about 8 minutes.

**This is the noise density about the fine tone, the noise density about the carrier is -179.4 dB.

The method of reconstituting the coarse tone is shown in Figure 2-7. The user detects (extracts) the carrier in the usual manner, i.e. with a phase locked loop, as shown in detail in Figure 2-5 earlier. This cleaned up carrier reference (VCXO output) is then multiplied with the incoming IF signal to demodulate both tones. Note that the discrete coarse tone frequency is not present, but rather, a sin x/x frequency spectrum is distributed about the frequency that would be the corase tone. The coarse tone carrying the data signal is then passed through a bandpass filter in order to obtain a positive signal-to-noise ratio. The output of the filter is split into two paths as shown in Figure 2-7. The upper path goes through a full wave rectifier and narrow bandpass filter, resulting in a steady-state sine wave at twice the coarse tone frequency and with the data information removed. (Note that the data transmission is either a 0° or a 180° phase shift of the coarse tone; now 2 times 0° = 0° and 2 times 180° = 360° is also equivalent

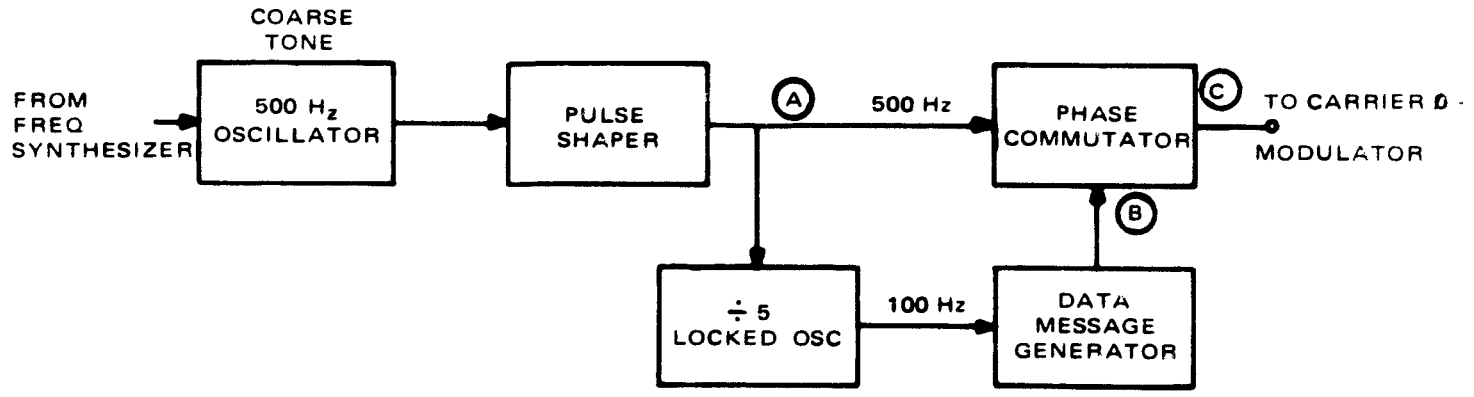

(a) DATA-LINK MODULATOR

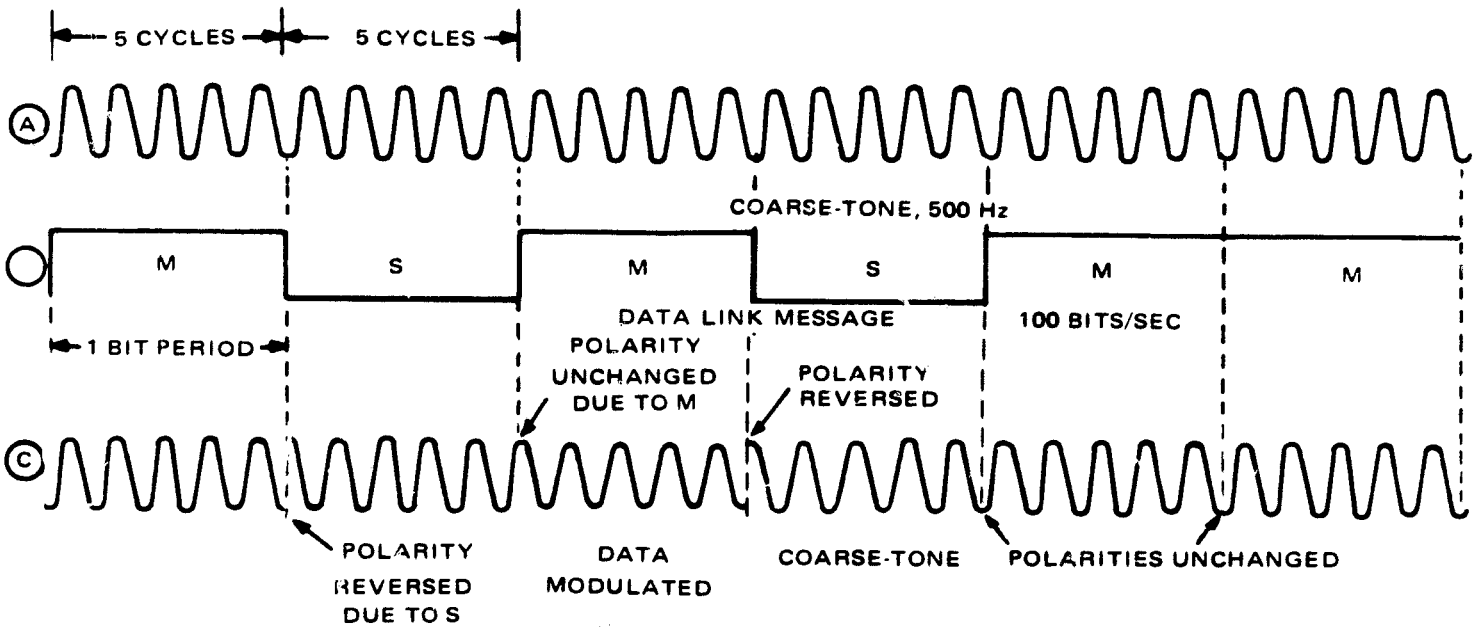

(b) SIGNAL WAVEFORMS AT POINTS A, B, C OF FIGURE (a)

Figure 2-6. Data Capability by Modulation of the Coarse Ranging Tone

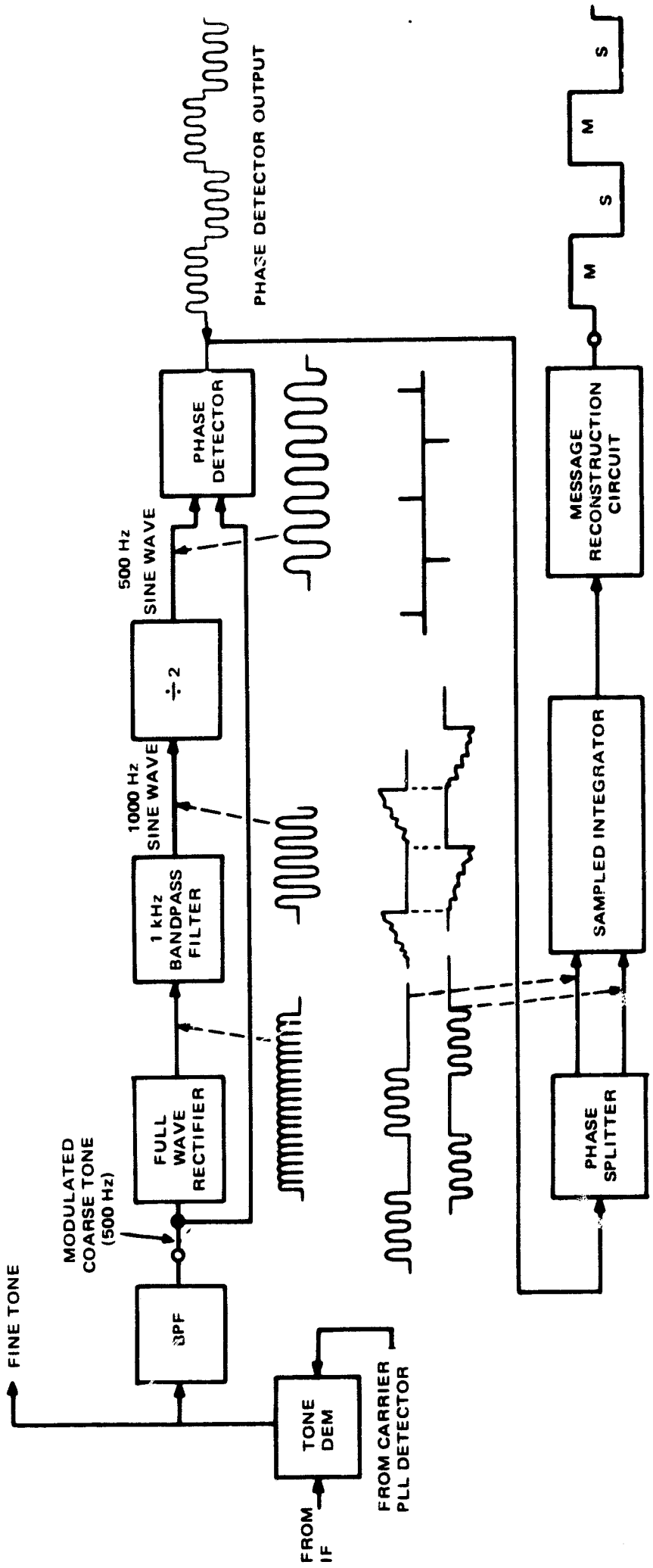

Figure 2-7. Data Demodulator

to 0°, so that the data is essentially removed.) This sine wave at twice the coarse tone frequency is then divided by 2; the output is multiplied with the modulated coarse tone coming from the lower path out of the bandpass filter. The result is a series of half wave pulses at the coarse tone frequency, of either + polarity or - polarity depending on the state of the data stream. It is to be noted that the polarity of the signal could have been reversed if the signal in the upper branch (entering the full-wave rectifier) was delayed by a half-cycle of the coarse tone anywhere in the upper path; therefore the absolute value of the phase information is lost. Figure 2-8 illustrates how the signal is restored to a mark/space square wave structure. Thus the output of the Message Reconstruction Circuit of Figure 2-7 is fed into two branches of the Message Restoration Circuit of Figure 2-8(a); the upper branch delays the data stream by one full bit and compares the n^{th} bit with the $n-1^{th}$ bit in the comparator circuit. If they are the same, the n^{th} bit is called a mark (1); while if they are opposite, the n^{th} bit is called a space (0). This results in message restoration as seen from parts (b) and (c) of Figure 2-8.

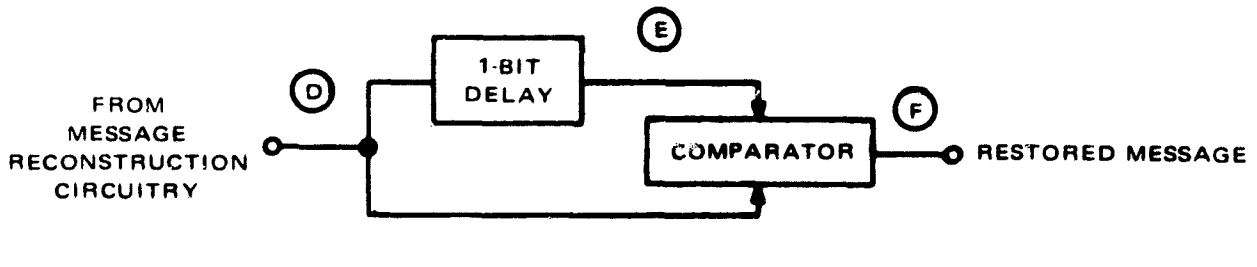

(a) MESSAGE RESTORATION CIRCUITRY

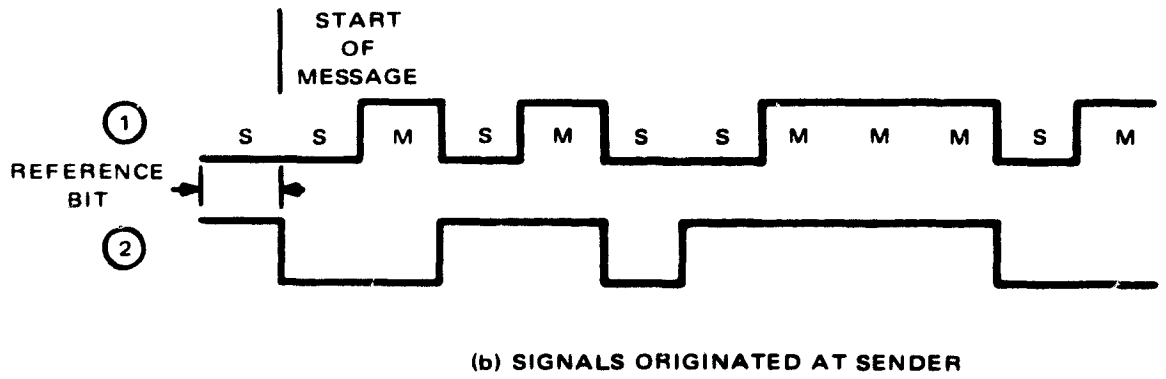

(b) SIGNALS ORIGINATED AT SENDER

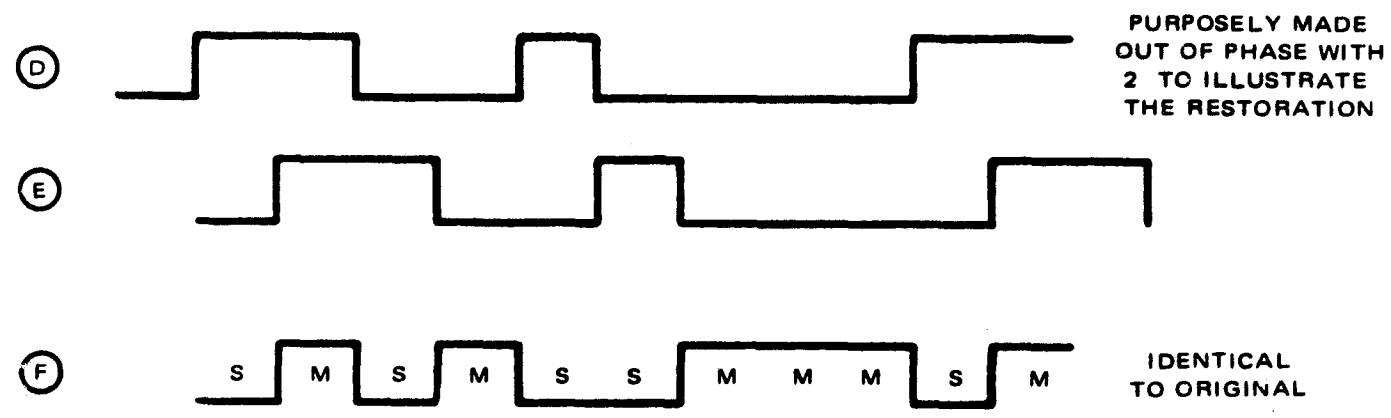

(c) SIGNALS PROCESSED BY RECEIVER

Figure 2-8. Restoration of Data Message

Data Format and Message Structure - For an operational Air Traffic Control (ATC) system, it is visualized that there will be many types of messages of varying priority. These messages could indicate position and velocity; weather information such as cloud coverage, wind velocity and direction, barometric pressure, and clear air turbulence; next checkpoint information such as latitude, longitude and time; destination information; fuel and fuel consumption; search-and-rescue commands, etc.

Because of the different precision requirements for the various data, the length of each type of "word" will be different; e.g. a latitude or longitude datum point will require at least 16 binary bits for a 0.1 minute of arc (0.1 nmi) precision, while a 4-bit word could indicate 1 of 16 possible sea states. Table 2-9 indicates some of the desired data parameters, precision requirements and resulting minimum binary word lengths. A total of 180 bits should suffice for each user message.

TABLE 2-9. TYPICAL ATC MESSAGE WORD LENGTHS

Parameter	Precision	Word Length (bits)
Address	65,000 Users	16
Format		
Sync	4-bits (8 - double rate)	4
Type	1/32 combinations	5
End	Reply/no reply, preceded by "0"	2
Position		
Latitude	0.1 nmi	18
Longitude	0.1 nmi	18
Height	100 ft/100,000 ft ceiling	10
Time	0.1 second/24 hours	20
Epoch	Present/last/next/other	2
Flight Origin	16,000 Locations	14
Destination	16,000 Locations	14
Weather		
Temperature	1°/128° and ± sign	8
Pressure	1 part/128	7
Wind Velocity & Direction	1 mph/256 mph and 1°/360°	17
Cloud Coverage	1% steps	7
Cloud Altitude	1000 ft/32,000 ft	5
Cloud Type	16 states	4
Turbulence	Yes/No flag	2
	TOTAL	173

A typical data link message is shown in Figure 2-9. All bits have the same duration except for the synchronization pattern which is at twice the bit rate in order to make it unique. The start pulse is used to trigger the user's starting gate. Upon reception of the start pulse, the address and all following bits are shifted into a shift register. After completion of the message the address is examined; if it is the correct one (for the specific user) the system responds. The reply/no-reply pulse at the end of the message informs the receiver of the sender's desire for a return message. Ample parity is provided for error detection and error correction bits are provided for the high priority data.

The bit-rate of 100 bits per second ensures a low bit error probability (i.e., about 2 bits in 10^4) for a signal to noise density ratio of 29.5 dB-Hz in the coarse tone, as discussed in Appendix 2.2.3.3-D.

The total duration of the message is 1.8 seconds, making the data link message compatible with the tone burst duration of 2 seconds. (Recall that each user is assigned this period in the ATC roll call mode of operation.)

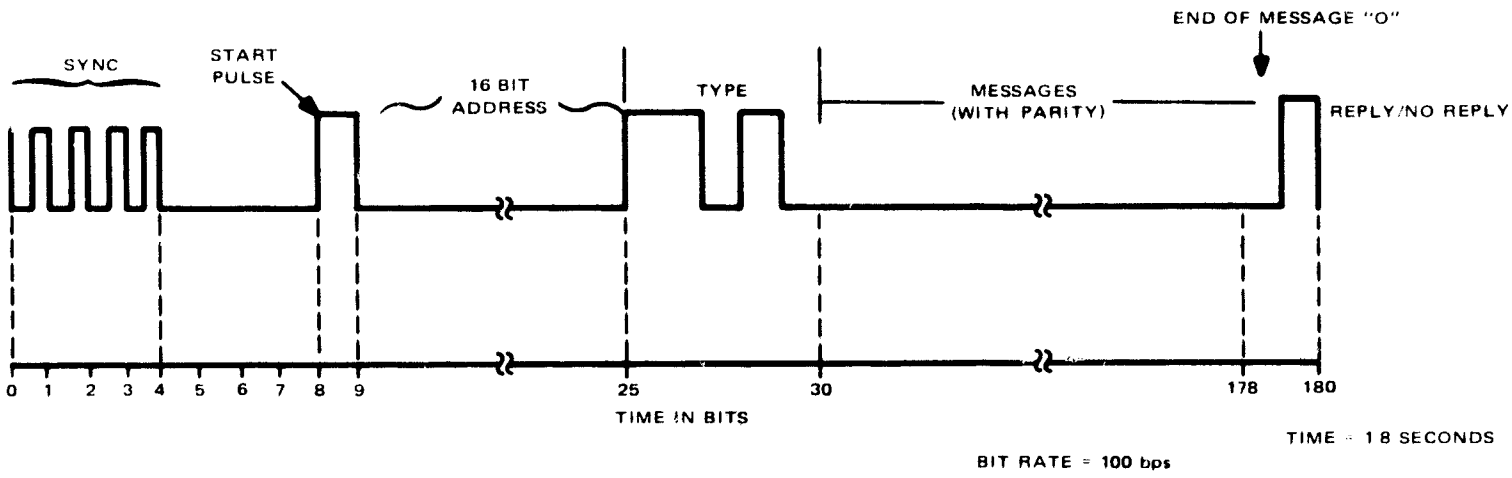

Figure 2-9. Typical ATC Data-Message Format

2.2.3.4 DIGITAL CODE MODULATION (BINOR)

The preceding section (2.2.3.3) was devoted to the discussion of a system using a CW carrier modulated by two sine wave tones for precise and unambiguous ranging; data communication was included by DCPSK modulation of the coarse tone. In the present section, we analyze a digital code technique for ranging which was developed by J. J. Stiffler[1] and discussed under the acronym BINOR by TRW.[2]

---

[1] J. J. Stiffler, "Block Coding and Synchronization Studies: Rapid Acquisition Sequences", JPL Space Programs Summary 37-42, Vol. IV, pp 191-197.

[2] A. Garabedian, "Range (Difference) Measurement Studies for a Navigation Satellite System", AIAA Paper #68-414, AIAA 2nd Communications Satellite Systems Conference, San Francisco, April 1968.

The BINOR code is generated from a series of N coherent, harmonically related square waves in which the period of the nth wave is twice the period of the (n-1)th wave. Usually, for ease of mechanization, N is chosen to be odd. The code is generated by the following rule: during each half-cycle of the "clock" frequency (which is the highest frequency wave in the series), the number of square waves in binary state "0"; are subtracted from the number of waves in binary state "1"; if the result is positive, the code is put in state "1", and if the result is negative, the code is put in state "0". This is illustrated in Fig. 2-10 for N=3. In general, for odd N, the code can be simply generated by basing the binary decision on the polarity of the sum of all square waves during each half-cycle of the clock frequency.

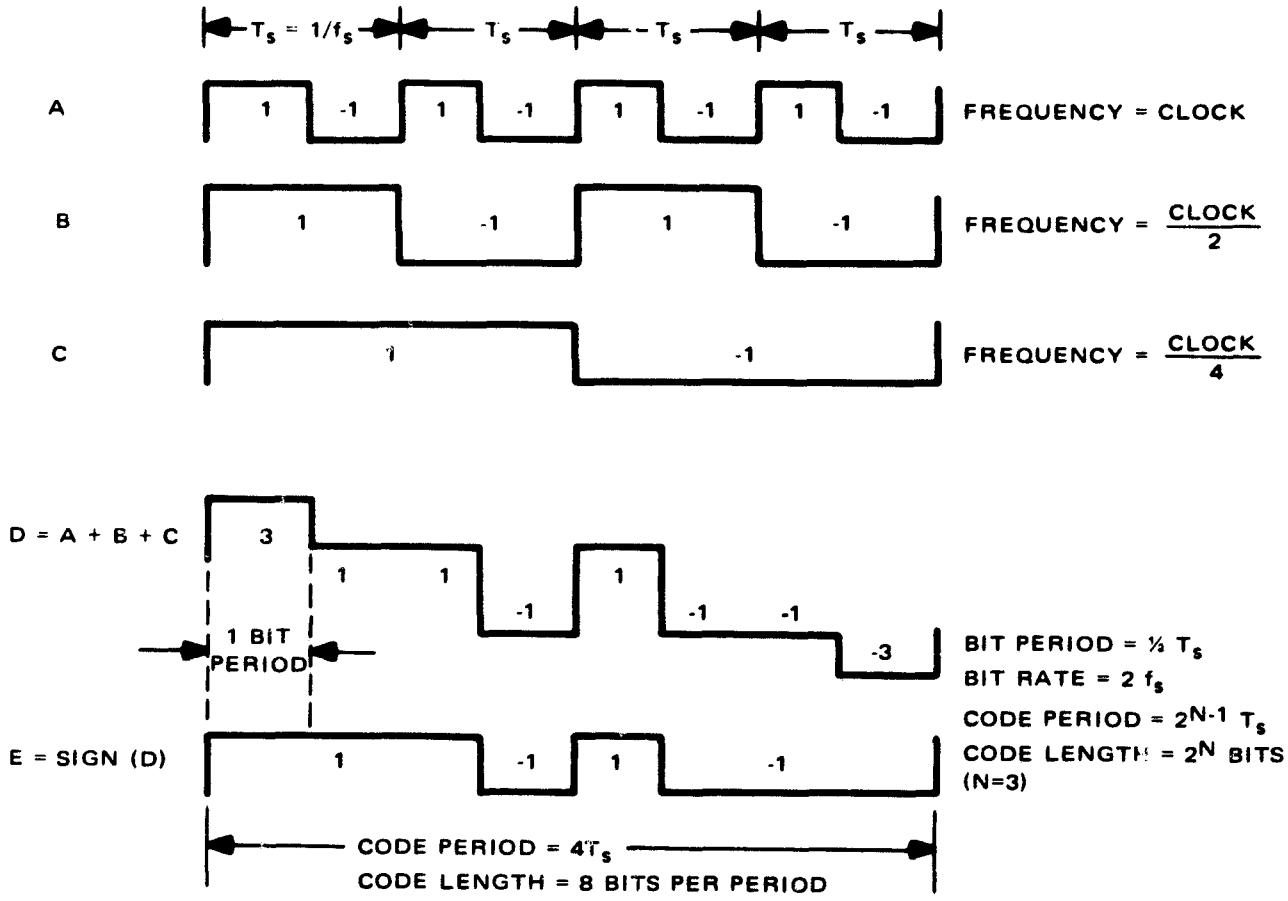

Figure 2-10. Formation of a BINOR Code Utilizing 3 Square Wave Trains

From the above discussion it follows that the code bit rate is $2f_s$ bits/sec, and the code period is equal to the period of the lowest frequency wave, i.e. $2^{(N-1)} \times T_s$ sec., where $T_s = 1/f_s$ is the period of the highest frequency wave, or the clock. The code length, that is number of bits per period, is 2^N bits.

The advantage of the BINOR code lies in its long period—which helps achieve unambiguous ranging over long distances—and its short acquistion time (compared to other codes with sequential acquisition schemes). As explained below, the acquisition time is the time required for carrying out N correlations. After acquisition, the phase information of the code is used to compute the range in a manner similar to that used for sine-wave ranging.

The acquisition process consists of (1) acquiring the "clock", by locking a free running oscillator to the "clock"; the procedure for doing this is identical to that of acquiring the fine tone in a 2-tone sine-wave modulation system and amounts to a correlation; and (2) making an additional set of (N-1) correlations between the incoming code signal and the (N-1) locally-generated square waves which are generated by a divide-by-two chain of flip-flops driven by the acquired clock. Thus a total of N correlations are needed in the acquisition process, requiring a total of N binary decisions to resolve the phase of a 2^N bit long code, which is the minimum number of decisions theoretically possible.

2.2.3.4.1 Description of the System Employing the BINOR Code

Required Number of Square-Wave Components - In the discussion of the two-tone sine wave modulation system, it was shown that a 16 to 1 ratio of fine tone (range resolution) to coarse-tone (lane ambiguity) would suffice if the fine-tone frequency is 8 KHz and the coarse-tone frequency is 500 Hz. This 16 to 1 ratio requires 5-square wave trains for a BINOR code. Therefore, the system to be analyzed will be derived from the following components:

A = an 8 kHz square wave train

B = a 4 kHz square-wave train

C = a 2 kHz square-wave train

D = a 1 kHz square-wave train

E = a 500-Hz square-wave train

Data Link Requirements - In order not to upset* the generation of the BINOR sequence by going to a 6^{th} square-wave with the data stream impressed on it, a separate sub-carrier will be utilized to bear the data information. This subcarrier will be modulated exactly like the coarse-tone in the 2-tone sine wave system discussed previously. The data-link message also will be identical to that of the above-mentioned system. In order to prevent excessive use of signal bandwidth, the subcarrier will be at a nominal frequency of 200 Hz. No carrier lock problems should arise because of false-lock on the sub-carrier, since the message will be balanced (equal number of marks and spaces) so

*An even number of square-wave trains result in a 3-level code. That is, the resultant amplitude is either positive, negative, or zero. The zero level introduces complicated logic and circuitry problems.

that either no discrete subcarrier component will be present, or the residual is very small (greater than 15 dB down from the carrier) if the circuitry does not phase shift the signals exactly 0° or 180°.

Modulation Index of Signal Components - The signal-to-noise ratio of the BINOR code is determined by the accuracy requirements of 1 nmi ground position error. As in the case of the 2-tone sine wave system (Section 2.2.3.3), this accuracy requires a S/N_0 of 17.3 dB-Hz on the fine tone, i.e. the highest frequency component of the modulation, which is the "clock" in the present case. Also, as shown in Appendix 2.2.3.3-C, the noise density about the fine tone is twice that about the carrier, so that the clock should really have a signal-to-noise density of 20.3 dB-Hz.

Now the clock S/N_0 is less than the code S/N_0 by the factor ρ^2, where ρ is the correlation coefficient between the clock and the code. For a code consisting of n square waves (n odd), Stiffler[1] has shown that

$$\rho = \frac{1}{2^{n-1}} \binom{n-1}{\frac{n-1}{2}}$$

Thus for n = 5, $\rho = 0.375$ and $\rho^2 = 0.141$ or -8.5 dB. Hence,

S/N_o clock = 20.3 dB-Hz

S/N_o code = 28.8 dB-Hz

The signal-to-noise densities for the carrier and the "coarse tone" (i.e. the lowest frequency wave in the code) are found from Appendix 2.2.3.3-C. Thus

C/N_o carrier = 27 dB-Hz (for C/N of 7 dB in 100 Hz reference[1] bandwidth)

S/N_o data = 29.5 dB-Hz (for E/N_0 of 8.9 dB in band $B = 1/\tau = 100$ Hz, with 0.6 dB allowance for degradation).

From Appendix 2.2.3.4-A, it is seen that the modulation index for the code, $B_C = 0.94$ while that for the data subcarrier, $B_D = 1.39$. The resulting normalized power levels are also derived in that appendix and are shown below:

Carrier, $P_C = -9.4$ dB
Code, $P_S = -7.6$ dB
Data, $P_D = -6.9$ dB

} Normalized with respect to the total RF power

[1] J.J. Stiffler, "Block Coding and Synchronization Studies: Rapid Acquisition Sequences", JPL Space Programs Summary 37-42, Vol. IV, pp 191-197.

[2] The 100 Hz bandwidth is nominal and represents the ideal case of no additional noise.

2.2.3.4.2 Link Calculation for the BINOR System

The parameters discussed above and those discussed in Section 2.2.3.2 (CW System Performance Parameters) are used to obtain the link analysis shown in Table 2-10. It is found from the table that satisfactory performance (as determined by the signal-to-noise criteria derived above) is obtained with the following RF powers and antenna gains, namely: 5W and 37 dB at the ground; 20 W and 2 dB at the user; and 20 W for the forward path and 10 W for the return path at the satellite, with an antenna gain of 16.5 dB in each direction.

TABLE 2-10. LINK CALCULATIONS FOR BINOR CODE MODULATION

Forward Path - Values for forward-path parameters are tabulated below:	
	Value
CONTROL CENTER	
Transmitter Power (5 W) (dBW)	7.0
Antenna coupling losses (dB)	1.5
Antenna gain (dB)	37.0
Rain and snow attenuation (dB)	0.2
Effective radiated power, ERP (dBW)	42.8
PROPAGATION	
Path loss (dB)	190.0
Atmosphere and ionosphere attenuation (dB)	0.5
SATELLITE	
Antenna gain (-3 db) (dB)	16.5
Antenna polarization loss (dB)	0.5
Antenna coupling loss (dB)	1.0
Received RF power (dB)	-133.2
SATELLITE NOISE POWER	
Receiver noise figure (dB)	5.0
Receiver noise temperature (°K)	809
Effective sun temperature (°K)	0
Total galactic noise temperature (°K)	2
Effective earth temperature (°K)	105
Total noise temperature (°K)	916
System noise figure (dB)	5.0

TABLE 2-10. LINK CALCULATIONS FOR BINOR CODE MODULATION (Cont.)

Forward Path - Values for forward-path parameters are tabulated below:

	Value
SATELLITE NOISE POWER (Cont.)	
Noise density (dBW/Hz)	-199.0
Satellite noise bandwidth (KHz)	100.0
Satellite noise power (dBW)	-149.0
RF power/noise (dB)	15.8
Transmitter power (20 W) (dBW)	13.0
Antenna coupling loss (dB)	1.0
Antenna gain (dB)	16.5
ERP (dBW)	28.5
Effective radiated noise, ERN, (dBW)	12.7
PROPAGATION	
Path loss (dB)	190.0
Atmospheric and ionospheric attenuation (dB)	0.5
USER	
Antenna gain (dB)	2.0
Antenna polarization loss (dB)	1.5
Antenna coupling loss (dB)	2.0
Received RF power (dB)	-163.5
USER NOISE POWER	
Receiver noise figure (dB)	5.0
Receiver noise temperature (°K)	1172
Total galactic noise temperature (°K)	2
Effective sun temperature (°K)	2
Total noise temperature (°K)	1172
System noise figure (dB)	6.1
Noise density (dBW/Hz)	-197.9
Received noise from satellite (dBW)	-179.3
Received noise density (dBW/Hz)	-229.3
Total noise density (dBW/Hz)	-197.9
Predetection noise bandwidth (kHz)	100.0

TABLE 2-10. LINK CALCULATIONS FOR BINOR CODE MODULATION (Cont.)

Forward Path - Values for forward-path parameters are tabulated below:

	Value
USER NOISE POWER (Cont.)	
Predetection noise power (dBW)	-147.9
RF power/noise (dB)	-15.6
Carrier/noise for P_C/RF Power = -9.4 dB (dB)	-25.0
Postdetection carrier noise bandwidth (Hz)	63
Reference carrier/noise (in 100-Hz bandwidth) (dB)	7.0
Code noise bandwidth (Hz)	10.0
Code signal/noise for P_S/RF power = -7.6 dB (dB)	16.8
Clock signal/noise (in 10 Hz bandwidth) for ρ = 0.375 (dB)	8.3
SELF-NAVIGATION MODE	
*Clock noise bandwidth (Hz)	1.0
Clock signal/noise (in 1 Hz bandwidth) (dB)	18.3

Return Path - Values for return-path parameters are tabulated below:

	Value
USER	
Transmitter power (20W) (dBW)	13.0
Antenna gain (dB)	2.0
Antenna coupling losses (dB)	2.0

*In active mode user tone-bandwidth is much larger (10-times) than control center clockbandwidth so that the integration time (reciprocal of the clockbandwidth) is predominantly determined by the control center. In the case where the user wants his position (either in the active or passive mode), the effective bandwidth of the user's navigation equipment is 1 Hz.

TABLE 2-10. LINK CALCULATIONS FOR BINOR CODE MODULATION (Cont.)

Return Path - Values for return-path parameters are tabulated below:	
	Value
USER (Cont.)	
ERP (dBW)	13.0
*Effective radiated noise density (dBW/Hz)	-21.4
PROPAGATION	
Path loss (dB)	190.0
Atmospheric and Ionospheric attenuation (dB)	0.5
SATELLITE	
Antenna gain (dB) (-3 dB beam edge)	16.5
Antenna polarization loss (dB)	1.5
Antenna coupling loss (dB)	1.0
Received RF power (dBW)	-163.0
SATELLITE NOISE POWER	
Noise density (same as forward path) (dBW/Hz)	-199.0
**Receiver noise density from user (dBW/Hz)	-197.4
Combined noise density (dBW/Hz)	-195.1
Effective noise power (dBW)	-149.0
Received RF power/noise dB)	-14.0
Transmitter power (10W) (dBW)	10.0
Antenna coupling losses (dB)	1.0
Antenna gain (dB) (-3 dB Beam edge)	16.5
ERP (dBW)	11.4
ERN (dBW)	25.4
PROPAGATION	
Path loss (dB)	190.0
Atmospheric and ionospheric attenuation (dB)	0.5

*Retransmitted noise in a 1 Hz bandwidth about the clock.

**Only affects the demodulated signal at the control center, since the noise is narrowbanded.

TABLE 2-10. LINK CALCULATIONS FOR BINOR CODE MODULATION (Cont.)

Return Path - Values for return-path parameters are tabulated below:

	Value
CONTROL CENTER	
Antenna gain (dB)	37.0
Antenna polarization loss (dB)	0.5
Antenna coupling loss (dB)	1.0
Received RF power (dBW)	-143.4
*CONTROL CENTER NOISE POWER	
System noise figure (dB)	3.3
System noise density (dBW/Hz)	-200.7
**Received noise density from satellite (dBW/Hz)	-175.5
Total noise density (dBW/Hz)	-175.5
RF Power/total noise density (dB-Hz)	32.1
Postdetection carrier noise bandwidth (Hz)	91
Reference carrier/noise (dB) (modulation loss = -9.4 dB)	7.0
***Clock noise bandwidth (Hz)	0.7
Clock signal/noise in 1 Hz bandwidth (dB) (ρ = 0.375)	17.3
EFFECT OF SUN	
Receiver noise figure (dB)	4.0
Receiver noise temperature (°K)	624
Solar noise temperature (°K)	3600
System noise density (dBW/Hz)	-192.4
Received noise density from satellite (dBW/Hz)	-175.5
Total noise density (dBW/Hz)	-175.5
Increase in noise due to sun (dB)	0.0
RF Power/Total Noise density (dB-Hz)	32.1
Demodulated carrier/noise (dB)	7.0
Clock signal/noise (dB)	17.3
Excess signal/noise (clock) (dB)	1.0

*This section excludes the effect of the control center antenna pointing directly at the sun which occurs at the spring and fall equinoxes for about a 7-day period with with the maximum duration during any one day about 8 minutes.

**This is the noise about the clock signal; the noise about the carrier is -179.4 dBW/Hz.

***In order to make comparisons with the sinewave modulation system (in Section 2.2.3.5) all the transmitter power levels for both systems are equal (at a specific location).

2.2.3.5 COMPARISON OF THE TWO CONTINUOUS-WAVE MODULATION SYSTEMS

In order to compare the "digital-code" system with the "sine-wave tones" system we will examine the critical parameters in the preceding link analyses. This will be done at the user location (for self-navigation) and at the ground control center (for air traffic control navigation). The critical parameters are shown in Table 2-11.

TABLE 2-11. COMPARISON OF SINE WAVE WITH SQUARE-WAVE MODULATION

Location	Parameter	(dB-Hz) Sine-Wave	(dB-Hz) Digital Code	(dB-Hz) Difference	Item No.
User	Total Power N_o	34.4	34.4	0.0	1
	Carrier N_o	28.5	25.0	3.5	2
	Fine Tone N_o (or clock)	22.3	18.3	4.0	3
	*Data Subcarrier/ N_o	31.2	27.5	3.7	4
Control Center	Total Power/N_o	36.0 (A) 32.1 (B)	36.0 (A) 32.1 (B)	0.0	5
	Carrier/N_o	30.1 (A)	26.6 (A)	3.5	6
	Fine Tone/N_o	20.0 (B)	16.0 (B)	4.0	7
	*Data Subcarrier/ N_o	32.8 (A)	29.1 (A)	3.7	8

NOTES: N_o is the noise spectral density.

A - the N_o is due only to the transmitted noise from the satellite.

B - the N_o is from both the user and the satellite.

* - In the case of the sine-wave this subcarrier is also the coarse tone.

We see from the table that for the same total-power to noise-spectral density in the two systems (as shown by item number 1 and 5), the system using sine wave tones achieves a higher signal to noise density ratio for all the other parameters (carrier fine-tone or clock as the case may be and the data subcarrier). In particular, the carrier to N_o (items 2 and 6) is 3.5 dB higher for the sine-wave system. If this "extra" 3.5 dB were to be converted into excess loop bandwidth over the code-modulation case the resulting bandwidth would be 2.25 times greater for the sine-wave case. Now, for moderate values of initial frequency offset Δf, Gardner[1] shows that the pull-in time, T_P,

[1] Floyd M. Gardner, "Phase Lock Techniques", John Wiley & Sons, 1966, page 46 formula (4-32)

of a 2nd order phase-locked loop, with the damping factor $\zeta = 0.707$, is given by:

$$T_p = 4.2 \frac{(\Delta f)^2}{B_L^3} \quad \text{(in seconds)}$$

Since the pull-in time is inversely proportional to the cube of the loop bandwidth B_L, the code-modulated system takes $(2.25)^3 = 11.4$ times longer than the sine-wave tone-modulated system to pull-in. It would not be practical to adjust the power levels in the various sideband components (code system) in order to bring up the power level of the carrier since this would cause further degradation of the clock signal and the data message error rate. Furthermore, if modulation lockup time were also considered the BINOR system would be further degraded since the square waves are locked up sequentially while the tones are locked up in parallel.

It is concluded from the above discussion that the sine-wave modulation is better than the BINOR code for equal RF powers at the user (or at the ground control center) because, with the optimum choice of modulation parameters in the two cases, the former results in higher signal-to-noise values and shorter acquisition time than the latter.

2.2.3.6 PROJECTION OF THE SINE-WAVE TONES SYSTEM TO 0.1 NMI GROUND POSITION ERROR

From Appendix 2.2.3.6-A we see that the signal to noise of the extra-fine tone (i.e. the 64 kHz tone) has to be at least 22.5 dB in order to meet the 0.1 nmi accuracy.

With the insertion of the 3rd tone the new modulation indices and the normalized power were determined by an iterative process and the results are shown in Table 2-12.

TABLE 2-12. SIGNAL PARAMETERS FOR 3-TONE (0.1 NMI) CASE

Parameter	Modulation Index	Normalized Power
Carrier	-	- 6.0 dB
Coarse Tone	1.25	- 5.0 dB
Fine Tone	0.50	-14.7 dB
Extra-Fine Tone	0.85	- 9.6 dB

The link analysis for the 0.1 nmi accuracy is shown in Table 2-13. It is to be noted that this system is fully compatible with the 1.0 nmi system. Users requiring an accuracy no better than 1 nmi need not demodulate the 3rd (extra-fine) tone.

We see in the link analysis that two minor changes need to be made to obtain the 0.1 nmi accuracy. They are:

1. A Control Center transmitter power increase of 3 dB, i.e. from 5 watts to 10 watts.
2. The satellite, user and control center predetection bandwidths must be increased by a factor of 2, i.e. increased to 200 kHz. This satellite bandwidth

will cause no degradation of the signals used for the 1.0 nmi ground accuracy so that this service will be unimpaired. Again, as in the previous link analysis (1.0 nmi accuracy) the effect of the increase in system noise temperature due to the sun (during the equinox periods) is negligible.

TABLE 2-13. POWER BUDGET - SAMPLE LINK CALCULATIONS (0.1 NMI ACCURACY)

Forward Path - Values for forward-path parameters are tabulated below:	
	Value
CONTROL CENTER	
Transmitter power (10W) (dBW)	10.0
Antenna coupling losses (dB)	1.5
Antenna gain (dB)	37.0
Rain and snow attenuation (dB)	0.2
Effective radiated power, ERP (dBW)	45.8
PROPAGATION	
Path loss (dB)	190.0
Atmosphere and ionosphere attenuation (dB)	0.5
SATELLITE	
Antenna gain (dB) (-3 dB)	16.5
Antenna polarization loss (dB)	0.5
Antenna coupling loss (dB)	1.0
Received RF power (dB)	-130.2
SATELLITE NOISE POWER	
Receiver noise figure (dB)	5.0
Receiver noise temperature (°K)	809.0
Effective sun temperature (°K)	0
Total galactic noise temperature (°K)	2
Effective earth temperature (°K)	105
Total noise temperature (°K)	916
System noise figure (dB)	5.0
Noise density (dBW/Hz)	-199.0
Satellite noise bandwidth (kHz)	200
Satellite noise power (dBW)	-146.0
RF power/noise (dB)	15.8
Transmitter power (20W) (dBW)	13.0
Antenna coupling loss (dB)	1.0
Antenna gain (dB)	16.5
ERP (dBW)	28.5
Effective radiated noise, ERN, (dBW)	12.7

TABLE 2-13. POWER BUDGET - SAMPLE LINK CALCULATIONS (0.1 NMI ACCURACY) (Cont.)

Forward Path - Values for forward-path parameters are tabulated below:

	Value
PROPAGATION	
Path loss (dB)	190.0
Atmospheric and ionospheric attenuation (dB)	0.5
USER	
Antenna gain (dB)	2.0
Antenna polarization loss (dB)	1.5
Antenna coupling loss (dB)	2.0
Received RF power (dB)	-163.5
USER NOISE POWER	
Receiver noise figure (dB)	5.0
Receiver noise temperature (°K)	1172
Total galactic noise temperature (°K)	2
Effective sun temperature (°K)	2
Total noise temperature (°K)	1176
System noise figure (dB)	6.1
Noise density (dBW/Hz)	-197.9
Received noise from satellite (dBW)	-179.3
Received noise density (dBW/Hz)	-229.3
Total noise density (dBW/Hz)	-197.9
Predetection noise bandwidth (KHz)	200
Predetection noise power (dBW)	-144.9
RF power/noise (dB)	- 18.6
Carrier/noise (Mod. Loss = 6.0 dB) (dB)	- 24.6
Post detection carrier noise bandwidth (Hz)	138
Reference carrier/noise (dB)	7.0
Tone noise bandwidth (Extra Fine) (Hz)	10.0
Tone signal/noise (Extra Fine) (dB) (Mod. Loss = 9.6 dB)	14.8
SELF-NAVIGATION MODE	
*Tone noise bandwidth (Extra-Fine) (Hz)	1.0
Tone signal/noise (dB)	24.8

*In active mode user tone-bandwidth is much larger (10-times) than control center tone-bandwidth so that the integration time (reciprocal of the tone-bandwidth) is predominantly determined by the control center. In the case where the user wants his position (either in the active or passive mode), the effective bandwidth of the user's navigation equipment is 1 Hz.

TABLE 2-13. POWER BUDGET - SAMPLE LINK CALCULATIONS (0.1 NMI ACCURACY) (Cont.)

Return Path - Values for return-path parameters are tabulated below:

	Value
USER	
Transmitter power (20W) (dBW)	13.0
Antenna gain (dB)	2.0
Antenna coupling losses (dB)	2.0
ERP (dBW)	13.0
*Effective radiated noise density (dBW/Hz)	- 21.4
PROPAGATION	
Path loss (dB)	190.0
Atmospheric and Ionospheric attenuation (dB)	0.5
SATELLITE	
Antenna gain (dB)	16.5
Antenna polarization loss (dB)	1.5
Antenna coupling loss (dB)	1.0
Received RF power (dBW)	-163.0
SATELLITE NOISE POWER	
Noise density (same as forward path) (dBW/Hz)	-199.0
**Received noise density from user (dBW/Hz)	-197.4
Combined noise density (dBW/Hz)	-195.1
Effective noise power (dBW/Hz)	-146.0
Received RF power/noise (dB)	- 17.0
Transmitter power (dBW) (10W)	10.0
Antenna coupling losses (dB)	1.0
Antenna gain (dB)	16.5
ERP (dBW)	8.4
ERN (dBW)	25.4

*Retransmitted noise in a ±1 Hz bandwidth about each tone.

**Only affects the demodulated signal at the control center since the noise is narrowbanded.

TABLE 2-13. POWER BUDGET - SAMPLE LINK CALCULATIONS (0.1 NMI ACCURACY) (Cont.)

Return Path - Values for return-path parameters are tabulated below:

	Value
PROPAGATION	
Path loss (dB)	190.0
Atmospheric & ionospheric attenuation (dB)	0.5
CONTROL CENTER	
Antenna gain (dB)	37.0
Antenna polarization loss (dB)	0.5
Antenna coupling loss (dB)	1.0
Received RF power (dBW)	-146.4
CONTROL CENTER NOISE POWER	
System noise figure (dB)	3.3
System noise density (dBW/Hz)	-200.0
*Received noise density from satellite (dBW/Hz)	-178.5
**Total noise density (dBW/Hz)	-178.5
RF Power/total noise density (dBW-Hz)	32.1
Post detection carrier noise bandwidth (Hz)	100
Reference carrier/noise (Mod. Loss = 6.0 dB) (dB)	7.0
Tone noise bandwidths (All) (Hz)	1.0
Tone signal/noise (Coarse) (Mod. Loss = 5.0 dB) (dB)	28.0
Tone signal/noise (Fine) (Mod. Loss = 14.7 dB) (dB)	17.4
Tone signal/noise (Ex. Fine) (Mod. Loss = 9.6 dB) (dB)	22.5

*This is the noise density about the fine tones, the noise density about the carrier is -179.4 dB.

**The increase in system noise due to the sun is negligible.

2.3 TIMING SEQUENCE FOR CW RANGING NAV/TC SYSTEM

2.3.1 SUMMARY DESCRIPTION

Figure 2-11 depicts a CW Range-Range Nav/TC system for North Atlantic coverage in the 1970's. As described in the introductory summary, the sequence of events leading to a user "position fix"* is initiated by a message sent from the ground control center (GCC) to a particular user via satellite A or B. The choice of satellite A or B is a computer decision based on user geometry for the purpose of minimizing the GDOP effect in the computation of the user's position "fix" as discussed in the section on error analysis for this system (Section 2.4.3.2). It can be made well before current fix time so as to avoid any transients that might otherwise occur if the satellite path to the user were changed when the fix was initiated.

When the user vehicle receives the GCC control message, it activates its transponder transmitter in order to transmit its identity, altitude data and the "turned around" ranging signal. The ranging signal is continuously available in this system configuration because the user receiver is phase-locked to the CW carrier at the beginning of the trip. A user equipment block diagram is given in Figure 2-12. It shows that ranging modulation is available continuously during a trip and can be transmitted back to the GCC immediately upon activation of the transmitter and programmer on the user.

The user data and ranging signal are then transmitted back through both satellites A and B to the GCC. The data message is transmitted simultaneously with the ranging signal by utilizing the low frequency tone as described in Section 2.2.3.3.

At the GCC the signals from satellites A and B are coherently demodulated and tracked after acquisition by the ground station receivers. The acquisition process will utilize either a doppler error elimination technique (implemented in the user equipment) or a user doppler "prediction" technique (calculated in GCC computer) to minimize the carrier frequency search time at the GCC. These techniques will be described in a later section.

From the demodulated ranging tones the user's position fix is calculated. This is followed by a user fix verification test which compares the calculated fix to an expected value based on previous fixes or initial user position information. Satisfactory acceptance of the user "fix" is followed by fix coordinate display and transmission of the fix to the user when required. Should the user fix fail the verification test, appropriate action is decided upon by the computer logic based on user traffic density, user priority and operational criteria, etc. Such action would be a decision to repeat the entire fix sequence immediately, as traffic allows, or wait until the next scheduled fix of the user in question.

---

* A "position fix" in the Active or Traffic Control mode requires that the user position be determined by a ground control center; this mode is more complicated than (and contains the capability of) the Passive or Navigation mode, in which the user determines his own position without sending this information to the control center. The present discussion relates to the Active mode.

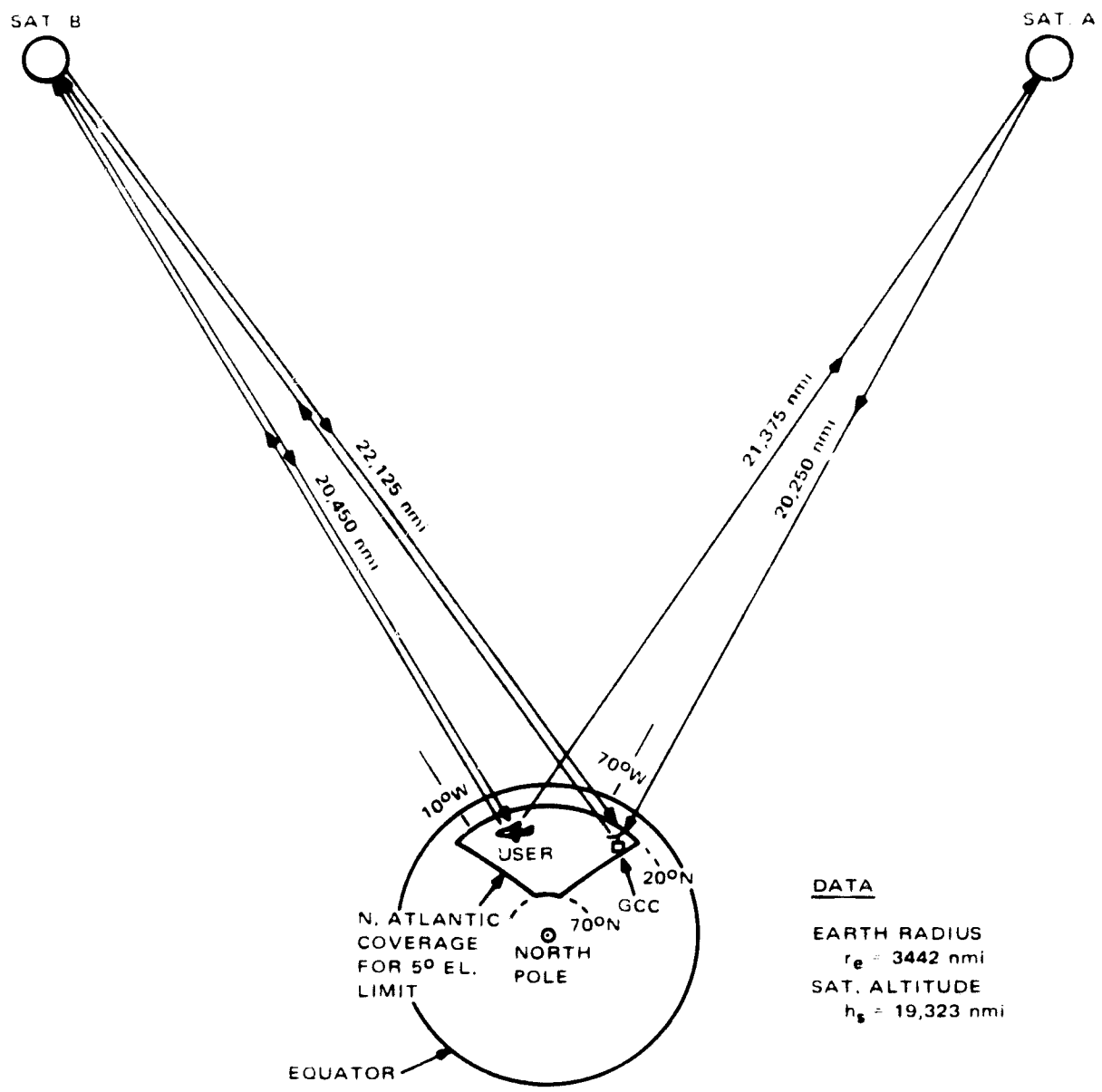

Figure 2-11. Range-Range Nav/TC System for North Atlantic

The following sections discuss the detailed timing sequence of operations for the CW Ranging Nav/TC System. Related discussions on the doppler correction technique and GCC user acquisition procedures are described as they occur in the sequence of events.

2.3.2 TIMING SEQUENCE CONSIDERATIONS (DATA MESSAGE AND TIMING FORMAT)

A typical data link message for traffic control consists of a synchronization signal, a start pulse, an address, a label (the first bit of which may indicate whether a fix is being made and thus activate the user's transmitter and programmer) a message, an end of message indication and a reply/no reply required indication. For the majority of traffic control transmissions from the GCC the data transmission would end with the indication to the user to return the required fix information. For others, however, such as sending the position fix coordinates to the user, additional message would be required. In these cases the user would not activate his transmitter until the end of the message and then only if a reply is requested.

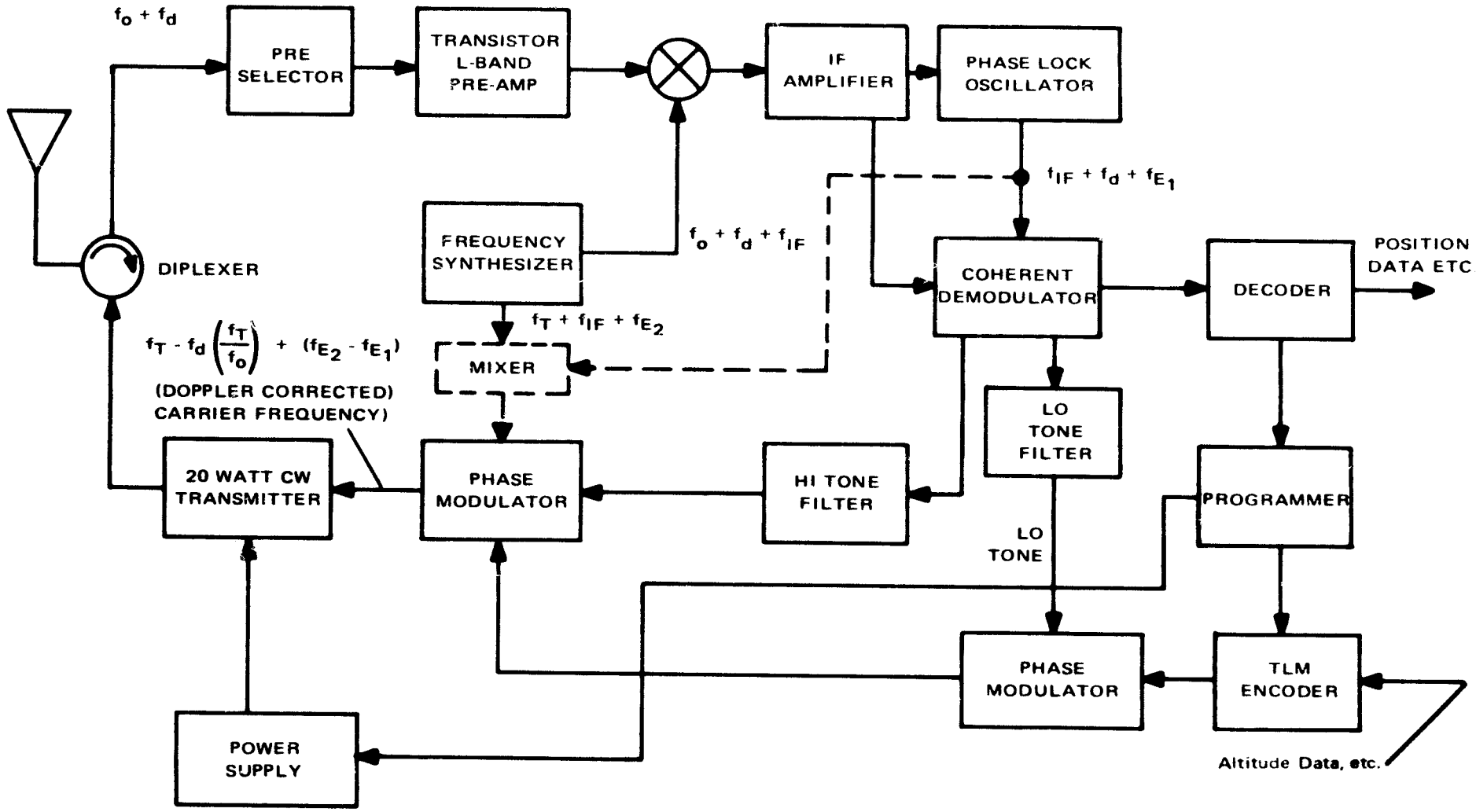

Figure 2-12. User Equipment Block Diagram

To illustrate a typical position fix timing sequence use will be made of the situation geometry indicated in Figure 2-11. The numbers involved are only intended to be representative and are therefore not limiting cases nor precisely determined values. The data message is assumed to be that of a GCC position fix interrogation of a user.

Figure 2-13 illustrates a user fix operational timing sequence. The space propagation time in seconds versus the total elapsed time in seconds illustrates the main time delays which occur in the system during a position fix determination. A more detailed breakdown of the user fix timing sequence is given in Table 2-14.

The sequence of events starts with the fix interrogation message for user N being encoded on the "coarse tone" ranging signal by means of a binary differentially coherent phase shift keying (PSK) technique described previously (section 2.2.3.3). The bit rate is 100 bps. The message duration of significance to the fix computation is indicated in Table 2-14 (0.2 second). Simultaneously, the space propagation time from GCC to satellite B is indicated at 0.137 seconds (22, 125 nmi at 161,000 nmi.sec). The satellite frequency shifts and repeats the message transmission to the user in 0.127 seconds for the illustrated geometry. The satellite repeater delay was estimated to be of the order of 3.5 μs and is therefore neglected as indicated in Table 2-14.

The initial transmitted message bit arrives at the user at 0.264 seconds and 0.2 seconds later the user (upon reception of the "activate-bit" of the "type" part of the transmission) activates the user programmer and transmitter. After a user activation delay of approximately 0.020 seconds the user transponds the ranging carrier and tones. The user encodes the "coarse tone" with his own sync, blank, start pulse, address, type and message containing his altitude, and other information including a request for the fix if he desired one (pre-set by user before fix).

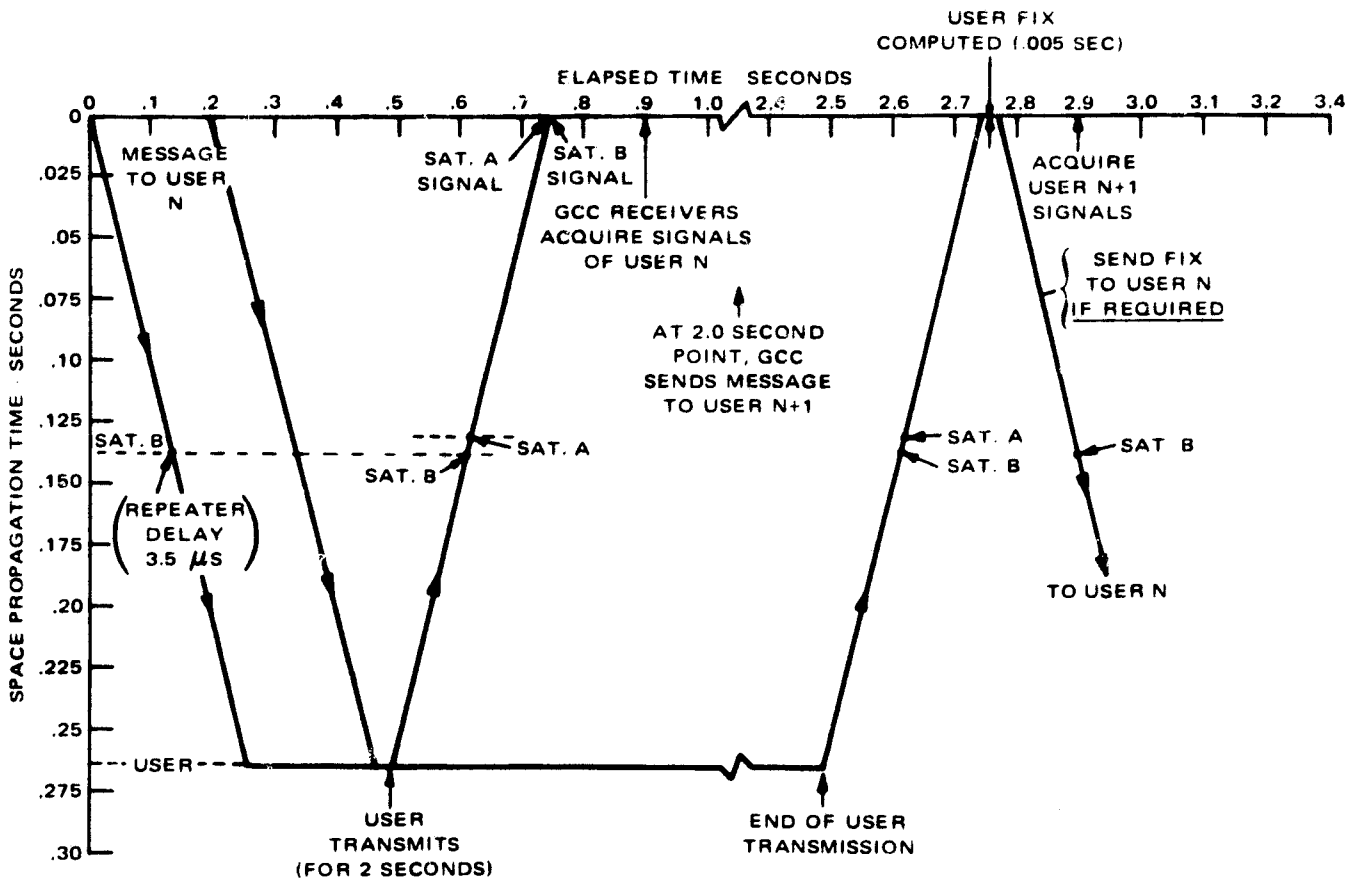

Figure 2-13. Illustration of User Fix Operational Timing Sequence

TABLE 2-14. ILLUSTRATION* OF USER FIX TIMING SEQUENCE

Item	Time (Sec.)		Elapsed Time (Sec.)
GCC Sends Fix Message to User N			
Data Message			
Sync	0.040		0.040
Blank	0.040		0.080
Start Pulse	0.010		0.090
User Address	.100		0.190
Type - Op. Diff. or Iter.	.010		0.200
Additional Type Bits	.040	May not be used for this type of transmission	
Message	1.480		
End of Message	.010		
Reply No Reply	.010		
Space Propagation			
GCC to Satellite B	0.137		0.337
Sat. Freq. Shift and Repeat	Neglect here and below (3.5 μs)		0.337
Sat. B to User	0.127		0.464
User Activation Delay	0.020		0.484
User Data Message and Ranging Signal			
Transpond Ranging Signal (incl. Data)			
Sync	0.040		
Blank	0.040		
Start Pulse	0.010		
User Address	0.100		
Type	0.050		
Messages (altitude, etc. requests)	1.480		
End of Message	0.010		
Reply No Reply	0.010		
Transpond Ranging Signals (includes data message above)	2.0		0.484
Space Propagation			
User to Satellite B	0.127		0.611
User to Satellite A	0.133		0.617
Satellite B to GCC	0.137		0.748
Satellite A to GCC	0.125		0.742
GCC Coherent Receiver Acquisition	0.15	(both signals)	0.900
GCC starts fix message to user N+1.	—		2.000
GCC Tracks Ranging Signals and Decodes User Message	1.85		2.750
GCC Computes User Fix	0.005		2.755
GCC Sends Fix to User N (If Required)			
GCC Acquires Signals from User N+1			2.900

*Based on a 100 B/S data rate and Geometry of Figure 2-11.

As noted in Figure 2-12 (by dashed lines), the user equipment may have a doppler correction feature to reduce the GCC acquisition time on the transponded ranging signal and user message. The technique will attempt to reduce the transponded carrier frequency by the incoming doppler offset. As noted in Figure 2-12, there will also be frequency offsets $f_{\epsilon 1}$ at the phase-locked oscillator and $f_{\epsilon 2}$ at the frequency synthesizer. The transmitted frequency will then be f_T (uncorrected) minus a frequency correction for doppler given as $(f_T/f_o)\, f_d$ and plus the difference of the offsets $(f_{\epsilon 2}-f_{\epsilon 1})$. It is expected that $(f_{\epsilon 2}-f_{\epsilon 1}) << (f_T/f_o)\, f_d$.

The user signal is then transmitted to both satellites A and B and repeated from each to the GCC. The GCC coherent receivers (one for each satellite signal) then acquire the user signals in an estimated time of 0.15 seconds.

This acquisition time estimate (which may be much greater if a frequency search mode is required if initial acquisition is not achieved during a specified interval) is based on the link analysis estimates (Section 2.2.3.3.2 of this volume) of a carrier-to-noise power ratio of 7 dB and a two-sided phase-locked loop (PLL) bandwidth ($2B_L$) of 200 hertz. The value of 0.15 seconds was estimated from published results (ref. 1,2)* based on a frequency offset of one half the loop noise bandwidth at the 7 dB signal-to-noise ratio.

The question of false-lock on the coarse or fine tones is not seen to be a serious problem. The coarse tone would appear as a noise-like signal with a sin x/x frequency spectrum characteristic offset by 500 hertz from the carrier. Even though the signal-to-noise level of the coarse tone may be greater than that of the carrier, the subtractive feature of the binary PSK message modulation reduces the effective SNR well below that of the carrier for acquisition purposes. Similarly the fine tone SNR is indicated to be well below (-10dB) that of carrier SNR and should cause no false-lock acquisition problem.

The assumption that the frequency offset will be within the PLL loop bandwidth is based on the use of the doppler correction technique, discussed above, or the use of a user doppler estimate computed from previous fixes and user geometry-flight plan information. In practice both techniques may be employed. It is also assumed in the above acquisition time estimate that any user frequency drifts may be calibrated out of the individual user's acquisition frequency estimate.

Should any unacceptable acquisition performance be indicated by simulation or actual development testing, use will be made of doppler filter banks for rapid carrier acquisitions. Such filter bank techniques are commonly used to locate a carrier frequency and designate the receiver to this frequency. The false-lock (false alarm) probability can be controlled by proper design for a given signal spectrum. Acqusition times well below 0.25 second are common for such filter banks especially if the doppler correction or user doppler estimate techniques discussed above are employed.

---

*1) D. Martin, Tech. Report No. 32-215, "The Pioneer IV Lunar Probe: A Minimum-Power FM/PM System Design," Jet Propulsion Laboratory, March 15, 1962.

2) R.W. Sannemann, J.R. Rowbotham, "Unlock Characteristics of the Optimum Type II Phase-Locked Loop," IEEE Trans. on Aerospace and Navigation Electronics, March 1964.

Following the acquisition of the user's transponded ranging signal the user message is decoded from the coarse tone and the GCC receiver coherently integrates the ranging phase signals for the remainder of the 2.0 second user transmission. The user altitude and estimates of phase are then sent to the GCC computer for computation of the user fix.

The fix may then be sent to the user if he has requested it, and be displayed as required, after successfully passing the fix verification test discussed earlier. Shortly after the fix is computed the GCC receivers acquire the next user's signals as indicated in Figure 2-13. These correspond to signals sent out about 0.9 seconds before the termination of user N's track. It can be seen from this illustration that one user fix each 2 seconds may be easily obtained for the CW ranging Nav/TC system illustrated.

2.4 ORBIT SYSTEM COVERAGE AND GDOP

2.4.1 SUMMARY

The ranging systems whose basic accuracies are described herein constitute one of the following:

1) Two satellite system. The range from navigator to each of the satellites is measured; these, together with altitude measurement, enable a position fix to be made. Lines of position are circular and the mode is passive.

2) Two satellite system for air traffic control; active mode. Range, range-sum, and altitude are measured. The lines of position are a circle and an ellipse, intersecting on the sphere of the user's Earth central distance.

3) Range difference - altitude system, requiring the use of at least three satellites, simultaneously in view. The system can be used in either passive or active mode.

Ranging may be accomplished either by the phase difference technique or by pulse timing. Error equations are developed for the circle-elliptic active mode. For a user latitude between 20°N and 70°N, and for 60° satellite spacing at synchronous altitude, it is determined that an rms surface position accuracy of 1 nmi can be obtained for the following parameters and source accuracies:

Carrier frequency	1.6 GHz
Fine tone frequency	8 kHz
Phase indicator resolution error	$1\sigma = 2°$
Signal noise and multipath error	$1\sigma = 5°$
ϵ RMS Error,	$1\sigma = 5.4°$

A .1 nmi accuracy can be achieved by means of a 64 kHz fine tone frequency. For a global system, in which three orthogonal orbits are used (one equatorial and two polar) for complete worldwide coverage, a hyperbolic (range-difference) mode of navigation provides 30% better accuracy than in the circular (range) mode. A "Y" orbit configuration, however, gives particularly bad GDOP's, resulting in coefficients greater than 14 at higher user latitudes.(1) Thus, circular orbits are preferrable for a precision Nav/TC global system.

2.4.2 ERROR SENSITIVITY EQUATIONS

In Figure 2-14, it will be assumed that the central distance from Earth center to navigator (possibly airborne) is at least approximately known; that is,

$$R_N \approx R_E + h$$

where R_E is the local Earth radius, a function of geodetic latitude, and his measured geodetic height above Earth surface. The ranges r_1, r_2 to two synchronous equatorial satellites are measured. Two equations in the unknown navigator (geocentric) latitude (ϕ) and longitude (λ) can be written:

$$R_s^2 + R_n^2 - r_1^2 = 2 R_n R_s \cos \phi \cos (\lambda - \lambda_1) = K_1 \qquad (1)$$

$$R_S^2 = R_N^2 - r_2^2 = 2 R_N R_S \cos \phi \cos (\lambda_2 - \lambda) = K_2 \qquad (2)$$

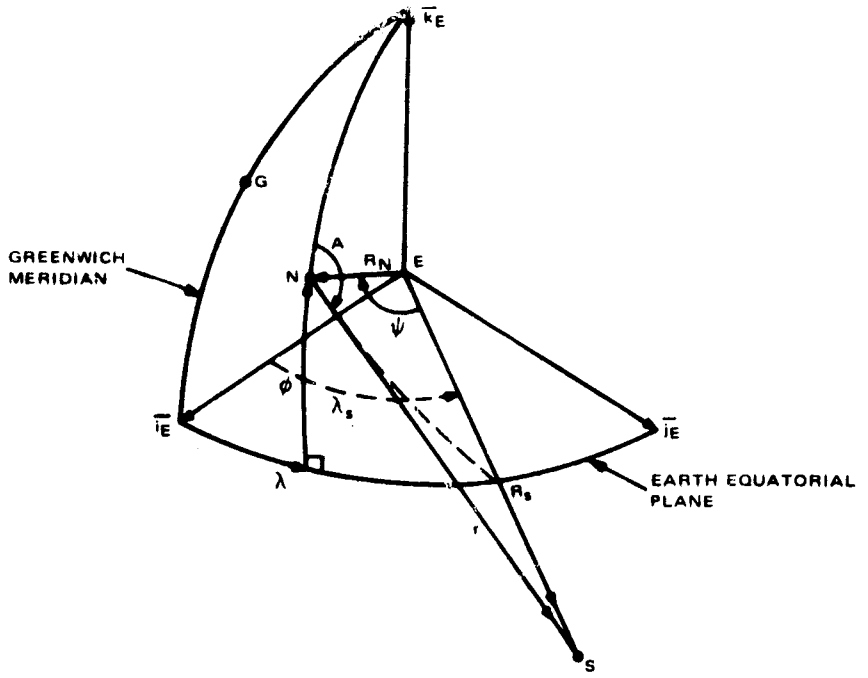

Figure 2-14. Navigator-Satellite Space Geometry

(1) Aerospace Corporation, Report No. TOR-0158 (3525-14)-1 "Parametric Summary - Influences of Synchronous, Inclined Elliptical Oribts on Performance of a Satellite Navigation System," Contract No. F04695-67-C-0158, 20 Dec. 1967.

wherein $\lambda_2 > \lambda > \lambda_1$, measured positive eastward from Greenwich meridian. Solving for ϕ and λ,

$$\phi = \cos^{-1} \sqrt{\frac{K_1^2 - 2K_1K_2\cos(\lambda_2 - \lambda_1) + K_2^2}{\left[2R_sR_N\sin(\lambda - \lambda_1)\right]^2}} \tag{3}$$

$$\lambda = \tan^{-1}\left[\frac{K_1\cos\lambda_2 - K_2\cos\lambda_1}{K_2 s_i \quad \lambda_1 - K_1\sin\lambda_2}\right] \tag{4}$$

No ambiguity exists in the use of eq. 3, if the user knows in which Hemisphere he is located. A refinement is made, through iteration, to obtain a more accurate value of $R_E(\emptyset)$ and thence a precise value of geodetic latitude.

Sensitivities to errors in the range and altitude measurements (and to errors in knowledge of the satellite positions) are most expeditiously found by taking total differentials of eq's. 1 and 2, solving simultaneously for $d\emptyset$ and $d\lambda$, and then identifying partials. Neglecting ephemeris errors, the required partials are

$$\frac{\partial\phi}{\partial 1} = \frac{r_1\sin(\lambda_2 - \lambda)}{R_sR_N\sin \quad \sin(\lambda_2 - \lambda_1)} \tag{5}$$

$$\frac{\partial\phi}{\partial_{\ 2}} = \frac{r_2\sin(\lambda - \lambda_1)}{R_sR_N\sin\phi\sin(\lambda_2 - \lambda_1)} \tag{6}$$

$$\frac{\partial\phi}{\partial R_N} = \frac{R_s\sin(\lambda_2 - \lambda_1)\cos\phi - R_N\left[\sin(\lambda - \lambda_1) + \sin(\lambda_2 - \lambda)\right]}{R_sR_N\sin\phi\sin(\lambda_2 - \lambda_1)} \tag{7}$$

$$\frac{\partial\lambda}{\partial r_1} = \frac{r_1\cos(\lambda_2 - \lambda)}{R_sR_N\cos\phi\sin(\lambda_2 - \lambda_1)} \tag{8}$$

$$\frac{\partial\lambda}{\partial r_2} = \frac{-r_2\cos(\lambda - \lambda_1)}{R_sR_N\cos\phi\sin(\lambda_2 - \lambda_1)} \tag{9}$$

$$\frac{\partial\lambda}{\partial R_N} = \frac{R_N\left[\cos(\lambda - \lambda_1) - \cos(\lambda_2 - \lambda)\right]}{R_sR_N\cos\phi\sin(\lambda_2 - \lambda_1)} \tag{10}$$

The square value of the error in the determination of horizontal position, in terms of measurement errors only, is

$$\epsilon^2 = R_N^2\left[\Delta\phi^2 + \Delta\lambda^2\cos^2\phi\right]$$

$$= R_N^2\left[\left(\frac{\partial\phi}{\partial r_1}\right)\Delta r_1 + \left(\frac{\partial\phi}{\partial r_2}\right)\Delta r_2 + \left(\frac{\partial\phi}{\partial R_N}\right)\Delta R_N\right]^2$$

$$+R_N^2\cos^2\phi\left[\left(\frac{\partial\lambda}{\partial r_1}\right)\Delta r_1 + \left(\frac{\partial\lambda}{\partial r_2}\right)\Delta r_2 + \left(\frac{\partial\lambda}{\partial R_N}\right)\Delta R_N\right]^2 \qquad (11)$$

Since the altitude measurement is independent of the range measurements, the mean square error is given by

$$\overline{\epsilon^2} = R_N^2\left[\left(\frac{\partial\phi}{\partial r_1}\right)^2 + \left(\frac{\partial\lambda}{\partial r_1}\right)^2\cos^2\phi\right]\overline{\Delta r_1^2}$$

$$+R_N^2\left[\left(\frac{\partial\phi}{\partial r_2}\right)^2 + \left(\frac{\partial\lambda}{\partial r_2}\right)^2\cos^2\phi\right]\overline{\Delta r_2^2}$$

$$+2R_N^2\left[\left(\frac{\partial\phi}{\partial r_1}\right)\left(\frac{\partial\phi}{\partial r_2}\right) + \left(\frac{\partial\lambda}{\partial r_1}\right)\left(\frac{\partial\lambda}{\partial r_2}\right)\cos^2\phi\right]\overline{\Delta r_1\Delta r_2}$$

$$+R_N^2\left[\left(\frac{\partial\phi}{\partial R_N}\right)^2 + \left(\frac{\partial\lambda}{\partial R_N}\right)^2\cos^2\phi\right]\overline{\Delta R_N^2} \qquad (12)$$

Note that the correlation of the range errors may be non-zero.

It is evident from inspection of the error sensitivities that the smallest position error occurs for a satellite spacing of 90°. Also, the latitude error becomes extremely large as the latitude approaches zero. The cos ϕ effect, in the denominators of the longitude partials, is cancelled in obtaining the east-west component of horizontal error; see eq. 11.

It is enlightening to re-cast the error sensitivities in terms of elevation and azimuth angles of the range lines, measured at the navigator's position. From Figure 2-14

$$\left.\begin{aligned}\sin(\lambda_1 - \lambda) &= \sin A_1 \sin\Psi_1\\ \cos(\lambda_1 - \lambda) &= \sec\phi\cos\Psi_1\end{aligned}\right\}$$

$$\left.\begin{aligned} \sin(\lambda_2 - \lambda) &= \sin A_2 \sin\psi_2 \\ \cos(\lambda_2 - \lambda) &= \sec\phi \cos\psi_2 \end{aligned}\right\}$$

whence

$$\sin(\lambda_2 - \lambda) \sin\phi = \sin\psi_1 \sin\psi_2 \sin(A_1 - A_2)$$

also,

$$\tan\phi = -\cos A_1 \tan\psi = -\cos A_2 \tan\psi_2$$

Finally, from Figure 2-15,

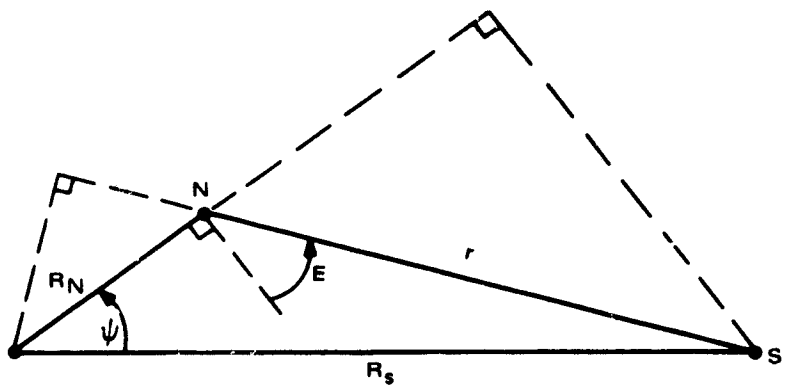

Figure 2-15. Navigator-Satellite Plane Geometry

$$\frac{r_1}{R_s} = \frac{\sin\psi_1}{\cos E_1} \; ; \; \frac{r_2}{R_s} = \frac{\sin\psi_2}{\cos E_2}$$

and

$$\frac{R_N}{R_s} = \frac{\cos(E_1 + \psi_1)}{\cos E_1} = \frac{\cos(E_2 + \psi_2)}{\cos E_2}$$

Making use of the above expressions in eq's. 5 through 10, we obtain

$$R_N \frac{\partial \phi}{\partial r_1} = \frac{\sin A_2}{\cos E_1 \sin (A_1 - A_2)} \tag{13}$$

$$R_N \frac{\partial \phi}{\partial r_2} = \frac{-\sin A_1}{\cos E_2 \sin (A_1 - A_2)} \tag{14}$$

$$R_N \frac{\partial \phi}{\partial R_N} = \frac{\sin A_2 \tan E_1 - \sin A_1 \tan E_2}{\sin (A_1 - A_2)} \tag{15}$$

$$R_N \cos\phi \frac{\partial \lambda}{\partial r_1} = \frac{-\cos A_2}{\cos E_1 \sin (A_1 - A_2)} \tag{16}$$

$$R_N \cos\phi \frac{\partial \lambda}{\partial r_2} = \frac{\cos A_1}{\cos E_1 \sin (A_1 - A_2)} \tag{17}$$

$$R_N \cos\phi \frac{\partial \lambda}{\partial R_N} = \frac{-\cos A_2 \tan E_1 + \cos A_1 \tan E_2}{\sin (A_1 - A_2)} \tag{18}$$

If the lines of position defined by the range measurements are circular, and Δr_1, Δr_2 are essentially independent, i.e., $\overline{\Delta r_1 \Delta r_2} = 0$. Insertion of eq's. 12 through 17 in eq. 12 then gives, for the circle-circle mode (applicable to the passive navigator):

$$\sin^2 (A_1 - A_2) \overline{\epsilon^2} = \frac{\sigma^2 (\Delta r_1)}{\cos^2 E_1} + \frac{\sigma^2 (\Delta r_2)}{\cos^2 E_2} + \sigma^2 (\Delta R_N) \left[\begin{array}{l} \tan^2 E_1 + \tan^2 E_2 \\ \\ -2 \tan E_1 \tan E_2 \cos (A_1 - A_2) \end{array} \right] \tag{19}$$

Significantly, both range and altitude error effects are severe as elevation angles approach 90°. A geometric interpretation of these effects is shown in Figure 2-16.

For simulation purposes, it can be shown that E and A are given in terms of latitude and longitude by the following:

$$\tan E_1 = - \frac{\cos\phi \sin A_1}{\tan (\lambda - \lambda_1)} + \frac{R_N}{R_s} \frac{\sin A_1}{\sin (\lambda - \lambda_1)}$$

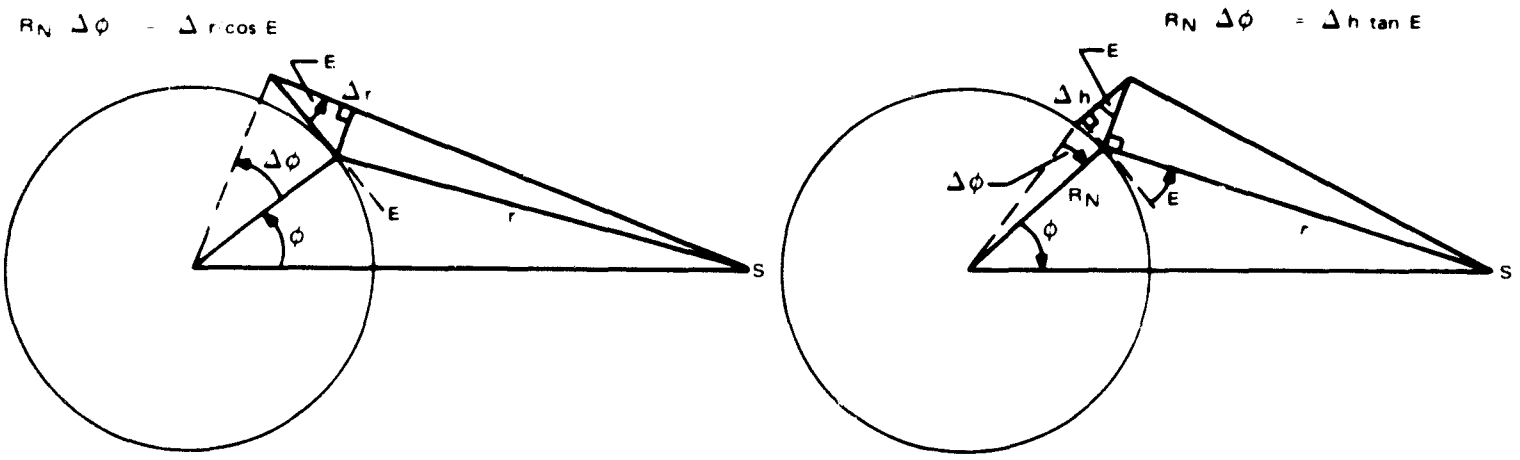

Figure 2-16. Range Error and Altitude Error Effects-Geometric Interpretation

where A_1 is given by

$$\tan A_1 = \tan (\lambda - \lambda_1)/\sin \phi$$

E_2 and A_2 are given by like expressions, subscript $1 \rightarrow 2$.

Now consider Figure 2-17. For the passive user, the signal transmitted by the ground control center to two satellites is received, after transponding by the satellites, at different times by the navigator. Thus, for a pulse-ranging system,

$$t_1 - t_o = \frac{D_1 + r_1}{c} \; ; \; t_2 - t_o = \frac{D_2 + r_2}{c}$$

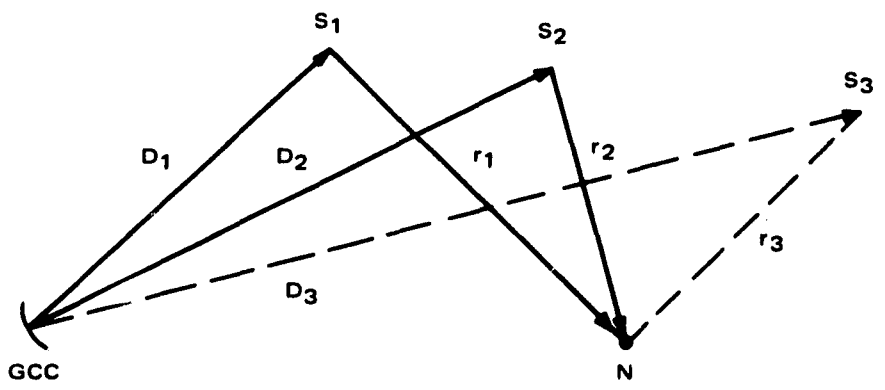

Figure 2-17. Passive Ranging from Satellites

where c = speed of light and t_0 = time of original transmitted pulse. The lines of position of intersecting arcs are circles and

$$c \cdot \sigma(\Delta t_1) = \sigma(\Delta r_1) \; ; \; c \cdot \sigma(\Delta t_2) = \sigma(\Delta r_2)$$

If a timing difference is measured,

$$t_1 - t_2 = \frac{(D_1 - D_2) + (r_1 - r_2)}{c}$$

so that $c^2 \cdot \sigma^2 \left[\Delta(t_1 - t_2) \right] = \sigma^2(\Delta r_1) + \sigma^2(\Delta r_2)$; that is, the time-difference measurement is essentially 41% larger in error than that for the single range measurement error, considering noise type errors only. Of course, another satellite must be used, giving an additional time-difference; thus two hyperbolic lines of position are defined, intersecting on the sphere defined by an altitude measurement. Evidently, $\sigma\left[\Delta(t_1 - t_3)\right] = \sigma\left[\Delta(t_1 - t_2)\right]$.

For traffic control usage, Figure 2-18, the ground station transmits to satellite 1, which transponds to the navigator; the navigator re-transmits to satellites 1 and 2 (and No. 3 for range-difference measurements) and thence the signals are transponded to the ground station for processing. We have

$$t_1 - t_o = \frac{2(D_1 + r_1)}{c} \; ; \; t_2 - t_o = \frac{D_1 + r_1 + D_2 + r_2}{c} \; ; \; t_3 - t_o = \frac{D_1 + r_1 + D_3 + r_3}{c}$$

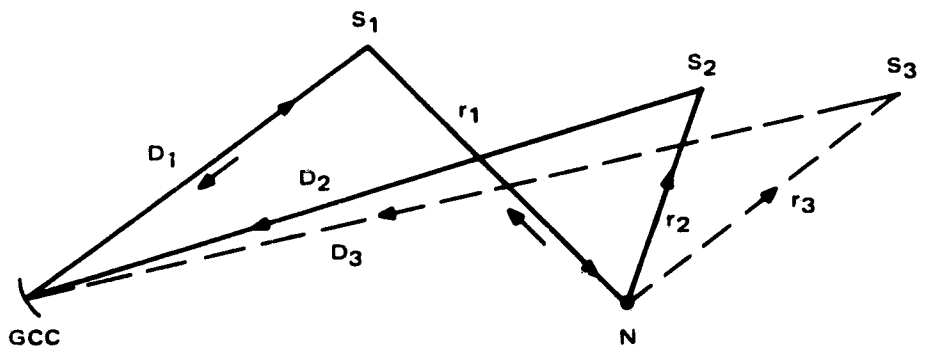

Figure 2-18. Traffic-Control Mode of Ranging

Solving the first two equations for r_1 and r_2,

$$r_1 = \frac{c}{2}(t_1 - t_o) - D_1 \; ; \; r_2 = \frac{c}{2}\left[2(t_2 - t_o) - (t_1 - t_o)\right] - D_2$$

Thus

$$\sigma^2(\Delta r_2) = c^2 \cdot \sigma^2(\Delta t_2) + \frac{c^2}{4}\sigma^2(\Delta t_1)$$

if Δt_1 and Δt_2 are considered independent random errors.

Insofar as noise is concerned, the error is proportional to the square of range; that is

$$\sigma(\Delta t_1) \sim (D_1 + r_1)^2$$

$$\sigma(\Delta t_2) \sim (D_1 + r_1)\,(D_2 + r_2) = \sigma(\Delta t_1) \cdot \frac{(D_2 + r_2)}{(D_1 + r_1)} \approx \sigma(\Delta t_1)$$

Thus

$$\sigma^2(\Delta r_2) = \frac{5}{4} c^2 \cdot \sigma^2(\Delta t_1) = 5\sigma^2(\Delta r_1) \qquad (20)$$

Note, also, that

$$\overline{\Delta r_1 \Delta r_2} = -\frac{c^2}{4}\sigma^2(\Delta t_1) = -\sigma^2(\Delta r_1) \qquad (21)$$

For the active hyperbolic mode,

$$t_1 - t_2 = \frac{D_1 - D_2 + r_1 - r_2}{c}; \; t_2 - t_3 = \frac{D_2 - D_3 + r_2 - r_3}{c}$$

Whence

$$\sigma^2\left[\Delta(t_1 - t_2)\right] = \sigma^2(\Delta r_1) + \sigma^2(\Delta r_2)$$

$$\sigma^2\left[\Delta\, t_2 - t_3)\right] = \sigma^2(\Delta r_2) + \sigma^2(\Delta r_3)$$

precisely the same as for the passive hyperbolic mode.

Let

$$\overline{\epsilon^2} = \overline{\epsilon_r^2} + \overline{\epsilon_h^2} = C_r^2 \sigma^2(\Delta r) + C_h^2 \sigma^2(\Delta R_N) \qquad (22)$$

Inserting relations 20 and 21 into eq. 12, the following are identified, applicable to the circular-elliptical mode (range, range-sum measurements) for the assumptions made regarding range-error correlation:

$$R_s^2 \sin^2(\lambda_2 - \lambda_1)\, C_r^2 = r_1^2 \left[\sin^2(\lambda_2 - \lambda) \csc^2\phi + \cos^2(\lambda_2 - \lambda)\right]$$
$$+ 5r_2^2 \left[\sin^2(\lambda - \lambda_1) \csc^2\phi + \cos^2(\lambda - \lambda_1)\right]$$
$$+ 2r_1 r_2 \left[\cos(\lambda_2 - \lambda) \cos(\lambda - \lambda_1) - \sin(\lambda_2 - \lambda) \sin(\lambda - \lambda_1) \csc^2\phi\right] \quad (23)$$

$$R_s^2 \sin^2(\lambda_2 - \lambda_1)\, C_h^2 = R_N^2 \left[\cos(\lambda - \lambda_1) - \cos(\lambda_2 - \lambda)\right]^2$$
$$+ \csc^2\phi \left[R_s \sin(\lambda_2 - \lambda) \cos\phi - R_N \sin(\lambda - \lambda_1) - R_N \sin(\lambda_2 - \lambda)\right]^2 \quad (24)$$

In the above, C_r is the sensitivity of horizontal error to range measurement error; C_h is the sensitivity to both altitude measurement error and imprecise knowledge of the Earth's shape, that is, the deviation of the true local Earth radius from the reference ellipsoid value. The equation for R_E is taken as

$$R_E = a_E \left[1 - \frac{\ell_E^2}{2} \sin^2\phi\right]$$

where

$$a_E = 3440\, n_1 \text{ miles}$$

$$\ell_E^2 = .006723$$

2.4.3 NUMERICAL EVALUATION

Coverage - In Figure 2-19, assume that a minimum elevation angle E_{lim} is assigned, so that refraction errors in range measurements do not become excessive. A navigator anywhere on the surface of the Earth spherical sector defined by the angle ψ will have a line-of-sight elevation angle greater than E_{lim}.

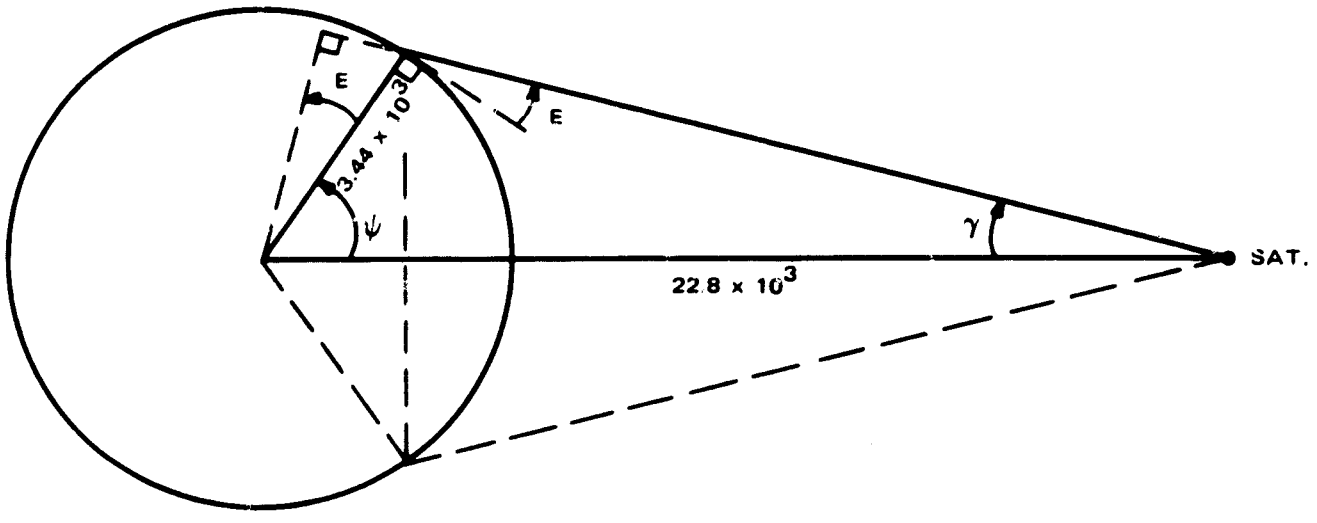

Figure 2-19. Satellite Limit of Visibility, Single Satellite

ψ is given by

$$\psi = \cos^{-1}\left(\frac{R_N \cos E_{lim}}{R_s}\right) - E_{lim} \tag{25}$$

For $E_{lim} = 5°$, $\psi = 76.4°$; for $E_{lim} = 10°$, $\psi = 71.4°$.

Denote $\lambda_{1-2} = \lambda_1 - \lambda_2$ as the longitude spacing of two equatorial satellites. The limiting range circles, from each satellite, intersect at a limiting latitude ϕ_{lim}; from Figure 2-20,

$$\phi_{lim} = \cos^{-1}\left[\cos\psi \sec\left(\frac{\lambda_{1-2}}{2}\right)\right] \tag{26}$$

For $\lambda_{1-2} = 60°$ and $E_{lim} = 5°$, $\phi_{lim} = 74.2°$; for $\lambda_{1-2} = 60°$ and $E_{lim} = 10°$, $\phi_{lim} = 68.5°$. Of interest is the longitude coverage, that is, the extent of navigator longitudes, at a specified latitude, such that the navigator can simultaneously view both satellites, subject to the elevation constraint. From Figure 2-21, this coverage is given by

$$\Delta L = 2\theta' - \lambda_{1-2} \tag{27}$$

where

$$\theta' = \cos^{-1}[\cos\psi \sec\phi] \tag{28}$$

The longitude limits, at ϕ, are then

$$L_{1,2} = \frac{(\lambda_1 + \lambda_2)}{2} \pm \frac{\Delta L}{2} \tag{29}$$

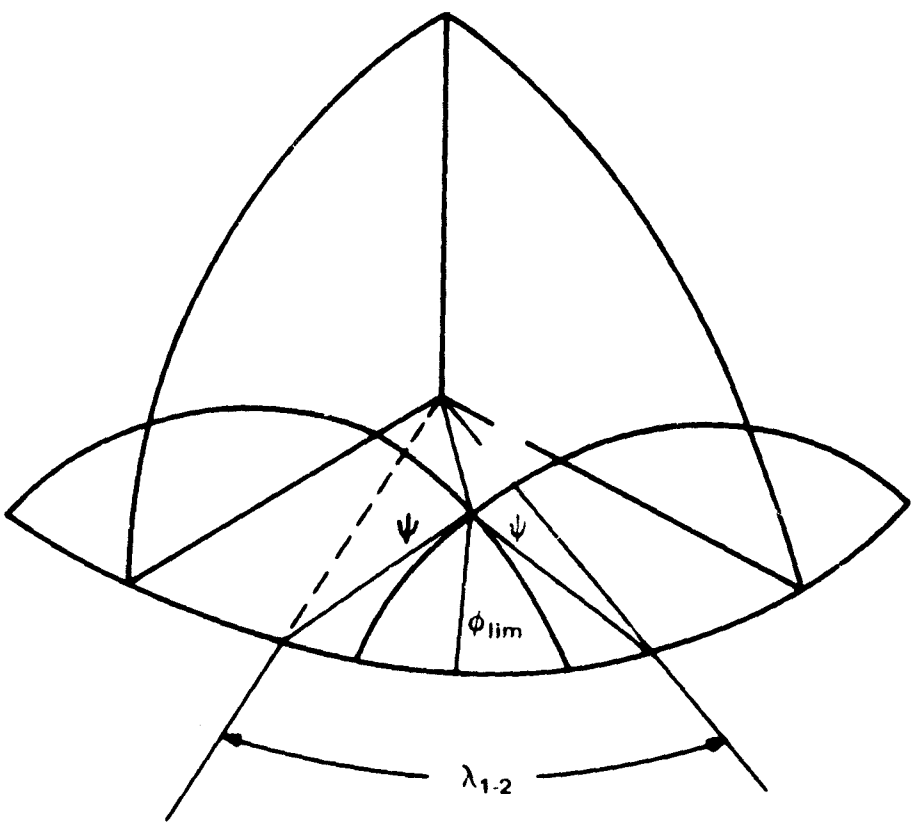

Figure 2-20. Navigator Position Limit for Simultaneous Viewing of Two Equatorial Satellites

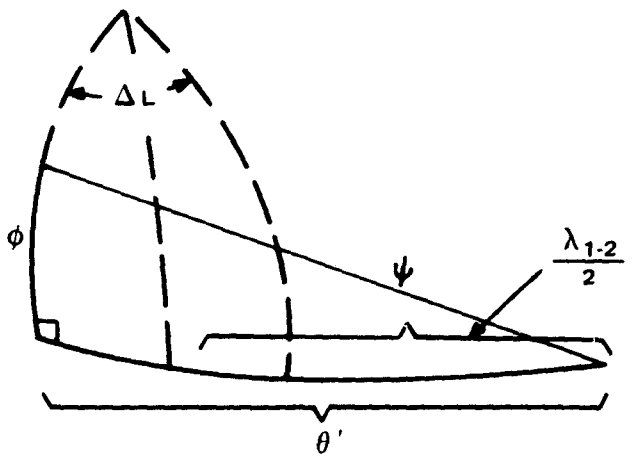

Figure 2-21. Navigator Longitude Limits for Simultaneous Viewing of Two Equatorial Satellites

Longitude limits are tabulated below, for $\lambda_1 = 10°$ W, $\lambda_2 = 70°$ W, and for $\phi = 20°$, $\phi = 70°$:

E_{lim}	ϕ	L_1	L_2
5°	20	5.5° E (Niger, North Africa)	85.5° W (Gulf of Mexico)
	70	23.1° W (Denmark Strait, Greenland)	56.9° W (Davis Strait, Canada)
10°	20	.2° E (Mali, North Africa)	80.2° W (Cuba)
	65	28.7° W (Denmark Strait, Greenland)	51.3° W (Davis Strait, Canada)

Error Results - Figures 2-22 and 2-23 give C_r and C_h, in miles/mile, for 60° satellite spacing, and for user latitudes of 20° N and 70° N; the error coefficients were calculated from eq.'s 23 and 24. Evidently, since the choice of designation of λ_1 or λ_2 is arbitrary, satellite 1 (double transmission) should be designated as that which is closer in longitude to the user's longitude. The curves reflect this transition at the midpoint longitude. Since the specified 1 nmi accuracy must be met at extreme points, the major concern is with coefficient values at 20° user latitude. Thus, for the circular-elliptic active mode, the following results obtain, noting that the factors given are not GD error but rather are error factors for the particular system.

E_{lim}	C_r	C_h
5°	4.8	1.25
10°	4.3	.95

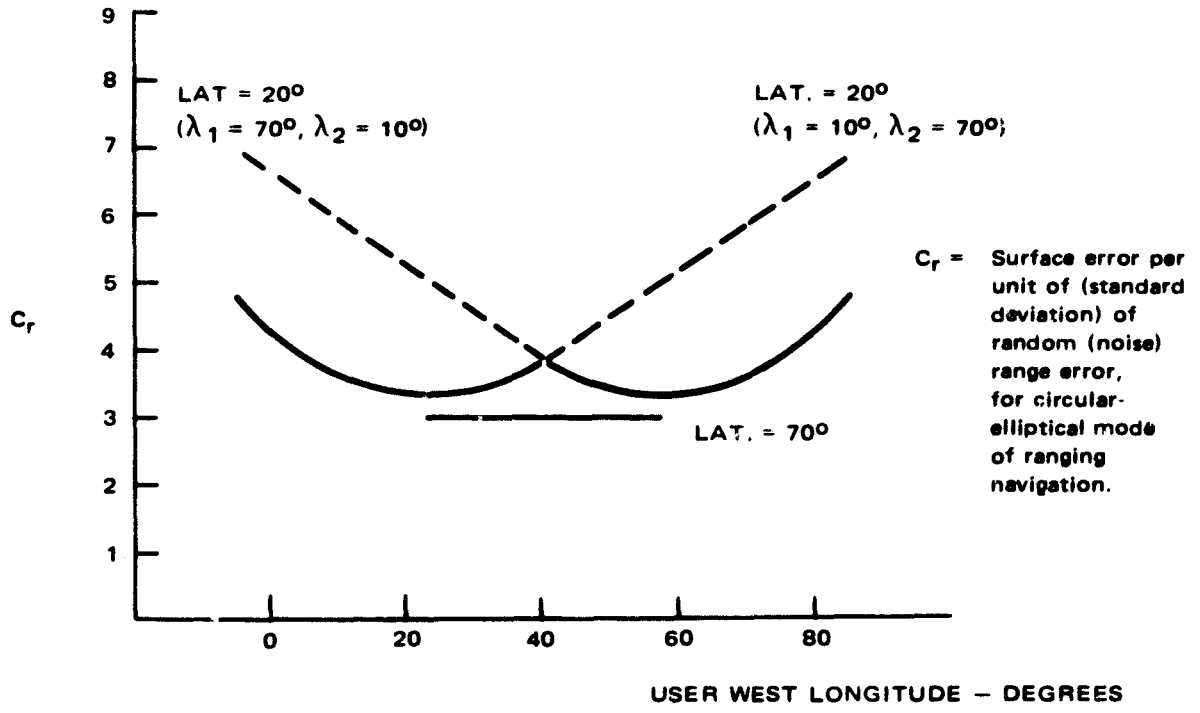

Figure 2-22. Horizontal Position Error per Unit Range Error (mi/mi) vs User Longitude for 60° Satellite Spacing

Referring now to a continuous-wave system, the phase angle (radians) of the signal received from satellite 1, at the GCC, is given by

$$(\Theta_1 - \Theta_o + 2k\pi) = \frac{2w_f}{c}(D_1 + r_1)$$

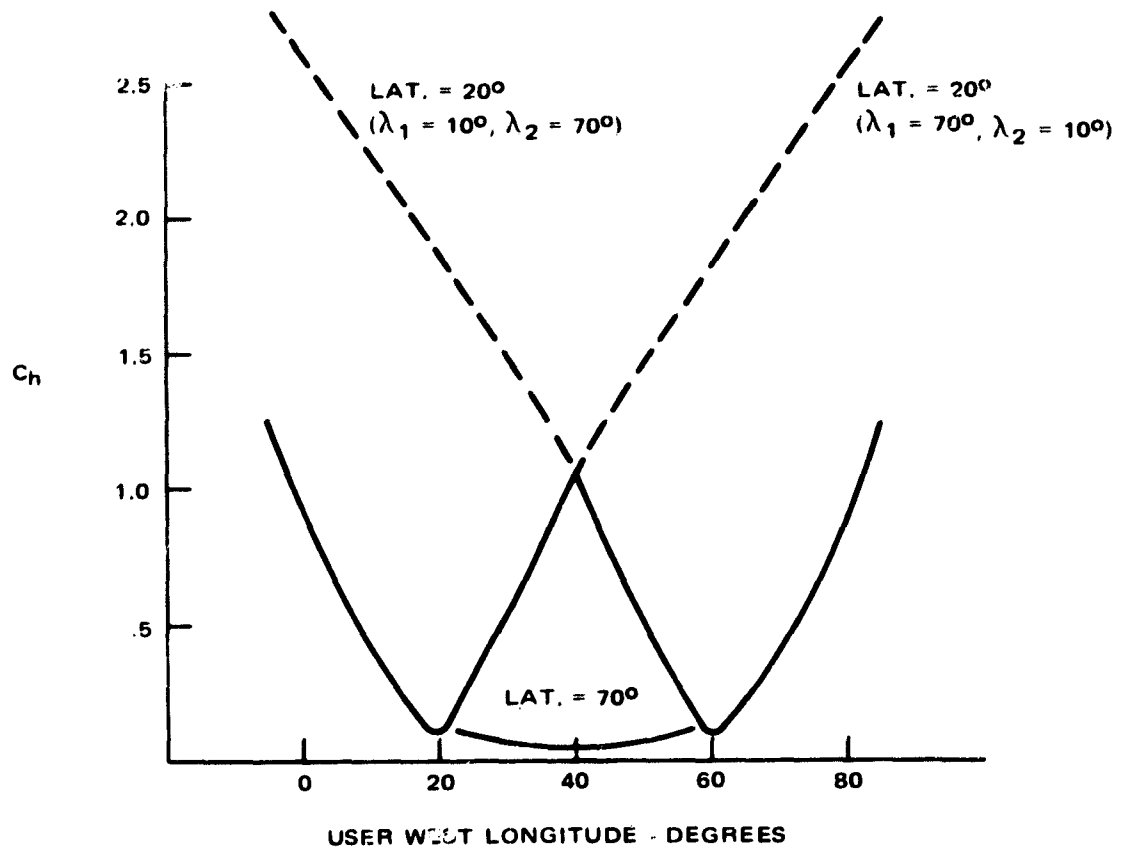

Figure 2-23. Horizontal Position Error per Unit Altitude Error (mi/mi) vs User Longitude

where θ_o = phase of original modulation signal, θ_1 = phase of return signal, k is an integer, W_f is fine tone frequency in rad/sec. Thus

$$\sigma(\Delta r_1) = \lambda_f \frac{\sigma(\Delta\theta)}{2} \tag{30}$$

where $\sigma(\Delta\theta)$ is in cycles, $\sigma(\Delta r_1)$ is in nmi if λ_f is expressed in nmi. Feasible 1σ values for contributory factors in phase measurement are

Indicator Resolution error, $\sigma(\Delta\theta_r) = 2°$

Noise & Multipath error, $\sigma(\Delta\theta_N) = 5°$

resulting in an RMS error of 5.38°. For a fine tone frequency of 8 kHz,

$$\lambda_f = \frac{c}{f} = \frac{186{,}000 \times 6076}{8 \times 10^3 \times 5280} = 26.8 \text{ nmi}$$

and the range error due to the above factors is

$$\sigma_N(\Delta r) = \frac{26.8}{2} \times \frac{5.38}{360} = .202 \text{ nmi}$$

The RMS ionospheric refraction errors, at 1.6 GHz carrier frequency, are given in reference 1 for two model atmospheres. For two-way ranging:

	Log-Normal	Normal
E_{lim}	$2\sigma_R$	$2\sigma_R$
5°	.0093 nmi	.0314 nmi
10°	.0079 nmi	.0265 nmi

The total range error, at $E_{lim} = 5°$, assuming the normal distribution as a conservative basis, is

$$\sigma(\Delta r) = \sqrt{(.202)^2 + (.0314)^2} = .204 \text{ nmi}$$

The error in R_N, reflecting both altitude measurement error and Earth-shape uncertainty, will be taken as

$$\sigma(\Delta R_N) = 300 \text{ ft} = .0493 \text{ nmi}$$

Taking the sensitivities, at the extreme field of view, from Figures 2-22 and 2-23, the rms horizontal error is

$$\epsilon = \sqrt{\left[(4.8 \times .204)^2 + (1.25 \times .0493)^2\right]} = .980 \text{ nmi}$$

so that the selection of 8 kHz for fine tone frequency is acceptable.

It is evident that a .1 nmi accuracy cannot be achieved, under the normal distribution model and for a 5° elevation angle limit, since the refraction error alone gives $\epsilon = 4.8 \times .0314 = .15$ nmi. If the log-normal ionosphere is assumed and E is limited to not less than 10°, and if the altitude error is decreased to $\sigma(\Delta R_N) = 100$ ft = .0164 nmi, then setting ϵ to .1 nmi the allowable phase measurement error can be found.

Thus

$$(4.3)^2\left[\sigma_N{}^2(\Delta r) + (.0079)^2\right] + \left[.95 \times .0164\right]^2 = (.1)^2$$

$$\sigma_N(\Delta r) = .0216 \text{ nmi allowable}$$

Assuming resolution and noise/multipath accuracies unchanged, an increase in tone frequency is required to reduce the effects on range error. Thus

$$f' = \frac{.202}{.0216} \times 8 = 75, \text{ say } 64 \text{ kHz}$$

and this would enable a .1 nmi accuracy to be achieved, under the assumptions and restrictions given.

If the more conservative ionospheric model is used, a possible approach to achieve the .1 nmi accuracy would be to emplace a satellite mid-way between the ones at 10° and 70°. A "hand-over" would occur when the navigator longitude is either side of the 40° meridian. In essence then, for the same N. Atlantic coverage, the elevation angles at the edge of the field would be considerably increased, diminishing the refraction errors to negligible amounts. The GDOP would, however, be essentially doubled, since the satellite separation angle would be halved. As a consequence, the fine tone frequency would need to be raised to 128 kHz to achieve the .1 nmi accuracy; or the signal/noise ratio or transmitted power would need to be increased as needed.

2.4.4 PASSIVE SYSTEM; GLOBAL COVERAGE

Reference 1 (in section 2.4.6) presents the results of computer simulation runs of horizontal error, for the circular-circular passive mode of navigation. Source errors assumed were $\sigma(\Delta r)$ = 1000 ft, $\sigma(\Delta R_N)$ = 100 ft, along-range satellite position error = 20 meters; user altitude was 6 nmi. Plotted were the semi-major and semi-minor lengths of the 29.3% probability error ellipse. Taking the root sum of the squares gives the RMS value; since the source error is predominantly range error, dividing the surface RMS error by $\sigma(\Delta r)$ = 1000 ft gives essentially the sensitivity to range error. This is summarized below for different satellite spacings, and for the navigator at the edge of the field ($E_{lim} = 5°$) and at latitude $\phi = 20°$.

$\epsilon/\sigma(\Delta r)$	Sat. Spacing
15.02	10° (90°W, 100°W)
3.16	50° (20°W, 70°W)
3.16	90° (50°W, 140°W)
4.57	130° (30°W, 160°W)

Taking 3.16 as the GDOP for 60° spacing, and assuming refraction error very small compared to resolution and noise error effects, the allowable maximum range error would be $\sigma(\Delta r) = \frac{1}{3.16} = .315$ nmi. Noting that transmission is now 1-way, and assuming $\sigma(\Delta\theta_r) = 2°$, $\sigma(\Delta\theta_N) = 5°$ as before, the fine tone frequency would need to be increased:

$$f' = \frac{.404}{.315} \times 8 = 10.2 \text{ , say 16 kHz for margin of safety.}$$

The meaning to be ascribed to the RMS position error is as follows: "The probability is no less than 39.3% that the computed position is within ϵ_{RMS} of the true position." A more satisfactory use for the RMS value is in the determination of the 99% probability

radius; this is, the value such that the probability is 99% that the computed position will lie within ϵ_{99} of the true position. It is given by

$$\epsilon_{99} = N \epsilon_{RMS}$$

where N is a function of the ratio of the semi-major to semi-minor axes of the 39.3% probability ellipse (see Figure 2-24). Note that $N = 3/\sqrt{2}$ when the ellipse becomes a circle, and N approaches 3 for large values of n.

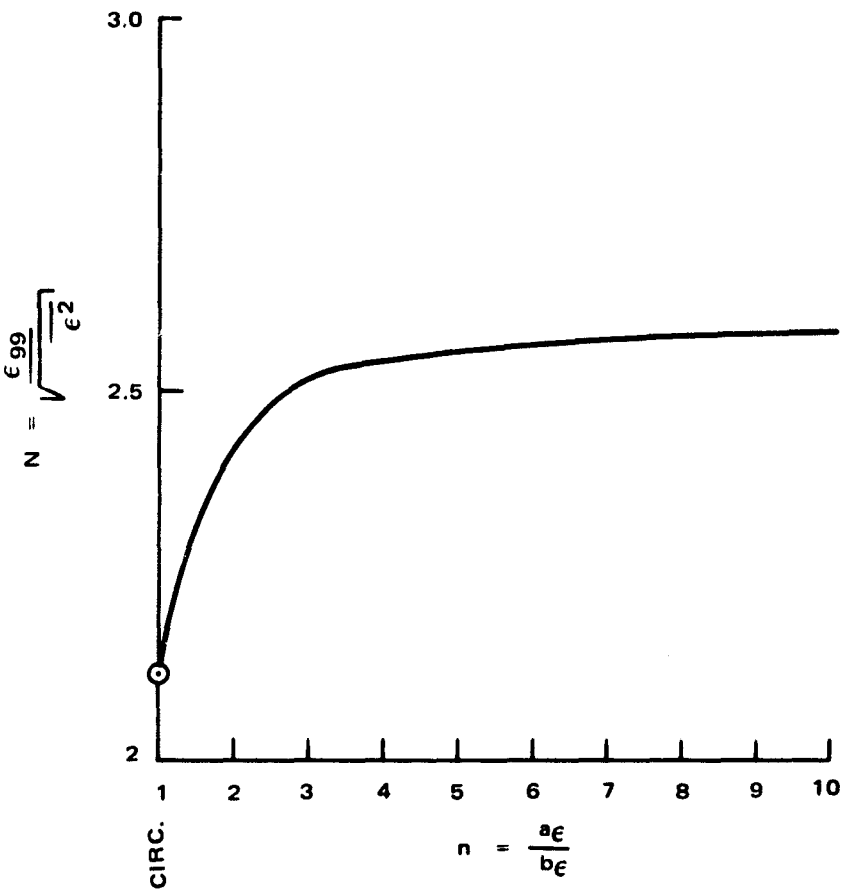

Figure 2-24. Ratio of 99% Probability Value of Position Error to RMS Position Error vs Ratio of Semi-Major to Semi-Minor Axis of 40% Probability Ellipse

An alternative parameter is the equivalent circle radius, defined by

$$\epsilon_{eq} = \sqrt{a_\epsilon b_\epsilon}$$

The area of this circle (of geometric mean radius) is equal to the 39.3% ellipse of concentration, but no formalistic probability can be ascribed to the radius. The radius of the RMS circle is of course always larger than the geometric mean radius circle, since

$$\frac{\epsilon_{RMS}}{\epsilon_{eq}} = \frac{\sqrt{a_\epsilon^2 + b_\epsilon^2}}{\sqrt{a_\epsilon b_\epsilon}} = \sqrt{n + \frac{1}{n}} \; ; \; n = \frac{a_\epsilon}{b_\epsilon}$$

Evidently, if the RMS value meets the 1σ circular value specified, the system performance is suitable.

In reference 2 the following range error budget is given at medium altitude (5600 nmi), for a pulsed ranging system:

Ionospheric bending (non-computable residual)	100 ft (at 500 MHz)
Range pulse timing uncertainty	
(noise contribution)	40 ft
(pulse height uncertainty)	50 ft

With ranging at 1.6 gHz, the refraction error is reduced to

$$\sigma_R(\Delta r) = 100 \times \left(\frac{.5}{1.6}\right)^2 = 9.7 \text{ ft, negligible}$$

The timing errors are proportional to frequency and range (for one-way ranging). Thus, for the satellites at synchronous altitude,

$$\sigma_N(\Delta r) = \sqrt{(40)^2 + (50)^2}\left[\left(\frac{1.6}{.5}\right) \times \left(\frac{19.6}{5.6}\right)\right] = 715 \text{ ft} = .117 \text{ nmi}$$

which is somewhat less than the maximum allowable range error, assuming a GDOP of 3, to obtain a 1 nmi RMS position error.

Reference 1 presents a range error analysis for the phase difference measurement technique, which shows the more significant effect of refraction errors when the fine tone frequency is 300 kHz. The equivalent error circle radius, for a 60° satellite spacing, passive mode of usage, is 129 ft at the edge of the field for a 20° latitude user. This indicates the possibility of attaining an ultimate .1 nmi accuracy for the passive user, North Atlantic coverage.

Reference 1 also presents results based on the same low range errors (1σ = 20 to 35 meters) when a global system of satellites is employed. This system employs 6 satellites each in 3 orbit planes (2 polar, 1 equatorial), all satellites being at synchronous altitude. The GDOP is 2 up to 80° latitude, and 5 for latitude between 80° and 90°; consequently, the RMS position error is nowhere greater than 575 ft.

2.4.5 RANGE DIFFERENCE SYSTEMS

The following is a simplified explanation of the error analysis equations, derived in Reference 3, for the deterministic case of 2 range difference measurements and one altitude measurement. In Figure 2-25, points 1, 2, 3 represent the instantaneous

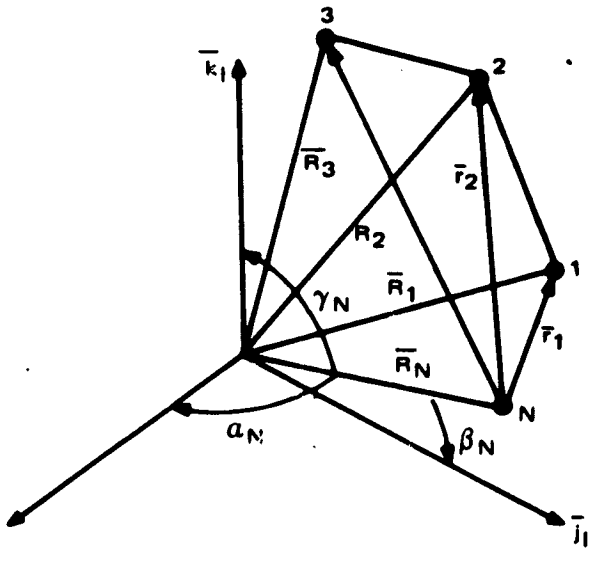

Figure 2-25. Range Difference System (Three Satellites)-Geometry

positions of three satellites, and N is the navigator position. The measurements m_1, m_2, m_3 are made, where

$$m_1 = r_1 - r_2$$

$$m_2 = r_2 - r_3$$

$$m_3 = R_N = R_E + h$$

(r_i is range to satellite i, h is measured navigator altitude.)

In matrix form,

$$\hat{m} = \begin{bmatrix} m_1 \\ m_2 \\ m_3 \end{bmatrix} = \begin{bmatrix} 1 & -1 & 0 & 0 \\ 0 & 1 & -1 & 0 \\ 0 & 0 & 0 & 1 \end{bmatrix} \begin{bmatrix} r_1 \\ r_2 \\ r_3 \\ R_N \end{bmatrix} = \hat{T}\hat{r} \tag{31}$$

so that

$$\Delta\hat{m} = \hat{T}\Delta\hat{r} \tag{32}$$

Evidently,

$$r_i = \left| \bar{R}_i - \bar{R}_N \right| = \left[(X_i - X_N)^2 + (Y_i - Y_N)^2 + (Z_i - Z_N)^2 \right]^{1/2} \tag{33}$$

$i = 1, 2, 3$

where X_i, Y_i, Z_i are position components of the i^{th} satellite in the ECI system of coordinates. Thus, neglecting satellite ephemeris errors,

$$\Delta r_i = \frac{\partial r_i}{\partial X_N} \Delta X_N + \frac{\partial r_i}{\partial Y_N} \Delta Y_N + \frac{\partial r_i}{\partial Z_N} \Delta Z_N$$

$$= \frac{(X_N - X_i)}{r_i} \Delta X_N + \frac{(Y_N - Y_i)}{r_i} \Delta Y_N + \frac{(Z_N - Z_i)}{r_i} \Delta Z_N \tag{34}$$

But

$$\bar{r}_i = \bar{R}_i - \bar{R}_N = (X_i - X_N)\,\bar{i}_I + (Y_i - Y_N)\,\bar{j}_I + (Z_i - Z_N)\,\bar{k}_I \tag{35}$$

$$= r_i \left[\cos \alpha_i \bar{i}_I + \cos \beta_i \bar{j}_I + \cos \gamma_i \bar{k}_I \right]$$

where $\cos \alpha_i$, $\cos \beta_i$, $\cos \gamma_i$ are the direction cosines of $\bar{r}_i$ in the ECI system. Thus,

$$\Delta r_i = -\left[\cos \alpha_i \Delta X_N + \cos \beta_i \Delta Y_N + \cos \gamma_i \Delta Z_N \right] \tag{36}$$

Note that

$$\bar{R}_N = R_N \left[\cos \gamma_N \bar{i}_I + \cos \beta_N \bar{j}_I + \cos \gamma_N \bar{k}_I \right]$$

$$= X_N \bar{i}_I + Y_N \bar{j}_I + Z_N \bar{k}_I \tag{37}$$

and

$$R_N^2 = X_N^2 + Y_N^2 + Z_N^2 \tag{38}$$

Then

$$\Delta R_N = \frac{\partial R_N}{\partial X_N}\Delta X_N + \frac{\partial R_N}{\partial Y_N}\Delta Y_N + \frac{\partial R_N}{\partial Z_N}\Delta Z_N$$

$$= \left(\frac{X_N}{R_N}\right)\Delta X_N + \left(\frac{Y_N}{R_N}\right)\Delta Y_N + \left(\frac{Z_N}{R_N}\right)\Delta Z_N \tag{39}$$

$$= \cos \alpha_N \cdot \Delta X_N + \cos \beta_N \cdot \Delta Y_N + \cos \gamma_N \cdot \Delta Z_N$$

Combining eq.'s 36 and 39, in matrix form we have

$$\Delta \hat{r} = \begin{bmatrix} \Delta r_1 \\ \Delta r_2 \\ \Delta r_3 \\ \Delta R_N \end{bmatrix} = \begin{bmatrix} -c\alpha_1 & -c\beta_1 & -c\gamma_1 \\ -c\alpha_2 & -c\beta_2 & -c\gamma_2 \\ -c\alpha_3 & -c\beta_3 & -c\gamma_3 \\ c\alpha_N & c\beta_N & c\gamma_N \end{bmatrix} \begin{bmatrix} \Delta X_N \\ \Delta Y_N \\ \Delta Z_N \end{bmatrix} = \hat{G}^T \Delta \hat{R}_N \tag{40}$$

Substituting eq. 40 into eq. 32,

$$\Delta \hat{m} = \hat{T}\hat{G}^T \Delta \hat{R}_N \tag{41}$$

Solving for $\Delta \hat{R}_N$,

$$\Delta \hat{R}_N = \left[\hat{T}\hat{G}^T\right]^{-1} \Delta \hat{m} \tag{42}$$

and the covariance matrix of the position errors, due to measurement errors, is given by

$$\overline{\Delta \hat{R}_N \Delta \hat{R}_N^T} = \left[\hat{T}\hat{G}^T\right]^{-1} \overline{\Delta \hat{m} \Delta \hat{m}^T} \left[\hat{T}\hat{G}^T\right]^{-1 T} \tag{43}$$

where superscript T denotes transpose, and a superposed bar line denotes expectation. The mean square position error is simply

$$\overline{\Delta X_N^2} + \overline{\Delta Y_N^2} + \overline{\Delta Z_N^2} = \text{trace } \overline{\Delta \hat{R}_N \Delta \hat{R}_N^T} \tag{44}$$

that is, the sum of the diagonal elements of $\overline{\Delta\hat{R}_N \Delta\hat{R}_N^T}$.

The mean squre horizontal error is

$$\overline{\epsilon^2} = \left[\overline{\Delta X_N^2} + \overline{\Delta Y_N^2} + \overline{\Delta Z_N^2}\right] - \overline{\Delta R_N^2} \tag{45}$$

wherein $\overline{\Delta R_N^2}$ is the mean square altitude error.

From eq. 32, it is to be observed that

$$\overline{\Delta\hat{m}\,\Delta\hat{m}^T} = \hat{T}\,\overline{\Delta\hat{r}\,\Delta\hat{r}^T}\,\hat{T}^T \tag{46}$$

If the range errors are essentially independent, with equal statistics,

$$\overline{\Delta\hat{m}\,\Delta\hat{m}^T} = \begin{bmatrix} 2\sigma_r^2 & -\sigma_r^2 & 0 \\ -\sigma_r^2 & 2\sigma_r^2 & 0 \\ 0 & 0 & \overline{\Delta R_N^2} \end{bmatrix}$$

wherein $\sigma_r^2 = \overline{\Delta r_1^2} = \overline{\Delta r_2^2} = \overline{\Delta r_3^2}$. Note that

$$\sigma^2(\Delta m_1) = \sigma^2(\Delta m_2) = 2\sigma_r^2$$

and Δm_1, Δm_2 are correlated, with the coefficient

$$\rho_{12} = \rho_{21} = \frac{\overline{\Delta m_1 \cdot \Delta m_2}}{\sigma_{m_1}\,\sigma_{m_2}} = -\frac{1}{2}$$

The satellite configuration, described in Reference 4, called the rotating "Y" configuration, consists of 4 satellite orbits. One satellite is in a circular, synchronous equatorial orbit; the other three satellites are in synchronous elliptical orbits, .3 eccentricity, 30° inclination, and spaced 120° apart in longitude of ascending mode. Continuous simultaneous visibility of three satellites is afforded for a user latitude of 70°N, with 80° width in longitude (5° elevation angle limitation), and for a user latitude of 20°N with 125° width in longitude. The sensitivity of 1σ semi-major surface position error component to 1σ range error is 20 at 75°N latitude; with 1σ range error of .1 to .2 nmi, as indicated in the previous section, the system is unacceptable for obtaining a 1 nmi accuracy. The GDOP can be decreased by resorting to higher orbit inclinations - see Figure 2-26, which is based on Figure 3.2-5 of Reference 4.

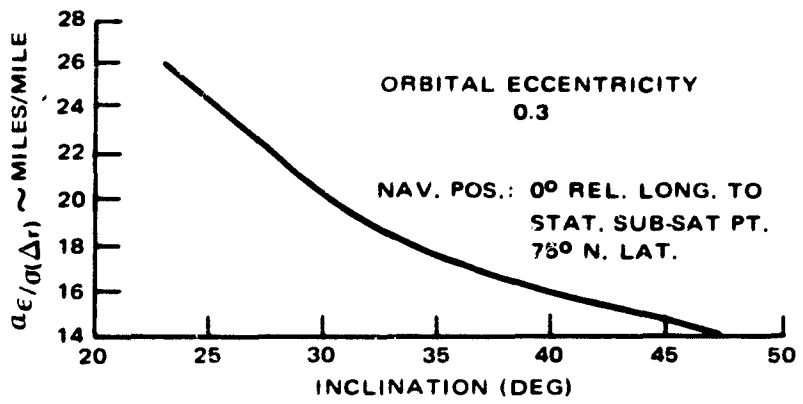

Figure 2-26. Ratio of Semi-Major Axis of 40% Probability Ellipse of Position Error to 1σ Range Error vs Inclination of Orbits for Y Configuration

Reference 1 indicates that when a global system is provided, of three mutually orthogonal near-synchronous orbits (one equatorial and two polar, with five satellites each), the GDOP for hyperbolic mode is uniformly less than 1.4; with a 1σ phase ranging error of no more than .2 nmi, an RMS position error of less than 1 nmi can certainly be achieved. A .1 nmi accuracy would require an order of magnitude decrease in range-measurement error.

2.4.6 REFERENCES FOR SECTIONS 2.4.4 and 2.4.5

1) Final Report - "Phase Difference Navigation Satellite Study" RCA - Dec.'67

2) "Study of Satellites for Navigation" - G.E. - Feb.'64

3) "A Static Error Analysis of a Class of Navigation Systems Employing Satellites" - P.W. Soule (Aerospace Corp.) - Nov.'67

4) "Parametric Summary - Influences of Synchronous, Inclined Elliptical Orbits on Performance of a Satellite Navigation System" - R.L. Dutcher (Aerospace Corp.) - Dec.'67

2.5 SYSTEM ERROR ANALYSIS

2.5.1 INTRODUCTION

The final ground position RMS error is the resultant of the RMS value of all the contributing elements. The elements, such as ionospheric and tropospheric refraction, multipath range error, satellite and user phase delay, cause an overall error in the slant range from the user to a specific satellite. If the errors from the user to both

satellites are uncorrelated, but with the same means and standard deviations a multiplication factor of $\sqrt{2}$ should be applied to the RMS error on the range to one satellite to obtain the RMS error of both ranges. Furthermore, this range error must be multiplied by the GDOP (geometric dilution of precision) factor in order to obtain the true ground position error. A GDOP value of 3 is used in this analysis. From a design point of view, this is a conservative estimate since it applies to the coverage area nearest the equator (20° N. Lat) where the GDOP is greatest. The relationship of the ground error ϵ_r, to the range error σ_{total} is:

$$\epsilon_r = 3\sqrt{2}\,\sigma_{total}$$

where

$$\sigma_{total} = \sqrt{\sigma 1^2 + \sigma 2^2 + \sigma 3^2} + \ldots$$

where the σ_i's are discussed next.

2.5.2 IONOSPHERIC AND TROPOSPHERIC RANGE ERRORS

Table 2-15 is reproduced from Table 4-5 of the "Final Report, Phase Difference Navigation Study, Dec. 1967, NASA Contract NAS-12-509, by RCA Systems Engineering, Evaluation and Research (SEER), Moorestown, N.J. For a 5-degree elevation angle the variance of the range error $(\sigma_I)^2$, is 840.0 meters^2 (for a normal distribution thus the RMS range error σ_I is 0.016 nmi.

TABLE 2-15. RANGE ERROR SUMMARY

Elevation Angle (Deg)	Log-Normal Ionosphere Distribution (m^2)	Normal Ionosphere Distribution (m^2)	Troposphere (m^2)	Multipath/ Noise (m^2)	Satellite Range Error (m^2)
1	84.2	990.0	81.8	386.01	400
5	74.4	840.0	3.3	111.25	400
10	53.5	604.0	0.4	36.04	400
15	28.1	318.0	0.2	18.49	400
45	5.0	57.4	0	10.0	400
90	1.8	20.7	0	10.0	400

The tropospheric range error can be completely ignored since the variance is only 3.3 m^2.

2.5.3 MULTIPATH RANGE ERROR

From Table 2-15, we see that the variance on the range due to multipath is 111.25 m^2, thus the range error due to multipath σ_M is 0.0057 nmi (shown later in Table 2-16).

2.5.4 SLANT RANGE ERROR DUE TO NARROW-BAND FILTER PHASE DELAY

In order to keep the predetection signal-to-noise ratio reasonable at the satellite, user, and control center, and to reject unwanted interference, narrow-band bandpass filters are utilized. The filters, by necessity introduce a phase shift to the arriving signal that is directly related to the displacement of the signal from the center of the passband. This displacement can result from a number of causes such as: receiver local oscillator drift, transmitter (received signal) frequency drift, doppler on the incoming signal, shift of the center frequency of the filter as a result of temperature change.

For a single-pole bandpass filter, the transfer function is given by

$$H\ (jw) = 1 / \left(1 - j\ \frac{\Delta f}{B/2}\right) \tag{1}$$

where

f = the frequency displacement from mid-band

B = the 3 dB bandwidth of the filter.

The phase shift of the filter output is

$$\phi = \tan^{-1} \left(\frac{\Delta f}{B/2}\right) \tag{2}$$

Let the filter bandwidth be 100 KHz. Then the upper and lower sidebands caused by the 8 KHz (fine) ranging tone have phase delays ϕ_u and ϕ_L given by

$$\phi_u = -\phi_L = \tan^{-1} \left(\frac{8}{50}\right) = 0.16 \text{ radian} = 9.1° \tag{3}$$

This results in a phase-bias error of $(\phi_u - \phi_L)/2 = \phi_u = 9.1°$, which corresponds to a range-bias error of 0.587 nmi. This bias error will be removed at the ground control center.

For a small frequency shift $d(\Delta f)$, the corresponding change in phase, $d\phi$, is found by differentiating eq. (2). Thus

$$d\phi = \frac{1}{1 + \left(\frac{\Delta f}{B/2}\right)^2} \cdot \frac{d(\Delta f)}{B/2} \tag{4}$$

For Δf = 8 KHz and B = 100 KHz as before, this reduces to

$$d\phi \doteq 1.95 \times 10^{-5}\ d(\Delta f) \tag{5}$$

Hence any change of frequency around the fine tone — caused by oscillator drift or one of the other factors named earlier — will result in a change of phase as given by eq. 5. This will be interpreted as a range error:

$$\sigma_f = \frac{c}{f} \cdot \frac{d\phi \text{ (degrees)}}{360} \qquad (6)$$

$$= 0.0559\ d\phi \text{ (degrees)}$$

where

σ_f = range error caused by filter, in nautical miles

c = speed of light = 161,000 nmi/sec

f = ranging tone frequency = 8 KHz

Values of differential phase error $d\phi$ and range error σ_f corresponding to various differential frequency shifts $d(\Delta f)$ are shown in the following table:

$d(\Delta f)$ (kHz)	$d\phi$ (rad)	$d\phi$ (deg)	σ_f (nmi)
1	0.0195	1.12	0.0625
2	0.0390	2.23	0.125
4	0.0780	4.47	0.25
8	0.1560	8.94	0.5
16	0.3120	17.88	1.0
32	0.6240	35.75	2.0

2.5.5 FREQUENCY OFFSET ERRORS

The following items will contribute to frequency offset (Δf) of the signal into the filter.

1. Doppler due to the rate of change of distance between a satellite and a user
2. User oscillator-frequency offset
3. Temperature drift of user's filter center frequency

User-Satellite Doppler -- An SST traveling at mach 3 directly in line toward a satellite (situated low on the horizon) will experience a doppler shift of approximately 4.8 kHz (one-way) on a RF carrier with a nominal frequency of 1600 MHz. Under the assumption that the aircraft velocity (speed and direction) is known to within 10% of the true value the frequency uncertainty of the 2-way doppler becomes:

$$\Delta f_d = 0.1 \times 2 \times 4.8 \text{ kHz}$$

$$\Delta f_d = 960 \text{ Hz}$$

User-Oscillator Error - If the user is equipped with a moderately accurate frequency standard such as a model FE 20-VPC-10P crystal VCO made by Frequency Electronics, Inc. the worst case frequency drift (published value) is 5 parts in 10^6 per year. Now if the user calibrates his standard as infrequently as once every two months the accumulated frequency error Δf_o is

$$\frac{2}{12} \times 5 \times 10^{-6} \times 1.7 \times 10^{9} = 1.42 \text{ kHz (at an injection frequency of 1.7 GHz)}$$

Filter-Temperature Effect - The resonant frequency f of a high-Q L-C filter is given by the formula:

$$f = \frac{1}{2\pi\sqrt{LC}} \tag{7}$$

where:

f is the frequency in hertz

L is the inductance in henrys

and

C is the capacity in farads

Differentiating (7) we have:

$$df = \frac{1}{2} \frac{1}{2\pi\sqrt{LC}} \left(\frac{dL}{L} + \frac{dc}{c}\right)$$

$$\frac{df}{f} = \frac{1}{2}\left(\frac{dL}{L} + \frac{dc}{c}\right) \tag{8}$$

Letting:

$$\frac{dL}{L} = \epsilon_L \Delta T$$

and

$$\frac{dc}{c} = \epsilon_C \Delta T$$

where:

ϵ_L is the temperature coefficient of the inductance

ϵ_C is the temperature coefficient of the capacitance

and

ΔT is the temperature change

therefore,

$$\frac{df}{f} = \frac{\Delta T}{2} \epsilon_L + \epsilon_C \qquad (9)$$

If we assume that ϵ_L and ϵ_C are 50 ppm ±10% but of opposite sign, that is $\epsilon_L(1 \pm 0.1) = -\epsilon_C(1 \pm 0.1)$, then the worst case error on the tolerance is 20%, i.e. 10 ppm.

Therefore:

$$\frac{df}{f} = \frac{\Delta T}{2} \left[(50 + 5) - (50 - 5)\right] \times 10^{-6}$$

$$\frac{df}{f} = \frac{\Delta T}{2} \times 10^{-5}$$

Now for a (ΔT) of 10°C (which is quite reasonable in the instrument compartment of a commercial jet aircraft,

$$\left|\frac{df}{f}\right| = 5 \times 10^{-5}$$

If the resonant frequency f, of the filter is 30 MHz, df is $30 \times 10^6 \times 5 \times 10^{-5} = 1500$ hertz.

Let us call this error Δf_T.

Summary of Frequency Offset Errors - In tabular form we have:

Δf_d = 960 Hz

Δf_o = 1420 Hz

Δf_T = 1500 Hz

Since the errors are all statistically independent the resulting frequency error Δf is:

$$\Delta f = \sqrt{f_o^2 + f_d^2 + f_T^2}$$

Δf = 2278 Hz

Putting Δf in (5) as $d(\Delta f)$ we have:

$$d\phi = 1.95 \times 10^{-5} \times 2.278 \times 10^{3} = 4.442 \times 10^{-2} \text{ radian}$$

or

$$d\phi = 2.545°$$

Finally by using this $d\phi$ in (6) we obtain:

$$\sigma_f = 0.0559 \times 2.545$$

$$\sigma_f = 0.1422 \text{ nmi}$$

2.5.6 SYSTEM ERROR SUMMARY

The resulting range errors are shown in Table 2-16; the resulting ground error in user position is then calculated below the table.

TABLE 2-16. SUMMARY OF ERROR SOURCES

Source	Symbol	Value (nmi)
Ionosphere	σ_I	0.0160
Multipath	σ_M	0.0057
Filter Phase Error	σ_f	0.1422

$$\epsilon = \sqrt{\sigma_I^2 + \sigma_M^2 + \sigma_f^2} \times 3\sqrt{2}$$

$$\epsilon = 0.6076$$

But since the total ground position error ϵ_r is 1 nmi, the ground range error due to the signal to noise $\epsilon_R = \sqrt{1 - \epsilon^2}$ or $\epsilon_R \approx 3/4$ mile.

The RMS range error corresponding to the 3/4 nmi ground range error due to the signal-to-noise is

$$\sigma_R = \frac{3/4}{3\sqrt{2}} = 0.177 \text{ nmi}$$

Now, a wavelength of an 8 kHz tone is

$$\lambda = \frac{161,740}{8,000} = 20.217 \text{ nmi}$$

Therefore, σ_θ, the RMS angular error is;

$$\sigma_\theta = \frac{2 \times \sigma_R}{\lambda} \times 360^\circ = \frac{2 \times 0.177 \times 360}{20.217}$$

$$\sigma_\theta = 0.354 \times 17.81$$

$$\sigma_\theta = 6.303$$

This σ_θ can be considered to be composed of two parts; one part the RMS instrumentation error which will be assumed to be 3°, and the remainder that due to the signal-to-noise $\sigma_{S/N}$,

$$\sigma_{S/N} = \sqrt{(6.303)^2 - (3)^2}$$

$$\sigma_{S/N} = 5.54^\circ = 0.0967 \text{ radian}$$

Now:

$$\sigma_{S/N} = \frac{1}{\sqrt{2\frac{S}{N}}} = 0.0967$$

therefore

$$S/N = 53.42 = 17.3 \text{ dB}$$

The system configured herein provides a S/N of at least 20 dB, thus providing ample margin.

2.6 COMMUNICATIONS REQUIREMENTS ANALYSIS

2.6.1 REQUIRED VOICE CHANNELS FOR NORTH ATLANTIC SERVICE

The pertinent parameters in the sizing of the number of voice channels required are (1) the total number of users in a specific time interval, (2) the frequency of a user call, (3) the mean duration of the call, and (4) the mean waiting time for a channel to become available to a user. The first two items will determine the required total population user rate, i.e. the number of calls per unit time. The population rate times the mean call duration determines the minimum allowable number of channels. Graphically, Figure 2-27 shows the above relationships. The figure shows average waiting time as a function of call density, for various numbers of channels, at an average conversation duration of one minute. The dependent parameter is the mean waiting time that the user has until a channel becomes available. For the hypothetical example, where 190 users are each required to make 3 calls per hour, the resultant user-population rate is 570 calls per hour. Since each call duration is 1 minute, a minimum of 10 channels would be required. For a 10 channel system, the average waiting time is 1.6 minutes. If the number of channels is increased (by 1) to 11, the mean waiting time drops to about 22 seconds.

A more revealing parameter is η, the channel efficiency. This number is obtained from the product of the user-population rate and the mean duration of the call, divided by the number of channels:

$$\eta = \frac{\text{No. of users X user rate X mean duration}}{\text{number of channels}} \qquad (1)$$

It should be noted that η must be less than unity in order to have a finite waiting time. Figure 2-28 illustrates this fact. It is seen that for a fixed number of channels, for example 3, the mean waiting time to obtain a clear channel increases from 0.25 minutes to 10 minutes as η increases from 0.50 to 0.97. However, as the number of users and channels increase for a given channel efficiency, the waiting time becomes monotonically smaller due to more efficient user channel utilization. This result is shown in Figure 2-29

To illustrate this point, another hypothetical case may be considered where there are 180 users and 4 available communications channels. It may be further assumed that the mean duration of the 2-way conversation is 1 minute and that the mean waiting time to acquire a free channel is also 1 minute. The cases that will be considered are:

1. The user population is divided into 4 equal groups (45 users per group) and each group is assigned a specific channel.
2. The user population is divided into 2 equal groups (90 users per group) and each member or a specific group can use either of two channels assigned to that group.
3. The total user population (180 users) can use any of the 4 channels as they may be available.

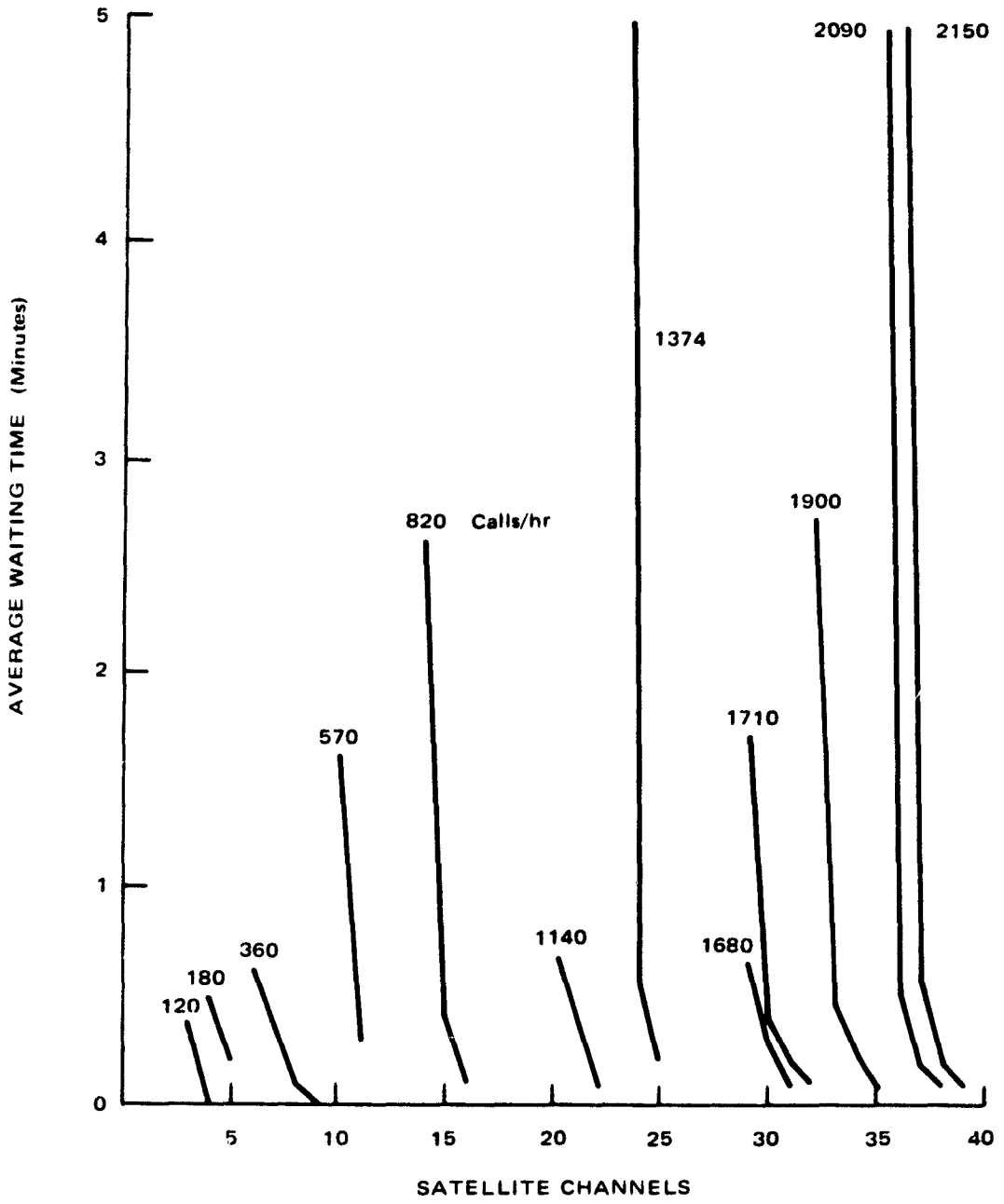

Figure 2-27. User Mean Waiting Time vs. No. of Satellite Channels (@ 1-Minute mean conversation time)

Table 2-17 is constructed by application of the formula

$$\eta = \frac{\text{No. of users x rate x duration}}{\text{No. channels}}$$ and by use of

Figure 2-28 (mean waiting time of 1 minute).

TABLE 2-17. USER-CHANNEL UTILIZATION & EFFICIENCY

Case	Groups	No. Users/ Group	Channels/ Group	η	Calls/ Hour	% Of Case 3
1	4	45	1	0.556	0.74	66.2
2	2	90	2	0.717	0.96	85.4
3	1	180	4	0.840	1.12	100

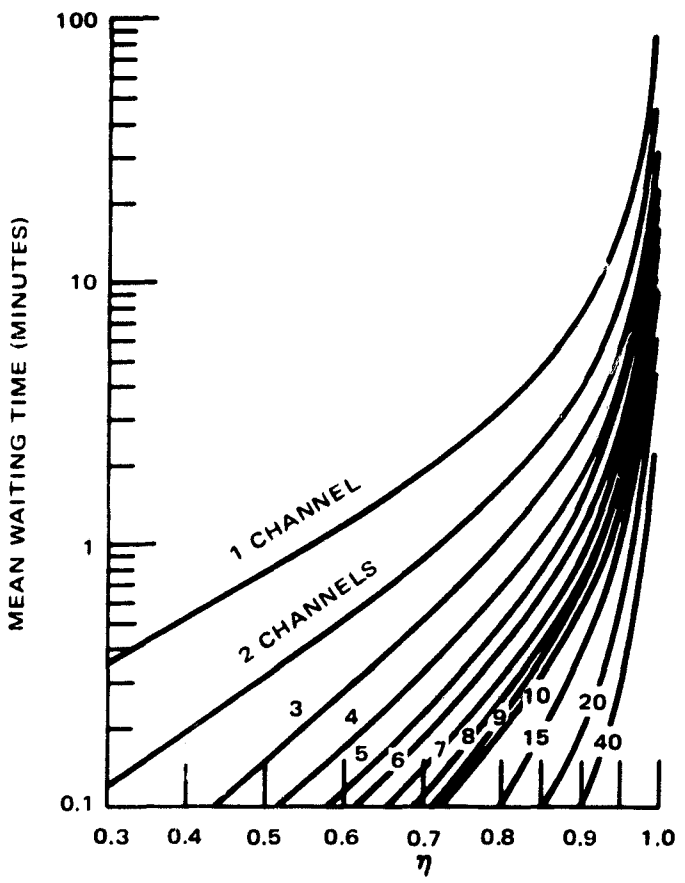

Figure 2-28. Mean Waiting Time vs. Channel Efficiency, $\left(\text{where: } \eta = \frac{\text{Calls/Hour X Mean Duration}}{\text{Number Of Channels}}\right)\eta$

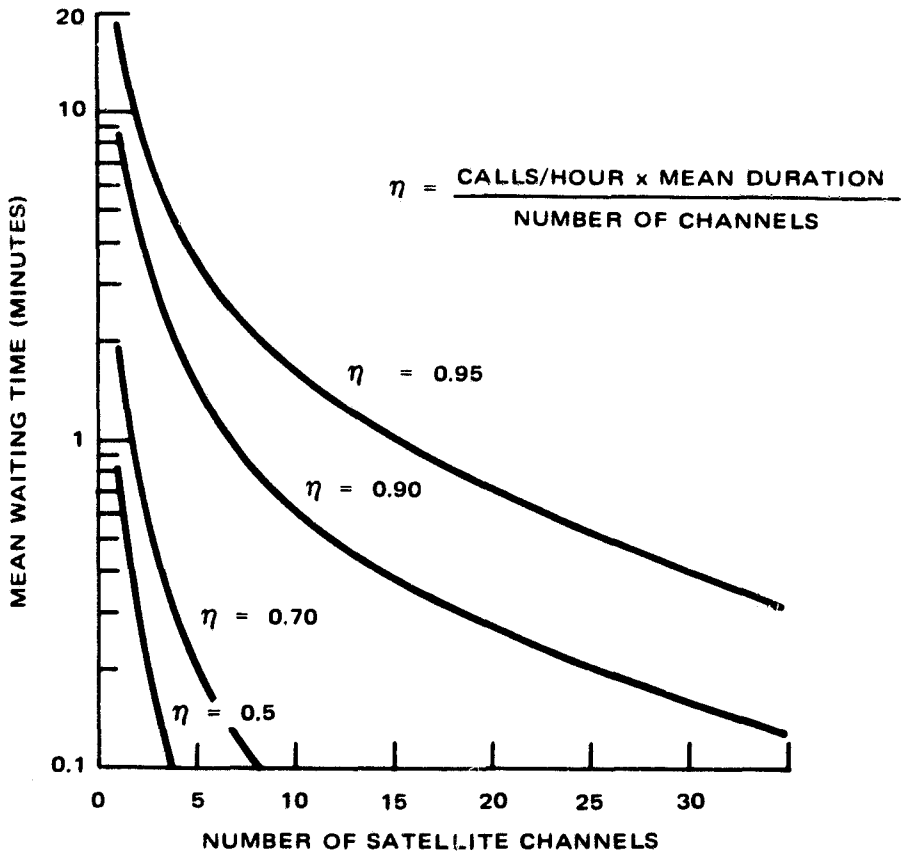

Figure 2-29. Mean Waiting Time vs. Number of Satellite Channels At Various Channel Efficiencies, η.

It is apparant that it is more efficient (more calls per hour) to allow the total user-population use of any one of the four channels. In fact there are almost 34% more calls per hour for case 3 compared with case 1.

It is now possible to determine the number of channels required for a North Atlantic aviation traffic surveillance system in which the pilot calls in his position to ground control at regular intervals. Table 2-18 shows a model based on estimates of 1975 peak traffic densities. In this table, the pilot reports his position whenever he traverses a particular distance in degrees of longitude. The mean duration of the 2-way conversation was specified as 1 minute with a mean waiting time of one minute or less. Figure 2-28 was utilized to obtain the n-values.

TABLE 2-18. REQUIRED NO. OF CHANNELS FOR NORTH ATLANTIC AIR TRAFFIC IN THE MID-1970's

Aircraft	Peak Traffic	Report Interval at 60° Lat. for 5 Longitudes (L)				
		L = 2.5°	L = 5°	L = 10°	L = 20°	L = 30°
S.S.T.	20	24/hr.	12/hr.	6/hr.	3/hr.	2/hr.
Subsonic	170	8/hr.	4/hr.	2/hr.	1/hr.	2/3 hr.
Total Calls per hour		1840	920	460	230	153
Calls/hr x duration		30.7	15.3	7.7	3.8	2.6
Total Channels (available to all)		32	16	9	5	4
Mean Waiting Time (seconds)		25	57	30	36	16

With the aircraft traffic model above and a reporting interval of 2.5° change in longitude, i.e. every 75 nmi at latitude 60°, 32 voice channels are required at a mean waiting time of 25 seconds.

The required number of voice channels for the maritime service was determined in Table 2-19 utilizing information found in Exhibit B of the Ad Hoc Joint Navigation Satellite Committee report of May 1966 and Reference[1].

---

[1] Final Report - Phase Difference Satellite Navigation Study, December 1968, NAS 12-509.

TABLE 2-19. MID-1970's NORTH ATLANTIC MARITIME SERVICE REQUIRED CHANNELS

User	Number	Position Fix Rate (Fixes/hr.)		Routine Messages (Calls/hr.)	
		Individual	Total	Individual	Total
Merchant (100 tons and over)	4,300	1/2	2,150	1/24	179
Fishing	15,000	1/12	1,250	1/48	312.5
Oceanic Survey	300	1/12	150	1/6	50
S.A.R. & Nav. Aid	300	4	1,200	1/24	12.5
Total (Calls/Hr.)			4,700		554
(Calls/Hr. x Duration)			78.33		9.23
Total Channels			79		10
Mean Waiting Time (in seconds)			100		48

The sizing of the maritime requirements, as shown in Table 2-19, ranges from 79 channels in the "position-fix" case to 10 channels in the "routine-message" case. The mean duration of the two-way conversation is again 1 minute. It can be seen that the bulk of the routine messages are from the 15,000 fishing vessels. Without these vessels, only five channels would be required. The mean waiting time would be 33 seconds.

If it is desired to reduce the number of channels, but maintain the same call rate the message duration has to be reduced proportionally; e.g. from 1 minute duration to 1/2 minute duration in order to decrease 79 channels to 40 channels. The mean waiting time becomes 66 seconds in this case.

Using voice communications as a means for reporting position or other routine data, calls for the utilization of many RF channels and is extremely inefficient.

2.6.2 REDUCTION OF VOICE CHANNEL REQUIREMENTS BY USING DIGITAL DATA LINKS

The previous section discussed the number of voice channels required to maintain a specific call rate, at given message duration and for a particular mean waiting time (desirably less than one minute) to obtain a free channel. If the mean duration were to be reduced to say 6 seconds, i.e. 10%, it is seen by application of formula (1) in Section 2.6.1, that the number of users can be increased by a factor of 10 for the same call rate and number of channels. One way to reduce the call duration to 6 seconds is to

digitally encode and transmit the information as a binary stream. Only the specific subject and value need be transmitted such as "altitude = 25,000 feet." All the redundancy and pauses of the spoken language could be eliminated, thus speeding up the transfer of information from the source to the receiver. Perhaps the simplest way to incorporate the digitizing of the message is for the user to have a small typewriter-like keyboard in which he types out the message onto a storage device such as a magnetic tape for transmission at the end of each line of a message and when a free channel is available. Each of the 26 letters and each of 25 punctuation symbols and controls could be represented by a unique 6-bit binary-word. Each of the 10 numbers (including zero, decimal point, sign, and parity) could be represented by a 6-bit binary-word. The numerical part of the text will incorporate an error detection bit because of the lack of redundancy in the digits. (If an error is made in a letter of a word, the word in general is still recognizable, e.g. in the line ALCITUDE = 25,000 FT. the correct word ALTITUDE is quite easily understood.) If transmission occurs at the end of each line, by depressing a specific control button such as "RETURN" for example and each line is no longer than say 40 characters and the transmission time for each line is 10 milliseconds, while the actual typing time for the line is about 12 seconds (at a moderate typing rate of 40, five-letter words per minute, an effective instantaneous 2-way communication can be maintained between the user and a control center, or perhaps another user. The principle is the same as used by computation centers in the "Computer Time Sharing Mode" of computation, i.e. a large type time/computation time ratio causes an apparent exclusive use of the computer by each one of the many users.

As a means of sizing the required number of channels for a purely digital service, a start may be made with a typical 1-line message as shown in Figure 2-30. Each transmitted line requires 65 bits so that the bit-rate is 65 bits/10 milliseconds = 6.5 kilobits/second. Such a data link will be called "high-speed" in order to distinguish it from the 100 bit/sec data link for routine information considered earlier. This bit-rate will just match a 3.3 kilohertz voice channel. If it is assumed that a typical message consists of 10 such lines, the total typing time is 2 minutes while the total transmission time is 100 milliseconds. The time compression ratio is therefore 120 seconds/0.1 second = 1200.

Channel Requirements - North Atlantic, Air Traffic - As an illustrative example of sizing the channel requirement, some of the data in Table 2-18 may be used as a starting point, i.e. the total user population is 190 and the average user message rate is 9.7 calls/hr.

Repeating Eq, (1) from section 2.6.1 then

$$\eta = \frac{\text{No. of users X user rate X mean duration}}{\text{No. channels}}$$

where: users = 190
user rate = 9.7 calls/hour = 2.7×10^{-3} call/sec
mean duration = 10^{-2} second/line x 10 lines = 10^{-1} second

$$\eta = \frac{5.6 \times 10^{-3}}{\text{No. channels}}$$

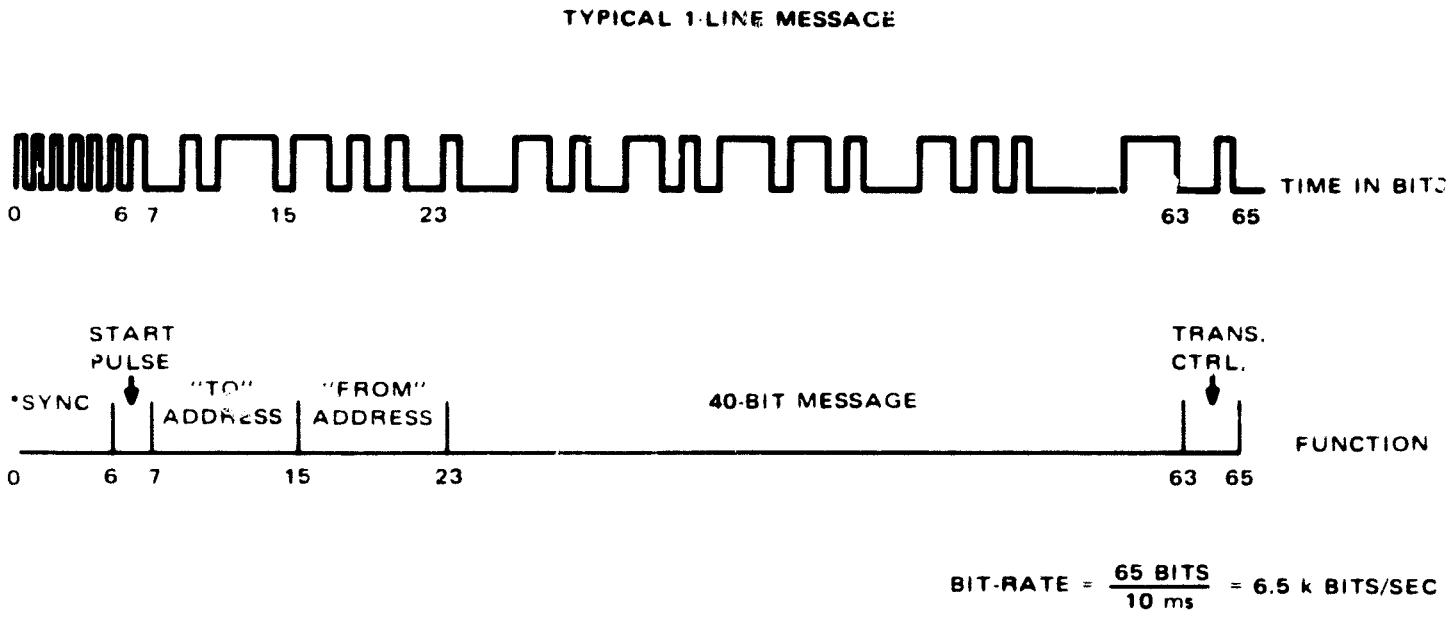

Figure 2-30. Data Link Line Message Structure

Even with 1 channel, the channel efficiency (η) and the waiting time are quite small. The expected waiting time to obtain the channel is 0.54 millisecond (see Appendix 2.6.2-A). This time represents only seven lost sync bits, leaving five remaining. Thus the probability of two or more users attempting to use the channel at any given time is very small. Thus it is seen that the 32 voice channels of the previous section can be replaced by one high speed data link channel (in the aircraft case).

A combination of voice channels and data link channels in the above case is not necessary, since the communications requirements could be met by one high speed data link channel having a bit rate of 6.5 Kb/sec.

Channel Requirements - North Atlantic, Maritime Service - From Table 2-19, it was seen that the maritime service required a routine message rate of 554 calls/hour. The resulting η is given by

$$\eta = \frac{554 \text{ calls/hour} \times \frac{1}{3600} \frac{\text{hours}}{\text{second}} \times 10^{-2} \text{ seconds/line} \times 10 \text{ lines/message}}{\text{No. channels}}$$

$$\eta = \frac{1.54 \times 10^{-2}}{\text{No. channels}}$$

We see that this value of η is also quite small even for a single channel.

In this case, the expected waiting time is 0.155 millisecond. This waiting time represents a loss of two synchronization bits leaving a remainder of 10, which is quite adequate.

Again, a combination of voice and data link channels is not necessary since the communications requirements could be met by one high speed data link channel at 6.5 Kb/sec. As a matter of fact, the estimated maritime position fix reporting rate of 4700 per hour can also be accommodated by one high speed data link channel.

2.6.3 BROADCAST MODE OF GROUND STATION TO USER-FIELD

2.6.3.1 VOICE COMMUNICATIONS

In order to simplify satellite equipment only one repeater will be used per voice channel. This means that the up-link transmission from the ground, be it from the control center or any user, will be at a specific frequency and the down-link signal, at another specific frequency, will be broadcast to the entire earth field as seen from the satellite. This enables users to talk to other users as well as the control center. If the user were to keep his volume control set so as to obtain an audible signal every time someone wished to communicate, an automatic broadcast mode would result. However, because of the large number of users (190) and few number of channels (4-6 per user category) the up-links and down-links would be quite busy with traffic most of the time and each user will receive many signals which are of no interest to him. However, the user need not keep his volume up since in general he is the one to initiate the call to the control center. The control center must always be in the audible receive mode.

One way for the control center to alert the muted users is to transmit a unique signal such as a tone at a specified frequency and amplitude. This tone would be received by each user with a working receiver, made to pass through a narrow band filter and (if the signal level is above a specific voltage level for a specific time duration it would unsquelch the receiver, or cause a visual signal (e.g. a flashing light), or an audible signal (e.g. a tone) to be sensed by all the muted users, thus warning them to turn up the volume control since a broadcast message will follow.

This procedure can also be used when one specific user wants to talk to another specific user. He first calls the control center in the usual way and states that he wishes to converse with a given flight number, and/or a particular pilot. The control center then activates the broadcast alert signal to the entire user population and then announces the number and/or name of the two parties that are to communicate. The other uninterested users could then go back to the "muted receiver" mode.

2.6.3.2 DIGITAL COMMUNICATIONS

In this mode of communications, the control center (or if desired, a user) would address the entire user population by transmitting a "universal address" in place of a specific "to address" as part of the message structure shown in Figure 2-30. Thus two distinct addresses can open a user digital receiver gate, his own address and the

universal address. The broadcast would then automatically be displayed on each user's video display console. Verification of the broadcast by the sender is made possible by comparing the downlink digital signal from the satellite with a stored replica of the transmitted signal. If they are not the same, because someone else has access to the satellite, the video display would then be garbled. In this case, he would press a retransmit button and try again. (This method also holds for the transmission of routine communications on a 100 bits/sec. low bit rate date link to or from the control center and/or a specific user. It also furnishes a visible error check on the signal arriving back down on the earth from the satellite.)

2.7 VOICE SIGNAL DESIGN AND MODULATION/DETECTION

The following modulation/detection analysis will consider AM, FM and PPM modulation. Voice processing is considered in the simplest and effective technique of clipping, and the amount of clipping is included as a variable in the modulation/detection technique analysis to minimize the average power requirement of the satellite transmitter.

Receiver and transmitter channel frequency instabilities used are compatible with ARINC anticipated specifications for the proposed time period, and cognizance is given to the proposed use of FM in ARINC documents. Dippler frequency effects are those considered for Mach 3 SST aircraft. Values of the clipping levels as well as the output SNR for a satellite to Earth voice link used in the analysis are those recommended by CCIR[1]*.

2.7.1 VOICE PROCESSING

Speech clipping provides an increased RMS level relative to peak level of speech over that of unprocessed speech which exhibits an RMS level about 14 dB below its peak level. In the limit of "infinite" clipping, the two levels are the same. The increase in RMS level due to any amount of clipping has been calculated by Wathen-Dunn et al [2] to be as shown by Figure 2-31; e.g. 5.5 dB increase for 6 dB of clipping, 8.5 dB for 12 dB clipping and 12.5 for 27 dB. Thus, from the unprocessed speech peak to RMS ratio of 14 dB, the resulting peak to RMS ratios are then 8.5, 5.5 and 1.5 dB respectively. These representative reductions in peak/RMS ratios will produce correspondingly higher average side-band power for AM and higher average modulation index without exceeding a limiting deviation for FM.

To insure that the intermodulation does not produce excessive side-band splatter for adjacent channel operation, filtering of the clipped signal is used and the amount is determined as follows. The spectral density of simulated speech is shown in Figure 2-32 with either 0, 12 or 30 dB of clipping. From this spectral density curve for differentiating and then clipping speech, it is fairly obvious that the intermodulation noise density above 3 kHz is about 10 dB greater than the unprocessed (0 dB curve) density. This increase in spectral width can be eliminated, by using only a 12 dB/octave filter starting at 3 kHz. In fact this would apply to the 30 db clipping curve also.

*References for Section 2.7 are listed in Section 2.7.3

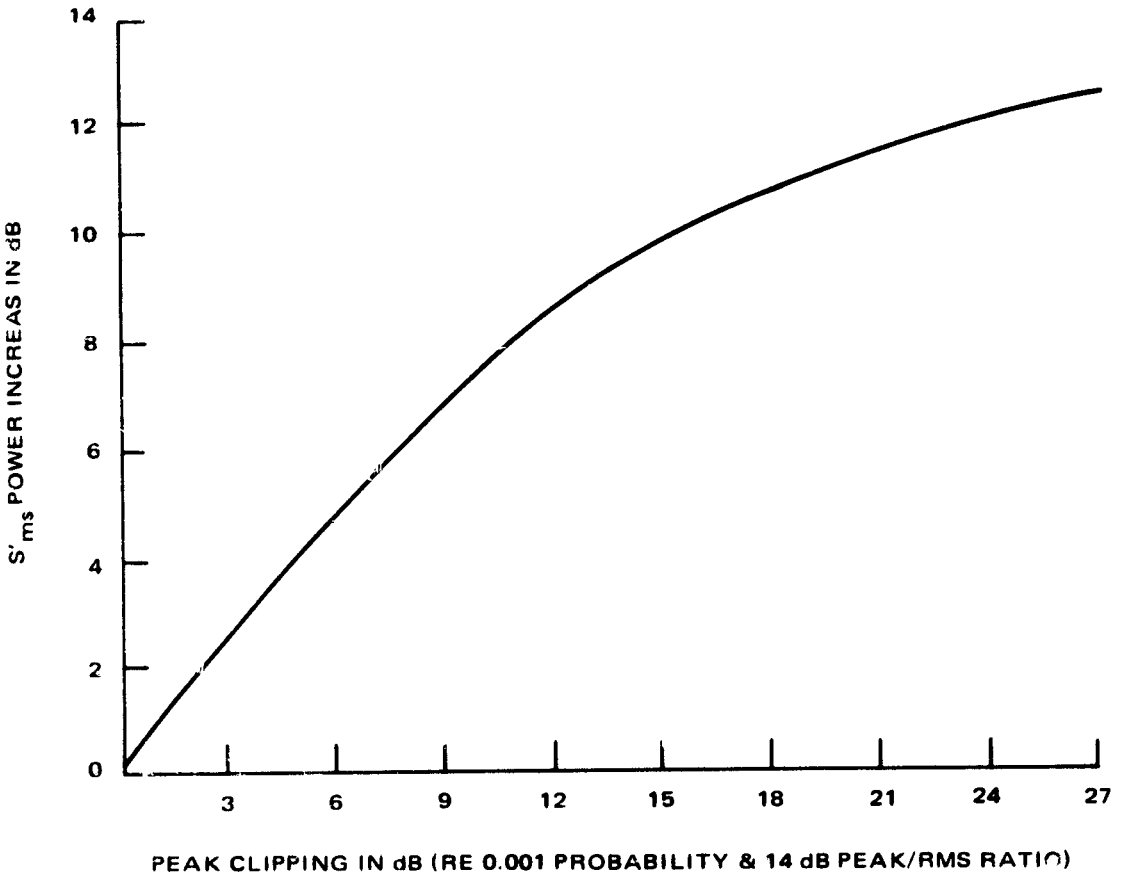

Figure 2-31. Power Increase as Function of Clipping Voice

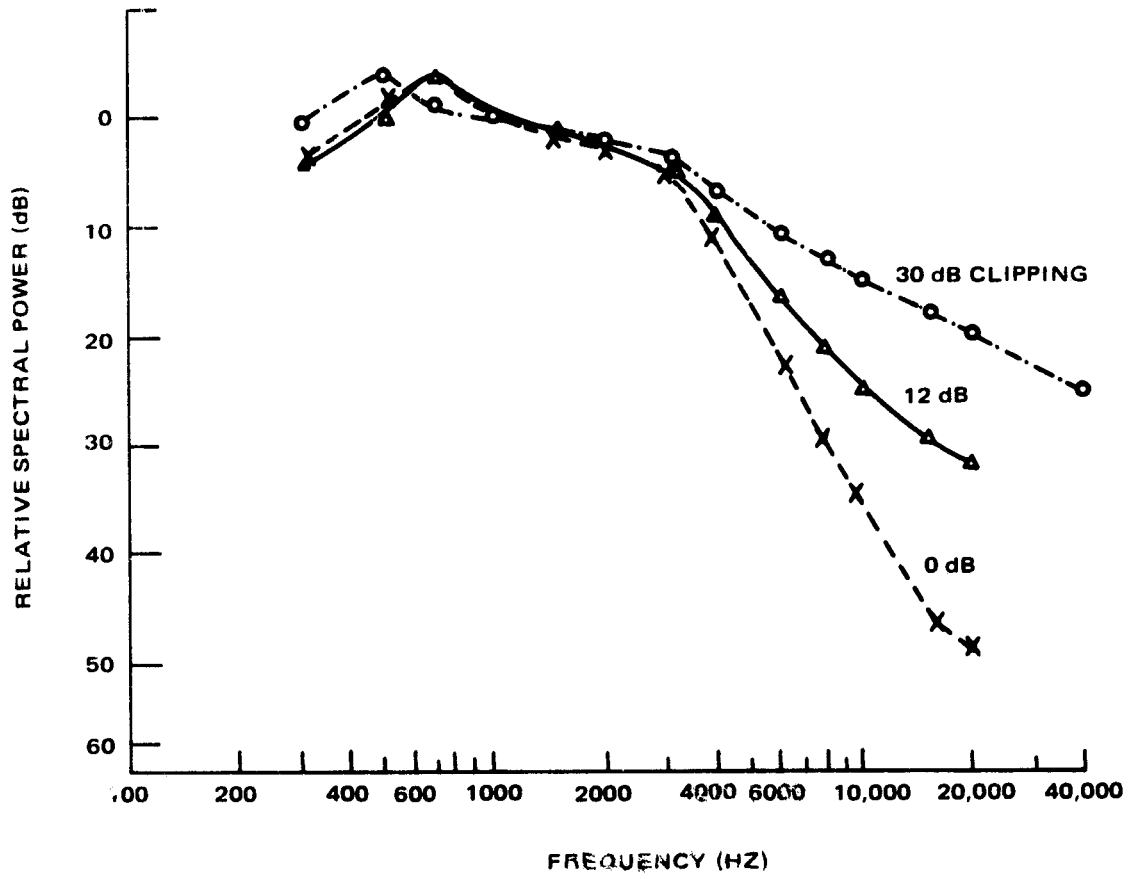

Figure 2-32. Relative Spectral Density of Differentiated Speech with Different Clipping Levels

The unprocessed speech curve applies to simulating the spectral density curve of speech by a low-pass filtering of flat Gaussian noise approximately 9 dB/octave above 500 Hz and in addition by an 18 dB/octave low pass filter starting at 3 kHz. This filtering both meets voice quality acceptance and typical filtering assignments in transmitter modulator amplifiers. Differentiation of a speech signal is performed by using a high pass filter between about 700 Hz and 3 kHz and this provides some useful gain word intelligibility by preventing serious suppression with unprocessed speech of the high frequencies by the stronger low frequencies during the limiting process.

A recent paper by Glasser[3] has shown that adjacent channel operation is possible with acceptably low intermodulation cross-talk with only 25 kHz channel spacing. Thus channel characteristics and filtering are the same as above with a deviation of 5 kHz, or a modulation index of 2 for his 2.5 kHz test signal. With this signal, the adjacent channel level can be about 60 dB greater than the in-channel level. Each one kHz less deviation produces about 5 dB greater immunity. This amount of filtering reduces adjacent channel interference to a level about the same as caused by an unprocessed voice with FM modulation.

Clipping up to 12 dB, which provides speech with acceptable audio distortion, can be filtered easily so that adjacent channel cross-talk is little worse than with no clipping. Greater than 12 dB of clipping introduces more than acceptable audio distortion for many services and in the limit of infinite clipping, close familarity with the speaker is required to not lose speaker identification capability. A clipping level of 12 dB provides the major amount (60%) of improvement possible in the increase of its RMS level by providing 8.5 dB of the 14 dB maximum improvement obtainable by infinite clipping. Thus, up to 12 dB of the clipping is preferred for the most efficient voice link with acceptably moderate distortion.

Without noise at the input to the microphone and headset, the word intelligibility of 12 dB clipped speech is 95% for a "random word test list." With only a 15 dB SNR input signal ratio at the microphone and 24 dB SNR output at the headset, the word intelligibility will fall to 87%, a level which still gives practically complete phrase and sentence intelligibility. Radio link noise in combination with environmental headset noise that provides the usual minimum of 10 dB SNR (RMS) at the headset output will lower the word intelligibility to 75% which provides phrase intelligibility of an acceptable level. Because this level of link noise occurs only about 1% of the time in the statistical analysis, the complete system intelligibility is still acceptably high 99% of the time, on the average. A 10 dB output RMS signal to RMS noise will be specified for the communication link. (Table 2-20 is from the referenced report and shows the relation of SNR and word intelligibility in more detail.)

Thus, the specification of the speech signal and its environment in terms of microphone and headset noise has been established. Twelve dB of clipping is recommended for as low as a 15 dB RMS input signal/noise ratio. Also 2700 or 3200 Hz speech bandwidth is recommended to minimize intelligibility loss, which is 20% and 15% for the two bandwidths respectively.

TABLE 2-20. WORD INTELLIGIBILITY AND SNR RELATION

Mike Input SNR (RMS)	Peak Clip Level (dB)	Word Articulation Scores For Headset Output S_{RMS}/N			
		24	19	14	10
30	6	94	92	87	78
	12	94.5	93.5	90	82
	18	94	93.5	91.5	86
	22	93.5	93	91.5	87
15	6	90	89	83	68
	12	87	84	82	75
	18	82	82	81	68
	22	76	76	68	60

This loss occurs due to frequency truncation before added noise degrades the quality further. A 2300 Hz bandwidth would lose an excessive 35% intelligibility. Filtering with 18 dB/octave before clipping together with differentation and 18 dB/octave filtering after clipping is advisable. A minimum of 15 dB input RMS SNR is to be considered which, used with 12 dB of clipping, optimizes the word intelligibility at 75% (see Table 2-20). Long hold time constants in the order of 5 seconds in the AVC amplifier are advisable to keep the output level noise at least 10 dB below the normal voice level during inter-syllable pauses. Push-to-talk operation also tends toward providing a low noise level with normal AVC attack times.

To provide a satisfactory voice link at L-band frequencies with an earth coverage antenna, the average transmitter power may be minimized by using the axis crossings only of heavily clipped speech to pulse position modulate (PPM) a high peak power transmitter for a short ON time to provide a low average power. (Table 2-20 then applies by using the 22 dB clipping lines of data.) An alternative method is to use a special (retrodirective) phased array at the satellite which provides high antenna gain along with wide-beam coverage, thus enabling FM voice links to be established with moderate RF power requirements.

2.7.2 MODULATION-DETECTION PERFORMANCE

The average carrier power required will also depend on the threshold C/N_t of the detection system as measured in the predetection noise bandwidth of B_{if}. For AM (see Figure 2-33) C/N_t is + 2 dB for a 1 dB loss efficiency; for FM it is 6 to 12 dB depending on the modulation index and the sophistication of the detection technique as shown in Figure 2-34. The minimum IF predetection bandwidth of the detector will vary as the modulation index m varies; viz., (by Carson Rule)

$$B_c = 2f_m (1 + m) \qquad (1)$$

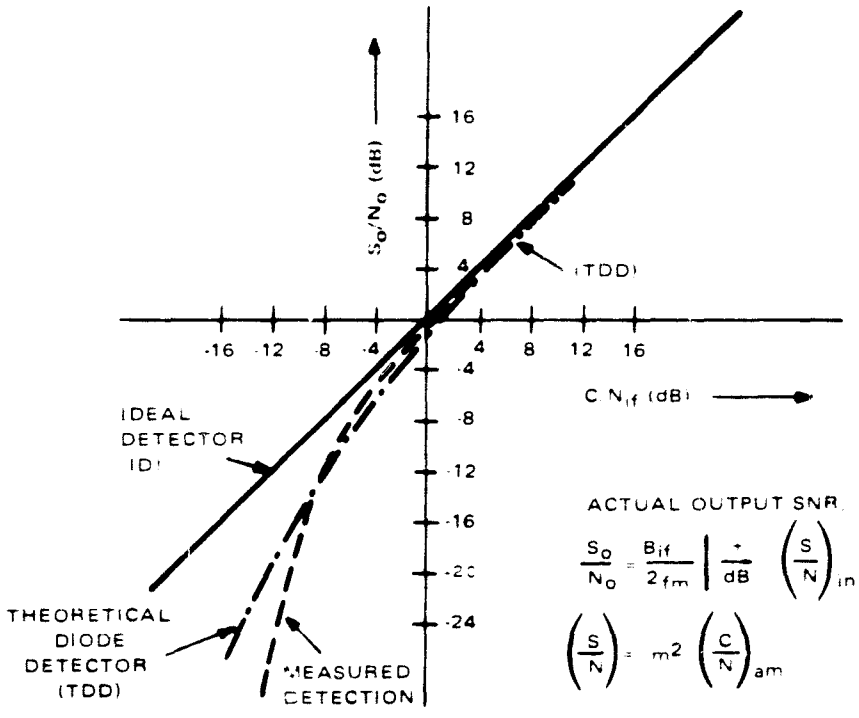

Figure 2-33. AM Detection

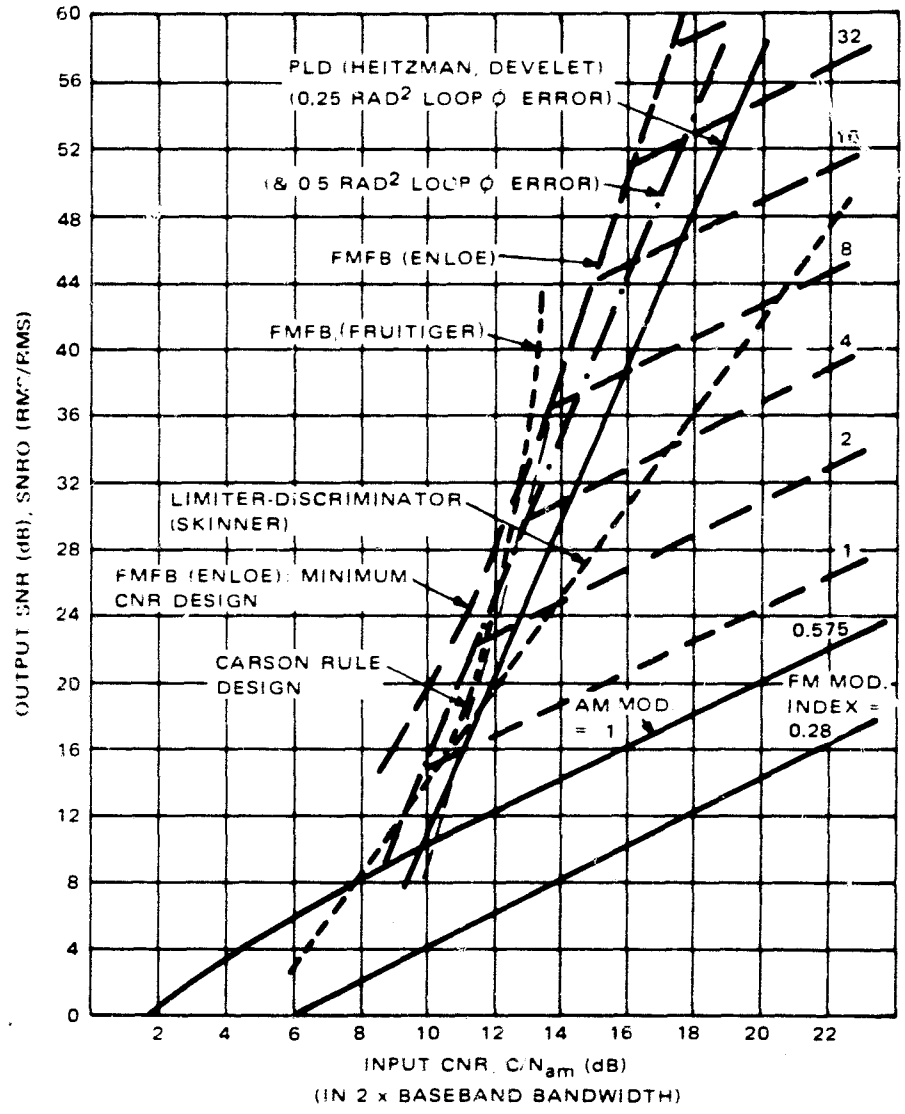

Figure 2-34. Detection Thresholds (Sinewave Modulation)

This expression is the usual definition of bandwidth for analog signals to secure acceptably low distortion in FM for m values of unity and above. With narrow band modulation, m of about 0.5 or less, the bandwidth may be taken as only $2f_m$, with some acceptable increase in distortion for particular applications like speech. Theoretical and measured thresholds are shown in Table 2-21.

TABLE 2-21. C/N_{ift}* THRESHOLDS OF FM DETECTION TECHNIQUES (dB)

Mod. Index, m OR $\frac{B_{if}}{2f_m} - 1$	FMFB			PLL (Develet,** Viterbi)	Limiter Disc (Foster Seely)		Pulse Count (Maclean, Baghdady)		Measured Performance		
	Enloe	Frutiger			Skinner	Dowling			LIM DISC MM 600 CW 60	Lunar Orbiter	
		C/N_{if}	C/N_{am}				L D	FMFB ***		FMFB	PLL
1	7.8	5.5	8.5	9.5	4	4	10	12	-	-	-
2	7.0	5.6	10.4	9.2	7	6	10	12	9	7.5	9.5
3	6.5	5.0	11	9.0	8	7	10	12	10	7.0	9.2
4	5.7	4.5	11.5	8.5	9.5	8	10	12	-	-	-

* Threshold values are those, in preselection IF bandwidths, dropping 1 dB below ideal realizable output SNR as the input CNR is decreased.

** PLL values correspond to a 0.25 mean square radian error in the loop, allowing 0.5 radian error would lower the PLL values by about two dB.

*** In narrow IF loop bandwidth.

There is variance between thresholds for even the same type of detector shown in Table 2-18. However, measured data is close to the performance predicted by Skinner[6] for the Foster Seely detector; data for PLL detection agrees with Develet's[7] analysis using his evaluation for a mean square radian error of 0.25 (which is close to Heitzman's[8] results for the same noise level); and the FMFB measured data is fairly close to Frutiger[9], and even closer to Enloe's[10] values. These values apply to the Carson rule predetection bandwidth B_c of $2f_m$ (1 + m).

Any bandwidth B_{if} exceeding this value to include channel instabilities lowers the thresholds of FMFB and PLL detectors by the ratio of 10 log (B_{if}/B_c); e.g. in ARINC letter #26, the closed loop bandwidth is 18.4 KHz for the new 25 KHz channelization whereas 43 KHz is the present channel bandwidth of the Bendix R-51 AM receiver. The 10.4 dB threshold for the closed loop bandwidth checks closely the measured performance of a PLL of Table 2-21. See Appendix 2.7.2-A for a full development of the limiter/discriminator detector. In the 43 KHz bandwidth, the $C/N_t = 10.4 - 10 \log (43/18.4) = 10.4 - 3.7 = 6.7$ dB. This is significant only in the sense that if the bandwidth exceeds the maximum bandwidth necessary it has only a slight effect on the lock-up performance of the loop and does not affect the loss of lock described by the threshold phenomenon over that for an 18 KHz bandwidth.

The thresholds then applicable for the different types of FM receivers will be assigned as favoring realizable measurable performance; viz. C/N values of 9.5, 7.5, and 9.5 dB for the standard Foster Seeley, FMFB and PLL types respectively for a modulation index of 2 and 18.4 kHz channel noise bandwidth. There is obviously some gain (2 dB) in using FMFB over the performance of the standard well designed limiter-discriminator. PLL shows no gain even though theoretically it should be better by some analyses.

2.7.2.1 AM MODULATION/DETECTION

A comparison with AM receivers on a threshold basis will be made in view of Figure 2-33 showing theoretical and measured thresholds of AM receivers. In the receiver used, sufficient gain is used to AGC on noise in the absence of carrier. This operation is normal and establishes a slightly better linear detection condition in the diode detector than is usually assumed to be a theoretical square law device. Figure 2-33 shows only about half the degradation measured as predicted, which is 1 dB loss from a linear detector at a C/N_{if} value of + 2 dB for a theoretical model and at a C/N_{if} value of -4dB for a practical receiver.

Just like output SNR and threshold effects in FM receivers with extra bandwidth, the extra bandwidth due to frequency and circuit instabilities and doppler frequency in AM also determines the output SNR, S_p/N, where S_p = peak output signal.

$$\frac{S_p}{N} = 2\,m^2\,,\ \frac{B_{if}}{2\,f_m}\,,\ \frac{C}{N_{if}} \qquad (2)$$

where:

$B_{if} = S + 2\,(f_i + f_d)$ (3)

S = spectral bandwidth of signal

f_i = channel instabilities

(for receiver oscillator stability of 2×10^{-5} and transmitter oscillator stability of 1×10^{-5})

f_i = 3.9 KHz at VHF (130 MHz)

= 48.0 KHz at L-band (1600 MHz)

f_d = doppler frequency

(for Mach 3 relative velocities)

f_d .39 KHz at VHF

4.8 KHz at L-band

Thus:

$f_i + f_d$ 4.3 KHz at VHF

52.8 KHz at L-band

2.7.2.2 FM MODULATION/DETECTION

The FM detection performance is similarly

$$\frac{S_p}{N} = 6\ m^2\ \frac{B_{if}}{2\ f_m} \cdot \left(\frac{C}{N_{if}}\right) \quad \text{if} \quad \frac{C}{N_{if}} \geq X \tag{4}$$

where X is the threshold value determined by the particular type of FM detector developed above as 9.5, 7.5 and 9.5 respectively for Foster Seeley Limiter/Discriminator, FMFB and PLL discussed above. Those numbers apply to a modulation index of 2 and a noise bandwidth of 18.4 kHz, which represents the ARINC type of FM system.

A more general analysis incorporating an optimum modulation index and dependent on the amount of speech clipping used is possible with its results shown in Table 2-22. The clipping levels selected are popular values with 6 and 12 dB values representing what ARINC is considering and 30 dB representing "infinitely" clipped speech processing. Peak signal to RMS noise ratios of the second column are values by Licklider[11] and others.

TABLE 2-22. SPEECH CLIPPING & DETECTION TECHNIQUES

Speech Clipping Level (dB)	Required * Peak Sig. / RMS Noise S_p N (dB)	Modulation Index (m)			Mod.** Spectral Width, S (kHz)	Receiver IF BW $B_{if} = S + 2(f_i + f_d)$ (kHz)	(C N_{AM}) Threshold Values in IF BW of 2 f_m			
		Lim. Disc.	FMFB	PLD			L/D	FMFB	0.5 rad² PLL	AM Detection
0	24	1.4	1.8	1.8	14.6	23.2	15.5	11.5	11	21
6	19	.83	1	1.1	11	19.6	14.5	11	10	16
12	15.5	.60	0.7	0.8	9.5	18.1	14	10.5	9	12.5
30	10	.33	0.4	0.5	8	16.6	13	10	8	7

* These provide 10 dB output SNR, S_{RMS}/N, for 70% to 80% word intelligibility.

** From Carson Rule, $S = 2\ f_m\ (1 + m)$ and $f_m = 2.7$ kHz.

The next three columns list the optimum modulation indices for different detection techniques used as a function of the clipping level. These are derived using bandwidths in the next two columns based on equations (1) and (3). The limiter/discriminator requires a special analysis found in Appendix 2.7.2-A because of the threshold determining ratio, B_{if}/f_m. The analysis develops both the optimum modulation index and the threshold CNR required. The remaining indices for FMFB and PLD are read from Fig. 2-34 curves which are based on published analyses (Ref. 6-10). Some slight modifications were made to the individual analyses to normalize their results along with combining features of the mathematical models used to provide the most comprehensive simulation. A number of receivers designed measure within a dB of the thresholds predicted by those of Figure 2-34.

In order to easily present the differences in transmitter powers required for the three detection techniques, the threshold CNR used is referrec to the noise in the equivalent AM IF bandwidth equal to $2f_m$, the output noise bandwidth for which the output peak signal to RMS noise, S_p/N, ratio applies.

An illustration showing the relative carrier powers of the systems will be considered by assuming no clipping; for example, the relative AM carrier power to the FM carrier power for a limiter/discriminator is 21 - 15.5 or 5.5 dB more for AM. To show the other extreme, the use of 30 dB of clipping shows 13 - 7, or 6 dB less carrier power is required for AM.

An interesting observation is that for 12 dB of clipping, the FM system is still about equal to the AM efficiency and because 30 dB of clipping does produce subjective problems for some applications, there is a clear cut choice to use FM with up to 12 dB of clipping and AM for 30 dB of clipping and particularly if FMFB or PLL detection is used. The choice of AM for high levels of clipping is reinforced by the poor impulse noise suppression for the low FM modulation index of only 0.5 which would suffice for FM with this level of clipping. This is not to say in converse that the poor suppression of impulse noise in AM detectors is a serious detriment to AM performance because impulse noise cancelling circuits in AM do almost the equivalent of wideband FM for noise impulses; in fact, what can be done for AM in this manner applies to narrow band FM (m = 0.5). The fact is simply that wideband FM essentially does this without the addition of noise cancellation circuitry. Further, limiting used in FM solves a good portion of the AGC problem of AM receivers and also provides better efficiency in transmitters by hard limiting with frequency division multiplexing if this type multiplexing is necessary and if the intermodulation noise power per channel is minimized by the proper choice of the channel frequencies.

A conclusion drawn from Table 2-21 is that once having decided in favor of FM by the above arguments with 12 dB or less of clipping, there is only one or two dB reduction in the carrier power required for a given detector system as clipping increases from zero to 12 dB, although there is 4.5 to 5 dB gain in choosing among the lim/disc, FMFB, or PLL techniques.

2.7.2.3 PULSE POSITION MODULATION (PPM), HEAVILY CLIPPED SPEECH SYSTEM

In an effort to reduce the requirement of transmitter power at L-band to mitigate the greater path loss than for a VHF link, a natural direction to pursue is to process voice more (greater than 12 dB of clipping), and to use a modulation technique compatible with it to improve SNR. The axis crossings that carry the intelligibility of infinitely clipped speech in the absence of any amplitude variation, may be transmitted at the nearest axis crossings of a clock frequency of 8 Kilobits/sec without any significant loss of intelligibility over that loss due to clipping alone. With this transformation of the random axis crossings of clipped speech to clocked crossings, both pulse position modulation and TDM multiplexing may be conveniently used to advantage for either a single or multiple channel speech system respectively.

Because some listeners describe clipped speech as losing significantly in speaker identification, this subjective side of system evaluation imposes listening tests for a final approval, although the recognition quality is still present to some degree and the need for recognition is a subjective value anyway in this application.

System Analysis - The analysis of one of the likeliest candidates for the modulation technique to be used is in appendix 2.7.2.3-A. The pulse-position modulation (PPM) system described there obtains improved signal-to-noise (SNR) by bandwidth expansion similarly to FM improvement. Although PPM gains only as the ratio of transmission bandwidth to the modulating signal bandwidth compared to the square of that same ratio for FM (see equations 14 and 17 of appendix), about the same threshold level of predetection SNR is attained by a high power, short duration pulse with PPM whereas FM refers to a continuous level carrier. The average power of PPM is about equal to the FM average power required for a typical voice system. For low to moderate SNR values applicable to speech systems for traffic control, PPM would seem most applicable, if characteristics of heavily clipped speech are put to use.

The mean-square SNR available from PPM is derived in appendix 2.7.2.3-A (equation 9) to be:

$$\frac{S}{N} = 0.077\left(\frac{f_b}{f_m}\right)^2 \cdot \frac{C}{N_b}$$

where f_m = 3.3 kHz for a speech system, speech mean-square S/N values are shown in Table 2-23 for different pulse widths of 2T and the predetection bandwidth, f_b = 1/T, (exclusive of any equipment channel tracking and doppler error effects on the bandwidths of the channel). A threshold value for C/N_b is assigned as 12 dB as derived in Appendix 2.7.2.3-A. In the equivalent AM bandwidth, the C/N_{am} threshold is $(C/N_b) + 10 \log (f_b/2f_m)$

TABLE 2-23. EFFECT OF PULSE WIDTH ON TRANSMITTER POWER

Pulse Width, 2T (μs)	f_b (kHz)	$(f_b/f_m)^2$	C/N_{am}	S/N (dB)	* C/N_{am}	3.3/2.7 (dB)	Net (dB)	P_t (kW)
61	33	100	19	21	+ 8	-1	+ 9	4.4
34	59	316	21.5	26	+ 10.5	1	11.5	7.8
19.2	104	1000	24	31	+ 13	1	14	14.0

* Compared to 11 dB of UHF Link Analysis.

In view of the previous analysis of the L-band link, the above values of C/N_{am} together with 3.3 kHz speech band, compared to 2.7 kHz used for the FM analysis, determine the increase in pulse power compared to CW power of the FM system. This comparison is shown in the column marked "Net (dB)," and the peak pulse power is then this many dB above the 550 watts of the FM analysis.

From equation 10 of Appendix 2.7.2.3-A, the mean-square power of the raised cosine pulse waveform is

$$P_{SC} = \frac{3 f_m P_T}{f_b}$$

For the values of the table, P_{sc} values are 1.3 kW for pulse durations of 61, 34 and 19.2 s, respectively.

Conclusions on PPM - Because certain academic luxuries are always assumed in analyses, those included in this analysis are listed:

1. No allowances for guard bands in modulating to the maximum time theoretically available, and
2. No allowance for bandwidth increase requirement for a doppler environment and frequency drifts and uncertainties of receiver/transmitter channelization oscillators.

These impose a modest reduction on the realizable SNR and a like increase in the power P_t of those values shown in Table 2-23; e.g., if oscillator stabilities in the order of 3 parts per million are in use in the 1970-1980 period for Mach 3 aircraft, an L-band R/T system will need about 20 kHz additional bandwidth so the signal remains in the receiver passband. This bandwidth added to those, f_b, of Table 2-23 will not reduce the 12 dB threshold C_{rms}/N_{rms} below AM detection threshold so the added IF bandwidth will not affect the recovered video SNR in the f_b baseband. Allowing 20% guard band with less than full time modulation, λ, about 1.5 dB less S/N is recovered.

A further consideration will help determine which of the three examples of pulse-widths should be used. As pointed out in the introduction, clipped speech intelligibility falls from 75% to 60% as the link SNR falls from infinity to 10 dB. Because infinitely clipped speech quality is significantly lowered by microphone noise a best trade-off between that noise and link noise is to keep the latter low. An overall S/N ratio of 10 dB can then be best realized by specifying the link S/N ratio to be at least 20 dB. This value can be provided by all pulse width listed in the Table. Since L-band channel bandwidths are expected to be at least 100 KHz, a pulse width of 34 μsec can be accommodated even with doppler and channel drifts of 20 KHz. A pulse width of 19.2 usec would exceed the 100 KHz channel bandwidth, provide an excessive SNR and require a peak power of 14 KW. This rationale leads to a choice of the 34 μsec pulsewidth system with a 100 kHz receiver bandwidth, which provides about 24.5 dB output SNR (including 1.5 dB loss for 20% guard band).

The speech characteristic made use of to reduce the PPM transmitter power below the power required of FM is the low average number of axis crossings of heavily clipped speech - about only 1400/second. This means that the 8 kHz clock which would be practical for normal speech of 3 kHz upper frequency does not need to produce a transmitted pulse at each clock interval but only at 1400/8000 or 17.5% of these. The 1.3 KW average power required will then reduce to 0.175 x 1.3 KW, equal to 230 watts.

Even though the required power for PPM compares favorably with the FM requirement, this favorable comparison is made possible by the use of severely clipped speech in the PPM analysis only. Because the quality of this type of speech is not acceptable for some services, FM is considered best for the aviation and maritime requirements now envisioned.

2.7.3 REFERENCES

1. "International Radio Consultation Committee (CCIR), Documents of the Xth Plenary Assembly," Vol. IV, Report 218, Geneva 1963, pp. 272-286.

2. W. Watken-Dunn and D.W. Lipke, "On the Power Gained by Clipping Speech in the Audio Band," JASA 30, 36 (1958).

3. J.R. Glasser, "Adjacent Channel Interference in FM Communications Systems," 18th Annual IEEE-VTG Conference (IEEE), Dec. 68, 1967.

4. H.E. Rose, "Performance Evaluation of Clipped Speech," 1967 Conf. on Speech Communication and Processing, MIT.

5. K.D. Kryter, "Methods for the Calculation and Use of the Articulation Index," JASA, Vol. 34, No. 11, Nov. 62, pp. 1689-1696.

6. F.J. Skinner, Unpublished Memorandum referred to in Enloe's paper (ref. below), page 485.

7. J.A. Develet, J.A., Jr., "A Threshold Criterion for Phase-Lock Demodulation," Proc. IEEE, Feb. 1963, p. 349.

8. R.E. Heitzman, "A Study of the Threshold Power Requirements of FMFB Receivers," IRE Trans. on Space Electronics and Telemetry, Dec. 1962, pp. 249-256.

9. P. Frutiger, "Noise in FM Receivers with Negative Frequency Feedback," Proc. IEEE, Nov. 1966, pp. 1506-1520.

10. L.H. Enloe, "The Synthesis of Frequency Feedback Demodulators, "Proc. National Electronics Conference, 1962, pp. 477-497.

11. J.C.R. Licklider, "Effects of Amplitude Distortion Upon the Intelligibility of Speech," Jour. of Acous. Soc. of America, Oct. 1964, pp. 429-434.

2.8 VOICE LINK ANALYSES

Voice link analyses have been made for both VHF and UHF (L-band) channels. The analyses shown for the VHF channel have been strongly influenced by equipment performance as described in current SATCOM receiver tests for which the carrier to noise ratio (CNR) at threshold is specified. The threshold is three to five dB higher than presented in Table 2-22. From the AEEC SATCOM Newsletter No. 26, the threshold is stated to be 53 dB/Hz which is confirmed from Figure 1 of this letter. With an 18.4 KHz loop bandwidth, this 53 dB converts to 53 less 10 log 18,400 or 10.4 dB; the threshold is stated to be 1 dB below this, i.e. 9.4 dB. Although a 2.25 KHz "Climax" voice filter is used, let 2700 Hz be its probable noise bandwidth; then, referred to an equivalent AM bandwidth of 2 (2.7) or 5.4 KHz, the threshold CNR, C/N_{am}, will be 10.4 plus 10 log (18.4/5.4) or 15.7. Theoretical considerations as shown by Figure 2-34, and supported in good measure by experiment, show a 12.5 dB (0.25 rad^2) threshold should be realizable. The 3.2 dB difference between the 15.7 and 12.5 dB values should be considered as a realizable additional reduction in transmitter power as PLD receivers attain improved performance.

Twelve dB of speech clipping will provide another two dB reduction in transmitter power as shown by Table 2-22. This gain is included in the final derived value of transmitter power for the UHF (L-band) channel analysis to lower the power significantly from its otherwise very high value at very little attendant degradation to speech quality. The level of clipping used does influence the parameters of the system by in general requiring less peak signal to RMS noise ratio as clipping increases which allows less modulation index with the attendant gain of lessening the channel bandwidth. The modulation/detection study shows that 12 dB clipping will theoretically allow 25 KHz channel spacing whereas no clipping indicates 50 KHz spacing would be preferred to minimize adjacent channel interference.

The link analyses for FM of an analog voice channel at either VHF or L-band use identical requirements of SNR, channel stabilities, etc., except as noted above. In order to minimize the heavy demands of transmitter power on the L-band system, 12 dB of clipping is included to arrive at the 275 watts specification. The two dB savings with 12 dB of clipping over that of unprocessed speech specified for the VHF system reduced the power from 550 watts. These L-band levels do not include any reduction possible with the use of a retrodirective satellite antenna.

The pulse-position-modulation system included in L-band analyses needs no separate link analysis from the L-band analysis for FM, all parameters being the same except for more efficient use of transmitter power by bandwidth expansion. In obtaining a most efficient system by reducing the equivalent digital speech bandwidth, heavily clipped speech is used to reduce the number of speech samples required for speech below that of straight sampling of voice or of even delta-modulation systems. A transmitter average power of 460 watts has been derived in the mod/det section compared to 275 watts of the FM system with 12 dB of clipping. The PPM peak power required is 7.8 KW.

2.8.1 NAV/TC VHF VOICE CHANNEL LINK ANALYSIS

The satellite-to-aircraft voice link is the most critical in the Nav/TC system since it requires more satellite prime power than does the satellite-to-ground control link. Table 2-24 gives the principal satellite, propagation, and aircraft parameters. The appendix details some of these parameters and gives an idea of some of the uncertainties in them.

The link shown has 0.0 dB margin in C/N in the phase locked loop and +3.1 dB margin in output S/N at threshold, for a 30 W VHF transmitter in the satellite. Most of the equipment parameters are worst-case (minimum power output, worst antenna pointing angle, etc.), and propagation parameters (multipath, scintillation, etc.) are believed to be for reasonably bad conditions. Propagation conditions between a satellite and an aircraft at VHF are just now being measured and are still very uncertain for many values of the path and temporal variables.

2.8.1.1 SATELLITE PARAMETERS

The satellite is earth-oriented in a synchronous equatorial orbit. Lines 1 through 9 of Table 2-24 define the satellite and free-space link parameters. Each VHF voice channel is transmitted through the earth-coverage antenna by a 30 watt (nominal) transmitter. Because of size limitations, the antenna has the conventional beamshape and 55% efficiency. Both could be improved at the sacrifice of a larger aperture. In particular, the beamshape could be modified to favor the edges of the earth where free-space path loss and the additional propagation loss due to scintillation and multipath are greater.

2.8.1.2 PROPAGATION PARAMETERS

These include the polarization loss and the scintillation and multipath losses, which are given in lines 10 and 11 of Table 2-24.

2.8.1.2.1 Polarization

At 130 MHz, Faraday rotation precludes the use of linear polarization on both satellite and aircraft antennas. To minimize polarization loss, both antennas are nominally circularly polarized. The satellite antenna has a maximum axial ratio of 3 dB over the full earth-coverage beamwidth. The aircraft antenna has an axial ratio of 3 dB or less at most look angles; however, the axial ratio may reach 6 dB at some look angles depending on the antenna location.

Angle between semi-major axes of antenna polarization ellipses = θ

Satellite antenna voltage axial ratio = $R_1 = 1.414$

Aircraft antenna voltage axial ratio = $R_2 = 1.414$ (nominal), 2.0 (maximum)

TABLE 2-24. NAV/TC VHF VOICE CHANNEL LINK CALCULATION

	Parameter	Value	Link Value
1	Frequency	130 MHz	
2	Transmitter Power (In Spacecraft)	30 watts	+ 14.8 dBW
3	S/C line and diplexer losses		- 1.0 dB
4	S/C antenna beamwidth (17.6° earth + 1° attitude error)	18.6°	
4A	S/C antenna diameter	28.5 feet	
5	Antenna gain at 55% efficiency		+ 18.7 dB
6	Beam edge loss		- 3.0 dB
7	Minimum A/C elevation angle to satellite	10°	
8	Maximum S/C to A/C range	25,250 s.mi.	
9	Path loss $(\gamma\ 4\pi R)^2$		-166.8 dB
10	Polarization loss (ARINC)		- 0.5 dB
11	Scintillation and multipath losses (54 hours/year) (2.5 σ value AFCRL)		- 5.0 dB
12	Line, diplexer, connector losses in A/C (Collins Radio)		2.0 dB
13	A/C antenna gain (Collins Radio)		- 0.0 dB
14	Receiver signal power		-145.8 dBW
15	Receiver noise figure and temperature	4 dB, 430°K	
16	System noise temperature	980°K	
17	Receiver noise density		-198.7 dBW/Hz
18	Phase locked loop bandwidth	18.4 kHz	+ 42.6 dB-Hz
19	System PLL noise power		-156.1 dBW
20	Carrier to noise ratio in PLL bandwidth		+ 10.3 dB
21	C/N threshold in PLL bandwidth		+ 9.4 dB
22	Link margin over C/N threshold		0.9 dB
23	Peak deviation	5.0 kHz	
24	Highest baseband frequency	2.25 kHz	
25	Modulation index m	2.22	
26	FM improvement factor = $3\ m^2\ \frac{BIF}{2fm}$		+ 17.8 dB
27	Degradation in S/N for threshold operation		- 1.0 dB
28	Output S/N* ($S/N = (C/N)_{IF}$ + FM Imp. - Degrad.)		+ 27.1 dB
29	Required Output S/N**		+ 24.0 dB
30	S/N Margin		+ 3.1 dB

* This does not include speech clipping, pre-emphasis, or noise weighting factors. This is test-tone-to-noise ratio.

** This gives 60 to 80 percent word intelligibility.

$$\text{Polarization loss} = -10 \log \frac{(R_1^2 + 1)(R_2^2 + 1)}{(R_1 + R_2)^2}$$

$$= -0.3 \text{ db } (R_1 = 1.414,\ R_2 = 1.414,\ \theta = 90°)$$

$$= -0.6 \text{ db } (R_1 = 1.414,\ R_2 = 2.0,\ \theta = 45°)$$

$$= -1.1 \text{ db } (R_1 = 1.414,\ R_2 = 2.0,\ \theta = 90°)$$

Assuming that maximum satellite antenna ellipticity, maximum aircraft antenna ellipticity, and worst-case angle θ do not all occur simultaneously, an allowance of -0.5 db is made for polarization loss in the link calculation.

2.8.1.2.2 Scintillation and Multipath

These parameters are probably the least well specified of any in the table. The amount of ionospheric scintillation at 130 MHz depends strongly on the sunspot cycle and on the transmission path geometry. Multipath depends on the aircraft antenna pattern, the terrain, and the transmission path geometry.

Measurements of these phenomena which have been made during the past three years do not reveal fully consistent results. The 136 MHz carrier of the Early Bird satellite was monitored for over 2000 hours during the summer of 1965 at the AFCRL in Massachusetts.(1) The results,(2) shown in Figure 2-35 are based on an additional 2000 hours during the summer of 1967. Propagation conditions did not change significantly over this period of 2 years. Note that over this particular path (elevation angle 25°), scintillation fading greater than 4 db occurs less than 1 percent of the time. Of these fades, 96 percent are less than 1 minute long, and 99 percent are less than 2 minutes long. These fades are not due to multipath reflections, but only to ionospheric scintillations.

---

(1) "Ionospheric Scintillations at 136 MHz from a Synchronous Satellite," Aarons and Whitney, AFCRL, Planet. Space Sci., pp. 21-28, 1967.

(2) "Comsat Corporation Data on Scintillation on VHF Satellite Communication," AEEC Satcom Newsletter No. 29, February 20, 1968.

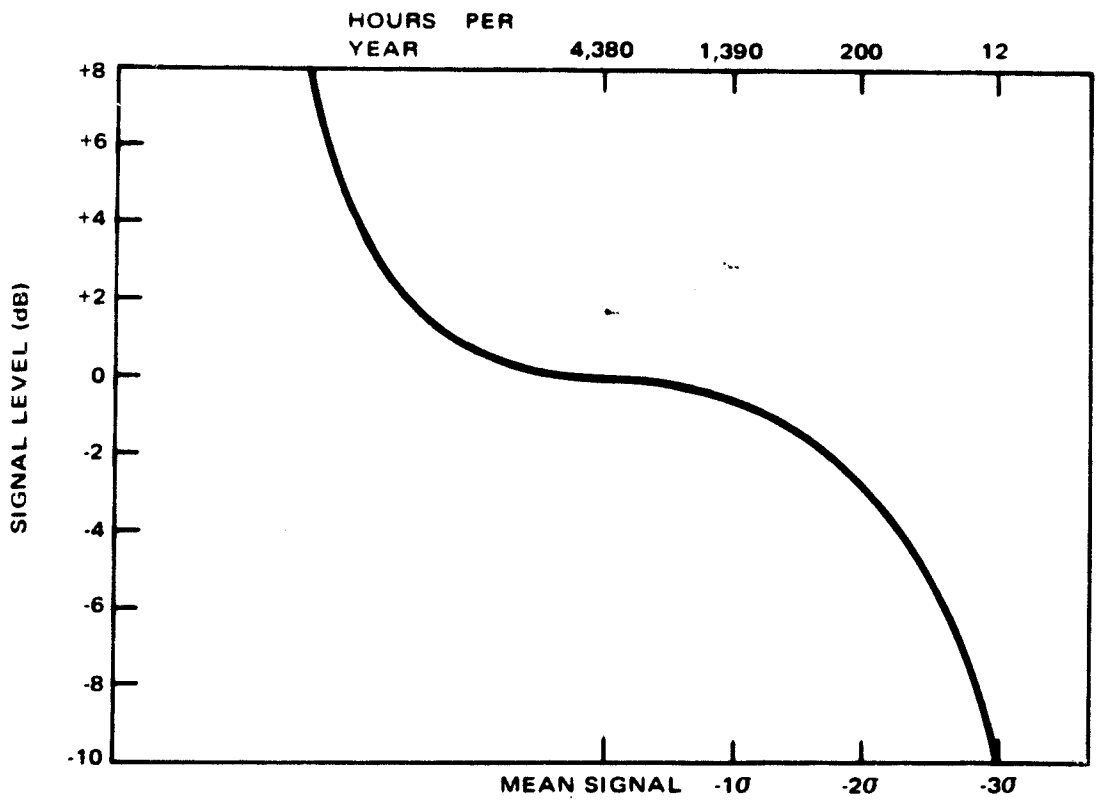

Figure 2-35. Ionospheric Scintillation At 136 MHz: Early Bird To AFCRL, Summer 1967 (25° Elev. Angle)

Multipath has been measured at 230 MHz,[3] 328 MHz,[4] and in the 225-400 MHz[5] band. At 230 MHz,[3] no fading attributable to ionospheric (scintillation) effects was observed. Below 2° elevation angle severe (20 to 30 db) fading, caused presumably by tropospheric ducting, was observed. Between 5° and 10° elevation angles, fading of 10 db occurred with a UHF blade, top-mounted, over smooth ocean water. Specular fading occurred for elevation angles up to 20°.

At 328 MHz,[4] over smooth land, fading of up to 23 dB was observed between two aircraft within optical line of sight. Actual elevation angles were -3° for each aircraft; UHF blade antennas were used on each aircraft. The authors also point out that severe fading due to antenna nulls occurred when either aircraft was turning with respect to the other or was otherwise not horizontal.

---

(3) "Measurement of Multipath Effects in a Satellite-Aircraft UHF Link," Jordan, MIT Lincoln Lab. Proc. IEEE, June 1967, pp. 1117-1118.

(4) "Air-to-Air Propagation Characteristics at Extreme Ranges," Ellington and Kirk, Electronic Communications, Inc., 1966 National Electronics Conference Record, pp. 401-406.

(5) "Multipath and Propagation Experiment Utilizing VHF-UHF Satellite Communication System," Foshee and LaVean, Electronic Communications, Inc., AIAA Paper 68-419, April 1968.

In the band 225 to 400 MHz,[5] the results of recent experiments with the LES-5 satellite show less fading at low elevation angles than the previous experiments. The principal conclusions are:

(a) Multipath fading, which can be characterized usually by the simple two-ray multipath model, is almost always encountered on over-water flights when the look angle to the satellite is below 20°.

(b) At angles greater than 25°, fading is not periodic, predictable, or significant (compare the Early Bird test results).

(c) The deepest fading occurs at angles between 10° and 15°.

(d) The level of fading encountered even at low look angles is in general 5 db or less; seldom are the fades as great as 10 db.

(e) To date, the airborne terminal has not experienced any effects which could be definitely identified as scintillation (140 hours of data over 6 months, throughout the world).

(f) Anomalous high-rate fading has been observed occasionally. It occurs for minutes or up to two hours, at high look angles to the satellite, only over water, and only within 30° of the equator. Its origin is unknown.

In summary, normal multipath occurs at elevation angles less than 20°. Its magnitude at 130 MHz is probably in excess of 10 db some of the time. Vertically polarized signals are less susceptible to multipath reflection at these angles; hence an aircraft antenna with polarization diversity may be of some use. The more severe scintillation occurs at the higher latitudes and near the peak of the sunspot cycle. Its magnitude at 130 MHz may exceed 5 db.

Line 11 of the calculation allocates a loss of 5 dB for scintillation and multipath. In addition, the signal level can be reduced 3 dB more than this with resulting output S/N degredation but without the PLL losing lock. This is to say the nominal link (Table 2-24) can support 5 dB propagation loss, and the worst-case link can support 8 dB loss with degradation in the output signal to noise ratio.

2.8.1.2.3 Receiving System Parameters

These include (a) the external environment at the aircraft, (b) the antenna and transmission line, and (c) the VHF SATCOM receiver. The values given in lines 15 through 23 of Table 2-24 are discussed in this section.

---

(5) "Multipath and Propagation Experiment Utilizing VHF/UHF Satellite Communication System," Foshee and LaVean, Electronic Communications, Inc., AIAA Paper 68-419, April 1968.

External Environment - The 130 MHz antenna receives noise from the earth, from thunderstorms, from the galaxy, from equipment on the ground, and from imperfectly shielded radiating sources on the aircraft itself. The first three sources are natural noise;[6,7] the last two are man-made noise.[7]

The aircraft antenna is more or less omnidirectional in the upper hemisphere. The galactic noise it sees will, therefore, not show strong variations as a function of time or latitude. The magnitude of the galactic noise for an upward looking antenna has been determined by several sources [8,9] to be the integrated effective regions of the sky showing small areas of 2000°K and for the greater part about 200°K. The integrated effective temperature is then 560°K.

The temperature of the earth[7] is 300°K (rural land) or 160°K (ocean), and the effect of this is further reduced by the lack of antenna directivity in the lower hemisphere. The noise resulting from thunderstorms is significant[7] at VHF within 100 miles of the storm. Equivalent noise temperatures of several thousand degrees Kelvin (extrapolated to 130 MHz) were recorded 2 miles from a thunderstorm.

Measurements on C-135 (jet) and C-131 (propeller) aircraft[7] indicated interference from both HF and UHF equipment, both of which could be reduced with additional filters. Precipitation static was also observed on the C-131 when flying through clouds; it was not observed on the C-135. The conclusion is that on-board aircraft-generated noise can be controlled to the required levels.

Steady state noise from electrical machinery and ignition circuits on the ground is very high when the aircraft flies over cities. At 226 MHz, a downward-looking dipole measured 20,000°K for most cities. (New York City was 75,000°K, however.) An upward and outward looking omni antenna reduced these temperatures by a factor of 10.

Transmission Line and Antenna[10] - The receiver will include a low-noise preamplifier at the receiver. The noise temperature could be reduced somewhat by placing the pre-amp at the antenna. However, operation in near-sonic and supersonic aircraft would cause such equipment to experience high thermal stress. Further, maintenance would be made more difficult.

(6) Hogg & Mumford, "The Effective Noise Temperature of the Sky," Microwave Journal, March 1960, pp. 80-84.

(7) Ploussios, "Electromagnetic Noise Environment in the 200 to 400 MHz Band on Board Aircraft," Proc. IEEE, Dec. 1966, pp. 2017-2019.

(8) Microwave Engineering Handbook, 1966, p. 208.

(9) MIT. T.N. 1966-59, "Noise Temperature of Airborne Antenna at UHF," Dec. 6, 1966.

(10) Based on AEEC SATCOM Newsletter No. 14, "Airborne VHF Communications Transceiver System," October 10, 1966.

The cable loss at 136 MHz is 2 dB. This is equivalent to more than 100 feet of RG/63, which is large enough to carry the 500 watt aircraft transmitter signal. The antenna VSWR does not exceed 2:1 over the frequency range 118 to 136 MHz. The gain of the pre-amplifier is 20 dB, and its noise figure is 4 dB,[9]

The system noise temperature, at the pre-amplifier input, is then:

$$T_s = \frac{T_a}{L} + \frac{(L-1)}{L} T_1 + T_p = 980°K$$

where

T_a = antenna temperature = average galactic temperature = 560°K (no allowance for aircraft-generated noise, or made-made terrestrial noise)

T_1 = coaxial line temperature = 533°K (500°F ambient of S.S.T. frame)

T_p = pre-amplifier noise temperature = 290°K (F-1) = 430°K

L = 2 dB = 1.59 power ratio

SACTOM Receiver - Based on measurements on 10 prototype SATCOM pre-amps and a standard ARINC 546 receiver,[11] the parameters to be assumed for the link calculation are:

- Noise figure: 4 dB (This is a conservative value, including effect of pre-amplifier and receiver. Measured values are 2.4 dB to 4.0 dB. Page 4)[11]
- IF bandwidth: 43 kHz (measurement on one ARINC 546 receiver)
- Loop noise bandwidth (2 sided): 18.4 kHz (Stated by the manufacturer, Bendix; not measured. Page 10)[11]
- Loop threshold: 10.4 dB (define as 1 dB departure from linearity in the S/N vs. C/N curve; defined in the 18.4 kHz loop noise bandwidth; based on base-band test tone of 1 kHz, m = 1.33, which is approximately 60% modulation. Pages 7-11)[11]
- Baseband bandwidth: 2.25 kHz (Page 9).[11] This bandwidth is determined by the audio output filter in the aircraft receiver ("climax filter")
- FM deviation: The loop C/N threshold is defined for a test deviation of ± 3 kHz (peak to peak). The maximum capability of the receiver, considering PLL design is ± 5 kHz, but the threshold may be slightly greater than 10.4 dB for this deviation.

---

(9) MIT. T.N 1966-59, "Noise Temperature of Airborne Antenna at UHF," Dec. 6, 1966.

(11) AEEC SATCOM Newsletter No. 26, "Test of a Current Airborne SATCOM Receiver," August 22, 1967.

2.8.2 NAV/TC UHF VOICE CHANNEL LINK CALCULATION - SPACECRAFT/USER

To compare with the VHF link analysis, the required transmitter ERP is determined first using unprocessed voice (zero dB clipping), a zero dB user antenna gain and a 6 dB noise figure user receiver preamplifier (remote antenna location). Values for the required threshold C/N_{am} for PLL detection of 11 dB is used from Table 2-22. The link losses are listed in Table 2-25.

TABLE 2-25. UHF MISCELLANOUS LOSSES

Item	Value, dB	Remarks
Scan Edge Loss	3.0	See Note
Polarization Loss	0.3	Ellipticity: Spacecraft 0 dB, User 5 dB
Relay Degradation	0.4	To allow reduction in CNR due to noise of other link (spacecraft - ground)
Multipath Fading	0.5	Estimated allowance; depends on user antenna pattern
Aircraft cable loss	2.0	Estimated (with 100' coax)
TOTAL	6.2	For one channel

Note: The Scan Edge Loss can be reduced to less than 1 dB by pointing the antenna array axis towards the north (say 45° North latitude) if earth coverage antennules are used (with 18.6° beamwidth) but only the North Atlantic region is of interest.

Table 2-26 (UHF L-band) shows that ERP values of 46, 50 and 54 dB W are required at the satellite for one channel, two channel, and four channel operation respectively. To compare with the VHF analysis using an earth coverage satellite antenna, transmitter powers required are 27.2, 31.2 and 35.2 dBW respectively. Thus, a single FM channel would require about 550 watts. Retrodirective antenna arrays reduce this power level to that practically obtainable at this L-band frequency; and additionally, the use of a switched, sector coverage user antenna can reduce the necessary amount of spacecraft antenna gain.

The link calculations assume a 0 dB aircraft antenna. The power requirements can be reduced by using a directional antenna at the aircraft, and various methods of achieving directivity within the necessary physical and aerodynamic constraints are available. It is quite possible that some of these (e.g. sector switching, multiple elements, steerable elements, etc.) may be used, especially because of the small physical size required at L-band and because the relative direction of the spacecraft is known fairly accurately at the aircraft. However, the aircraft power and spacecraft ERP requirements are so modest even with a 0 dB aircraft antenna, given a retrodirective array at the spacecraft that an increased gain is not essential from the power point of view.

TABLE 2-26. UHF LINK CALCULATIONS: SPACECRAFT - USER LINK

Item	Value	Remarks
1. f, frequency, MHz	1560	Nominal, in 1540-1660 MHz band
2. L_p, Path Loss, dB	-188.9	For 26,000 miles, maximum
3. L_m, Miscellaneous Losses, dB	-6.2	For one channel: add inter-modulation loss for multiple channels, see Table 2-25
4. G_a, Aircraft Antenna Gain, dB	0.0	Assumed
5. Sum of Lines 2 thru 4, dB	-195.1	For one channel. See Line 3
6. CNR desired, dB, in IF spectral bandwidth of 14.6 KHz	7.0	No clipping, 24 dB SNR, PLL, (11 dB in baseband of 6 KHz)
7. B, Noise bandwidth, dB-Hz	41.7	B = 14.6 KHz
8. N_o, Noise density, dBW/Hz	-198.0	6 dB noise figure aircraft receiver
9. N, Receiver noise, dBW	-156.3	Line 7 + Line 8
10. C, Required carrier power per channel, dBW	-149.3	Line 6 + Line 9
11. ERP required, dBW, 1 ch	45.8	Line 10 - Line 5
for "good" quality 2 ch	49.8	Includes 1 dB intermodul. loss
voice 4 ch	53.8	Includes 2 dB intermodul. loss
12. Satellite Earth Coverage antenna of gain (dB)	18.6	Same as VHF analysis
13. Transmitter Power, P_t (dBW)		
1 ch	27.2	550 watts
2 ch	31.2	
4 ch	35.2	

For one channel with 30 dB satellite antenna gain:

P_T = 46 - 30 = 16 dBW = 40 watts

With 12 dB of clipping, CNR is 9 dB and with aircraft preamp at antenna:

P_T = 12.4 dBW = 17 watts.

The aircraft antenna pattern is important, however, insofar as multipath is concerned. Thus to avoid multipath fading it is necessary to reject the earth-scattered signal arriving at the aircraft, and this can be done by ensuring that the antenna pattern has a large suppression in the direction of arrival of the earth-scattered signal. In view of the small size of the antenna and its location over a very large conducting surface, it is reasonable to expect that it will be well-shielded from the earth and the undesired earth-scattered signal will be adequately suppressed. (This justified the low allowance of 0.5 dB for multipath fading in Table 2-25.)

The user aircraft must have adequate power to support a voice channel as well as a pilot channel. The latter is necessary for beam formation and beam steering of the spacecraft retrodirective array. Thus the pilot signal is received by the spacecraft with an effective antenna gain corresponding to a single antennule rather than the whole array. The pilot power requirement can be kept reasonably small by appropriate narrowbanding. The voice channel has a wider bandwidth but it uses the full array gain, thus requiring a modest power.

Calculations for both voice and pilot channels are shown in Table 2-27. The array receiver noise figure is assumed to be 5 dB, and allowance is made for the full earth temperature in computing the noise power density. With a 0 dB antenna, the aircraft needs about 20 watts for a pilot channel (6 dB CNR in 1000 Hz) and approximately 20/N watts for a medium quality voice channel, where N is the number of antennules (each with about 19 dB gain) in the spacecraft array. Typically, the array will use 15 to 25 antennules; for N = 16, the aircraft RF power requirement is less than 20 W for a single voice channel. Since the aircraft duty factor is low for this channel (on the order of 2 to 3%) 3 dB additional power margin appears entirely reasonable for the user equipment.

TABLE 2-27. LINK CALCULATION: USER - SPACECRAFT LINK

Item	Value		Remarks
1. f, frequency MHz	1640		Nominal, in 1540-1660 MHz band
2. L_p, Path Loss, dB	-189.3		For 26,000 miles, max.
3. L_m, Misc. Losses, dB	- 6.2		For single channel (100 ft. of coax in A/C)
4. G_s, Spacecraft antenna gain, dB	+19.3		Single element
5. Sum of Lines 2 thru 4, dB	-176.2		
	Pilot	Voice	
6. CNR desired, dB	6	7.5	
7. B, Noise Bandwidth, dB-Hz	30	39.8	1000 Hz for pilot, 9.6 KHz for "medium" quality voice
8. N_o, noise density, dBW/Hz	-199.0	-199.0	5 dB noise figure receiver, plus earth temperature
9. N, Receiver noise, dBW	-169.0	-159.2	Line 7 + Line 8
10. C, Required carrier power, dBW	-163.0	-151.7	Line 6 + Line 9
11. P_a, Aircraft power required for 0 dB antenna) dBW	13.2	24.5	Line 5 + Line 10
Watts	21	280*	Assumes a single element in spacecraft array

*The aircraft power for a voice channel will be 280/N watts if the array uses N elements. Typically, N = 16 so that aircraft power requirement is 16 W for a single channel, at this particular frequency and at 19.3 dB element gain.

Section 3

USER EQUIPMENT

This section describes the user equipments that are recommended for use in the North Atlantic navigation and traffic control satellite system.

The equipments described are:

- Ranging transponder and digital communication equipment for air traffic control.
- Passive ranging equipment for aircraft and marine navigation.
- Interim VHF Voice communications transceiver.
- L-band Voice communications transceiver.
- In addition, antenna and ground support requirements are discussed for the airborne equipment, and critical technology associated with the development of the user equipments is identified.

3.1 USER EQUIPMENT DESCRIPTION

This section describes the recommended design approaches for the following user equipments in the subsections shown in parentheses:

- Airborne user traffic control equipment (3.1.1)
- Airbone passive user navigation equipment (3.1.2)
- Marine user navigation equipment (3.1.3)
- Interim VHF voice communication equipment
- L-band voice communication equipment

} (3.1.4)

A list of preliminary design specifications for each of the above equipments appears in Appendix 3.1-A. This list provides some guidelines for estimating component requirements and costs.

3.1.1 DESCRIPTION OF AIRBORNE USER TRAFFIC CONTROL EQUIPMENT

This equipment is intended for large ocean-crossing commercial aircraft. Figure 3-1 shows the user equipment in simplified form. (Figure 3-2 is a more detailed diagram of this same equipment.)

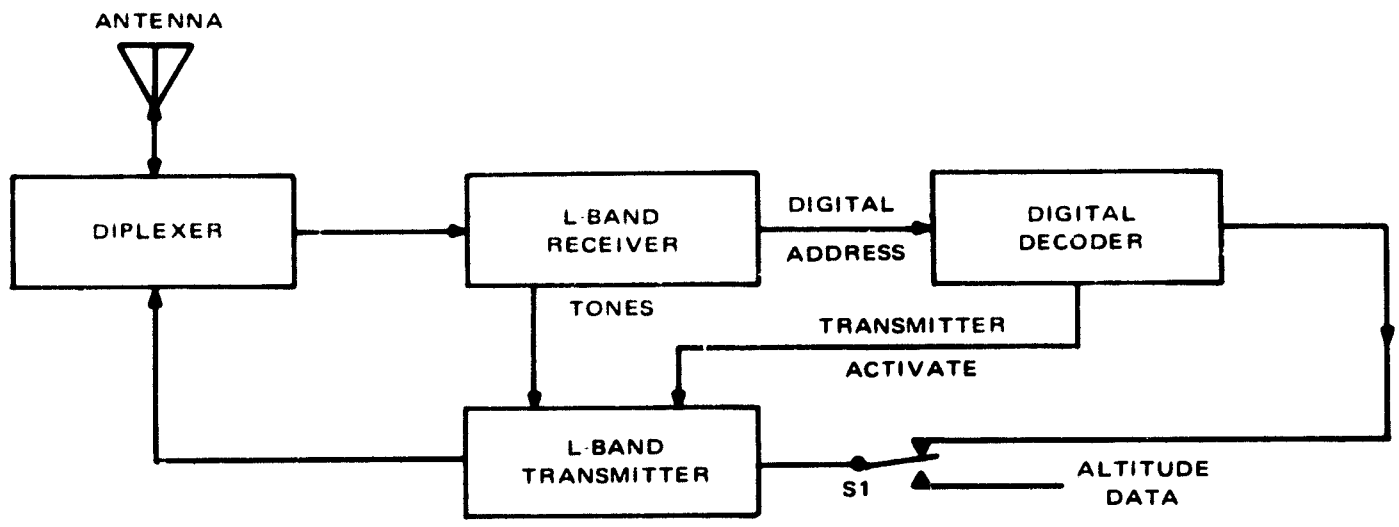

Figure 3-1. Active Mode Aircraft User Equipment (Simplified)

Referring to Figure 3-1, an L-band signal is continuously received from one satellite. This signal contains two range tones (500 Hz and 8 KHz) which are phase-modulated on the carrier frequency. The 500 Hz tone is, in turn, itself bi-phase modulated with digital messages which tell the aircraft user that he is being interrogated.

A single antenna is used and a diplexer routes the incoming signal to the L-band receiver. The receiver detects the two range tones and sends these to the transmitter. The transmitter is activated (turned on) for about two (2) seconds only when the user is interrogated. The Digital Decoder monitors the incoming interrogations and provides an activate signal to the transmitter when the interrogation "matches" the code which is unique to him.

The transmitted signal consists of an L-band carrier which is phase-modulated by the two received range tones. The lower of these tones (500 Hz) is initially bi-phase modulated with the user's address which informs the ground station that the proper user is replying. After the address is sent, S1 of Figure 3-1 is switched to the down position to allow the aircraft's altitude to be relayed to the ground station. S1 is switched automatically by the user equipment.

Referring to Figure 3-2 for the more detailed treatment, the received signal is routed to an L-band pre-amplifier and then to an L-band mixer. The local oscillator signal is offset from the received signal by 60 MHz (nominal), thus giving the desired 60 MHz IF signal. The 60 MHz signal is amplified, then hetrodyned to 7 MHz, and amplified further in a 7 MHz IF amplifier.

The output of the 7 MHz IF amplifier is applied to a phase lock loop (PLL) which locks to the carrier component of the received signal. When the PLL is locked, the 7 MHz VCO (voltage controlled oscillator) output is coherent with the received carrier. The VCO output is therefore available for use as a phase detector reference signal, affording a means of extracting the phase-modulated range tones (8 KHz and 500 Hz).

The 8 KHz detected tone is filtered and sent to a summing network. The summing network, in turn, routes the 8 KHz tone to the transmitter phase modulator for retransmission back to the ground station.

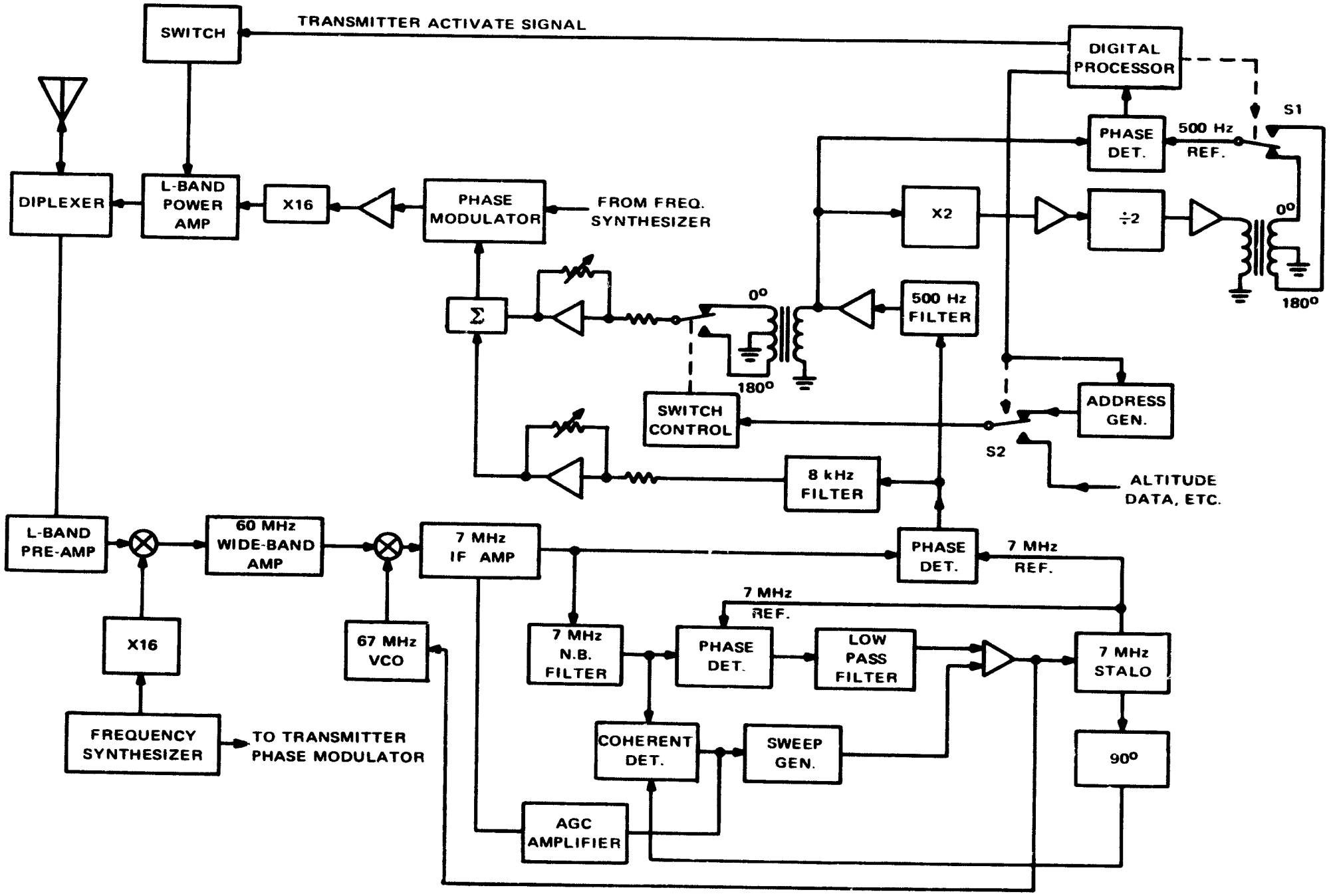

Figure 3-2. Active Mode Aircraft User Equipment (Voice Channel Not Shown)

The 500 Hz tone gets more extensive processing because it contains the interrogation codes. After filtering the 500 Hz tone goes two routes: one of these sends it to the transmitter for retransmission; and the other route goes to the digital demodulation circuits. The output of the digital demodulator is fed to the digital processor where incoming interrogations are compared with the unique address associated with this particular user.

Digital demodulation occurs as follows. The filtered 500 Hz tone is sent to both a phase detector and a times-two-multiplier. The output of the phase detector contains the interrogation codes.

The 500 Hz phase detector reference signal is obtained by times-two-multiplication which removes any bi-phase (0° or 180°) phase modulation. The resulting 1000 Hz signal is then divided by two to obtain the required 500 Hz phase detector reference.

The ground station precedes every interrogation with a synchronizing code. The digital processor determines at this time if the 500 Hz reference is in-phase or 180 degrees out-of-phase with the 500 Hz signal being detected. If an out-of-phase condition exists, S1 of Figure 3-2 is actuated to correct the detected code polarity.

When the digital processor senses that this user is being interrogated, it sends a "transmitter activate signal" (after an appropriate delay) to the transmitter. This activate signal applies prime power to the final stages of the L-band power amplifier, permitting the generation of a 20 watt signal for a duration of approximately two seconds.

Shortly after transmitter activation, the address generator (see Figure 3-2) supplies a digital message which bi-phase modulates the 500 Hz tone being transmitted. (The received 500 Hz tone contains no digital information at this time.) The digital message consists of a synchronizing code followed by the interrogation verification code which is unique to this user.

After the interrogation verification code is sent, the digital processor actuates S2 (of Figure 3-2) to permit relaying of aircraft altitude and other data to the ground station. During the remainder of the two-second reply, only unmodulated 8 KHz and 500 Hz tones are transmitted.

The data rate of digital messages is 100 bits per second. The sync signal will consist of 4 to 5 bits. The user address will be about 16 bits in length, and about 10 bits will be used to supply altitude data.

Some important design parameters for this user equipment will now be discussed.

Receiver Front End - The receiver front end should exhibit a very low noise figure. A maximum noise figure of 5 db is acceptable, although lower noise figures will provide additional margin and improved performance during aircraft maneuvers. At a nominal receiver frequency of 1600 MHz, a transistor RF preamplifier may be used to obtain a noise figure of less than 5 db. In large quantity production, the cost of these amplifiers should be on the order of $100 in the 1975 period. An alternate choice has recently been made available by the development of miniature parametric amplifiers. These

amplifiers have built-in diode pump sources and exhibit noise figures of less than 2.5 db. The cost of these units, in large quantity production, is expected to be competitive with the transistor amplifier.

Receiver IF Amplifiers - The first IF amplifier operates at a frequency of 60 MHz. This amplifier can be fabricated in integrated circuit form to provide a broad band 4 MHz power gain of 70 db. The second IF amplifier operates at a frequency of 7 MHz. This amplifier can also be fabricated in integrated circuit form. A nominal power gain of 70 db is desired with a 3 db bandwidth of 200 KHz. The second IF amplifier should exhibit an AGC control range of 25 db to compensate for variations in the received signal level and the receivers power gain. This second IF amplifier should also have an output capability of at least + 13 dBm to drive the receiving detectors.

Phase-Lock Loop - The phase-lock loops bandwidth should satisfy the following constraints:

1. During acquisition, the bandwidth should be made as wide as possible to result in a minimum acquisition time. The maximum limit on this bandwidth is determined by the requirement that the signal to noise ratio in this bandwidth be at least +7 db and, preferably, +9 db.

2. After acquisition the bandwidth of the phase-lock loop should be reduced to avoid (cross talk) the undesired retransmission of received modulation.

The maximum bandwidth during acquisition will now be calculated, based on an assumed received noise figure of 5 dB, an assumed received signal power level of 133.5 dBm, and a desired signal to noise ratio of +7 dB.

Thus

$$BN = +174\ dB - 133.5\ dB - 7\ dB - 5\ dB = 28.5\ dB \approx 700\ Hz$$

To insure that the noise bandwidth during acquisition does not exceed 700 Hz, a loop natural frequency of 500 radians is recommended. This natural frequency (f_n) of 500 Hz will permit a frequency search rate of

$$\frac{W_n^2}{4} \approx 19\ KHz/sec, \qquad \text{where: } W_n = 2\pi f_n$$

This maximum sweep rate in co-function with the required phase-lock loop search range determines the user equipment acquisition time. The required phase-lock loop frequency search range is the sum of the following frequency uncertainties, based on modest equipment standards:

Doppler shift	± 4 KHz
Satellite frequency drift	± 2 KHz
User local oscillator drift	± 16 KHz

Total frequency uncertainty = ± 22 KHz or 44 KHz peak to peak.

The acquisition time is thus equal to $\frac{44\ \text{KHz}}{19\ \text{KHz/sec}} \approx 2.3$ seconds. For normal operation, the user is continuously locked to the signal. If the receiver loses lock at the precise moment the GCC interrogates the user, a highly unlikely event, the GCC can recycle the call a few seconds later.

Upon acquisition, the phase lock loop bandwidth may be reduced to 100 Hz which will insure negligible loop response to the received 500 Hz and 8 KHz modulation tones. The 100 Hz phase-lock loop bandwidth is also sufficient to accommodate the expected relative acceleration between the user and the satellite. The loop phase error (θ_E) due to an acceleration of lg is equal to approximately

$$\frac{2.5\pi}{(B_N)^2} \times 32\ F/S^2 \times \frac{F}{C} = \theta_E$$

where F is the nominal carrier frequency of 1.6×10^9 Hz

C is the velocity of light $\approx 10^9$ FPS

$B_N = 100$ Hz

Thus $\theta_E \approx 0.04$ radian, which is a satisfactory value.

Transmitter - The user's transmitter consists of a phase modulator followed by a X 16 frequency multiplier and an L-band transistor power amplifier. The phase modulator will be a simple device consisting of a varactor diode in an L-C tuned filter operating at a nominal frequency of 100 MHz. The required phase deviation in this phase modulator is less than 0.15 radians so that very low distortion can be obtained. The required bandwidth of the phase modulator and the entire transmitter is less than 200 KHz to accommodate the 8 KHz ranging tone.

The output of the phase modulator is amplified and then multiplied in frequency in a single step recovery diode multiplier to result in a nominal transmitter frequency of 1600 MHz. The desired power output from this multiplier is on the order of 20 milliwatts. The phase deviation at the output of the multiplier will be 16 times the phase deviation obtained from the phase modulator. Thus phase deviations in excess of two radians will be obtainable.

The L-band transistor power amplifier must exhibit a power gain of 30 db to provide an output power of 20 watts. The transistors that are expected to be available by 1970 will permit the amplifier configuration that is illustrated in Figure 3-3.

Frequency Synthesizer - The frequency synthesizer will consist of two temperature compensated crystal oscillators providing output frequencies on the order of 100 MHz. The desired stability in these oscillators is one part in 10^5 which is well within the state of the art.

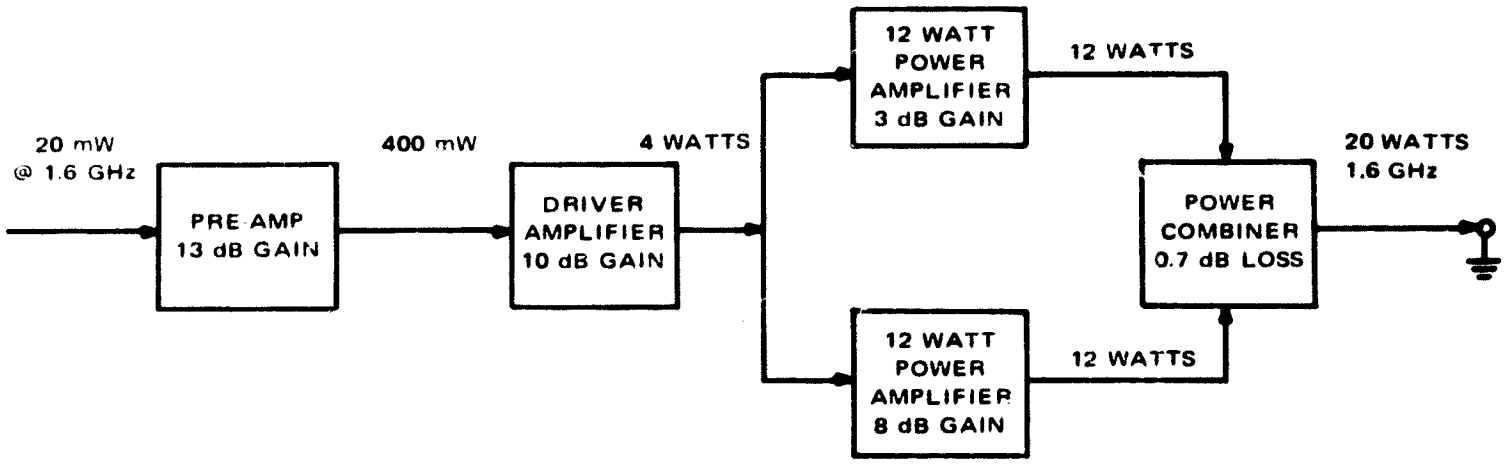

Figure 3-3. L-Band Power Amplifier

3.1.2 AIRBORNE, PASSIVE USER NAVIGATION EQUIPMENT

This equipment is intended for use in aircraft over the North Atlantic Ocean. Figure 3-4 shows the equipment in simplified form, and Figure 3-5 is a more detailed diagram of this equipment.

Referring to Figure 3-4, the antenna receives L-band signals continuously from two satellites. These two signals are somewhat separated in frequency. Each of these signals contains range tones of 500 Hz and 8 KHz phase-modulated onto the carrier.

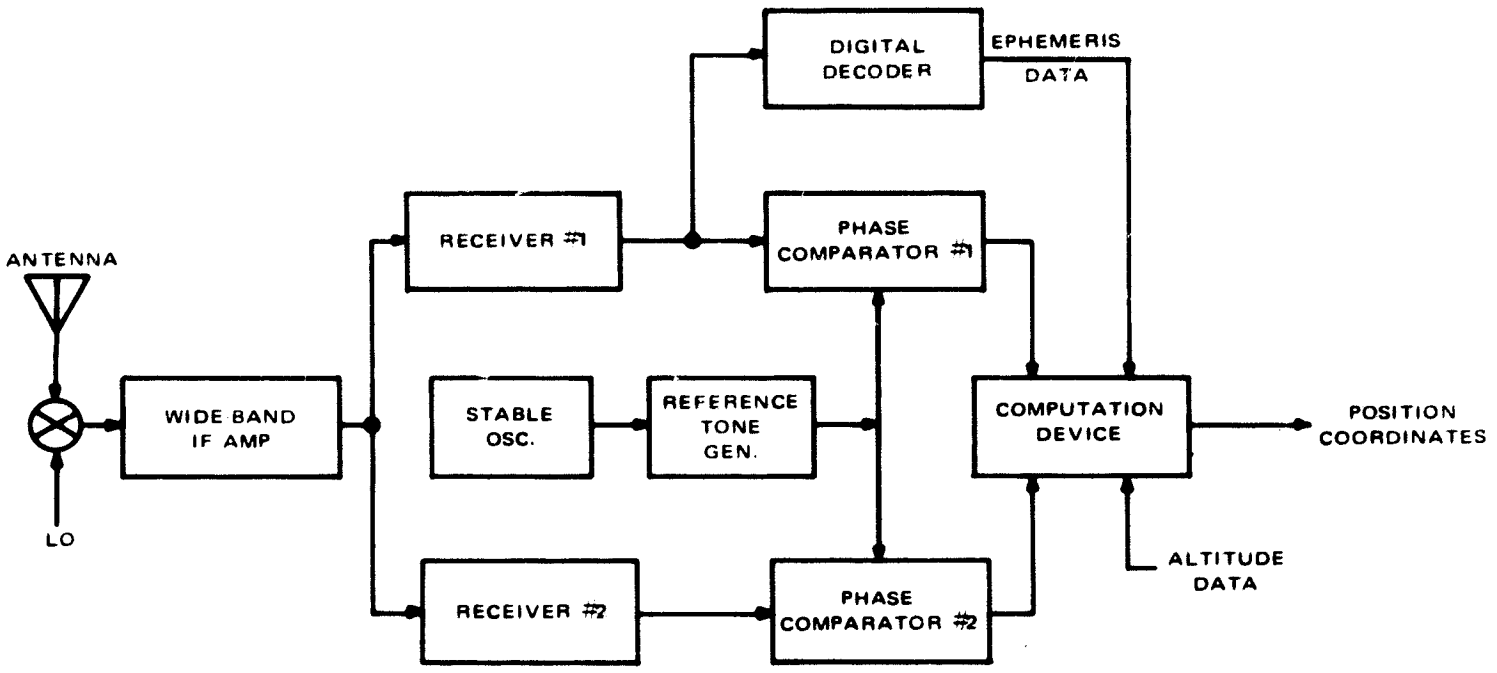

Figure 3-4. Passive User Equipment (Aircraft) (Simplified)

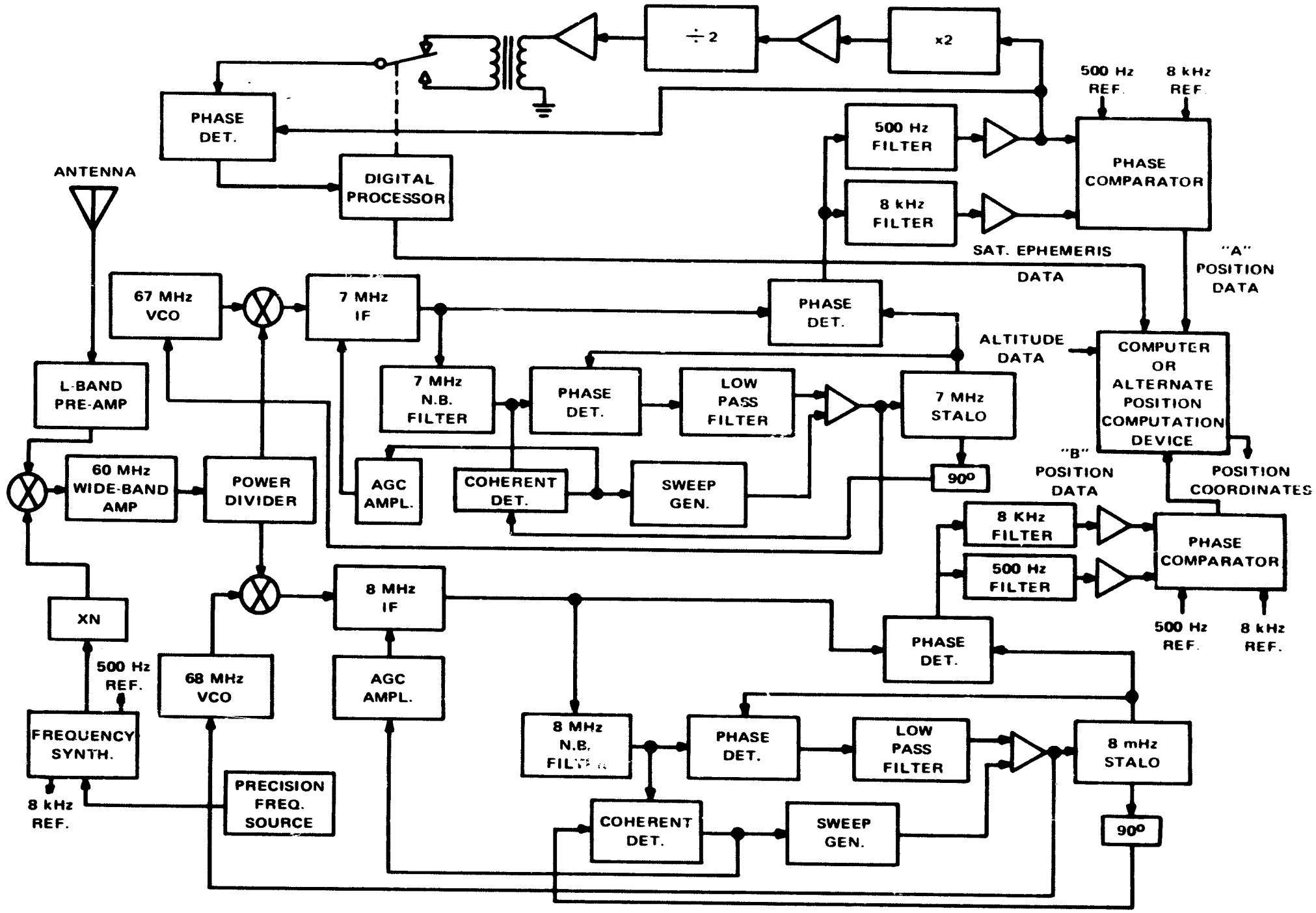

Figure 3-5. Passive User, Aircraft or Marine North Atlantic

The 500 Hz tone from one of the satellites is bi-phase modulated to carry satellite ephemeris data. (Interrogation codes will also be impressed on the 500 Hz tone for use by active users, but the passive users will ignore these messages.)

The incoming signals are hetrodyned to an IF frequency and amplified in a common wide-band IF amplifier. The output of the IF amplifier is sent to two receiver channels, one for each of the two received signals. Each receiver channel detects and filters the range tones associated with the received carrier frequency. The detected tones are sent to phase comparators where a measurement is made of the phase difference between the recived tones and reference tones generated within the user. A stable oscillator (clock) is required to drive the reference tone generator in order to maintain accuracy in position determination.

The two sets of phase data from the phase comparators is sent to a computational device. The computational device determines user position coordinates from phase and altitude data, and satellite ephemeris data. Ephemeris data is obtained by de-modulating the bi-phase modulated 500 Hz tone out of Receiver Channel #1. The computational device can be either a computer or a manual operation using tables and/or charts. Generally, aircraft users would employ a computer, whereas marine users would compute positions manually.

Referring to the detailed user diagram (Figure 3-5) it is seen that the two receivers are essentially identical to the receiver of Figure 3-2, therefore no further treatment is required. The reference tones are generated by the frequency synthesizer, which is, in turn, driven from a precision frequency source. Ephemeris data is extracted by means of circuits identical to those described previously for monitoring interrogations.

3.1.3 MARINE USER NAVIGATION EQUIPMENT

The marine user navigation equipment can be a simplified version of the aircraft user navigation equipment. Only a single channel receiver is required and this channel will be time shared between the incoming signals from the two satellites. The switching of the receiver from one satellite signal to another can be performed manually by the ship's navigator, by switching the receiver VCO frequency between the 67 MHz second local oscillator frequency and the 68 MHz second local oscillator frequency.

The outputs from the receiver phase comparator would be calibrated in terms of range, so that the ship's position can be calculated on the basis of the measured range to the satellites, the published satellite ephemeris data, and the estimated position of the ship (which would be used to resolve ambiguities.

Navigation Computer for Passive User - In an earlier study [1] a preliminary design of a general purpose computer was described which was capable of storing all the data

(1) Final Report - "Phase Difference Navigation Satellite Study" by RCA, Dec. 1967. Contract NAS-12-509

and effecting all the computations required for a position fix in satellite ranging navigation systems. This computer was designed to handle the equations for a range-difference (hyperbolic) three-satellite configuration, and has about twice the capacity necessary for a range-range, two satellite configuration.

Input and output equipment has to handle satellite ephemeris insertions, altimeter input for the aviation users, clock signals and output longitude and latitude data.

A version of a simple control panel is presented in Figure 3-6.

The bulk of the input problem is concerned with the loading of orbital ephemeris data for two or more satellites. A single card reader is utilized in this design.

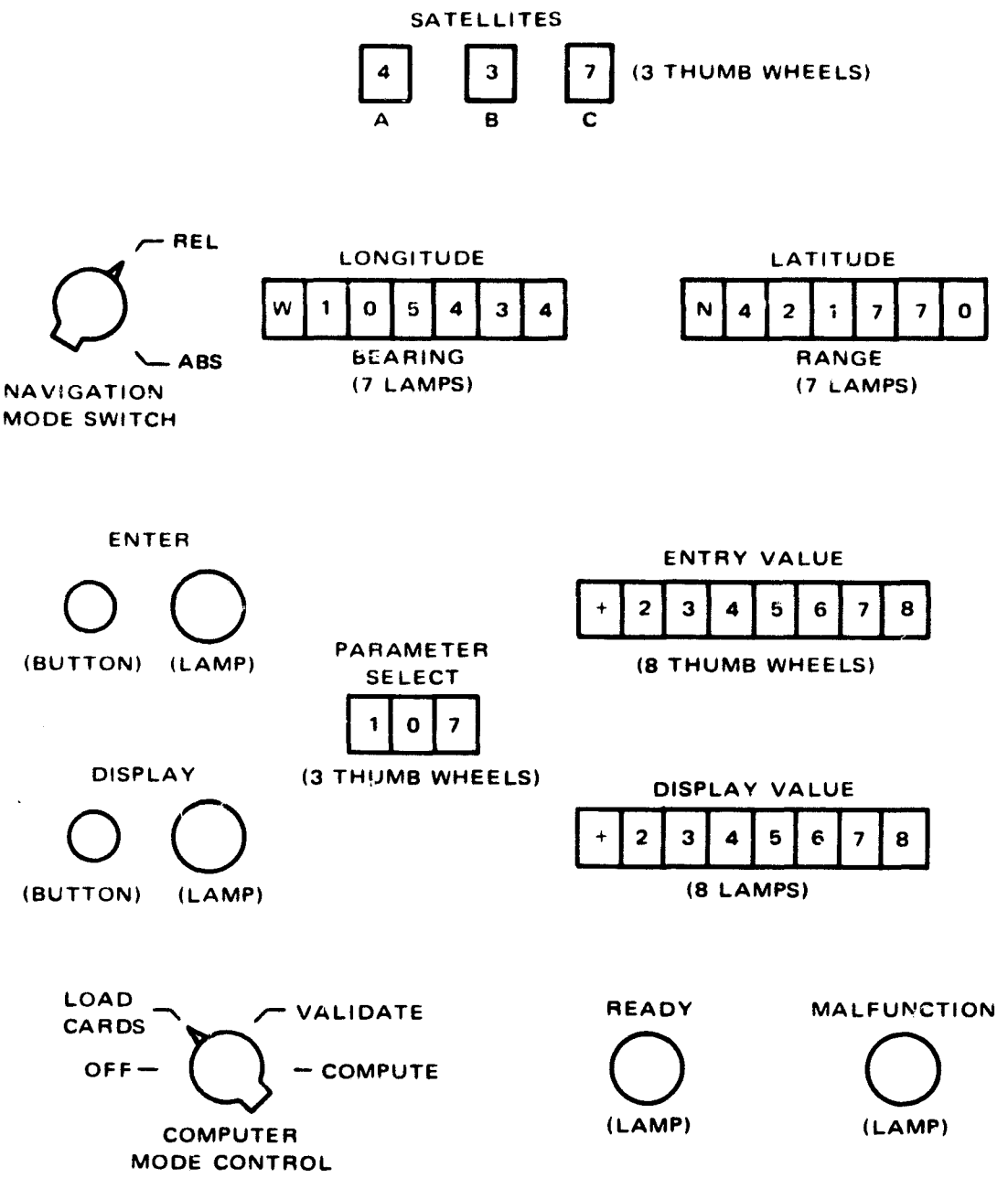

Figure 3-6. Control Panel

Input and output control is effected by energizing the desired set of gates, and transferring the data from a bank of specially assigned memory registers. Each input or output quantity is organized in "words"; e.g. the data is presented to the computer in parallel. Discrete lines are organized into words and each discrete is assigned a particular bit location. The postulated input/outputs are summarized in Table 3-1.

The general functional specifications of this computer and its estimated physical characteristics are shown in Table 3-2.

The computer design includes a complement of 27 basic instructions for arithmetic logic, shift control, and data transfer operations, 24 bit word length, memory count of 2048 words and a memory cycle time of 100 microseconds. The word length provides range quanta sizes of less than 100 feet, allowing for adequate computational resolution for even 0.1 nmi precision.

These requirements can easily be met by a number of aircraft-qualified digital computers and the operations may well be time-shared on the more advanced computers being proposed for SST and 747 type aircraft. There appears to be suitable excess capability in such machines to reduce sample interval significantly and operate with a globally deployed satellite net.

A simplified block diagram of the computer subsystem is depicted in Figure 3-7. It is comprised of a control box, the computer and interconnecting cables. The control box receives, filters and controls all of the DC power (28 volt for aviation user) required to operate the subsystem, and provides means to enable manual mode selection, data insertion, display control, course selection, and fault display. The remainder houses the power supply, precision oscillator, computer core memory, and arithmetic, control and input/output logic sections. Details of this design are available in the earlier referenced report.

The computational equipment for slow flying aircraft or marine users who can tolerate considerably longer intervals between fixes, may be greatly simplified and can include almanac type look up tables, analog devices, map plotting and other equipments associated with manual navigation.

3.1.4 VOICE COMMUNICATION TRANSCEIVER DESCRIPTIONS

This section describes the recommended design for the following voice communication transceivers:

- Aviation VHF voice communications transceiver } Interim
- Marine VHF voice communications transceiver }
- Aviation L-band voice communications transceiver
- Marine L-band voice communications transceiver

TABLE 3-1. SUMMARY OF COMPUTER INPUT/OUTPUT

Name	Signal	Characteristics	Rate
COMPUTER INPUTS			
1. Navigation Mode Switch	1 bit	0 - Relative Navigation 1 - Absolute Navigation	N/A
2. Computer Operating Mode Switch	2 bits parallel	00 - Off 01 - Load Cards 10 - Validate 11 - Compute Position	N/A
3. Enter Button	1 bit	Off/On	N/A
4. Display Button	1 bit	Off/On	N/A
5. Enter/Display Parameter (3 thumb wheels)	12 bits parallel	3 BCD characters designating one of 1000 parameters for Display or Entry	N/A
6. Entry Value (Manually Inserted) (8 thumb wheels)	31 bits parallel	8 BCD characters first 3 bits represent +, -, N, S, E, W remaining bits are decimal values	N/A
7. Satellite Designators (3 thumb wheels	12 bits parallel	3 BCD characters. Indicate which three sets of orbital elements are to be used.	N/A
8. Data Channel from Card Reader	1 computer word length plus 5 control bits all in parallel	One parallel binary computer word. 1 bit for ready fit. 4 bits designate row on card.	16 ms/word or 0.02 sec/card
9. Phase Channel	14 bits parallel	1 ready bit 6 bits for coarse tone 6 bits for fine tone 1 identify bit (0: B - A) (1: B - C)	1 pair of values available per second

TABLE 3-1. SUMMARY OF COMPUTER INPUT/OUTPUT (Continued)

Name	Signal	Characteristics	Rate
10. Altimeter	11 bits parallel Greycode, encoder	-1,000 to +80,000 feet	Continuous discrete 11 wires sampled by program.
11. Binary Clock	24 bits parallel	LSB = 0.0491 sec time for 8 day period	20 cps
COMPUTER OUTPUTS			
1. Enter Lamp	1 bit	0 - Off 1 - On, data entry completed	N/A
2. Display Lamp	1 bit	0 - Off 1 - On, display completed	
3. Ready Lamp	1 bit	0 - Off 1 - On, computer ready for next mode	N/A
4. Fault Lamp	1 bit	0 - Off 1 - On, indicates malfunction	N/A
5. Display Channel I (7 lamps)	26 bit parallel	One 2 bit character for N, S, E or W Six 4 bit decimals (used for longitude or bearing)	N/A
6. Display Channel II (7 lamps)	27 bits parallel	One 3 bit character for 0, N, S, E or W Six 4 bit decimals (used for latitude or ground range)	N/A
7. Display Channel III (8 lamps)	31 bits parallel	One bit character for +, -, N, S, E or W Seven 4 bit decimals	N/A

TABLE 3-2. SUMMARY OF COMPUTER CHARACTERISTICS

OPERATIONAL	
Type:	General purpose, parallel, stored program
Word Length:	24 bits
Arithmetic:	2's complement
Instructions:	32 general purpose
Index Registers:	3 (in memory)
Clock Frequency:	1.43 MHz
Memory Size:	2048 words
Type:	Coincident current core
Memory Cycle:	3.5 microseconds
Basic Order Time:	15 microseconds
PHYSICAL	
Size:	587 cubic inches
Weight:	13 pounds
Power:	47 watts, 28 vdc
Integrated:	Logic, sense amplifiers, drivers and switches

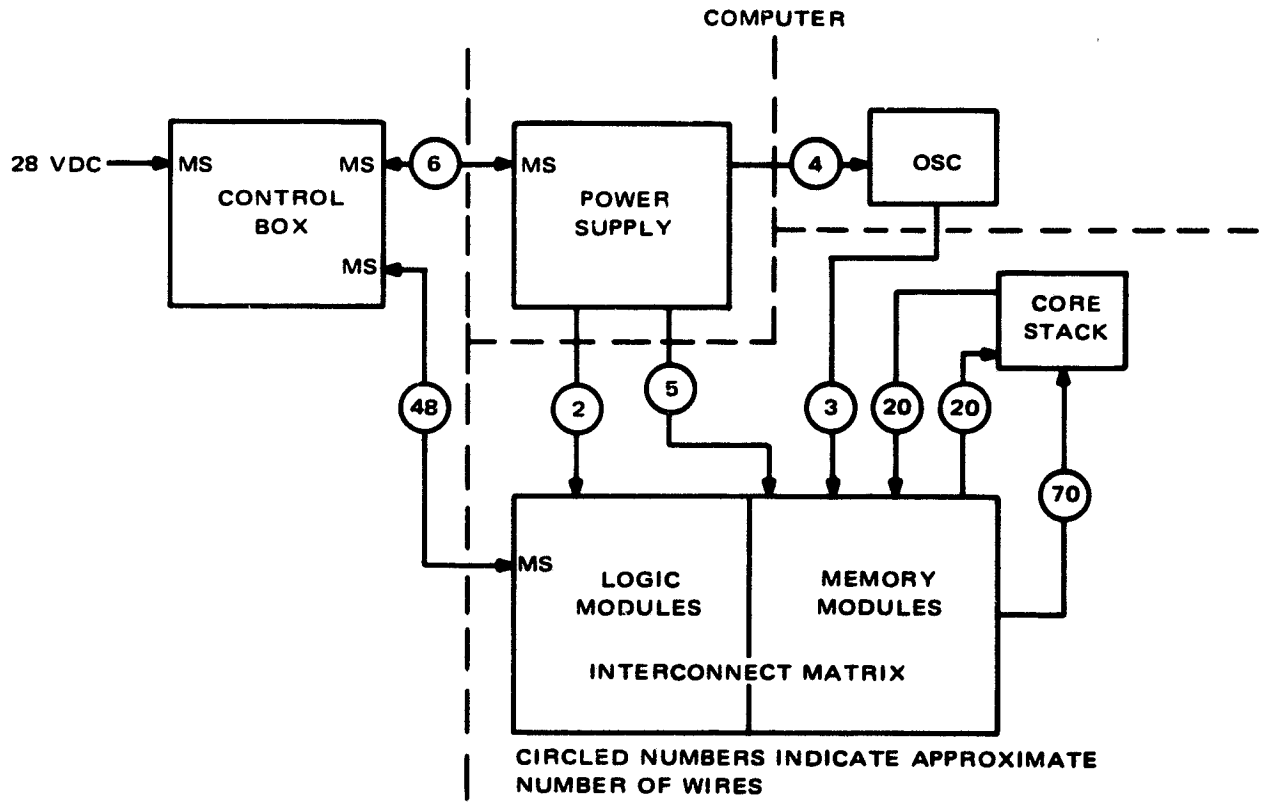

Figure 3-7. Computer Subsystem Cabling

3.1.4.1 DESCRIPTION OF AVIATION VHF VOICE COMMUNICATION TRANSCEIVER

This equipment is required to implement an aircraft-satellite voice communications link over ocean areas where conventional line of sight communications with ground terminals are not feasible. Figure 3-8 is a block diagram of the recommended aviation VHF communication transceiver.

This equipment may be characterized as a frequency modulation transceiver exhibiting very high sensitivity (-116 dBm) to minimize the transmitter power burden on the satellite. This high sensitivity is obtained through the use of a low noise (3 dB noise figure) transistor front end and a phase lock demodulator. This approach has recently been demonstrated by industry and reported in the Airlines Electronic Engineering Committee letter No. 67-2-63 dated August 22, 1967.

Since the voice communications will be in the form of a frequency modulated carrier, a limiting receiver will be used. A double superheterodyne receiver is indicated by the required -116 dBm sensitivity which dictates a total IF gain in excess of 115 dB. The bandwidth of the IF amplifier should be on the order of 25 kHz to minimize adjacent channel interference. This bandwidth is adequate to pass the signal spectrum of less than 20 kHz in the presence of doppler shifts (less than ±400 Hz) and receiver local oscillator drift (less than ± 1.3 kHz).

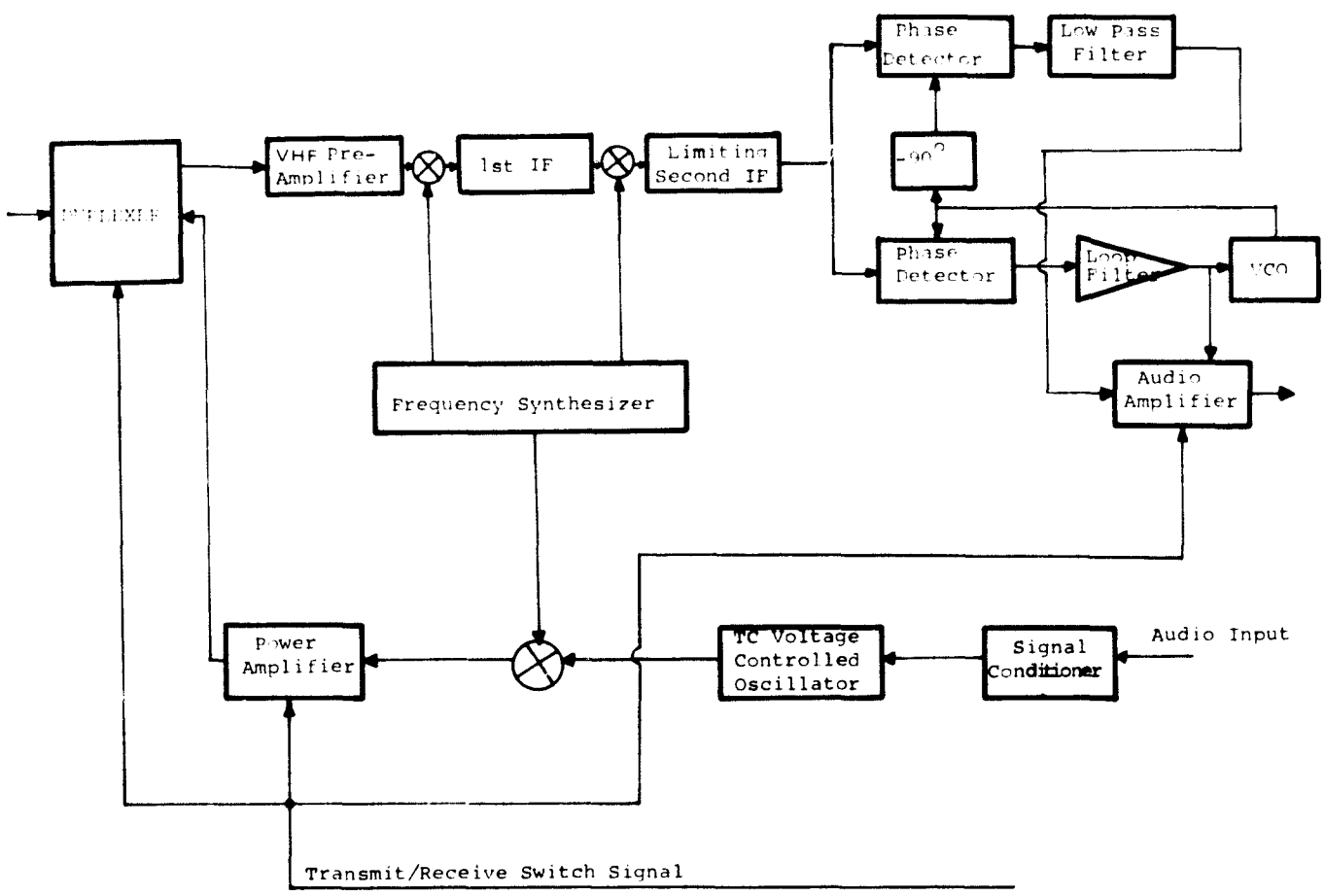

Figure 3-8. Block Diagram, VHF Transceiver

The output of the receiver IF amplifier is used to drive a phase locked demodulator and a coherent in-lock detector. The phase lock demodulator exhibits a two sided noise bandwidth of approximately 18 kHz which is sufficient to accommodate 5 kHz peak frequency deviation at modulation rates up to 2.5 kHz. The coherent in-lock detector senses when the receiver is phase locked and provides a control signal to squelch the receiver audio output.

The transceiver transmitter consists of a signal conditioner, a temperature compensated voltage controlled crystal oscillator, a transmitted carrier up-converter and a VHF power amplifier. The signal conditioner provides the following functions:

- Filters the audio input derived from a microphone and limits the baseband width to approximately 2.25 kHz.
- Provides automatic gain control of the audio input.
- Provides clipping to limit the peak deviation of the transmitter to 5 kHz. This clipping level is adjustable between 0 and 12 dB with respect to the expected peak audio input signal.
- Provides a pre-emphasis of the audio signal at the rate of 6 dB/octave for audio frequencies above 800 Hz.

The output of the signal conditioner is used to drive and frequency modulate the transmitter voltage control crystal oscillator. A nominal VCXO frequency of 15 MHz is recommended to obtain adequate bandwidth and to simplify the design of the transmitter up converter. The VCXO design should incorporate simple temperature compensation to obtain a frequency accuracy of within $\pm$ 0.002 %.

The transmitter up converter generates an output frequency in the 130 MHz to 135 MHz frequency range by mixing the VCXO output signal with a reference frequency that is derived from the transceiver frequency synthesizer. The output signal from this up converter is used to drive the transmitter power amplifier.

The airlines plan to provide about 150 watts, and this power level results in approximately 7 dB of additional margin on the aircraft to satellite link as compared with the satellite to aircraft link. This additional margin will increase the voice quality and reliability to the aircraft to satellite link. Since the expected drive power to this power amplifier will be on the order of 0 dBm, approximately 52 dB of power gain will be required to obtain the 150 watt output power level. This gain can be obtained with four stages of amplification. A competitive transistorized power amplifier can be made available before the mid-1970's.

The reference signal from the transmitter's up converter and the local oscillator signals for the receiver are generated by a frequency synthesizer. The changing of channels is accomplished through the changing of the output frequencies from the synthesizer. Since the channel frequencies have not been established, the exact nature of this frequency synthesizer cannot be defined at this time. However, frequency accuracies within 0.001% are required.

3.1.4.2 DESCRIPTION OF MARINE VHF VOICE COMMUNICATION TRANSCEIVERS

The marine VHF voice communications transceiver will be identical to the aviation transceiver with the following exceptions:

(1) The frequency band of the marine transceiver will be approximately 23% or 30 MHz higher than the aviation transceiver. This will require minor modifications in the receiver front end, the frequency synthesizer, the transmitter up converter and the transmitter power amplifier.

(2) The required transmitter power is only 20 watts as compared to 150 watts in the aviation transceiver. This will simplify the transceiver's transmitter and power supply.

3.1.4.3 DESCRIPTION OF AVIATION L-BAND VOICE COMMUNICATION TRANSCEIVER

Figure 3-9 is a block diagram of the recommended L-band communications transceiver. As can be seen by comparing this block diagram with that of the VHF transceiver in Figure 3-8, the L-band transceiver will be similar to the VHF transceiver. The differences between these two equipments will now be discussed.

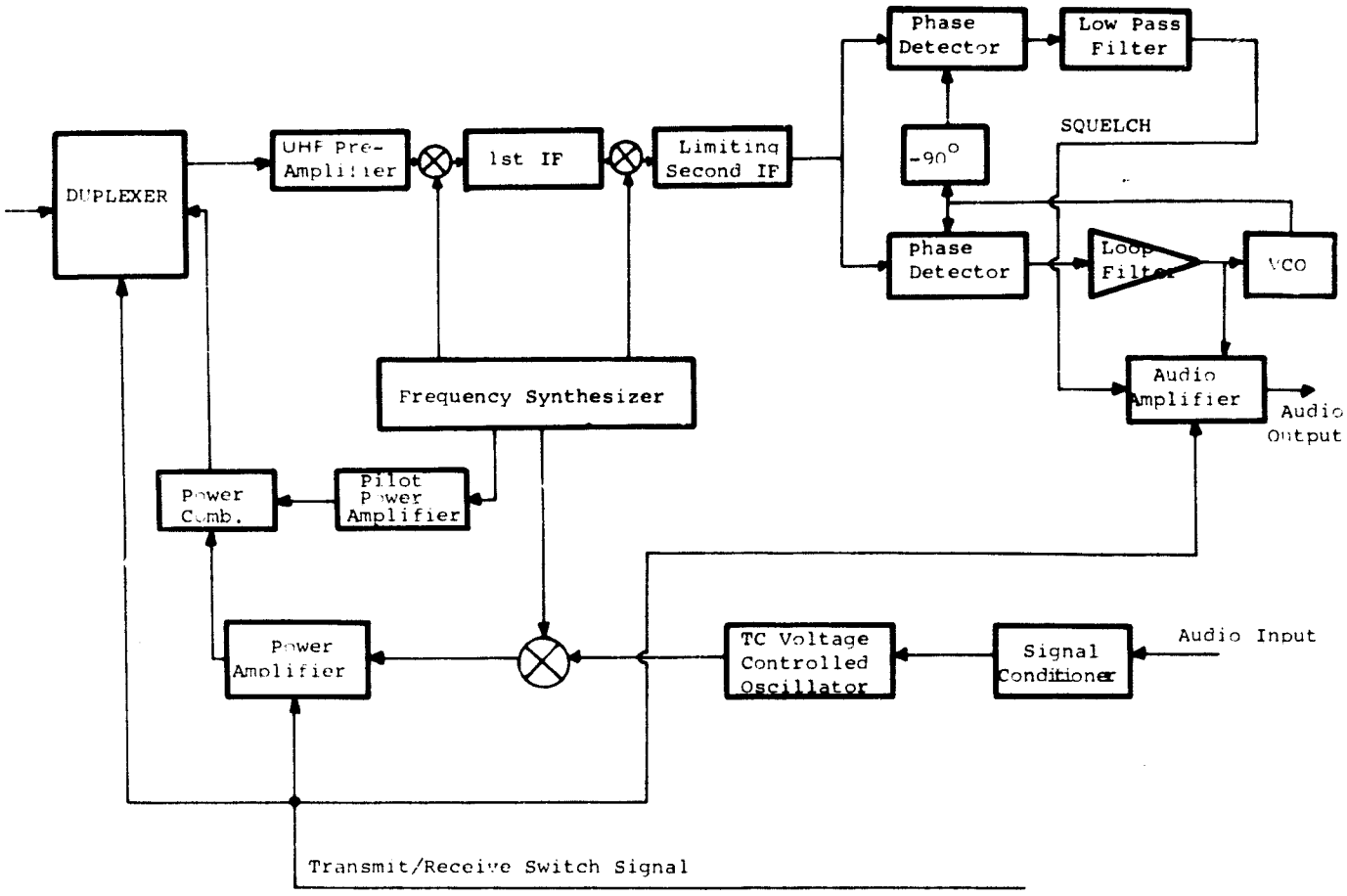

Figure 3-9. Block Diagram, L-Band Transceiver

The higher frequency of operation requires a new receiver front end. It is presently beyond the state of the art to obtain a 3-dB noise figure at 1600 MHz from transistor amplifiers. However, research and development funds are presently being expended with the objective of obtaining low noise transistors at S-band. Thus, 3-dB transistor amplifiers will probably be available and economical before the mid-1970's.

An alternate approach would be to make use of the recently developed L-band and S-band miniature parametric amplifiers. These amplifiers have built-in diode pump sources, exhibit uncoded noise figures of less than 3 dB and occupy a volume of several cubic inches. The production cost of these amplifiers is expected to be several hundred dollars in very large quantities.

The remainder of the L-band receiver will be identical to the VHF receiver with the following exceptions:

(a) The VHF mixer will be replaced with an L-band mixer.

(b) The 25 KHz bandwidth IF filter will be replaced with a 40 KHz bandwidth IF filter to accommodate the large doppler shifts and local oscillator drifts at L-band.

The L-band transceiver frequency synthesizer must provide L-band receiver local oscillator and transmitter reference signals in place of the VHF output signals. Two transmitter reference signals must be provided; one for the communications signal and one for the transceiver pilot signal. The required frequency accuracy of 3 parts in 10^6 dictates the use of a high quality temperature compensated crystal oscillator within the synthesizer.

The L-band transceiver transmitter will contain an L-band up converter and two power amplifiers. One power amplifier will be used to transmit the pilot tone at a 20 watt level. This amplifier can be fabricated with four or five transistor amplifier stages.

The communications power amplifier is required to provide at least 34 watts of output power, which will provide the aircraft to satellite link approximately 3 dB of additional margin as compared to the satellite to aircraft link. This 34 watt output level at 1600 MHz can be obtained by adding an additional high power amplifier stage to the 20 watt pilot power amplifier design. This final power amplifier stage can utilize either a triode tube or paralleled transistors. However, some advancement in the state of the art of high power L-band transistors will be required to make the all solid state amplifier economically competitive to the 34 watt amplifier that uses a triode tube in its output stage.

3.1.4.4 DESCRIPTION OF MARINE L-BAND COMMUNICATION TRANSCEIVER

The marine L-band voice communication transceiver will be identical to its aviation counterpart with the following exceptions.

(a) Although the marine transceiver will also operate somewhere in the 1540 to 1640 MHz frequency band, the precise channel frequency allocations will be slightly different to avoid conflicts. This will require a minor difference in the transceiver frequency synthesizer.

(b) The marine transceiver will operate with a 10 dB gain antenna. Thus the pilot and communications transmitter power levels can be reduced by 10 db compared to the airborne units; allowing a 3 db margin, the necessary powers are 2 watts and 4 watts respectively. Both transmitter power amplifiers should utilize an all solid state design.

3.2 USER ANTENNA DESIGNS

The general performance requirements for a user antenna for traffic control, navigation and voice transmission have been reported in previous studies (see Interim Scientific Report, June 1967, prepared for NASA ERC on Contract NAS 12-509). Investigations of current antenna technology reveal that the stated requirement can be met with existing designs and that no critical antenna technology problems exist. The major problems are associated with selection and installation in specific aircraft, wherein aerodynamic effects (thermal and drag), visibility, multipath interference from aircraft structures, etc., constitute major selection criteria.

Requirements - The receiving antenna to be employed for navigational purposes should have the following characteristics:

(1) Conical sector beam of about 160°, with very low sidelobes. The net gain within this sector should be equal to or greater than 0 dB.

(2) Circular polarization to minimize polarization loss (axial ratio < 5 dB).

(3) 10% impedance bandwidth (VSWR < 1.5)

(4) Low pattern degradation within the frequency band

(5) Multipath rejection capability as required, by reduced gain in downward direction

(6) Small size, shaped to minimize drag and temperature effects.

(7) Flush-mounted for high speed aircraft such as the SST.

These requirements also are valid for the voice channel link of the North Atlantic Traffic Control System, provided sufficient channel gain is achievable between the user and the satellite. The system described in this report permits use of a 0 dB user antenna with reasonable user radiated power since high link gain is provided by the retrodirective array on the spacecraft.

Recommendations - A slotted dipole cavity backed antenna as the basic element is recommended, with the exact configuration determined by the particular user. Circular polarization requirement can be fulfilled by a four-slot configuration (see Figure 3-10). Here two pairs of slots are oriented at right angles, 90° out of phase. Each pair has a separation of approximately $\lambda/2$, with a slot length less than λ. Such a configuration can be contained in a near-flush mounted fairing with the selection of a low loss dielectric material capable of withstanding mechanical and thermal conditions of the skin of the SST.

The design of such an antenna is straightforward and well within the capabilities of a number of companies.

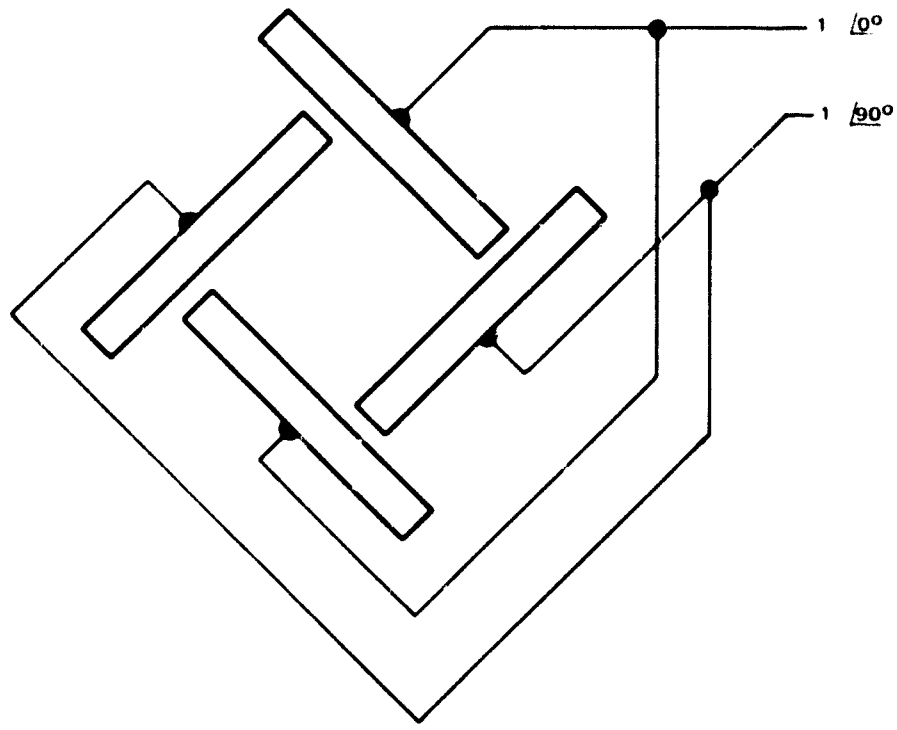

Figure 3-10. Four-Slot Configurations

Integration with Traffic Control, Navigation and Communication User Equipments - For VHF voice and L-band navigation, electrically separate antennas need to be provided, although both might be contained in a single faired or flush section of the aircraft. For those configurations employing L-band for both functions, a single antenna and diplexer may be more effective, depending on the frequency separation involved. Conceptually, a single RF diplexer can be used for both functions, and the user equipment block diagrams in this report reflect this approach.

3.3 USER EQUIPMENT ESTIMATED WEIGHTS AND COSTS

3.3.1 AVIATION USER EQUIPMENTS (L-BAND)

A summary of the weights and DC power requirements of the L-band aviation equipments is shown in Figure 3-11. The separate "packages" reflect

1) the voice communication equipment set

2) the traffic surveillance set, and

3) the passive navigation set

The aviation user who is part of a traffic control system would probably only require sets No. 1 and 2. The Traffic Control Center can provide updated position data within a few seconds if the pilot wishes to check his on-board navigation equipment. However, the general aviation user with transoceanic ambitions may wish to avail himself with set No. 2 as his primary navigation system.

Set No. 1 consists of a PLL receiver and a transmitter with selectivity for six FM channels. One of these channels is for emergencies purposes only and would be kept on in the receive mode except for those periods when the equipment is being used for voice communications.

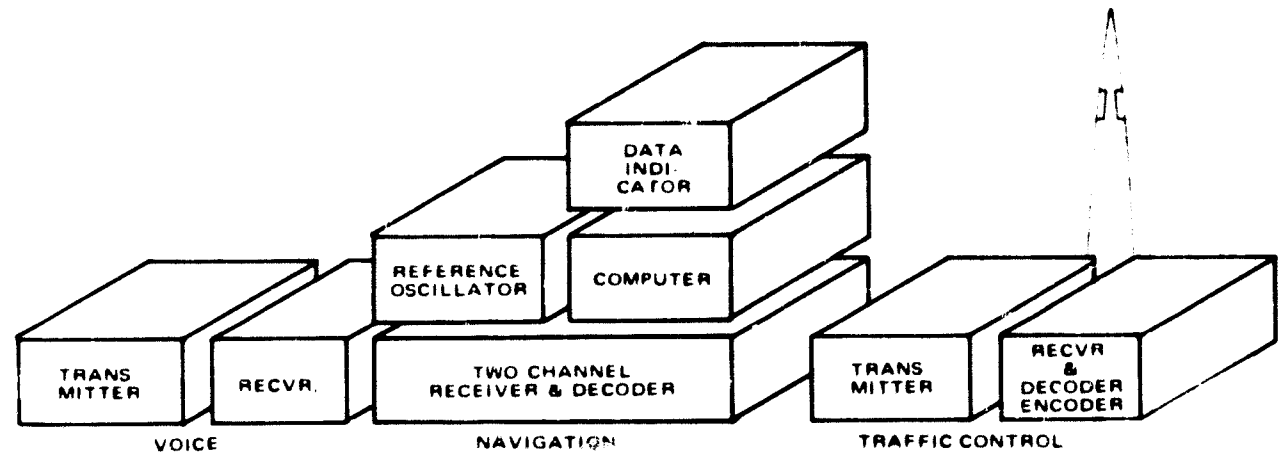

	WT.	DC POWER
TRANSMITTER	30 lb	200 W
RECEIVER	15 lb	60 W
	45 lb	260 W

	WT.	DC POWER
RECEIVERS	16 lb	76 W
REF. OSC.	16 lb	17 W
DATA IND.	1 lb	2 W
COMPUTER	13 lb	47 W
	46 lb	142 W

	WT.	DC POWER
TRANSMITTER	5 lb	10 W
RECEIVER	8 lb	38 W
	13 lb	48 W

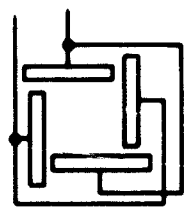

ANTENNA

	WT.
ANTENNA	2 lb.
DIPLEXER	3 lb.
	5 lb.

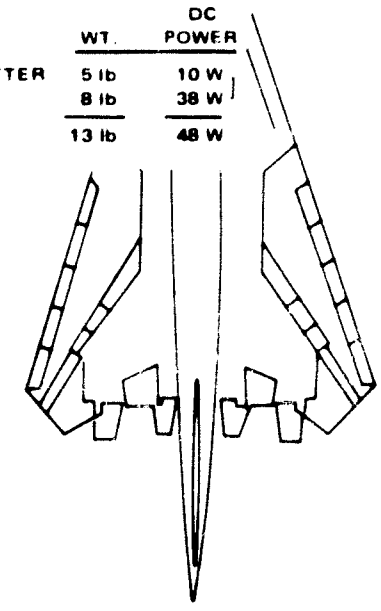

Figure 3-11. Aviation User Equipments

Set No. 2 contains a single channel PLL receiver, a decoder-encoder, a transmitter and a display.

Set No. 3 is comprised of a two-channel PLL receiver, an oven controlled stable crystal reference clock with stabilities on the order of 1×10^{-10} or 5×10^{-11} per 24 hour period, phase angle detectors, a decoder, a navigation digital computer and a display.

One antenna with a multiplexer can serve all of the receive transmit functions. The unit depicted is a flush mounted, circularly polarized, hemispherical beam antenna with cavity backed-slotted dipoles.

Component power, weight, and cost breakdowns of a typical CW ranging receiver and transmitter are shown in Tables 3-3 and 3-4.

A summary of the L-band equipment costs for the aviation user is shown in Table 3-5. These are predicated on production runs of at least 1000 projected to the early 1970's and do not include the cost of development or installation. The design and component requirements are present day state-of-the-art. A preliminary estimate of the development costs for each of the equipment sets I and II is approximately $300K to $500K. Set No. 3 by itself would run between $500K to $1000K, but in conjunction with set No. 2 would drop to about $500K. A reasonable addition to the estimated costs shown in Table 3-5 for amortization of development expenses would be about 15% to 20%.

TABLE 3-3. CW RANGING TRANSMITTER TABULATION

Item	Power (W)	Weight (lb-oz)	Size (in^3)	Cost ($)
530 MHz Power Amp	-	-	-	-
4 transistors	-	-	-	75
Stripline circuitry (6" x 2-1/2" x 1")	-	0 - 6	15	120
x3 Output Mult (2" x 2" x 1")	-	0 - 2	4	105
x3 and x5 low power mult	-	0 - 2	6	50
106 MHz Buffer Amp (2 stages)	-	0 - 3	6	60
35 MHz Limiter	-	0 - 4	10	100
Solid State switch (low cost power transistor will do)	-	0 - 8	6	75
60 volt power supply	10	1 - 8	30	120
Sub-totals:	10	3 - 1	77	705
Mounting case	-	1 - 0	53	60
Wiring	-	0 - 7	-	240
Check-out	-	-	-	120
Totals after packaging	10	4 - 8	130	1125

3.3.2 MARINE USER EQUIPMENT (L-BAND)

A summary of the weights and DC power requirements of the L-band marine equipments is shown in Figure 3-12. These are essentially the same as those for the aviation user with the exception that the 10 dB antenna for the marine user relaxes the RF power requirements of the transmitters. This category of user can also use charts and hand computations in lieu of a digital computer for the passive navigation set.

The marine user equipment costs are summarized in Table 3-6. The same conditions stated for the aviation user apply here as well.

TABLE 3-4. CW RANGING RECEIVER TABULATION

Item	Power (W)	Weight (lb-oz)	Size (in^3)	Cost ($)
Transistor RF pre-amp and mixer		0 - 4	10	150
IF Amplifier (3 IC chips plus 2 filters)	1	0 - 6	15	200
Phase Lock Oscillator	4	0 - 8	25	--
Temp Cont. VCXO				125
Phase Detector				45
Operational Amplifier				45
Acquisition sweep oscillator				30
Buffer amplifiers				30
Coherent Demodulator		0 - 3	4	40
Tone filters	2	0 - 8	10	50
Frequency Synthesizer	5	1 - 0	50	--
2 Temp Cont. Crystal Oscillators				180
RF switch and driver				35
L-Band multiplier (20 parts plus filter)				210
Signal Decoder (15 IC chips plus 50 parts)	4	0 - 10	30	455
Programmer (8 IC chips plus 40 parts)	3	0 - 8	20	335
Telemetry Encoder (15 IC chips plus 50 parts)	4	0 - 9	30	455
Telemetry phase modulator				40
Transmitter phase modulator		0 - 7	8	100
Power Supply	15	1 - 5	20	150
Sub-totals	38	6 - 4	222	2675
Case, Wiring and Checkout	--	2 - 2	80	535
Receiver Totals	38	8 - 6	302	3210

TABLE 3-5. ESTIMATED AVIATION USER EQUIPMENT COSTS
(Based on Production of 1000 Units)

Item	Cost
I - Voice Equipment:	
Receiver	$ 2,500
Transmitter	3,500
	$ 6,000
II - Traffic Control Equipment:	
Receiver, Decoder and Encoder	$ 3,200
Transmitter	1,100
	$ 4,400
III - Passive Navigation Equipment:	
Two Channel Receiver & Decoder	$ 6,000
Reference Oscillator	1,500
Digital Computer	6,000
Data Display	500
	$14,000
IV - Antenna Equipment:*	
Flush Mount Antenna	$ 250
Diplexer	250
	$ 500
*Installation costs not included.	

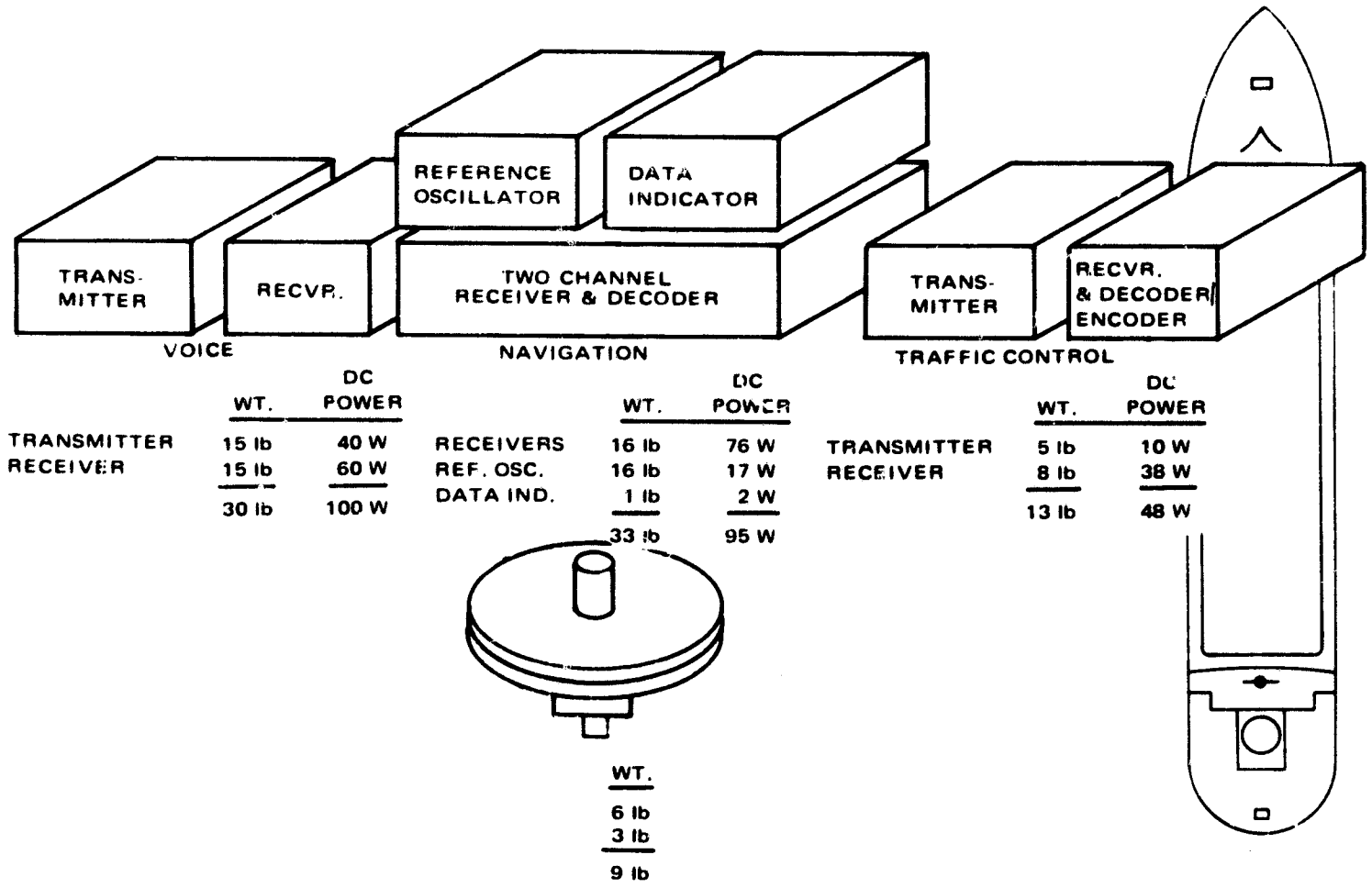

Figure 3-12. Marine User Equipments

TABLE 3-6. ESTIMATED MARINE USER EQUIPMENT COSTS
(Based on Production of 100 Units)

Item	Cost
I - Voice Equipment:	
Receiver	$2,500
Transmitter	2,500
	$5,000
II - Traffic Control Equipment:	
Receiver, Decoder and Encoder	$3,200
Transmitter	1,100
	$4,400
III - Passive Navigation Equipment:	
Two Channel Receiver and Decoder	$6,000
Reference Oscillator	1,500
Data Display	500
	$8,000
IV - Antenna Equipment:	
10 dB Parabolic Antenna	$ 500
Diplexer	250
	$ 750

3.4 USER GROUND SUPPORT EQUIPMENT

Maintenance and general support requirements for the User System have been considered from both ground and in-flight aspects. Though ground support is an obvious requirement established a priori by the total aircraft/ship and its electronics, in-flight and/or on-board support is dictated by more subjective criteria. For aircraft, these criteria include:

(a) System complexity and likelihood of failure between departure and destinations.

(b) Criticality of continuously knowing status of system because of impact on flight profile and safety of mission.

(c) Economic gains derived from knowing source of failure in flight so that appropriate logistic channels can be activated by radioing ahead the identification of the faulty unit.

(d) More accurate appraisal of true operability of the equipment in actual flight environment from built-in monitoring system which ground support systems can never exactly duplicate.

Additionally, the trend for the new large capacity aircraft and SST's is in the direction of an on-board integrated data system which provides centralized processing of significant test data from all aircraft systems.

Because of these considerations, a small built-in test system for the user equipment is recommended which can operate independently of, or associated with, a centralized

data system such as AIDS. The built-in test system would provide, on a qualitative basis, a level of confidence of User System performance and in conjunction with monitoring points isolate a majority of failures to the line replaceable unit (LRU) level. Basic design objectives would be high reliability, low power and weight, and low cost. Simplicity of operation and concise display of results would also be required in keeping with flight personnel work loads and technical backgrounds.

Requirements for ground support equipment, on the other hand, include: detailed quantitative test, fault isolation, and calibration capability; semi-mobility to meet both hanger and some flight line use; controls, displays and print-outs compatible with ground crew skill levels; and system flexibility that will permit some future tie-in with a centralized computer controlled maintenance system as some airlines are currently planning. As one ground support system would service a fleet of aircraft, its design should incorporate enough time saving read-out and a control feature to allow a test rate that is compatible with aircraft short turn around times.

3.4.1 IN-FLIGHT/BUILT-IN TEST (BIT) SYSTEM

Test Requirements - The principal test parameters which provide the most significant information on the status of the User System are:

(1) Receiver sensitivity (MDS)

(2) Receiver lock-up verification

(3) Transmitter power output

(4) Tone and synchronizing code demodulation

These parameters, on a self test activate basis by flight crew, would provide a realistic appraisal of equipment performance without need for complex additional circuitry. The power output would be monitored continuously if desired without self test initiate as it would have no detrimental affect on primary operating conditions. The remaining parameter in combination with a few strategically placed test points would provide fault isolation to the LRU level.

Design - The built-in test system design contains two basic functions. These are a self test signal source or stimulus and a series of monitoring test points for determining loss of signal path between major User System functions. Figure 3-13 shows the location of a transmitter output monitoring point between the L-band final amplifier and diplexer via a coupler. The power sensor will provide a discrete threshold indication on a go, no-go basis if power falls below an acceptable level.

The self test signal source, shown in Figure 3-14, is an IF carrier phase modulator with the 500 Hz tone. The test signal simulates the transmission characteristics of the ground station with the synchronizing and interrogation codes appropriate for this User equipment. A properly functioning system will demodulate and process this signal and respond by activating the transmitter. Monitoring transmitter activate signal (Figure 3-15) will verify that tone and synchronizing code demodulation process functioned properly and that receiver lock-up took place. A time period measurement between self-test initiate and transmitter activate signal would be a measure of lock-up time.

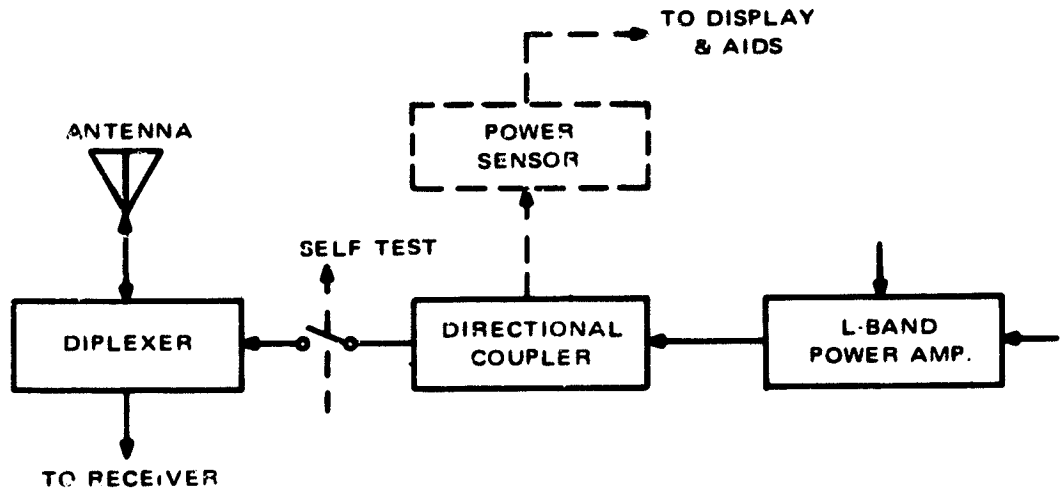

Figure 3-13. Power Monitor

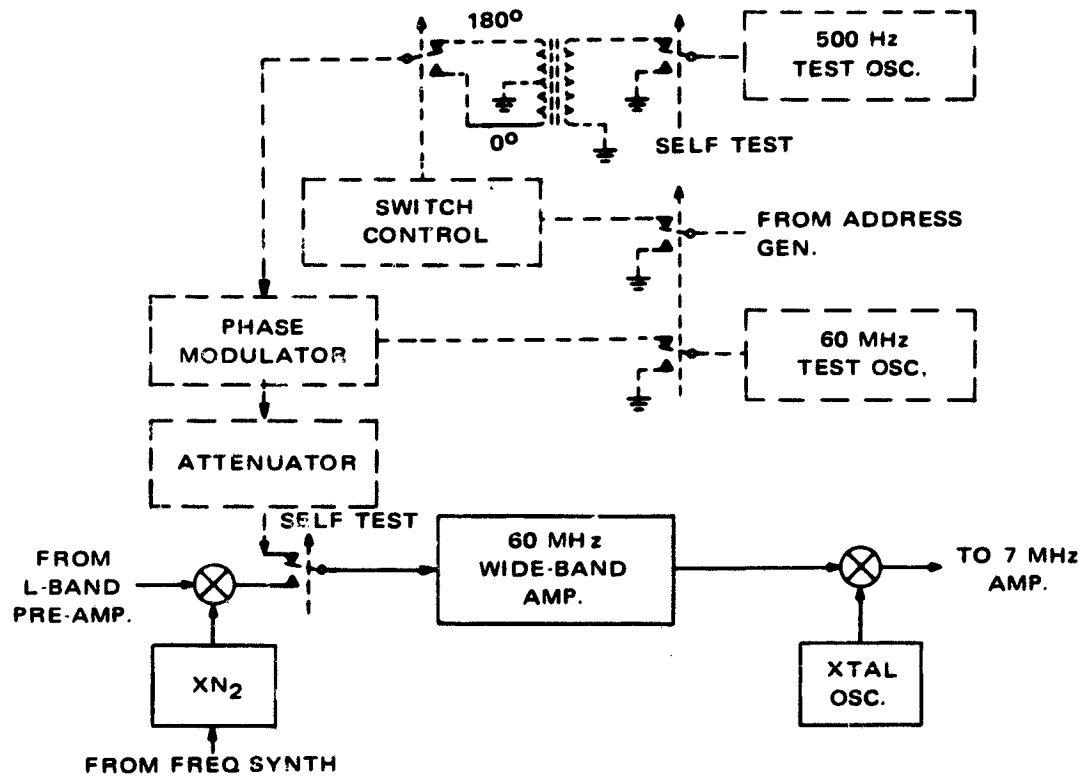

Figure 3-14. Self Test Signal Source

Referring again to Figure 3-14, a proper synchronizing and interrogation code is sent from the User Equipment Address Generator which bi-phase modulates a 500 Hz test oscillator signal. This signal in turn phase modulates a 60 MHz test carrier which passes through a calibrated attenuator to provide proper level for MDS as test of receiver sensitivity. The signal is then injected ahead of the 1st IF stage. Though this test does not pick up the L-Band front end, it covers most of the receiver system while preserving simplicity and reliability as a built-in test source.

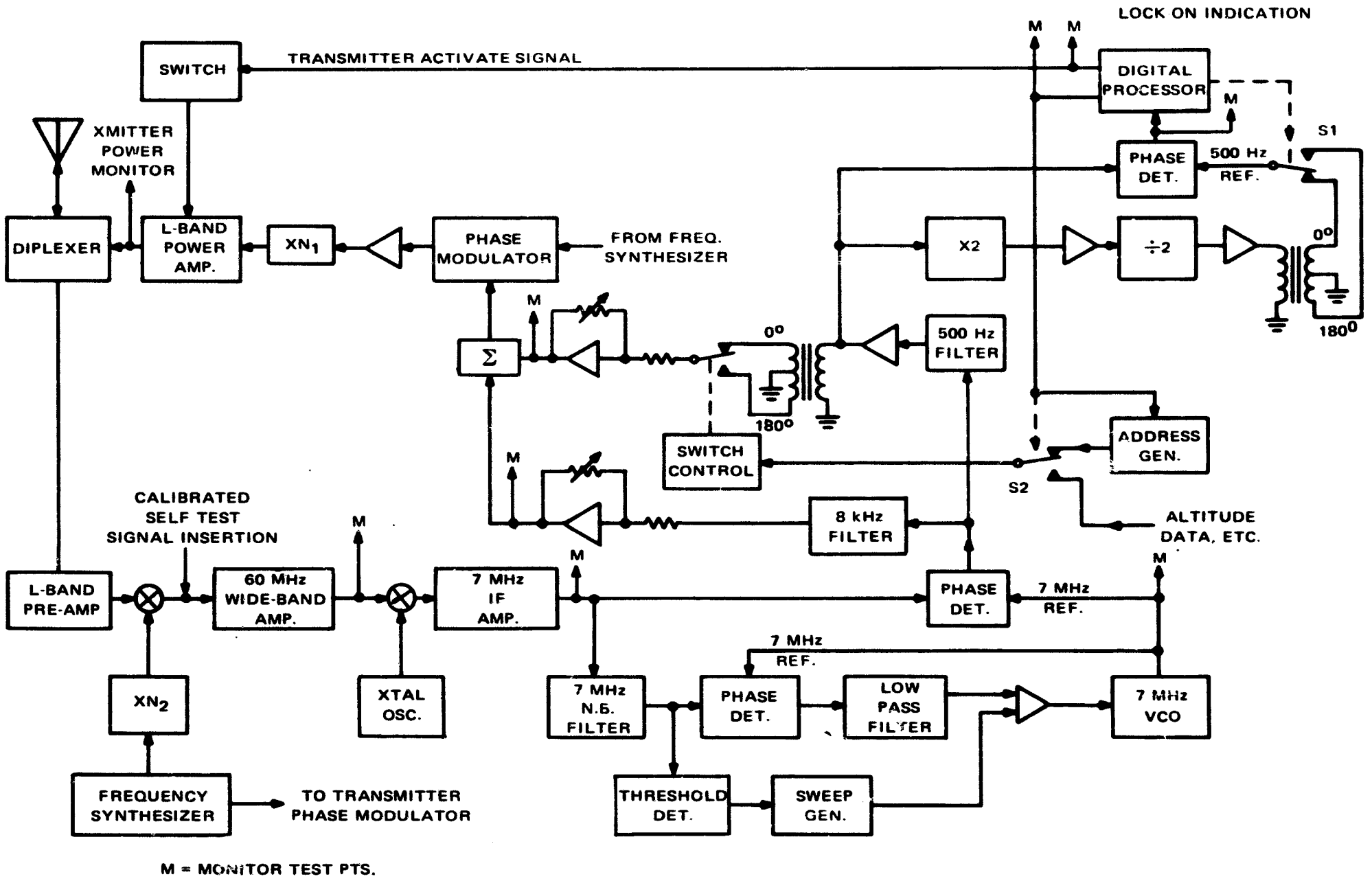

Figure 3-15. Active Mode, Aircraft User North Atlantic (Voice Channel not Shown)

Selectively placed monitoring points (Figure 3-15) follow the path of the test signal through the receiver. Diode detectors and other threshold devices would condition signals to go, no-go indications on the display panel or for tie-in with AIDS.

For the Passive Mode User, the same design applies except that tone phase relationship would be controlled to simulate a specific navigational fix for test of the phase comparators and Position Computation Device.

3.4.2 GROUND SUPPORT SYSTEM (GSE)

Test Requirements - In addition to the four test parameters identified in Section 3.4.1, the ground support system shall also test for:

(1) Address verification transmission

(2) Two tone (500 Hz and 8 KHz) phase delay between receiver input and transmitter output

(3) Modulation indices

(4) Transmitter output carrier frequency, and stability.

While accomplishing the above, the GSE provides a primary reference standard for precision alignment, calibration, and basis of rejection for marginal or below performance equipment. It basically simulates a ground station except for not having to simulate interrogation of more than one User equipment simultaneously (though conceivably that could become a requirement in the future). Fault isolation capability will be required to the replaceable board or sub-assembly level.

Semi-mobile or cart installed systems would increase convenience around the hanger and on the flight line. One system should be able to handle a dozen aircraft at a typical maintenance facility.

Because automation is the trend in expanding civilian GSE facilities, the TC/Nav GSE should be capable of future semi-automatic to automatic control from a central computer. Used independently, the system should provide some internal data smoothing or summarizing to simplify readouts. Hard copy display from standard digitally driven printers will be required.

Design - A general design concept for the User System GSE is shown in Figure 3-16. The control function is a manual system that can receive digital commands remotely. The stimulus is basically a ground station transmitter with precision controlled L-band and tone frequency sources. The power supplies provide energy for the receiver under test.

The measurement system ties into receiver test points through cable connections. Phase, frequency, and lock-up time is referenced against basic oscillator sources in the stimulus through the central control function. The digital processor provides decode verifications of the UUT synchronizing and interrogation codes, and altimeter data.

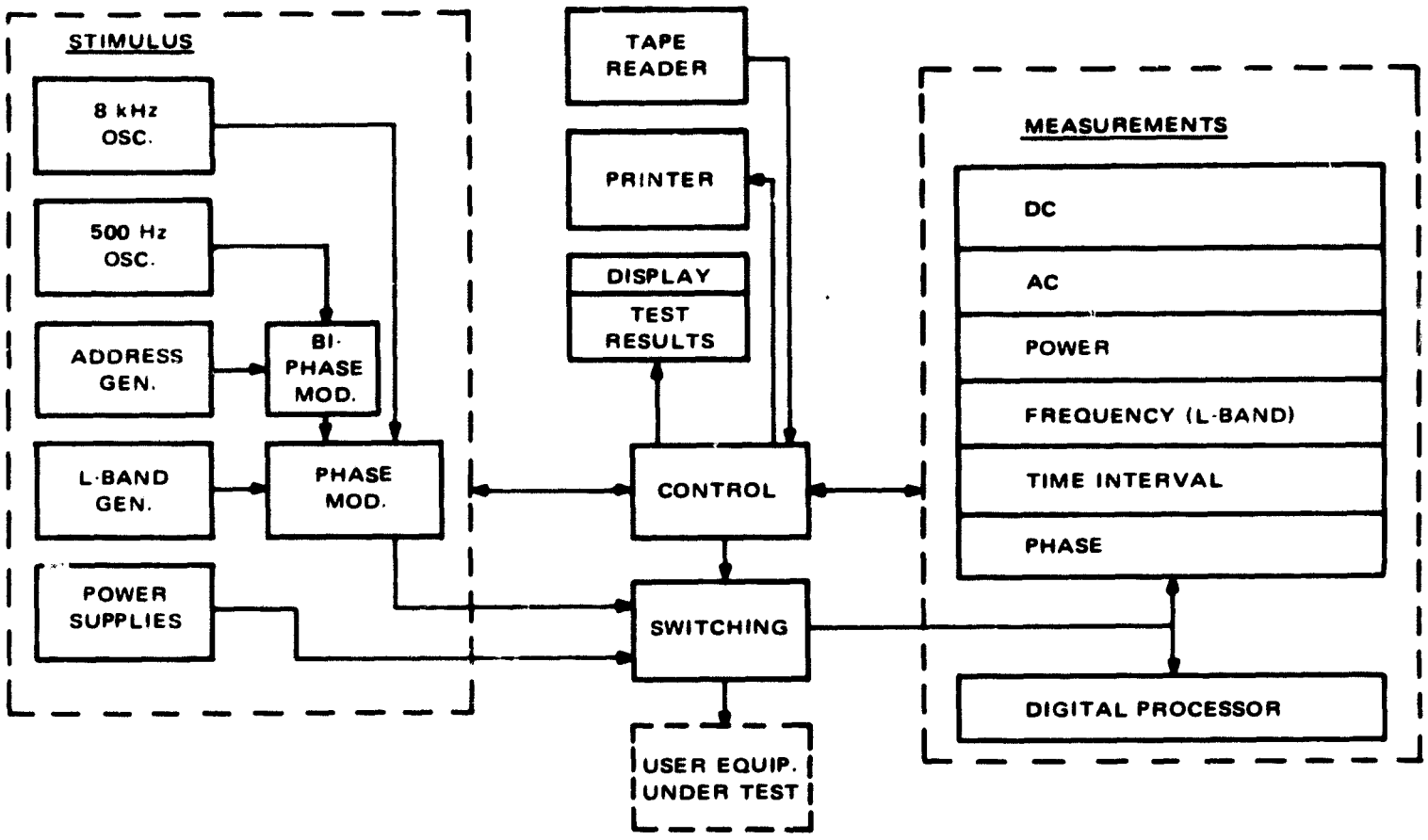

Figure 3-16. Ground Support System

For the peripheral equipment, the tape reader supplies bulk storage for analog comparator limits where go, no-go read-out is used in lieu of analog print-out. The Printer and Display provide both hard copy and visual test results respectively.

SECTION 4

SPACE SEGMENT DEFINITION (VHF VOICE)

4.1 INTRODUCTION & SUMMARY

The spacecraft that has been configured in this portion of the study is a multipurpose vehicle, a pair of which form a system able to satisfy present requirements. The satellite, acting as a relay station, has been designed utilizing techniques and equipment that are present state of the art and no significant new developments would be required for implementation.

The system consists of two synchronous equatorial satellites separated by about 50 degrees of longitude, providing L-band navigation service as well as VHF voice communication capabilities. Each spacecraft carries two-L-band hard limiting navigation repeaters, which are compatible with carriers that are phase modulated with tone-ranging and digital data subcarriers, and four separate VHF transponders for four voice channels (two in the 120-130 MHz aviation band and two in the 150-160 MHz maritime band).

The satellite, which has been given the acronym NAVOX, has been configured for a dual launch aboard an Atlas-Centaur-Burner II, this particular arrangement being selected on the basis of preliminary estimates that the spacecraft was in the 600-800 lb. class. As such, from cost effectiveness considerations as well as availability of appropriate launcher configuration in the U.S. stable of boosters, the multiple launch on Atlas Centaur, using the Burner II as essentially an apogee kick motor, proved preferable. In addition to having adequate payload capacity, the ten foot diameter shroud permitted the design of a cylindrically shaped non-oriented solar array of reasonable height. Figure 4-1 depicts the two satellites stowed for launch inside a lengthened Centaur shroud.

Figure 4-2 shows the satellite fully deployed in mission mode. The basic elements of the configuration are the spinning solar array section containing power supply, attitude control and propulsion equipment, and the despun equipment canister, containing communication and TT and C equipment and nutation dampers, and the antennas which are attached to the despun platform. There are three different antennas shown in this figure: the largest is the 28.5 foot diameter VHF voice antenna; the 2.5 foot L-band antenna is mounted at the feed of the VHF parabola; the third antenna is a VHF whip for TT and C. The dish antennas provide earth coverage at the 3 dB points from synchronous altitude. The TT and C antennas have a broad pattern to permit telemetry at 136 MHz and commands at 148 MHz to be transmitted and received during the transfer orbit as well as in mission mode.

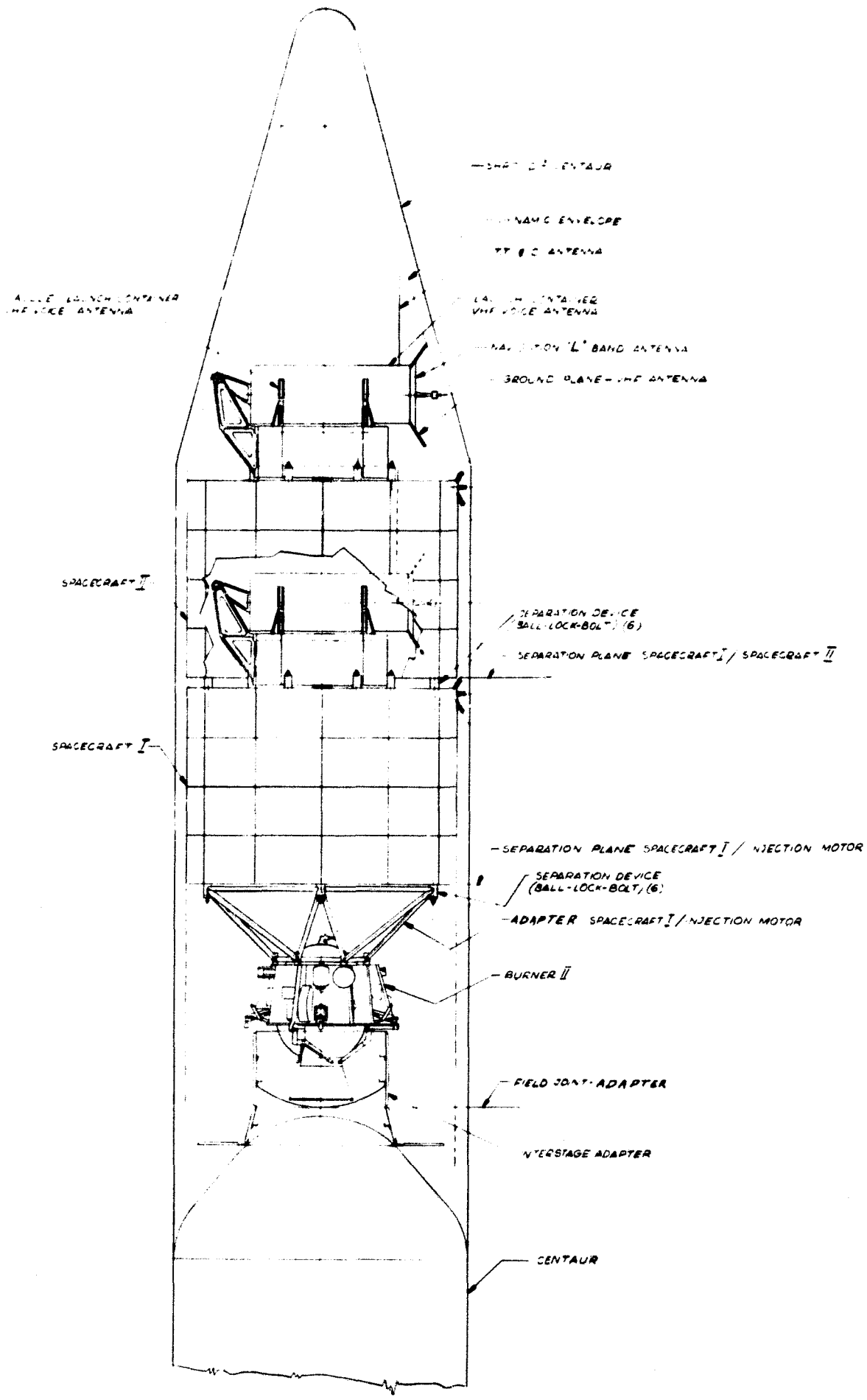

Figure 4-1. VHF Dual Payload on Centaur

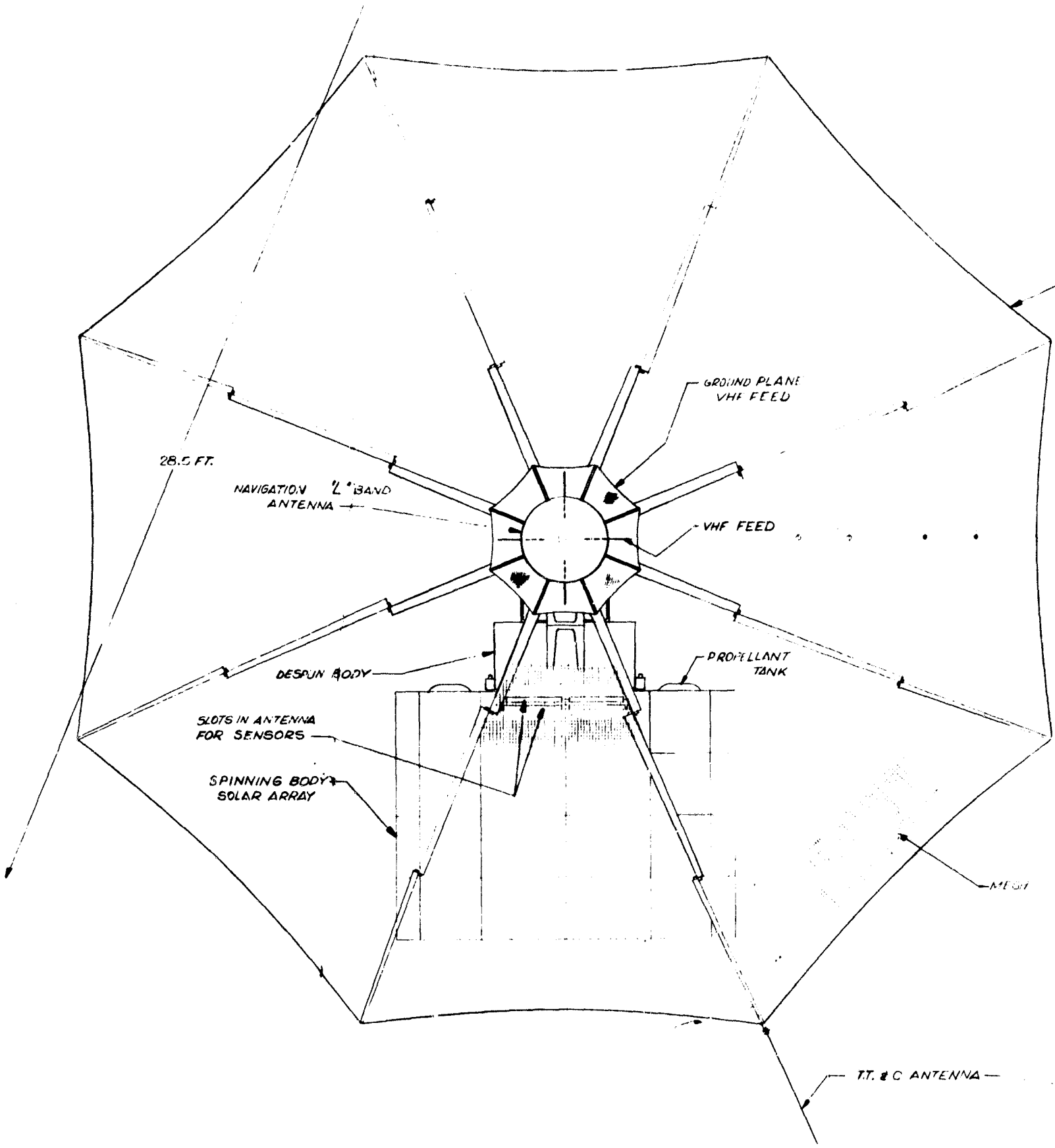
GROUND PLANE
VHF FEED
28.5 FT.
NAVIGATION "L" BAND
ANTENNA
VHF FEED
DESPUN BODY
PROPELLANT
TANK
SLOTS IN ANTENNA
FOR SENSORS
SPINNING BODY
SOLAR ARRAY
T.T. & C. ANTENNA

4-3A

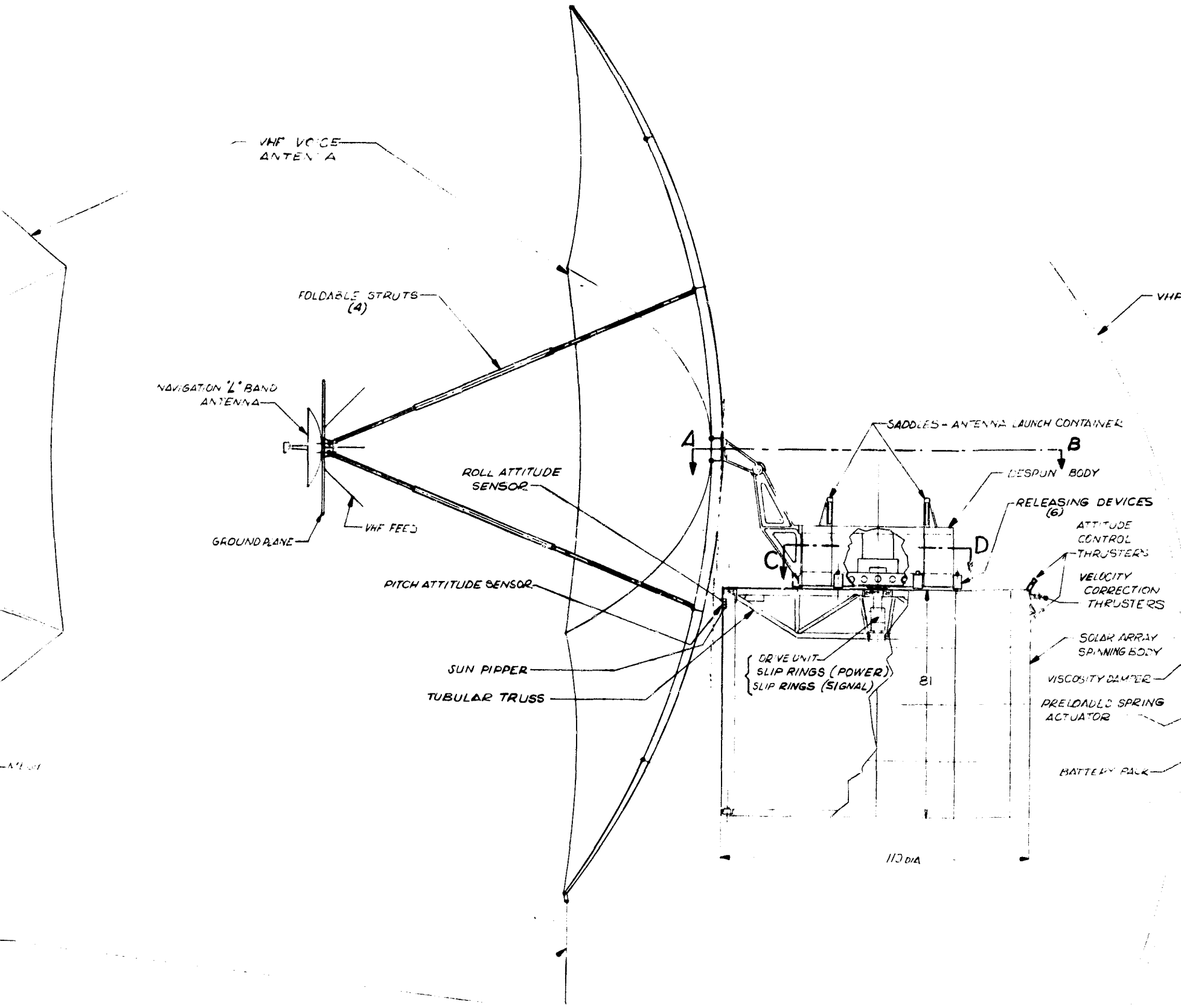
VHF VOICE ANTENNA
FOLDABLE STRUTS (4)
NAVIGATION 'L' BAND ANTENNA
ROLL ATTITUDE SENSOR
GROUND PLANE
VHF FEED
PITCH ATTITUDE SENSOR
SUN PIPPER
TUBULAR TRUSS
SADDLES - ANTENNA LAUNCH CONTAINER
A
B
C
D
DESPUN BODY
RELEASING DEVICES (6)
ATTITUDE CONTROL THRUSTERS
VELOCITY CORRECTION THRUSTERS
SOLAR ARRAY SPINNING BODY
VISCOSITY DAMPER
PRELOADED SPRING ACTUATOR
BATTERY PACK
DRIVE UNIT
SLIP RINGS (POWER)
SLIP RINGS (SIGNAL)
81
110 DIA

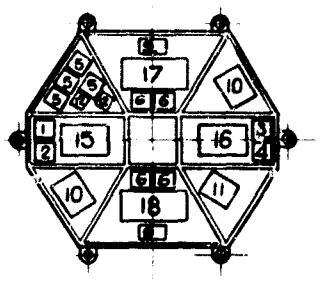

SECTION C-D

EQUIPMENT ARRANGEMENT-DESPUN PLATFORM

LEGEND

1 - VHF AVIATION POWER AMPL. #1
2 - VHF AVIATION POWER AMPL. #2
3 - VHF MARITIME POWER AMPL. #1
4 - VHF MARITIME POWER AMPL. #2
5 - VHF LOCAL OSCILLATOR (4)
6 - VHF MIXERS, IF AMPLIFIERS, & BANDPASS FILTERS (4)
9 - VHF COMMAND RECEIVER (2)
10 - COMMAND DECODER & CDU (2)
11 - TELEMETRY BASEBAND ASS'Y UNIT & MODULATOR
12 - VHF TELEMETRY TRANSM. (2)
13 - T.T. & C. DIPLEXER
15 - FORWARD LINK L-BAND NAVIGATION TRANSPONDER
16 - BACK LINK L-BAND NAVIGATION TRANSPONDER.
17 - FORWARD LINK POWAMP (TWTA)
18 - BACK LINK POWER AMPLIFIER (TWTA).

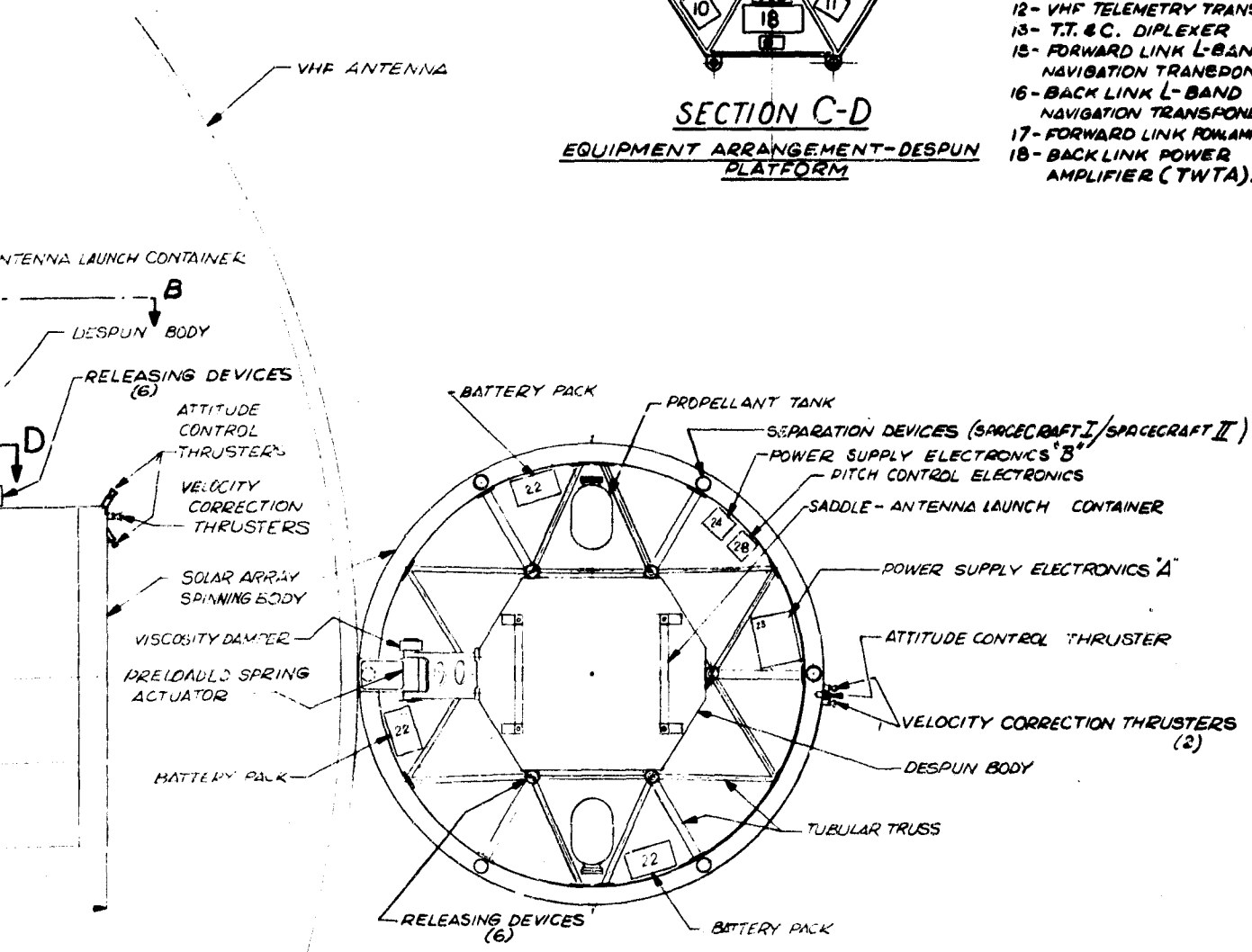

VIEW A-B

Figure 4-2. VHF Spacecraft Deployed Configuration

Operationally, the satellite is oriented with its spin axis normal to the orbit plane. The equipment canister and antennas are despun by a motor between the spinning solar array (120 rpm) and the canister. Horizon sensors mounted on the array, scanning nearly normal to the spin axis, provide position data with respect to the local vertical which, when compared to an index on the canister, is used to continuously orient the antennas along the local vertical. An additional pair of horizon sensors configured in a "Vee" with respect to the pitch plane (the plane normal to the spin axis) provides roll/yaw attitude data for ground processing.

Also contained on the shaft between the array and canister is a set of slip rings for electrical power transfer and for horizon sensor signal transfer.

A monopropellant hydrazine propulsion system using Shell 405 as a catalyst is mounted in the spinning section. This system, operating in a blowdown mode, provides orbit station acquisition and station keeping by appropriately phased firing cycles over a fraction of spin period. It also is used for occasional correction of the spin axis attitude (roll/yaw).

The solar array has been sized to provide a minimum of 350 watts continuous load power under worst case conditions at the end of five years in a synchronous orbit. The array dimensions are 110 inches in diameter by 81 inches high. Included as factors in sizing the array were power required for battery recharge, power loss due to shadowing by the large mesh VHF antenna and radiation damage losses. Power storage in the NiCd batteries is 50% redundant in supplying 288 watts for the 70 minute maximum eclipse time at a maximum depth of discharge of 43%.

Following sections of this report describe in more detail the major subsystems, the system deployment and finally the estimated system costs. The major subsystems of a single NAVOX spacecraft are listed below with their estimated weights:

Subsystem	Weight (lb)
Structure	75
Communications	174
Telemetry, Tracking and Command (TT&C)	25
Power	259
Attitude Control	31
Propulsion	67
Total	631

4.2 SPACECRAFT STRUCTURE

4.2.1 GENERAL ARRANGEMENT

The NAVOX spacecraft shown in Figure 4-2 has two major parts: a despun body platform and a spinning body, interconnected by a shaft and drive assembly.

The despun platform is an eight-sided container 5.5 feet in diameter and 1.5 feet high. It houses all communication and TT&C equipment as well as the nutation dampers.

(See Figure 4-2 View C-D for the equipment layout.) All antennas are also located on this platform:

1) The VHF voice antenna mounted by means of a single pivot arrangement as depicted in Figure 4-2.

2) The navigation "L" band antenna located on the ground plane of the VHF antenna feed

3) The TT&C antenna attached to the outboard end of one of the eight ribs on the VHF reflector.

The bottom plate of the despun platform is rigidly attached to the upper end of the drive shaft, which is located on the spacecraft spin axis. This shaft is part of a drive assembly which provides pitch control of the despun platform. The drive assembly is comprised of bearings, drive torque motors, encoders, slip rings for power transfer, and slip rings to carry signals from attitude sensors to the T/M subsystem. The assembly is enclosed and sealed by a single set of labyrinth seals. Sacrificial lubrication is provided to ensure a proper environment for the rotating parts throughout the lifetime of the satellite.

The spinning portion of the spacecraft is in the form of a cylinder 110 inches in diameter and 81 inches long. The cylindrical surface is covered with solar cells. Storage batteries, equipment associated with power regulation, and the secondary propulsion subsystem are installed inside this section as shown in Figure 4-2 View A-B. The secondary propulsion system, consisting of attitude control and velocity correction thrusters, propellant tanks and associated hardware, is mounted in the plane perpendicular to the spin axis containing the spacecraft center of gravity. The attitude sensors are also mounted on the cylindrical surface, flush with the solar cells.

4.2.2 STOWED LAUNCH CONFIGURATION

Figure 4-1 shows the multiple launch arrangement whereby a Burner II injection stage supports two identical NAVOX spacecraft stacked one on top of the other. An adapter attached to the Centaur stage carries the Burner II module. The Burner II is mated to the lower spacecraft by a tubular truss adapter. The upper spacecraft is attached to the lower using six separation devices on the periphery of the cylindrical solar array.

As shown in the figure, both spacecraft are configured to lie within the standard dynamic envelope of the Centaur shroud, with the exception of the secondary propulsion thrusters which protrude into the space between stringers in the shroud, and hence satisfy payload constraints.

In the launch configuration both despun platforms are locked to the respective cylindrical sections by six restraining devices, thereby assuring that the ascent loads are carried through these hard points and minimizing loads in the shaft and drive assembly. Prior to activation of the torque motor the restraint devices are energized, torsionally freeing the despun platform. At the same time a spring loaded mechanism, located on the shaft, lifts the despun platform on a keyway from the spinning body and locks it rigidly on the shaft. This provides the necessary clearance between the two

bodies and assures sufficient rigidity to allow accurate pointing of the despun platform and antennas. The major loads on the two bodies are inertial at this time since the satellite is in a "zero G" environment.

The separation of the payload occurs first at the separation plane between the Burner II and the Centaur adapter. The next separation is between the lower Spacecraft (I) and the Burner II adapter assembly, ejecting the spent Burner II and adapter subsequent to spin up. The third separation takes place at the Spacecraft I/Spacecraft II interface.

All separation devices are of the "Ball-Lock-Bolt" type actuated by manifolded gas generators as shown on Figure 4-3 and 4-4. Compression springs mounted coaxially with the separation bolts provide separation forces.

4.2.3 CONSTRUCTION

The structure of the despun platform is of riveted sheet metal, with honeycomb panels and several machined fittings (shaft attachment, launch hard points for separation devices, etc.) The electrical equipment is mounted on the lower base plate which acts as a heat sink. The structure is enclosed by a top plate and side walls for thermal and structural reasons. Thermal control is achieved by passive techniques, using second surface mirrors on the side walls or surfaces of the platform. The radiator area (the top and bottom surfaces of the platform) is coated so as to provide adequate radiation cooling for the predicted power dissipation of the platform mounted equipment.

The spinning body is of a similar structural design. The cylindrical portion has a frame made of rings and longitudinal stringers onto which sections of cylindrically shaped honeycomb are attached. These honeycomb sections are the substrate for solar cells and form the solar array. The lower and upper edges of the cylindrical frame each have 6 hard points, where the separation devices are installed. The longitudinal members between the upper and lower hard points are sized to carry the launch loads. Attached to the upper edge of the cylindrical section is a three-dimensional tubular truss which provides hard points for the separation devices for the despun platform, for support for the drive assembly, for attach points for electrical equipment and for the components of the propulsion system.

The material used for the structures of the despun platform and the spinning body is aluminum alloy 2024 commonly used for airframe construction. Tubular trusses are 6063 weldable aluminum alloy or its equivalent. Honeycomb panels are spacecraft type. The panels are 1/4 to 3/8 inches thick using a honeycomb aluminum core of 1/4 to 3/8 cell size and material thickness of .001 inch. The faces of the honeycomb are .0037 inches thick.

4.2.4 VHF VOICE ANTENNA

Because the VHF voice antenna is so large and requires deployment, this separate section of the report is devoted to its description. The reflector of this antenna is 28.5 feet in diameter. The feed, consisting of four whips with a ground plane, is supported by four struts from the reflector. The antenna and its feed are foldable for launch. Based on prior experience of rib-type parabolic antennas with taut metal mesh reflecting surfaces, it was deduced that eight ribs would provide acceptable dish

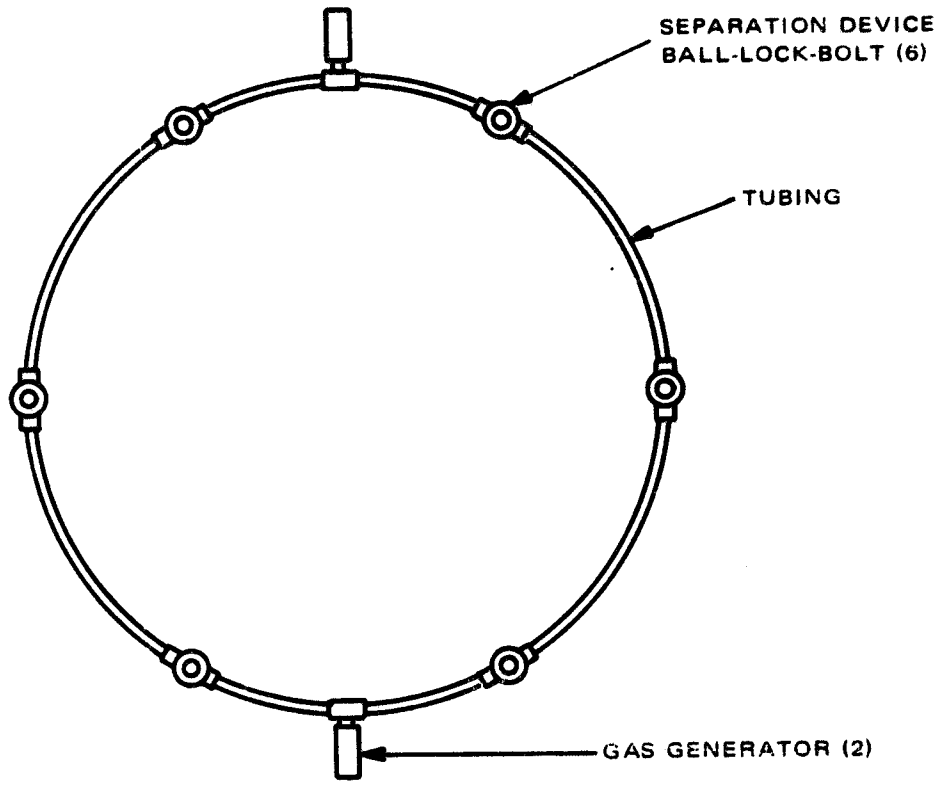

Figure 4-3. General-Arrangement-Separation

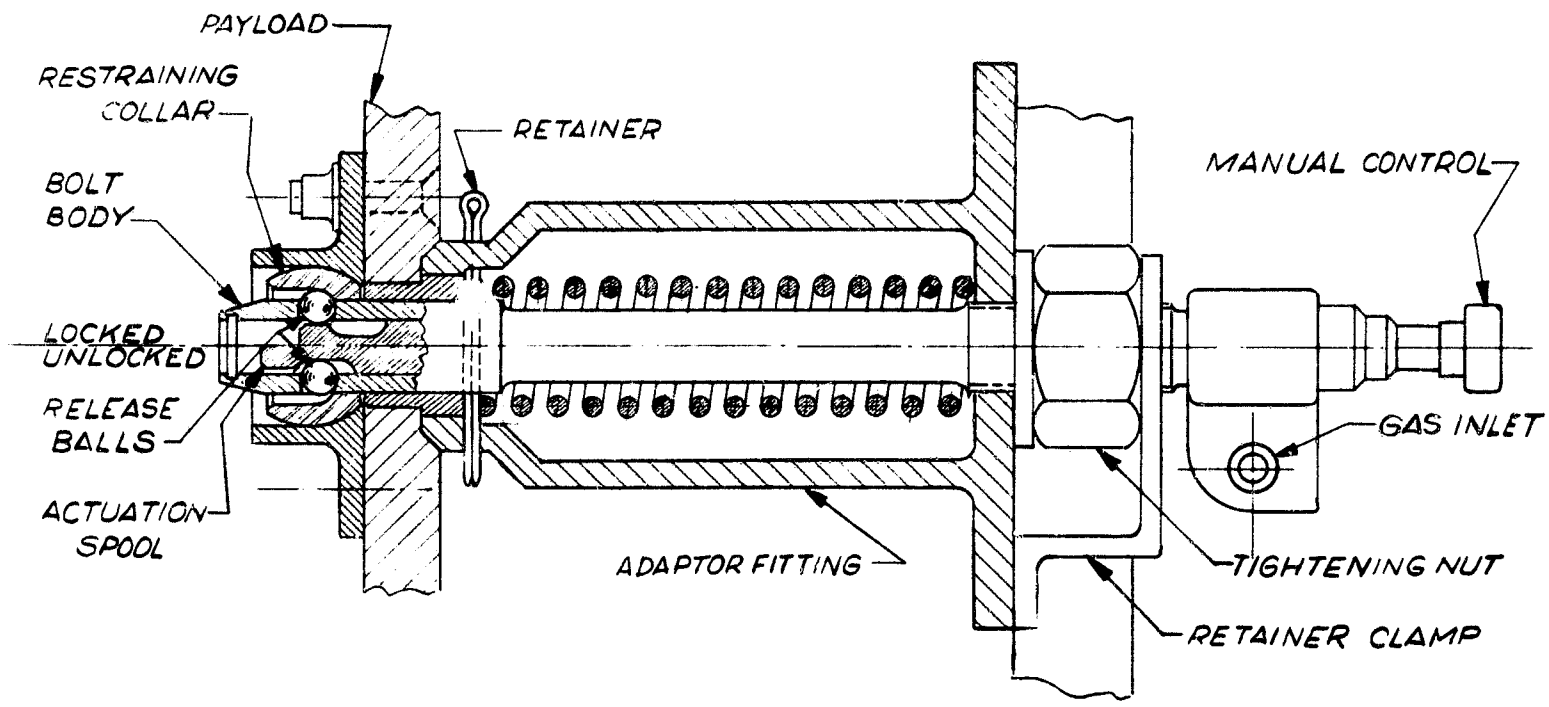

Figure 4-4. Separation Device-Ball-Lock-Bolt

efficiency in this application. These ribs are hinged to a central hub, which is attached by a fitting to a bracket on the side of the despun platform. The attach fitting is free to pivot on one axis with respect to the bracket. Each of the eight ribs consists of three hinged sections. The struts supporting the feed are hinged once, and telescope at the outer segment. The ribs, struts and feed all fold and are stowed inside a container in the launch configuration as shown on Figure 4-1. During launch, this container is supported by two saddles located on top of the despun platform. In order to deploy the antenna the saddles are released first, allowing the container to swing 180°. This motion is actuated by a preloaded spring at the main pivot and is controlled by a viscosity damper. The unfolded position is determined and maintained by mechanical stops and by the remaining preload force in the actuating spring. Half-way during the above described motion, the two halves of the stowage container are ejected, allowing the ribs of the reflector, the struts of the feed and the feed ground plane, to unfold. This unfolding is also accomplished by preloaded springs at the various pivot points. The unfolding sequence, which is critical to avoid mechanical interference, is again controlled by viscosity dampers (of different damping characteristics). Again, the final configuration of the antenna is achieved by mechanical stops and by the remaining force in the springs.

The ground plane for the VHF feed has a light collapsible frame supporting a mesh which unfolds in the first stages of deployment, during the period while the telescoped struts of the feed are being extended.

The deployment sequence for the antenna system is depicted in Figure 4-5.

In the final configuration the unfolded reflector ribs stretch a conductive mesh which is attached to the ribs. At the VHF frequencies of interest a rather coarse mesh with 1.25-inch diameter holes provides adequate performance. In the area where the fields of view of attitude sensors located on the spinning body intersect the antenna reflector, the mesh is removed, forming two slots for the roll/yaw attitude sensors. The pitch attitude sensor and the sun pipper have fields of view passing through the lower slot for the roll attitude sensors.

4.2.5 WEIGHT AND INERTIA ESTIMATES

Table 4-1 presents a detailed breakdown of the weight and size distribution by element in the NAVOX spacecraft. Also included in this table are the average electrical power requirements.

Based on the layout shown in Figure 4-2, the inertia of the spinning cylindrical section about its spin axis has been calculated to be 7,495 lb-ft^2. The transverse inertias for the total spacecraft (with the antenna deployed) are computed to be 15,310 lb-ft^2 and 22,460 lb-ft^2 on each of the two transverse principal axes.

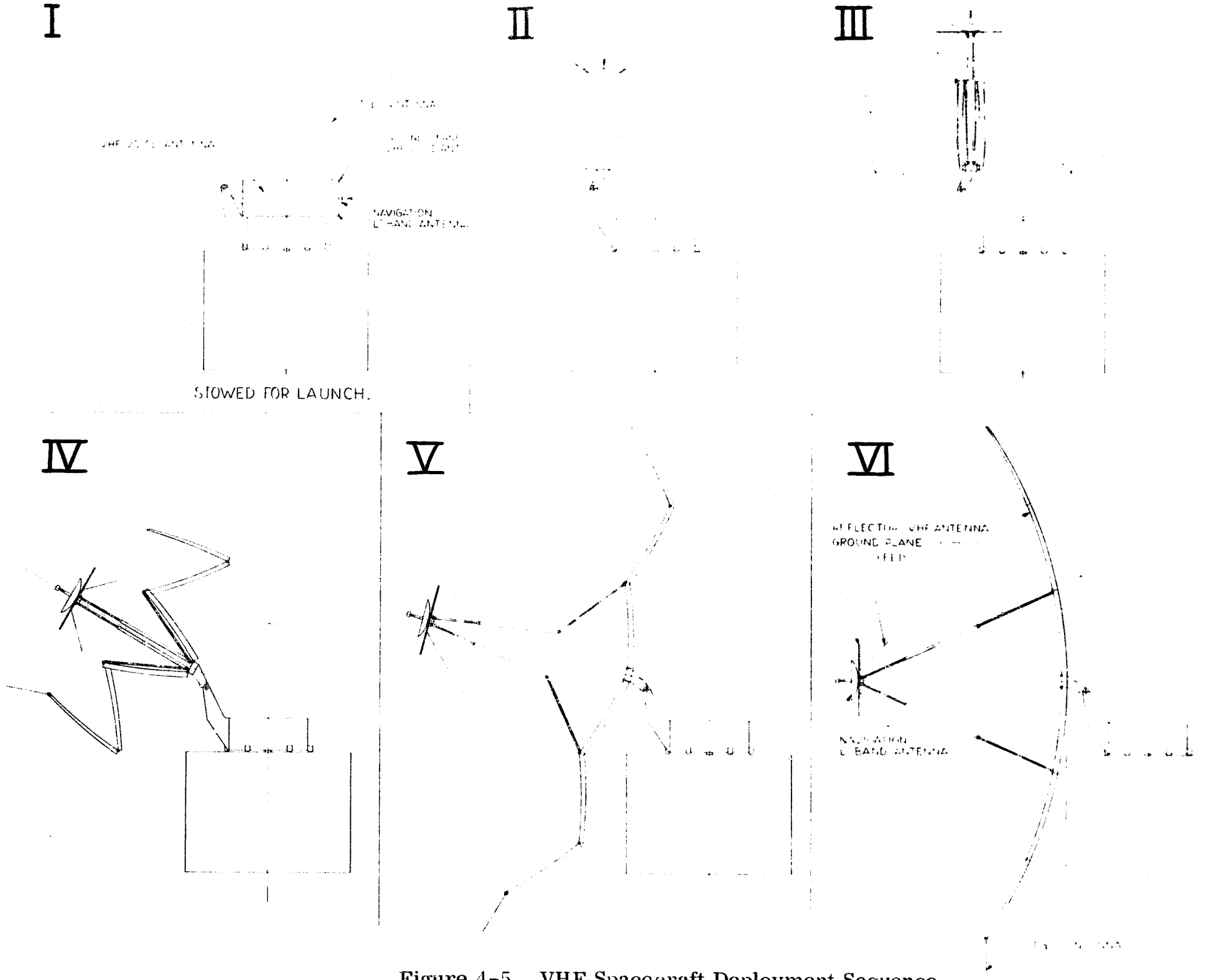

Figure 4-5. VHF Spacecraft Deployment Sequence

TABLE 4-1. PHYSICAL AND ELECTRICAL DETAILS OF NAVOX COMPONENTS

Component	Weight (Lb.)	Power (W)	Size (in)
Structure Subsystem			
Array Support	20.0		
Despun Platform	25.0		
Thermal Control	10.0		
Misc. (Harness, Bal. Wts., etc.)	20.0		
Subtotal	75.0		
Communications Subsystem			
Voice Communications Subsystem			
VHF Aviation pwr. amplifier #1	2.0	61.3	1.5 x 4.0 x 4.0
VHF aviation pwr. amplifier #2	2.0	61.3	1.5 x 4.0 x 4.0
VHF maritime pwr. amplifier #1	2.0	6	1.5 x 4.0 x 4.0
VHF maritime pwr. amplifier #2	2.0	6	1.5 x 4.0 x 4.0
VHF local oscillators (four)	4.0	4	2.0 x 4.0 x 4.0
VHF mixers, IF amplifiers and bandpass filters (4 sets)	3.0	4	2.0 x 4.0 x 4.0
VHF antenna diplexer	5.0		-- -- --
VHF communications antenna	110.0		28.5 foot diameter
Subtotal	130.0	142.6	
Position Location Subsystem			
Forward link L-band navigation transponder	8.0	10	7.0 x 6.0 x 10
Back link L-band nav. transponder	8.0	10	7.0 x 6.0 x 10
Forward link power amp. (TWTA)	10.0	66	5.0 x 6.5 x 14
Back link power amplifier (TWTA)	10.0	33	5.0 x 6.5 x 14
L-band antenna diplexer	5.0	--	-- -- --
L-band navigation antenna	3.0	--	2.3 foot diameter
Subtotal	44.0	119	
TT&C Subsystem			
VHF command receiver (2)	2.5	1	2.0 x 3.0 x 6.0
Command decoder and CDU (2)	10.0	2	5.5 x 6.0 x 7.5
Telemetry baseband assembly unit and modulator (1)	8.0	6	7.0 x 5.0 x 6.5
VHF telemetry transmitter (2)	1.5	5	3.0 x 3.0 x 3.0
TT&C diplexer	1.0	--	-- -- --
TT&C antenna (omni, VHF)	2.3	--	40 inch dipole
Subtotal	25.3	14	
Power Subsystem			
(1) Solar Array	153.5		108" D x 81.2"
(2) Batteries (3)	83.0	58	(3) 4 x 9 x 4.4
PSE A	8.5	2	10 x 12 x 3
PSE B	4.0	4	6 x 6 x 3
(3) Slip Ring Assembly	10.0	3	
Subtotal	259.0	67	
Attitude Control Subsystem			
Roll Horizon Sensors	1.4	.5	3 x 3 x 4
(4) Pitch Horizon Sensors	2.0	.5	4 x 7 x 4
Pitch Control Electronics	8.0	4	5 x 6 x 5
Despun Platform Drive Assembly	15.0	5	
(5) Nutation Damper	5.0		12" x 72"
Subtotal	31.4	10	
Secondary Propulsion Subsystem			
(6) Tanks (2) A-24 Surv.	47.3		10" D x 15.4"
Thruster Block (4)	7.2		
Support Structure	10.0		
Miscellaneous	2.6		
Subtotal	67.1		

(1) 61 ft^2 Projected Area
(2) 29 W required for C/20 charge. One battery switched out.
(3) Integ. with despun platform drive assembly
(4) Includes threshold amplifiers
(5) Approximate Toroid Shape
(6) Includes 39-lb. propellant

4.3 COMMUNICATIONS

The communications equipment on the satellite is divided into two major subsystems:

- L-band position location transponders
- VHF voice-channel transponders

In addition of course there is the telemetry and command subsystem. The L-band position location transponders are hard-limiting repeaters whose characteristics are compatible with carriers which are phase modulated with tone-ranging and digital sub-carriers. There is one transponder for the forward (ground station - satellite - aircraft) link and a second transponder for the back (aircraft - satellite - ground station) link.

Four separate VHF transponders provide voice communication. Two are in the 120-130 MHz aviation band, and the other two are in the 150-160 MHz maritime band. With each transponder, all up-link communications to the satellite are at one frequency; all down-link communications are at another. Thus communications between an aircraft and the control center or between a ship and the shore station are in the simplex, push-to-talk mode.

4.3.1 L-BAND NAVIGATION SUBSYSTEM (See Figure 4-6)

The components of this subsystem are (a) a 2.3 foot diameter earth-coverage antenna and its diplexer-duplexer; (b) a low-noise pre-amplifier for the received forward and back link signals; (c) separate hard-limiting transponders for the two channels; and (d) traveling-wavetube (TWT) amplifiers for the two channels.

The antenna will be mounted on the feed structure of the VHF voice communications antenna. The aperture blockage caused to the VHF antenna results in less than 0.1 dB gain reduction for the VHF antenna. The L-band antenna has a beamwidth between the 3 dB points of 18.6° at 1.6 GHz. Allowing 0.5° satellite attitude error, the antenna gain at the edge of the earth exceeds 15.5 dB at both the 1.55 GHz receive frequency and the 1.63 GHz transmit frequency. The receive and transmit signals are circularly polarized with opposite senses of polarization to increase the isolation between them. Bandpass filtering in the diplexer-duplexer further increases the isolation.

Both received signals are first amplified in the low-noise preamplifier. This will be of the tunnel-diode type, with a noise figure not exceeding 5dB. Note that the two input frequencies are considerably separated and are well within the 1.54 to 1.66 GHz aeronautical navigation band. These parameters are relatively arbitrary at this time and can be modified as specific channels are allocated for the satellite-aided navigation service and user equipment standards are formulated. The two spacecraft would be somewhat separated in frequency.

The two received signals are separated at the output of the pre-amplifier and go to individual IF transponders. This type of transponder, at the expense of some increase

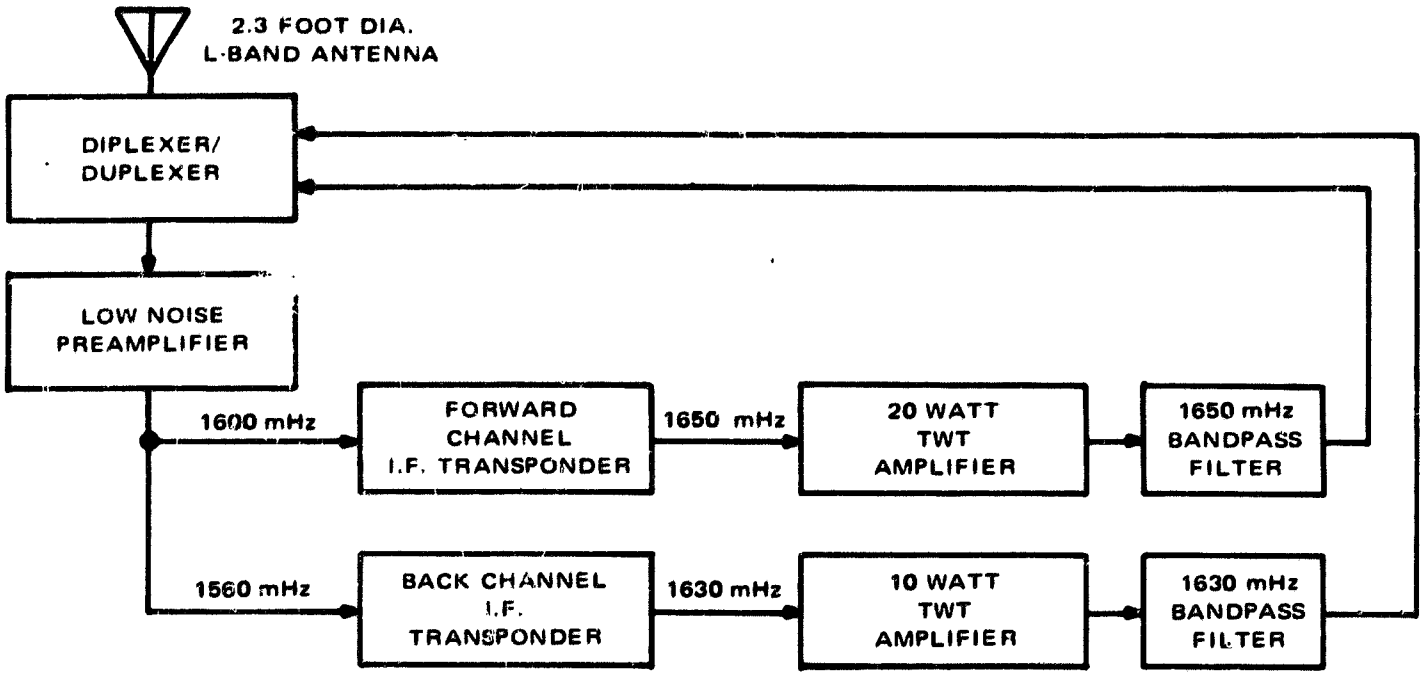

THESE FREQUENCY SELECTIONS ARE SOMEWHAT ARBITRARY, AND ARE FOR ONE SPACECRAFT OF THE PAIR ONLY. THE OTHER SPACECRAFT WOULD HAVE DIFFERENT ALLOCATIONS. (EXCEPT FOR THE NORMALLY 1551 mHz BACK CHANNEL UPLINK)

Figure 4-6. Nav/TC Satellite L-Band Navigation Transponders

in complexity, has two advantages over the all-RF transponder: (1) automatic gain control may easily be included in the IF stages so that a constant level input is available to the TWT, and (2) demodulation of the signal is possible -- this feature may be desirable in future versions of the navigation satellite although it is not required in the interim NAVOX spacecraft. The satellite repeater bandwidth is 100 KHz. This is adequate for the modulated carrier (which has first-order sidebands at 500 Hz and 8 KHz and second-order sidebands at twice these frequencies), frequency instabilities in user and satellite equipment, and the maximum anticipated doppler shifts.

The RF power required at the TWTA is 20 watts for the forward channel and 10 watts for the back channel. This includes the effect of 1 dB loss in the filter, diplexer-duplexer, waveguide or cable, and connectors. There are not presently any space-qualified TWT's at exactly these power levels in this frequency band. The probable solution to this problem is the "scaling" of existing 2.2 to 2.4 GHz TWT's to the 1.6 GHz band. Several TWT manufacturers have space qualified 2.2-2.4 GHz tubes; the output powers available range from 10 to 50 watts. The DC to RF efficiency for such a tube, scaled to 1.6 GHz, is expected to be 30 percent, including the power supply.

4.3.2 VHF VOICE CHANNEL SUBSYSTEM (FIGURE 4-7)

This subsystem is the most complex and the one which requires the greatest amount of DC power of all the communications subsystems. It is configured to be completely compatible with the VHF voice channel system standards being formulated by the FAA

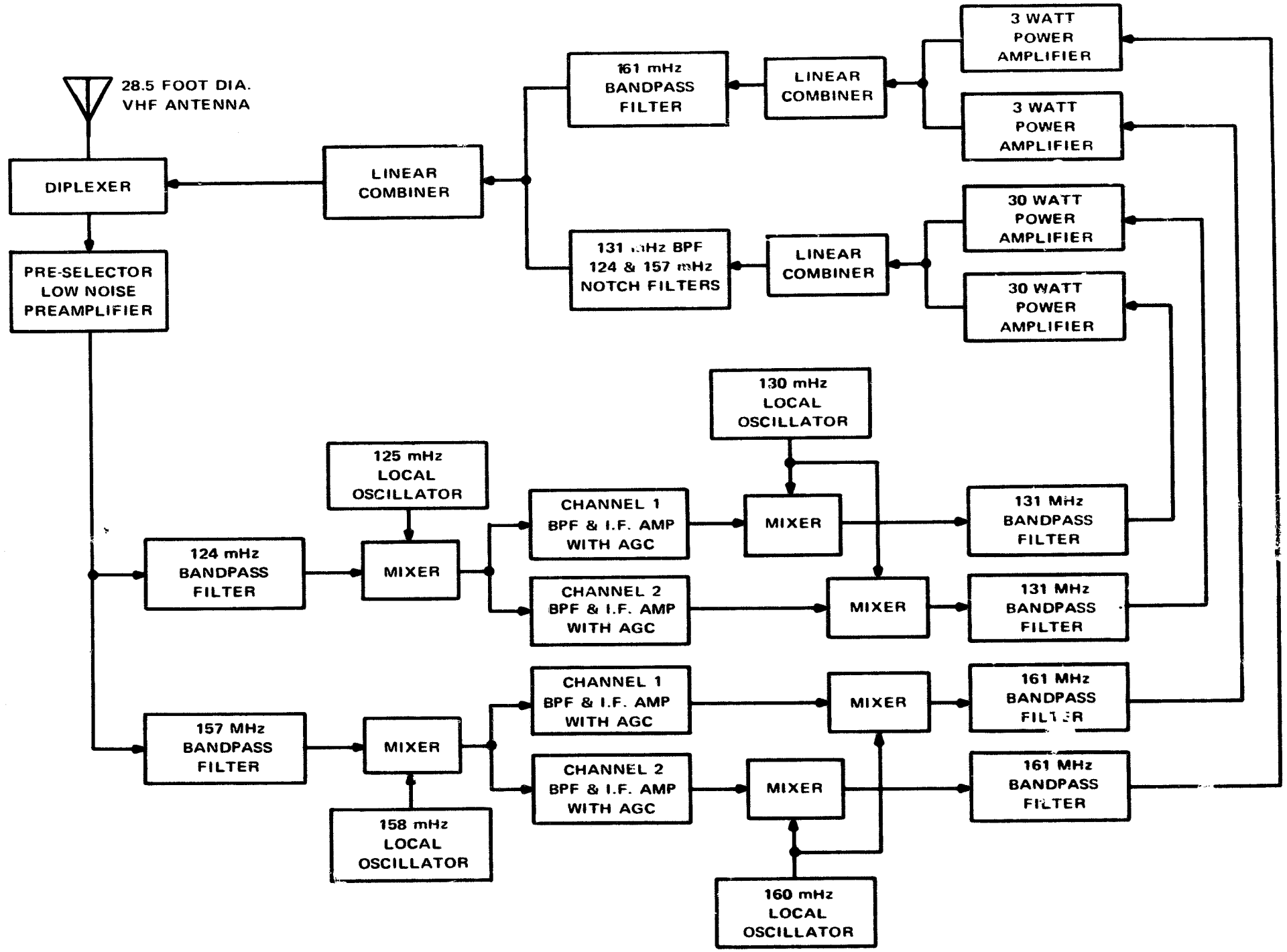

Figure 4-7. Block Diagram, Satellite NAVOX Aviation and Maritime Voice Communications Equipment

and the airlines. These standards are described in the "Satcom Newsletters" of the Airlines Electronic Engineering Committee (AEEC) and, in summary, are as follows:

- Modulation: FM with pre-emphasis of a 2.7 kHz voice baseband, having no speech-clipping or other processing, with an RF modulation bandwidth of approximately 15 kHz.
- RF bandwidth of channel: 25 KHz, including all oscillator instabilities, doppler shifts, and the above modulation spectrum.
- Spacing of channels: Adjacent Satcom channels might be as close at 50 kHz together; adjacent channel interference from other services 25 kHz away may be anticipated. All up-link channels to the satellite will be in a single 1 MHz band; all down-link channels from the satellite will be in a second 1 MHz band. The spacing between the receive and transmit halves of a given channel will be constant, for example, 7 MHz.

System standards for a maritime Satcom service have not been completed, but are expected to be similar in that frequency modulated carriers, spaced in 25 KHz bandwidth channels will be used. However, the spacing between the receive and transmit halves of a given satellite channel is expected to be 4.6 MHz instead of 7 MHz as for the airlines. The subsystem of Figure 4-7 is composed of the following major parts: (a) a 28.5 foot diameter earth-coverage antenna, (b) diplexer-duplexer to permit the four received carriers and the four transmitted carriers to share the antenna, (c) a low-noise preamplifier and preselector for the received carriers, (d) bandpass filters to separate the 124 MHz aviation carriers from the 157 MHz maritime carriers, (e) local oscillators and mixers to convert the received carriers to intermediate frequencies of 1 to 2 MHz and to convert the amplified signals back to the required transmit frequencies, (f) the 1 to 2 MHz center frequency IF amplifiers which include automatic gain control and noise bandwidth filtering for each channel individually, (g) separate solid-state power amplifiers for each channel.

The antenna has a beamwidth of 18.6° between the 3 dB points at 130 MHz. Its gain exceeds 15.5 dB at the edge of the Earth in both the 130 MHz band and the 160 MHz band. The configuration is based on experience with the LEM erectable antenna designed and built by RCA for the Apollo program. The antenna, when unfurled and deployed, consists of metallic mesh stretched between supporting ribs.

Following preamplification and initial bandpass filtering, each of the four channels is handled separately. To reduce the effect of oscillator instabilities, the number of local oscillators shown in Figure 4-7 could be reduced by the use of a frequency synthesizer. To minimize the effect of up-link noise on the down-link, the noise bandwidth of each channel will be reduced to 25 KHz in the IF amplifiers. The center frequencies of these amplifiers, of course, will depend on the actual channel allocations. Alternatively, the local oscillator or frequency synthesizer frequencies could be selected to permit a common IF design for all channels.

The power amplifier power output must be 30 watts per channel for the aviation voice channels and 3 watts per channel for the maritime channels. This allows approximately 1 dB for losses in the output bandpass filters, combiners, and diplexer. A level of 30 watts per channel at 130 MHz is well within the capability of present day transistor amplifiers. The gain per stage is 6 dB for the high-level stages, and the overall efficiency of the amplifier exceeds 40%.

The satellite-to-aircraft voice link is the most critical in the NAVOX system since it is the one requiring the greatest amount of satellite prime power. Table 2-24 (Section 2.8.1) gives the principal satellite, propagation, and aircraft parameters.

The link shown has 0.9 dB margin in C/N in the phase locked loop and + 3.1 dB margin in output S/N at threshold. Most of the equipment parameters are worst-case (minimum power output, worst antenna pointing angle, etc.) and propagation parameters (multipath, scintillation, etc.) are believed to be for reasonably bad conditions. Propagation conditions between a satellite and an aircraft at VHF are just now being measured and are still very uncertain for many values of the path and temporal variables.

4.4 TELEMETRY, TRACKING AND COMMAND

The TT&C subsystem operates at VHF with the telemetry carrier at 136 MHz and the command carrier at 148 MHz. Carrier modulation parameters, RF bandwidths, and carrier frequencies will be compatible with the NASA STADAN system. A separate omnidirectional VHF antenna is provided for TT&C to allow monitoring and commanding the satellite as necessary during ascent and station-keeping maneuvers.

The TT&C subsystem (Figure 4-8) operates in the standard VHF bands and is compatible with the STADAN system. It consists of (a) a single element omnidirectional antenna (half-wave dipole) and associated coupling network, (b) redundant 148 MHz command receivers and command decoders, (c) a command distribution unit, (d) telemetry commutator and sub-commutator, (e) baseband assembly unit for multiplexing analog telemetry information with on-off "discretes", digital data, and attitude sensor information, and (f) a redundant 5 watt solid state 136 MHz telemetry transmitter.

The TT&C antenna has a pattern sufficiently broad to permit reception of commands during station-keeping maneuvers which may disorient the earth-coverage VHF antenna. The omni antenna is a single 40 inch dipole similar to the one used on the TIROS M satellite. On TIROS M, the antenna pattern approaches that of an ideal dipole; however, the pattern is dependent on the presence of the remainder of the satellite and so cannot be predicted exactly in advance of simulation. The omni-antenna location shown in the NAVOX satellite configuration, (Figure 4-2), may require modification for this reason. The coupling network, consisting of tuned lines, produces circular polarization at the transmit frequency and permits the simultaneous use of either telemetry transmitter and both command receivers. Depending on the final location of the TT&C antenna, the filters shown between the coupler and the command receivers may have to be supplemented by notch filters at the 131 MHz aviation transmit frequency and the 161 MHz maritime transmit frequency.

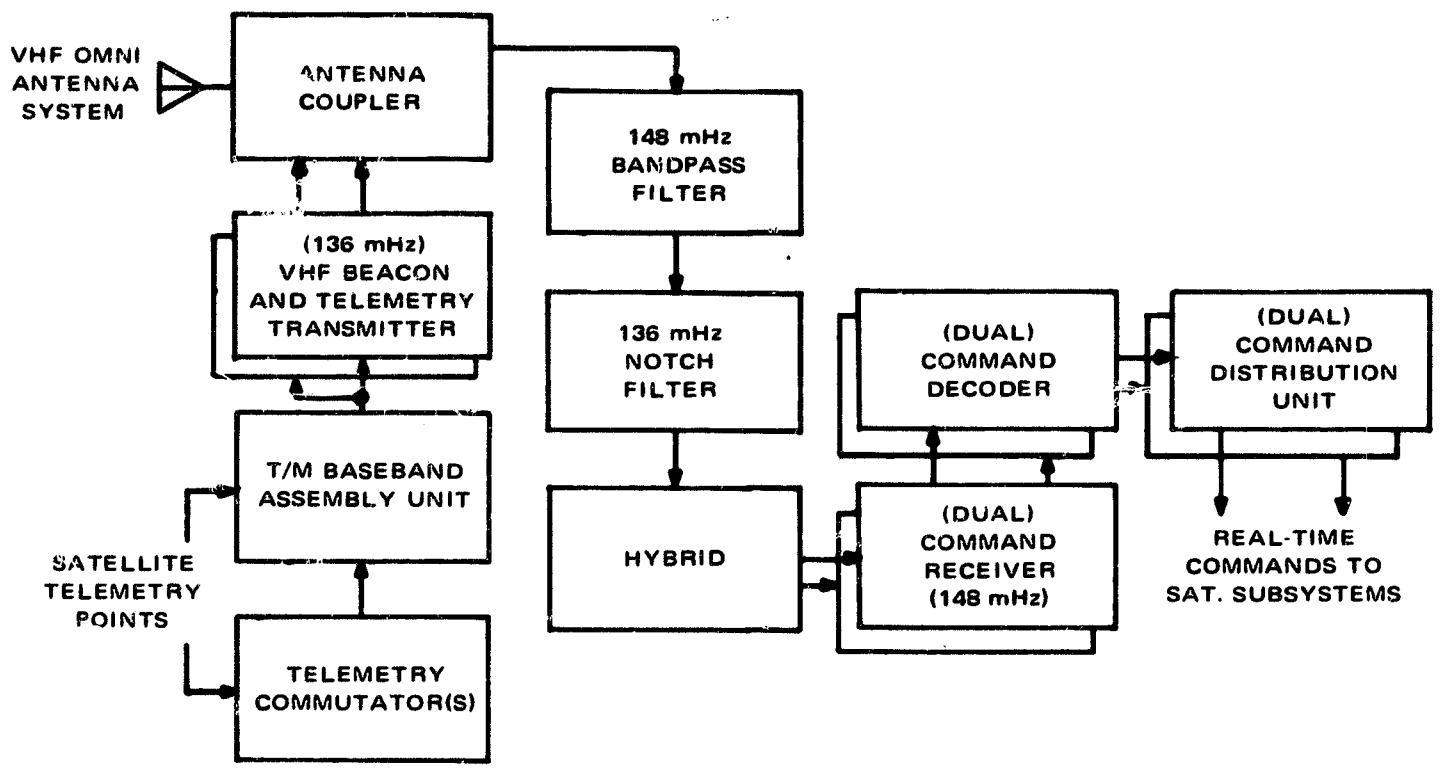

Figure 4-8. NAVOX Satellite TT&C Subsystem

The command portion of the subsystem is based on that used in the TOS satellite. The command signal consists of an enable tone followed by an FSK tone which is modulated by 10 bit per second, bi-polar, return-to-zero digital data. This baseband amplitude modulates the command transmitter at 148 MHz. The satellite command receiver demodulates the AM carrier and delivers enable and FSK tones to the decoder. The decoder and command distribution unit provide on-off and magnitude commands to the satellite subsystems.

The telemetry portion of the subsystem is based on the TIROS M design. Since the NAVOX satellite itself is of a new design, a certain number of satellite parameters will be monitored through the telemetry. In addition, the outputs of the attitude horizon sensors will be telemetered continuously so that attitude correction may be accomplished as required. Finally, the telemetry RF carrier will provide a VHF beacon for tracking of the satellite by the STADAN ground stations during ascent to near synchronous orbit. Final tracking to precise orbit station will be accomplished through the L-band navigation transponder. Depending on the particular design of the attitude control system, the horizon sensor data may be in the form of modulated subcarriers which modulate the telemetry carrier or in the form of digital data which are read out periodically during the main telemetry frame. The housekeeping telemetry points will be sampled at the rate of one per minute (subcommutated) to one per second (main frame commutation rate), conditioned to a zero to five volt range, converted into seven bit digital form, and read out as 8-bit serial words (including a parity bit) which modulate a subcarrier. All subcarriers will phase modulate the RF carrier. Their center

frequencies will be compatible with STADAN and will be sufficiently far from the carrier frequency that carrier tracking by means of a phase locked loop is possible.

Link calculations for the command up-link and the telemetry down-link are given in Tables 4-2 and 4-3. There is adequate margin in both links with the standard STADAN ground equipment assumed.

The use of a VHF TT&C subsystem is predicated on a relatively quickly implemented satellite having VHF voice capability. VHF TT&C spacecraft and ground components are readily available. If the program should be delayed until, say 1975, the satellite would probably have an S-band TT&C subsystem. The S-band TT&C would be constructed around a Goddard Range and Range Rate Transponder (which would serve as command receiver and 5 watt solid state telemetry transmitter) which could also be used for precise orbit tracking. (This latter function is now accomplished through the navigation transponders and calibrated navigation ground stations.)

4.5 ELECTRICAL POWER SUBSYSTEM

4.5.1 GENERAL

A block diagram of the proposed electrical power subsystem is shown in Figure 4-9. It comprises three major elements, the solar-cell array, the battery pack, and the electronics packages. This subsystem will generage electrical power by means of solar cells and will supply this power in the required form to operate all spacecraft equipments and to store sufficient energy in the batteries for dark-time operation of those equipments. The subsystem will supply a regulated bus voltage of -28 volts (±0.7%) at power levels consistent with mission requirements.

The solar-cell array consists of cells mounted on the curved side of the spinning cylindrical section. The cells are the radiation-resistant N-on-P type, 2 cm by 2 cm, having a base resistivity of 10 ohm-cm. The thickness of the protective cover glass is 6 mils.

The battery pack consists of three packages each containing 18 twenty-ampere-hour, nickel-cadmium cells connected in series. These batteries are configured so that any two with their associated charge controller connected in parallel can provide for all mission functions. Load and battery switching commands permit the selection of any two.

The basic components used to regulate the array output are the mode selector and the shunt regulator. The shunt regulator is connected directly across the solar array, and regulates the array output by limiting the output voltage to the desired value within the specified tolerance.

During dark time, the regulated load power is supplied by the two selected 18-cell nickel-cadmium batteries through the battery booster. The mode selector senses small voltage changes in the solar-array output bus. During the illuminated portion of flight, the correct amount of array current is delivered to the load. Any excess current

TABLE 4-2. UP-LINK, COMMAND, 148 MHZ

Line	Parameter	Value	Comments
1.	Ground transmitter power	+67.0 dBm	5000 watts, minimum
2.	Ground antenna gain	+23.7 dB	NASA X-530-66-33, p. 2-91 (SATAN)
3.	Space Loss	-167.1 dB	22,250 s. mi
4.	Receiving Antenna Gain	-1.8 dB	Theoretical Dipole at ± 40° from beam center
5.	Polarization Loss	-3.0 dB	Circular transmit, linear receive antennas
6.	Loss of two 137 MHz notch filters and one 148 MHz BP Filter	-5.0 dB	TOS APT-TR, Contract NAS 5-9034
7.	Hybrid splitter loss	-3.5 dB	
8.	Total received power	-89.7 dBm	
9.	Noise power spectral	-165.8 dBMHz	Receiver F = 8 dB = 1540° K, T circuit = 320° K, Tsky = 700 k, Circuit losses = 8.5 dB
10.	Receiver bandwidth	+46.2 dB Hz	TOS receiver: 42 KHZ BW
11.	Noise Power	-119.6 dBm	
12.	RFI from VHF transmitters	-120.6 dBm	TOS APT-TR, Contract NAS 5-9034
13.	Total noise + RFI	-117.0 dBm	
14.	Required signal power	-107.0 dBm	Threshold, for 0.7 volt RMS to decoder:
15.A	Link margin based on signal	+17.3 dB	TOS Receiver Specification
15.B	Link margin based on S/(N + RFI)	+27.3 dB	
16.	Subcarrier improvement factor	+10.2 dB	AM mod. index = 0.9 AM S/C Bandwidth = 3.2 KHZ TOS APT-TR, Contract NAS 5-9034
17.	Decoder FSK/FM Improvement Factor	+10.5 dB	FM mod. index = 3.7
18.	Threshold C/N	+10.0 dB	Line 14 - Line 13
19.	Decoder S/N at system C/N threshold	+30.7 dB	Line 16 + Line 17 + Line 18
20.	Bit error rate at threshold.	$<10^{-6}$	

NOTES: 1. The NASA STADAN high-powered command transmitter and associated SATAN antenna are assumed for this command link.

2. The RFI in TOS comes from one 5-w data transmitter at 136 MHz. The NAVOX command link calculation shows 26 dB RFI margin, based on the single 5-w transmitter. It is expected, therefore, that the NAVOX command link will work in the presence of the two 30-W, 130 MHz aviation voice transmitters and the two 3-W, 160 MHz maritime voice transmitters, although this has not been studied.

TABLE 4-3. DOWN-LINK (TELEMETRY AND ATTITUDE INFORMATION INTO CDA), 136 MHZ

Line	Parameter	Value	Comments
1.	Transmitter Power	+37.0 dBm	5 watt transmitter
2.	Spacecraft Circuit Loss	-1.7 dB	Diplexer 0.4 dB, Cable 0.5 dB, Feed Network 0.7 dB, notch filter 0.2 dB
3.	Spacecraft Antenna Gain	-1.5 dB	Includes pointing loss at 40° antenna angle
4.	Polarization Loss	-3.0 dB	Linear (spacecraft, worst case) into circular (ground)
5.	Space Loss	-166.2 dB	Slant range 22,250 s. mi. at 5° elev. angle.
6.	Receiving antenna gain	+22.2 dB	SATAN antenna (NASA X-530-66-33.)
7.	Total received power	-113.2 dBm	
Carrier Channel			
8.	Modulation Loss	-2.2 dB	$m_1 = 0.7$ $m_2 = 0.7$ radians.
9.	Power in carrier	-115.4 dBm	
10.	Noise power spectral density	-168.0 dBm	Receiver F = 3.5 dB, Receiver T = 360°K Tsky = 800°K, T system = 1160°K
11.	Loop bandwidth	+24.7 dB Hz	Electrac Receiver (Bandwidth 3 to 300 Kz; 300 Hz chosen here for rapid acquisition)
12.	Received noise power	-143.3 dBm	
13.	C/N in loop	+27.9 dB	Adequate
Subcarrier Channel 1 (Channel 7, 2300 Hz ± 20%, $m_1 = 0.70$)			
14.	Modulation Loss	-7.7 dB	$m_1 = 0.70$ rad. peak, $m_2 = 0.70$ rad. peak

TABLE 4-3. DOWN-LINK (TELEMETRY AND ATTITUDE INFORMATION INTO CDA), 136 MHZ (Continued)

Line	Parameter	Value	Comments
15.	Power in subcarrier	-120.9 dBm	
16.	Subcarrier bandwidth	+30.9 dB	TIROS M system ((Deviation ± 20%) (Baseband 160 Hz) BW = 1240 Hz.
17.	Noise Power	-137.1 dBm	
18.	Subcarrier C/N	+16.2 dB	
19.	FM detector threshold	12.0 dB	assumed
20.	Margin above threshold	+4.2 dB	Adequate in this worst case
21.	FM improvement factor	+19.9 dB	20% deviation; m = 2.9; I = $3m^2$ (m + 1)
22.	Baseband S/N at link C/N	+36.1 dB	rms/rms
23.	Baseband S/N at threshold	+31.9 dB	rms/rms
Subcarrier Channel 2 (Channel 9, 3900 Hz, ± 12%, m_2 = 0.7 rad.)			
14A.	Modulation Loss	-7.7 dB	m_1 = 0.7 rad. peak, m_2 = 0.7 rad. peak
15A.	Power in subcarrier	-120.9 dBm	
16A	Subcarrier Bandwidth	+30.9 dB	Deviation + 12% Baseband 160 Hz, BW = 1240 Hz
17A	Noise power	-137.1 dBm	
18A	Subcarrier C/N	+16.2 dB	Same as Channel 1
20A	Margin above threshold	+4.2 dB	Same as Channel 1
22A	Baseband S/N at link C/N	+36.1 dB	Same as Channel 1

NOTES:

1. A 5-watt satellite telemetry transmitter and dipole-like satellite antenna pattern are assumed.
2. Two data subcarriers modulate the 136 MHz telemetry carrier. These may used to carry the telemetry data and the outputs of two horizon sensors on a time-shared basis.

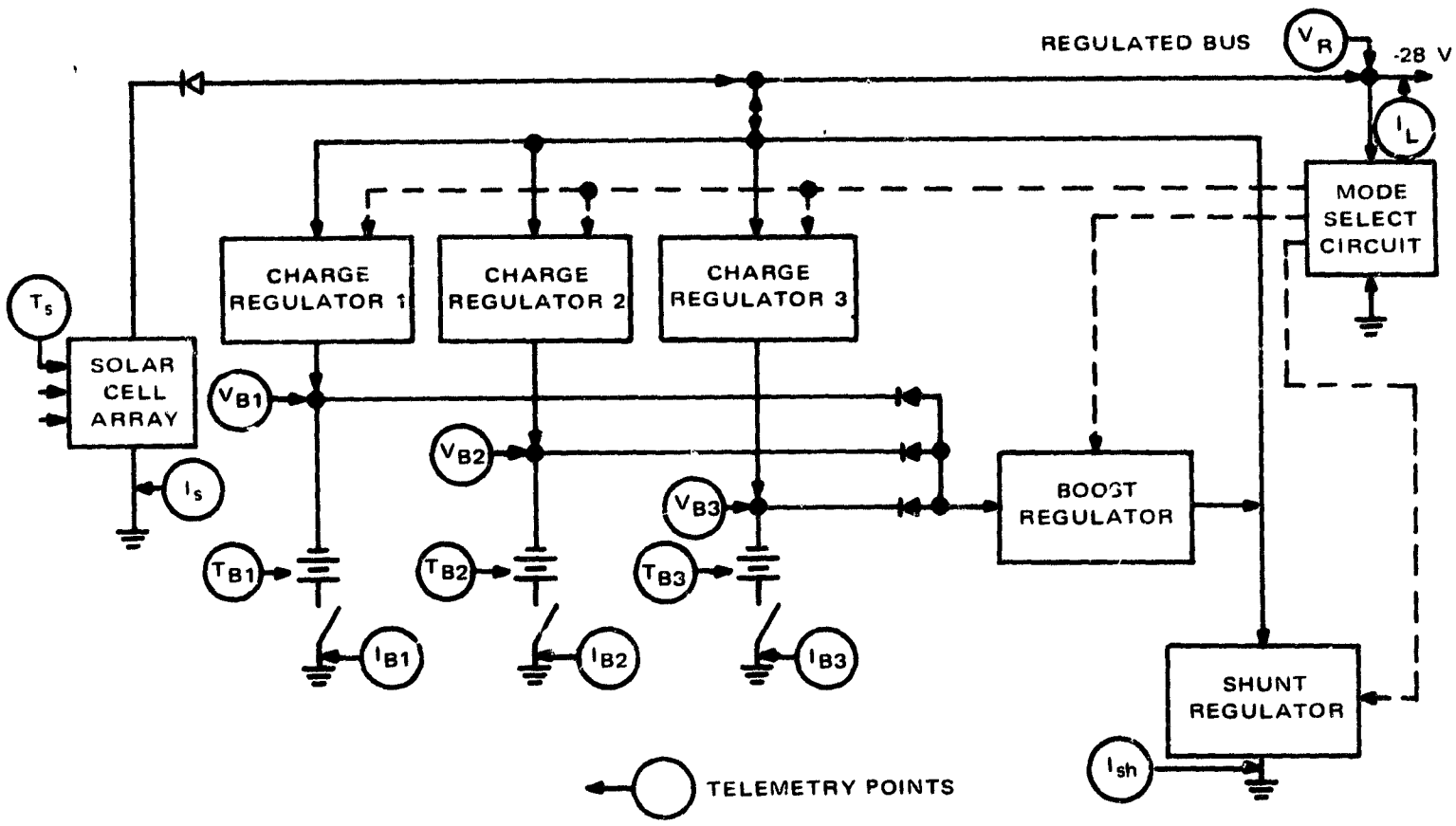

Figure 4-9. Power Subsystem

causes the bus voltage to increase slightly; this increase is sensed by the Mode Selector, which then turns on the charge controllers, allowing excess array current to flow into the battery. All excess current (i.e., the difference between the total available array current and load plus power-subsystem loss) is thus delivered to the battery unless the excess is too large for safe charge. In the latter case, the charge controller limits the charge current, and any remaining excess current is bypassed to the shunt regulator.

If the load should increase, or during the transition from light to dark, the action of the power subsystem is as follows: First, the shunt regulator is unloaded to a point where practically no current flows through it. The bus voltage then drops slightly, causing the mode selector to reduce the charge current to the battery and to supply that current to the load until the added current matches the load requirement or until the charge current is reduced to zero. At that point, the array capability just equals the load-plus-loss requirement. Further load increase (or array current decrease) is accompanied by the mode selector action to turn the battery booster on by an amount proportional to the terminal load requirement. The entire sequence (i.e., no load/shunt regulator turned on, to full load/battery booster turned on) causes a net change in the bus voltage equal to a fraction of the regulation tolerance. (Note: The battery booster and charge controller are never on at the same time.)

4.5.2 POWER SYSTEM ANALYSIS

The array power requirements considered in the design of the NAVOX power subsystem are listed in table 4-4. This tabulation was used in sizing the solar array, selecting battery sizes, and determining charge rates.

TABLE 4-4. ARRAY POWER REQUIREMENTS SUMMARY

Element	Average Power (watts)
Communications - Voice	143
Communications - Navigation	119
TT and C	14
Power	6
Attitude Control	10
Subtotal	293.6
Battery Charge	58
Power Transfer	3
Total	353.6

Further considered as factors in evaluating the required solar cell area was the effect of sun angles on the minimum projected area and the effect of antenna shadowing. Since inclination change correction capability is not included in sizing the propulsion subsystem, the maximum range of sun angles for the NAVOX five year mission is $\pm 26.5^\circ$ with respect to the plane normal to the spin axis. This includes a tolerance of $\pm .5^\circ$ in attitude control but assumed that the initial orbit inclination is biased to minimize the inclination excursion in five years. Based on illumination tests run at RCA on the effects of the LEM erectable antenna which uses a much finer mesh than that required in the large VHF voice antenna, an estimate of a 20% average loss was also assumed. The LEM mesh tests resulted in losses of between 25% and 40% depending on the aspect angle between the light source, the mesh and the solar cells. Because of the larger mesh size and the fact that the array is shadowed for less than 40% of the orbit, the 20% average loss should be conservative.

Utilizing all the aforementioned factors, the total solar cell area required is 192 ft^2, for an array degraded by radiation in the five year synchronous orbit.

The minimum number of battery cells in series required to support the electrical load requirements for the selected power system is 18 for a 28 volt bus voltage assuming a 1 volt charge regulator loss. As described earlier the storage system consists of three 18-cell batteries, any two of which can be selected by ground command to provide dark time load power. The cells have a 20 amp-hour capacity. This configuration was based on a design goal that the depth of discharge be no greater than 50% and that in addition 50% redundancy be provided. Using the load power requirements given in Table 4-4 and considering the maximum eclipse time of 70 min for a synchronous

orbit, the per orbit discharge is 17.3 amp hours. This results in a 43% depth of discharge for the two batteries. The batteries are recharged during the sunlit portion of the orbit. However, the minimum charge rate for NiCd cells must be greater than C/20, where C is total battery capacity, otherwise the battery will not accept an adequate charge. With this requirement, two amps are required from the array for this function.

4.5.3 POWER SUPPLY ELECTRONICS

Mode Selector - The mode selector shown in Figure 4-10 consists of a differential amplifier (Q1, Q2) and several other stages (Q3, Q4, Q5). All are biased to activate the battery booster, the charge controller, or the Shunt Regulator in the appropriate sequence. If the bus voltage is low, the differential amplifier is unbalanced and the Q2 collector is less negative than the Q1 collector. The shunt regulator does not therefore have adequate voltage to turn on, and the base-emitter junction of Q5 is reversed-biased, resulting in no activation signal delivered to the Charge Controller. The collector current of Q3, however, is in the control range for turning on the battery booster, and the battery is made to supply bus power. When approaching sun time causes the bus voltage to increase, the collector current of Q3 increases and tends to turn off the battery booster. At one condition of bus voltage, the Battery Booster is completely deactivated.

As the bus voltage again rises, a dead band is traversed to the point where CR1 and CR2 conduct sufficient current to activate the charge controller. Increasing bus voltage then increases battery charge current until the limiting value of current, as determined by the controller circuitry, is reached. After this, another dead band is traversed, and the voltage at the collector of Q2 becomes high enough to activate the shunt regulator.

Shunt Regulator - The shunt regulator shown in Figure 4-11 was designed by the Bell Telephone Laboratories. The circuit has substantially no shunt losses other than a small current bleed to maintain operation of CR1, which sets the threshold of conduction for the circuit. When the mode selector input exceeds the threshold voltage, transistors Q1, Q2, and Q3 conduct and dissipate excess array energy. Dissipation is shared between these transistors and their respective collector resistors.

Figure 4-11 also illustrates the method of increasing shunt regulator power capacity, should this be required. Transistor Qa, diodes CRa and CRb, and resistors Ra through Rd (all shown with dotted connections) would be added and would increase power capacity by approximately 50%. Additional capability may be had by adding more power transistors in the same manner as for Qa.

Battery Booster - The Battery Booster shown in Figure 4-12 is a constant-frequency, pulse-width-modulated device capable of providing an output voltage of -28v, for an input voltage which varies from -21 to -27 volts.

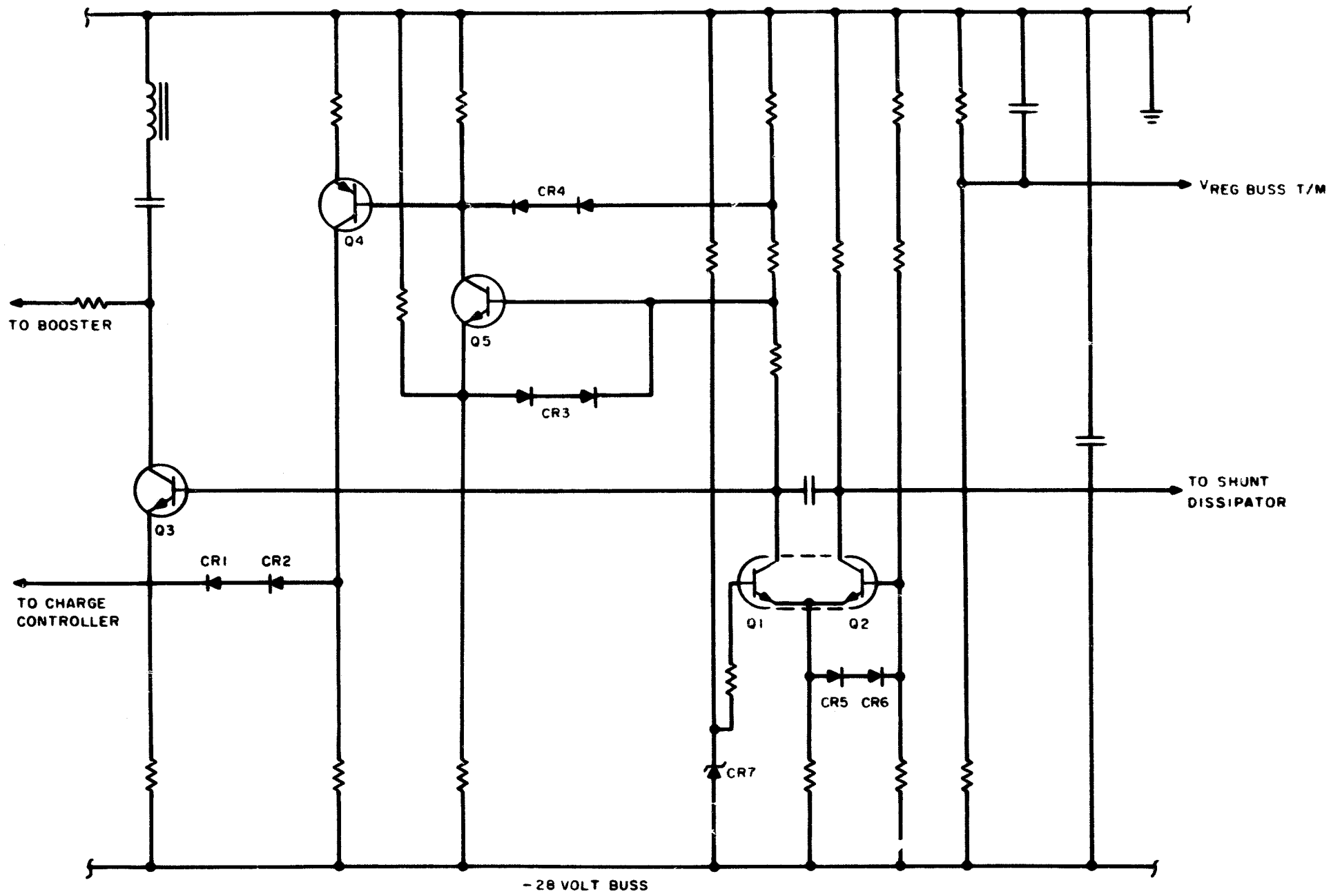

Figure 4-10. Mode Selector

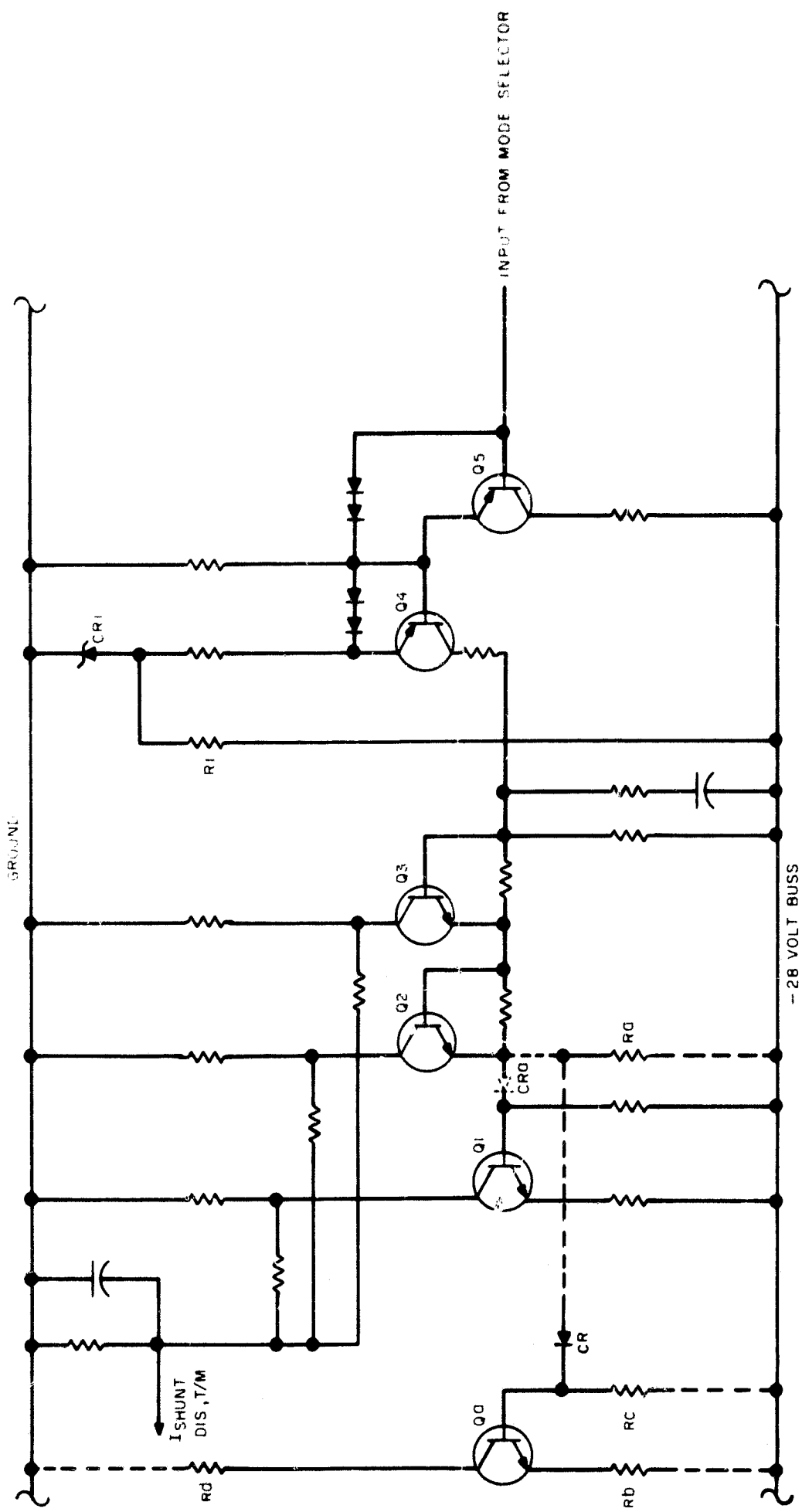

Figure 4-11. Shunt Regulator

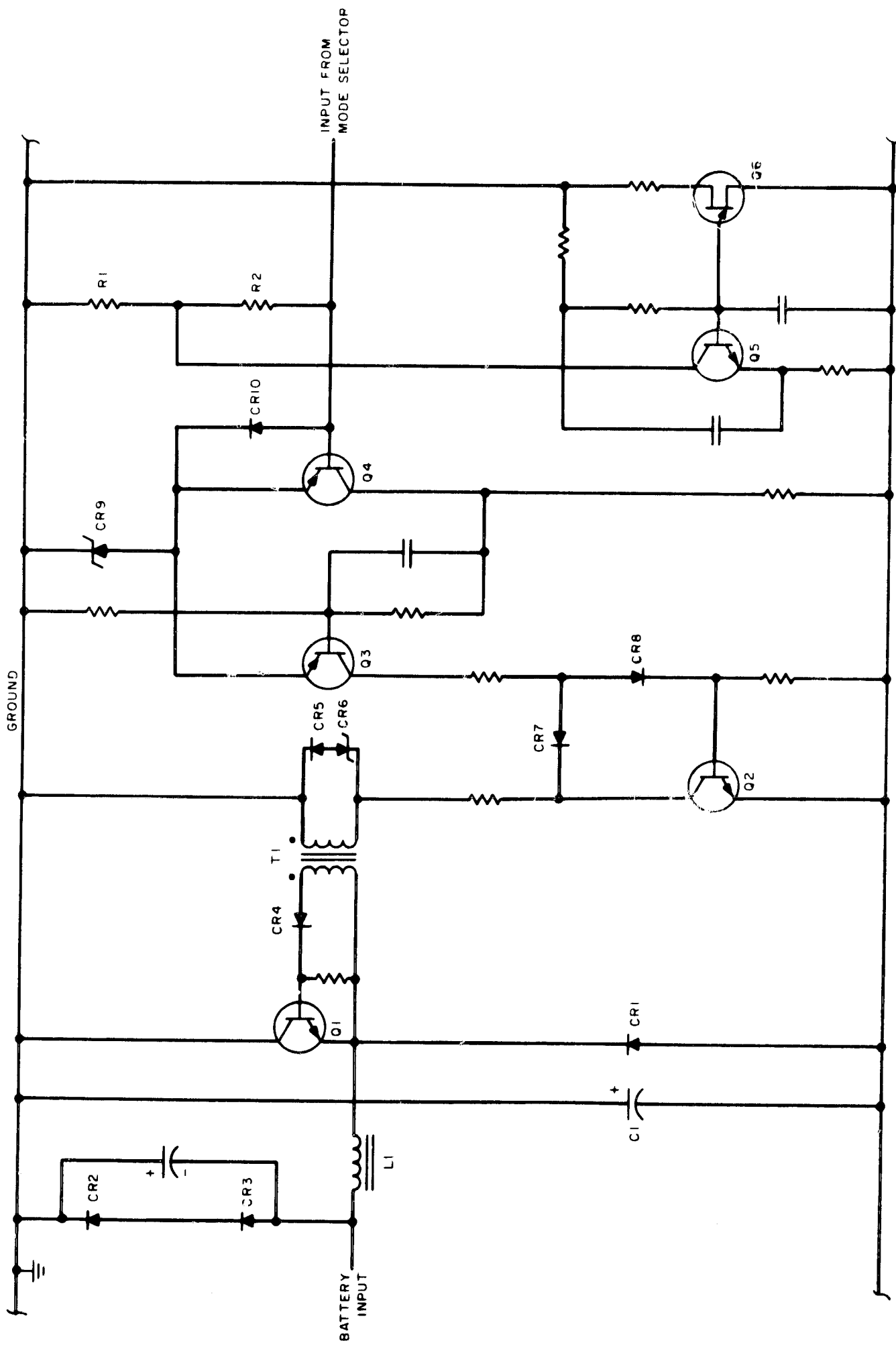

Figure 4-12. Battery Booster

Choke L1 is charged by the battery through high-power transistor switch Q1. L1 discharges into the -28-volt bus through CR1 when Q1 is turned off. Capacitor C1 serves as the main ripple-filtering element. Drive power for Q1 is delivered via transformer T1 and unsaturated switch Q2. Drive power for Q2 is duty-cycle modulated and is derived from Schmitt trigger Q3-4 which serves as a modulator. The input from the Mode Selector is summed with the output of a fixed-frequency sawtooth generator, Q5 and Q6, in resistor network R1-R2. The resultant voltage at the base of Q4 causes the output of Q3 to be time-variant and with a duty-cycle inversely proportional to the current input from the mode selector.

Battery Charge Controllers - The battery charge controllers, upon receipt of the appropriate command from the mode selector, delivers solar-array current in excess of that required by the spacecraft loads to the battery as charging current. The charge-current level is proportional to the mode selector signal until the maximum value, as determined by the mission requirements, is reached. At this point the charge controllers limit and allow no further increase in charging current. The current limit will be held over the spacecraft life to within 20% of the initial setting.

The charge controller, shown in Figure 4-13, is activated by a signal input from the mode selector at the base of Q8. The Mode selector signal reduces the current drawn by Q8 and hence causes the voltage at Q7 base to become more positive. This in turn causes Q3, Q2, and Q1 to conduct. The battery charge current, Q1 collector current, is sensed by Q4 and Q5 which produce a voltage V_a, proportional to charge current. V_a is fed back to the input divider, R1-R2-Q8, in such a manner as to balance differential amplifier Q6-Q7. Charge current then increases with the activation signal from the mode selector until transistor Q8 is cut off. The value of charge current at which the circuit limits is determined by the selection of resistors R3 and R4.

4.6 ATTITUDE CONTROL SUBSYSTEM

4.6.1 GENERAL

The attitude control subsystem includes the roll/yaw sensing elements, the despun platform control and associated sensors, and nutation control. Roll/yaw orientation control is provided via the secondary propulsion subsystem and is implemented by open loop ground control.

Basic stabilization of two axes (roll-yaw) of the spacecraft is derived from the gyroscopic stiffness property of the spinning cylindrical section (120 rpm nominally). Control of the third (pitch) axis is by modulation of the rate of the spinning section. This system, in derivation at least, is similar to the single momentum flywheel control system (called Stabilite) being developed by RCA for NASA/ESSA for the next generation operational weather satellite, TIROS M.

The gyroscopic inertial rigidity of the spin axis also permits a simplified roll/yaw sensing system. It can be shown that both roll and yaw vary sinuscidally at orbit rate, 90° out of phase, at the same amplitude. Hence by obtaining a roll history, the yaw

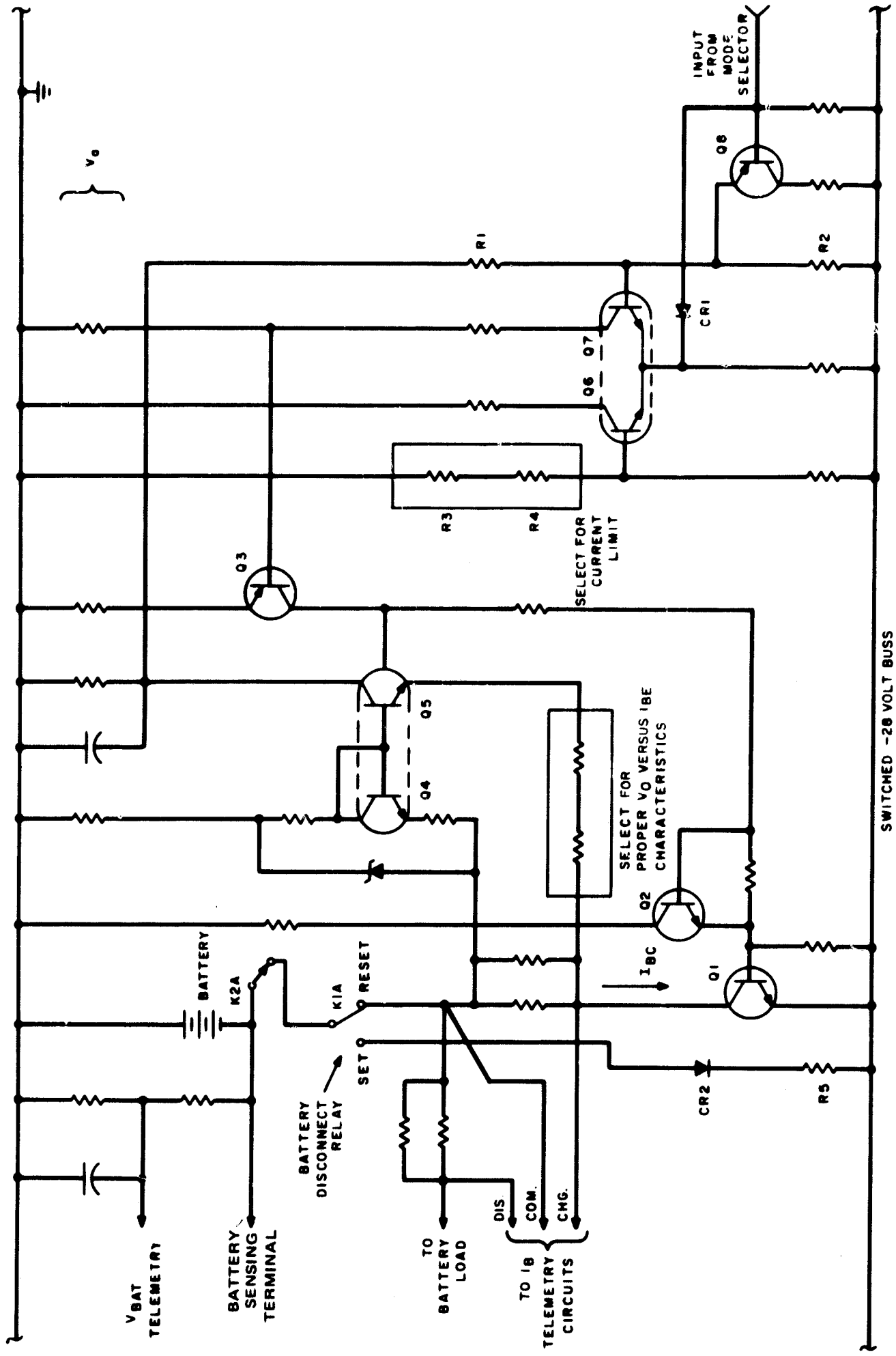

Figure 4-13. Battery Charge Controller

history can be derived. The sensing system itself consists of a pair of IR horizon sensors rigidly attached to the spinning body and configured with their optical axes in a "Vee." The "Vee" is arranged to be symmetric about the pitch plane (a plane normal to the spin axis). In operation the optical axes trace out two cones in space as the spacecraft rotates. The intercepts of these sensor paths with the earth and the corresponding sensor outputs are depicted in Figure 4-14 (only the spinning section of the NAVOX satellite is shown for clarity). When the spacecraft spin axis is normal to the orbit plane or equivalently normal to an earth radius (the condition of zero roll), the outputs of each channel will show equal time durations of earth intercept paths. If however, the spin axis is not normal to an earth radius so that a roll angle exists, the earth intercept paths will not be of equal durations. And the difference is a direct measure of the roll angle. Roll angle is defined as the angle between the spin axis and the local vertical, minus 90°. The measurement of the instantaneous roll angle at several points along the orbit obtained from the output of the "Vee" sensor and telemetered to ground stations is used to derive the phase and amplitude of the roll angle history. Whenever the amplitude exceeds 0.5°, a command is sent from the ground station to fire an attitude control thruster. The phase and pulse duration and the number of pulses are determined from the phase and magnitude of attitude error.

Closed-loop control is required for the pitch axis of the despun section. It is accomplished by momentum interchange between the rotating and non rotating sections through a servo controlled motor drive. An additional pair of IR horizon sensors (one is redundant) mounted on the spinning solar array provides relative position between the local vertical and the spinning section (i.e. - the optical axis of the sensor). The relative position of the spinning section and the non spinning parts is derived from an index on the shaft. By measuring the time difference between the index pulse and the local vertical determined by the sensor, an error signal is derived to change the distribution of momentum in the spacecraft. This in conjunction with a tachometer feedback loop provides stable pitch control, i.e. local vertical orientation, of the despun platform and antennas. Also included in the pitch control system is an RCA patented sun interference circuit utilizing a sun pipper to avoid the situation when the sun is near the horizon and in the scan path of the pitch sensor.

One of the more interesting features of dual spin spacecraft such as the NAVOX satellite is that nutational stability can be assured by mounting the nutation damper on the despun platform provided the spinning portion is axisymmetric, regardless of the interial properties of the satellite. That is to say that the usual property for nutational stability for passively damped spinning satellites that they spin about a principal axis of maximum moment of inertia no longer applies to dual spinners. This basic result now used extensively by most of the spacecraft attitude control industry for dual spinners was derived and presented for publication first by RCA in 1962.[1] The nutation damper for the NAVOX satellite consists of a passive toroidally-shaped liquid filled tube mounted on the despun canister with the plane of the toroid parallel to the spin axis. This type damper has been used very successfully by RCA on the TOS-ESSA satellites.

(1) The results were finally published by the Journal of Spacecraft Vol. 1, No. 6, 1964 entitled "Rotational Stability of an Axisymmetric Body Containing a Rotor" by V. Landon and B. Stewart.

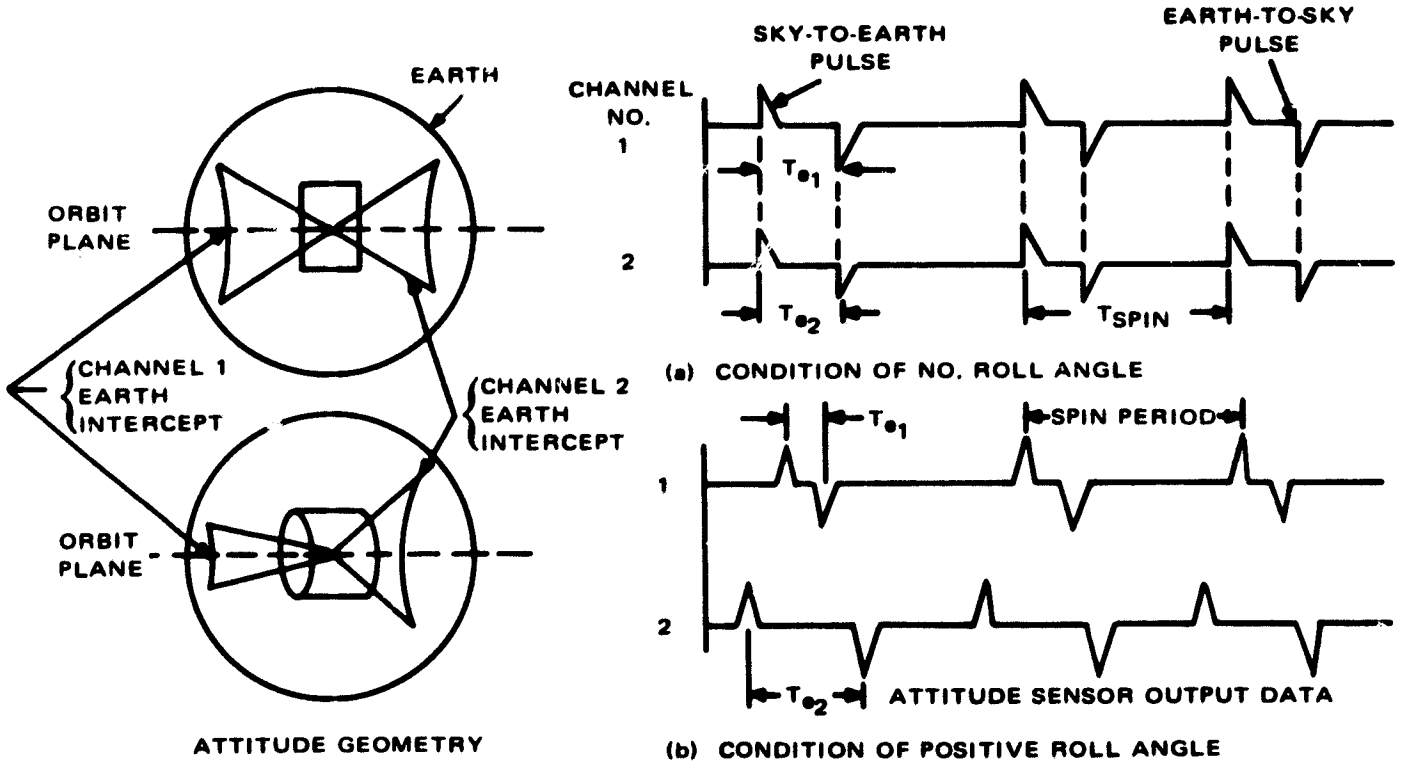

Figure 4-14. Sensor Geometry

4.6.2 ROLL/YAW SENSING AND CONTROL

The output of the "Vee" sensor is telemetered to the ground for data processing which consists of measuring the duration (t_e) that the sensor intersected the earth relative to spin period (t_s). It can then be shown that the output of a single side of the "Vee" can be used to compute roll angle by the equation

$$\mathrm{Cos}\left(\frac{t_{e_i}}{t_{s_i}}\pi\right) = \frac{\mathrm{Tan}\varphi}{\mathrm{Tan}\alpha_i} + \frac{\mathrm{Cos}\mu}{\mathrm{Sin}\alpha_i\,\mathrm{Cos}\varphi}\ , \quad i = 1 \text{ or } 2$$

where

φ = roll angle

α_i = angle between the selected sensor (i) optical axis and the spin axis

$$\mu = \mathrm{Sin}^{-1}\frac{R_e}{R_e + h}$$

R_e = earth radius

h = instantaneous orbit height

If data is available from both sensors and the "Vee" is truly symmetric about the pitch plane, the altitude dependence can be eliminated resulting in the equation

$$\text{Tan}\,\varphi = -\frac{\tan\alpha_1}{2}\left\{\text{Cos}\left(\frac{t_{e_i}}{t_{s_i}}\pi\right) - \text{Cos}\left(\frac{t_{e_2}}{t_{s_2}}\pi\right)\right\}$$

Making several measurements of φ throughout the orbit and fitting a sinusoid to the data of the form

$$\text{Sin}\,\varphi_j = \text{Sin}\,\varphi_{max}\,\text{Sin}\,(W_o t_j - \lambda)$$

where

φ_j = j^{th} measurement of φ

t_j = time at j^{th} measurement

W_o = orbit rate

λ = phase parameter

φ_{max} and λ, which uniquely determine the inertial position of the spin axis, can be determined.

A detailed error analysis on measurement accuracies with this system revealed that by the appropriate choice of the cant angle, α, instantaneous roll can be measured to within 0.5°. By taking many samples and using statistical techniques in deriving φ_{max} and λ, the inertial attitude can be determined to 0.2°.

Whenever φ_{max} which by definition is the angle between the orbit normal and the spin axis exceeds 0.5°, a roll/yaw correction must be made by the secondary propulsion attitude control thrusters. λ provides the necessary geometric information for selecting the phasing of the pulse centroid for cancelling the φ_{max} error.

The two largest disturbance factors causing φ_{max} changes are due to the solar torque and to misalignment in the velocity correction thrusters. Utilizing the data given in figure 4-2 regarding dimensions and c.g. location (in the plane of the propulsion system) and assuming that the antenna is 5% mesh material reflecting specularly, and that the spinning solar array reflects 50% of incoming radiation diffusely and absorbs the other 50%, then an unbalanced momentum input of 4.4 in-lb-sec per day can be calculated. Further assuming a 4-foot moment arm for the thrusters as well as a spacecraft weight of 650 pounds, the total ΔV required from the propulsion system to cancel solar pressure for a five year mission is 18 ft/sec. This includes 100% excess capability to account for possible errors in the assumption of surface characteristics. With the inertias

given in Section 4.2.5 and a spin rate of 120 rpm, φ_{max} should be corrected every 63 days to maintain the attitude error less than 0.5°.

The disturbances due to misalignment in the velocity correction thrusters can be analyzed similarly. Typical alignment tolerance for these devices amounts to 1°. Since the thruster is approximately 4 feet from the spacecraft c.g., this results in a moment arm of approximately one inch. However, in addition to this there is a further factor associated with c.g. location errors (assumed for the purposes of this analysis to be 2 inches). As listed in the next section on propulsion, the required velocity corrections amount to 375 ft/sec. Again assuming a moment arm of 48 inches for the attitude control thruster, the ΔV required for attitude control to correct misalignment torques is thus 24 ft/sec. The total ΔV requirement for attitude control is then 42 ft/sec. Notice that 50 ft/sec is allowed in the propulsion subsystem requirements. The margin is to account for inefficiencies due to the finite burn time of the thrusters.

The spin axis direction is changed by pulsing the axial (attitude control) rockets once per spin over a short duration of spin. For the nominal momentum of the system and a 5-lb thruster, the attitude can be changed about .05° per pulse. The nutation induced by this pulsing has a stepwise history never exceeding .1°. Any residual nutation subsequent to thrusting will be cancelled by the passive nutation damper. Extreme care must be exercised to minimize error in the pulse phasing. Even the unavoidable tolerance in the delay time between rocket actuation and the centroid of the pulse should be removed by in-flight calibration. By selecting the appropriate start time of the thrust period relative to the local vertical in the spin cycle, either roll or yaw may be corrected by this technique. It is recommended that roll be corrected since induced changes can be measured immediately after activation. Yaw changes may be detected six hours after the correction (when yaw interchanges with roll due to the inertial rigidity of the spin axis). Actual firing times are determined on the ground and programmed by real time ground commands.

4.6.3 DESPUN PLATFORM CONTROL (PITCH CONTROL)

The basic function of the DPC is to orient the NAVOX antenna system continuously along the local vertical. The subsystem block diagram is shown in Figure 4-15. As shown, the basic servo is a sampled data loop referenced to the earth's horizon crossing. A sky earth transition pulse is generated by the pitch IR horizon sensors mounted on the spinning array. The relative position between this pulse and the despun platform is derived (against an index pulse on an encoder in the drive assembly). This encoder also provides the relative rate between the two bodies. High resolution in the difference between the horizon pulse and index pulse is obtained through an analog error-detector based on pulse-width-modulation techniques. The resolution, limited only by preamplifier noise, is estimated to be as high as .002°.

The recommended system for meeting the antenna pointing-accuracy and jitter requirements is the position loop shown in Figure 4-15. Rate feedback is included primarily for damping. Accordingly, the rate feedback device does not have to be of high precision. The only important requirements for the minimization of jitter are

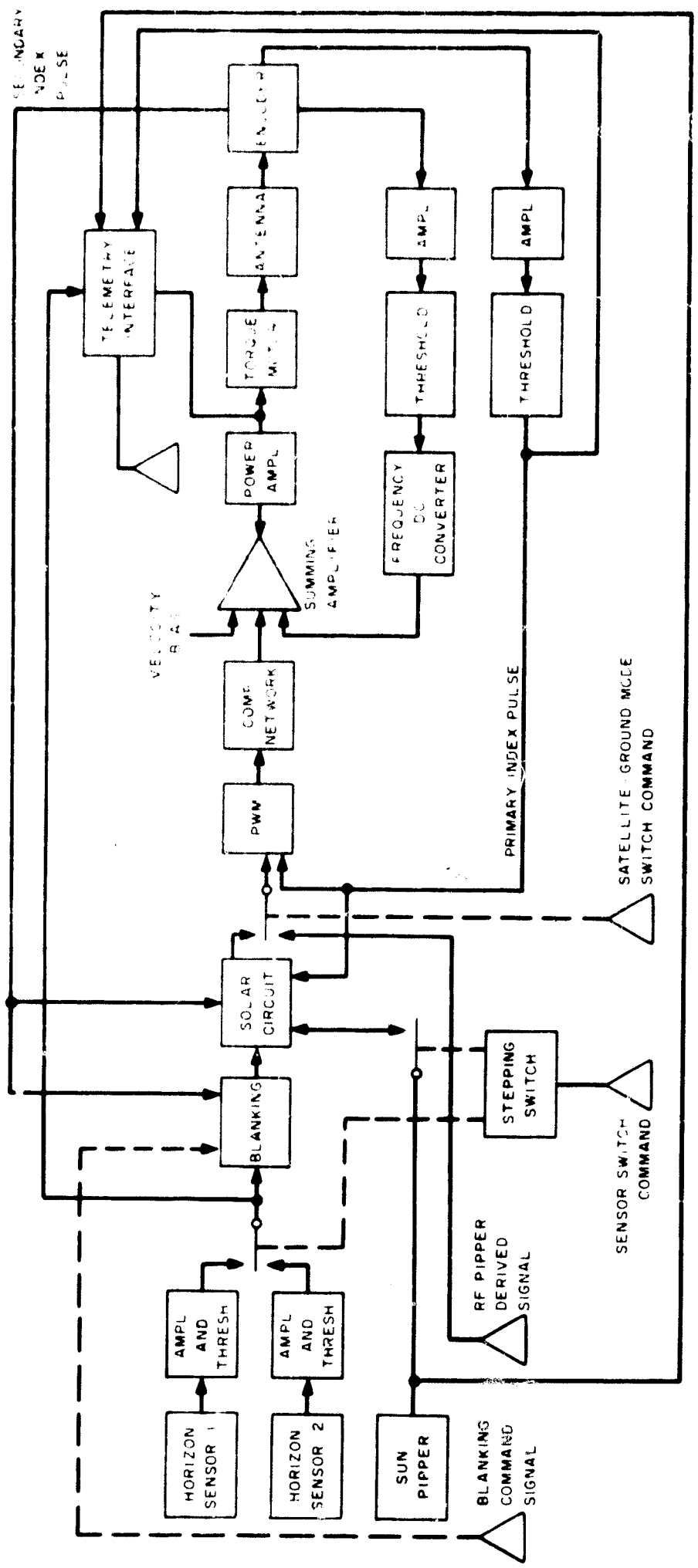

Figure 4-15. Block Diagram of DPC Servo

low ripple content and high resolution. The rate function can be derived by means of either a tachometer or a serial encoder in tandem with a frequency-to-dc converter.

In operation, the rate feedback output is compared with a bias voltage commanding the nominal speed of the antenna with respect to the vehicle. Any error voltage is amplified and applied to the motor in such a direction as to reduce the error. The position error voltage is generated by the pulse-width modulator (PWM) error detector and is processed through a frequency-sensitive lag-lead network in the compensation amplifier before being applied to the motor loop.

For a satellite having the nominal spin rate (120 rpm), the bias voltage is sufficient to maintain the proper rotational speed with essentially zero position error. However, initial momentum tolerances, decay rates due to external disturbances, and misalignment of attitude-control jets might cause the nominal spin rate of 120 rpm to vary. Therefore, the relative speed must be adjusted to maintain the despun platform rotation equal to the orbital rate and so have the antennas properly oriented with the local vertical. For a Type I servo, this velocity change results in a finite position error, but maintaining a high velocity gain (K_V) minimizes this steady-state position offset.

In addition to this Type I (proportional with lag-lead compensation) system, consideration was also given to a Type II (proportional plus integral) control, which tolerates a steady-state velocity offset with zero position error. However, the Type I system is chosen for this application, because response to larger upsets is generally less oscillatory than for Type II; moreover, the presence of an integrator in the Type II system represents a potential drift problem which could result in an offset error.

Referring now to Figure 4-15, it is of interest to note that, for small errors and a bandpass much less than $2\pi/T$ (sampling period T), the PMW error detector can be represented by a constant gain and negligible phase shift.

There are two components that precede the PWM error detector, namely the blanking and solar circuits which are included to assure that extraneous signals due to earth noise, antenna interference and sun interference do not give a false earth horizon and therefore a false local vertical. The secondary index pulses indicated in the block diagram locate the antenna interference areas, as well as providing coarse and fine blanking for acquisition and tracking modes, respectively, eliminating earth noise problems. As shown in figure 4-2 slots are provided in the VHF antenna mesh corresponding to 30° of scan thereby permitting an unobscured view of the earth. However the scan path does intercept part of the antenna and this data must be blanked. If the sky earth transition should occur in the blanking period the servo will change the momentum distribution in the satellite and cause the transition to "walk" out of this area.

The solar circuit provides for proper DPC reference for the singular condition of sun interference (sun near the sky-earth horizon in the vicinity of the orbit plane). Should the sun-pipper pulse (pulse of the solar sensor mounted on spinning array) occur within the window defined by the secondary and primary index pulses (16° from horizon), the

solar circuit will substitute the sun pipper for the horizon sensor as the DPC reference. A five-bit backward counter will decrease an initial 16° delay of the sun-pipper PWM input in 0.5° increments in accordance with the orbital rate. Once the count is completed and the sun is outside the reference pulse window, the reference automatically reverts to the horizon sensor. At synchronous orbit, this arrangement results in a sun-referenced despun platform system for a continuous period of about one hour per day for 100 days per year. When the horizon is again utilized for local vertical reference, the system will almost immediately remove any small error due to clock instability or granularity of the backward counter. The basic DPC reference is the earth-generated signal; no commands are required to assure the continuous local vertical orientation after the initial acquisition. Prior to acquisition, the solar circuit is deactivated by opening the sun-pipper line, in order to prevent the occurrence of an incorrect sun reference. The circuit, which has been patented by RCA, is shown in Figure 4-16.

The remaining elements of the DPC system are the horizon sensor, horizon sensor amplifier and threshold circuit, PWM error detector, compensation network and amplifier, summing amplifier, power amplifier, AC-to-DC converter, encoder, encoder amplifiers and threshold circuits, and a DC motor. All electronic components are transistorized solid-state devices.

The horizon sensors to be used in the NAVOX configuration are identical with those used on TOS . Figure 4-17 is a photograph of this device. Since a failure here aborts the mission, two such units are used, as shown, for redundancy. A block diagram of the sensor, amplifier and threshold circuit is shown in Figure 4-18.

The PWM circuit is shown in block diagram form in Figure 4-19. Index and horizon pulses trigger their respective flip-flops. Algebraic summing of the flip-flop outputs results in a PWM pulse of fixed absolute height, with sign dependent upon the first pulse (index or horizon) to occur. The pulse width is a direct function of the elapsed time between the occurrence of the two pulses. The "and" circuit output drives a single-shot, which resets the flip-flops for the next sample. Thus, after the occurrence of both pulses, the system is reset and ready for the next sample. Output offset voltage is minimized through the use of push-pull switching transistors.

The compensation network and amplifier providing lead-lag compensation is shown in Figure 4-20.

The summing amplifier is an operational type used to algebraicly sum and amplify two or more analog voltages. The bias voltage applied to this component (Figure 4-15) permits a wide dynamic range and eliminates proportional offset at nominal system momentum. The AC-to-DC converter converts the 256 pulses-per-revolution encoder output into DC voltage, thus providing a DC rate feedback signal required for proper damping of the servo loop. The electromagnetic encoder not only served the purpose of rate feedback but simultaneously furnishes the index pulses for phase lock requirements. These output pulses are shaped by the encoder amplifier and threshold circuit.

The motor which together with the drive shaft labyrinth seal, oil storage, bearings, slip rings and encoder form the drive assembly is a d-c brush type torque motor. RCA

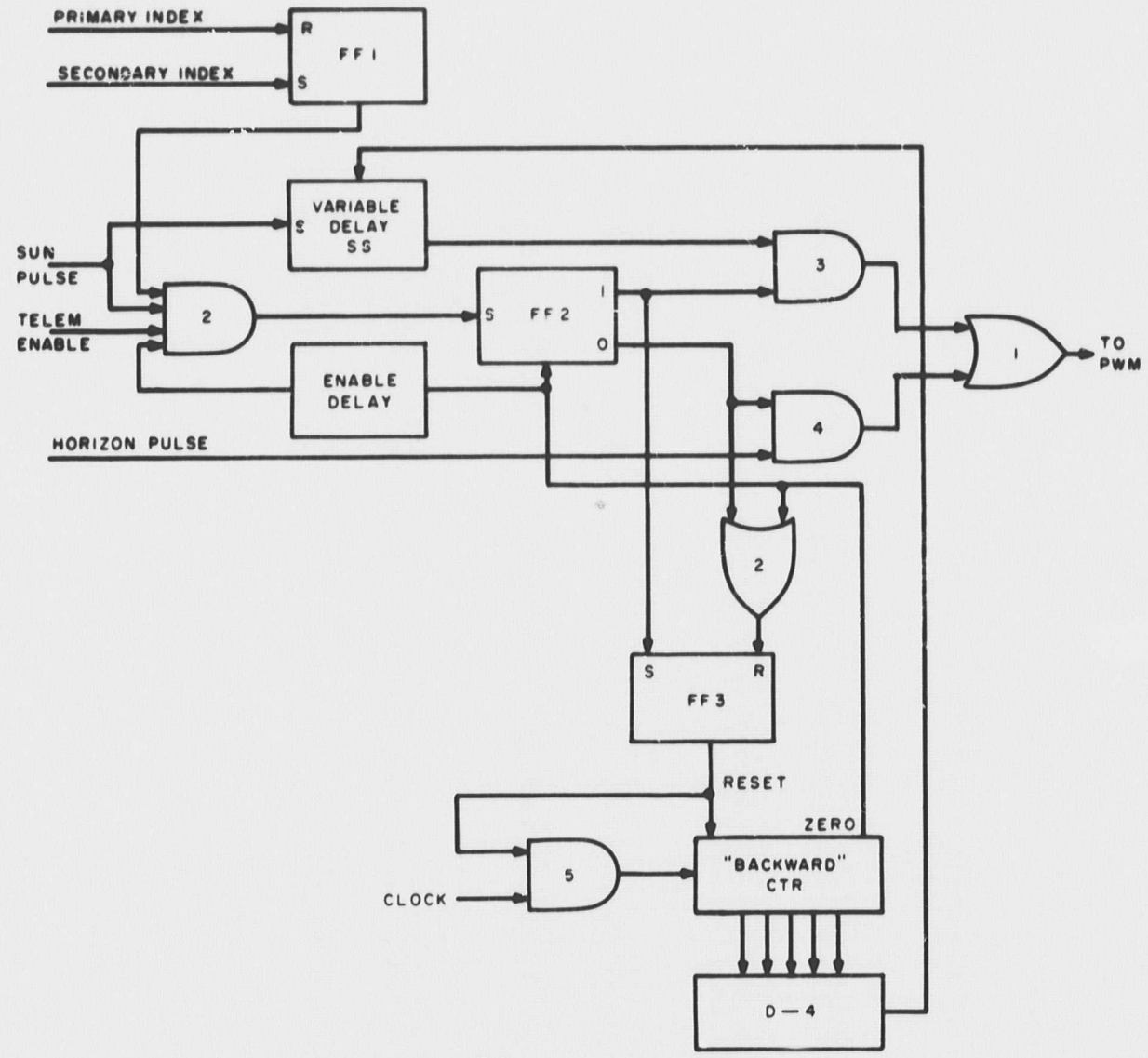

Figure 4-16. Solar Circuit

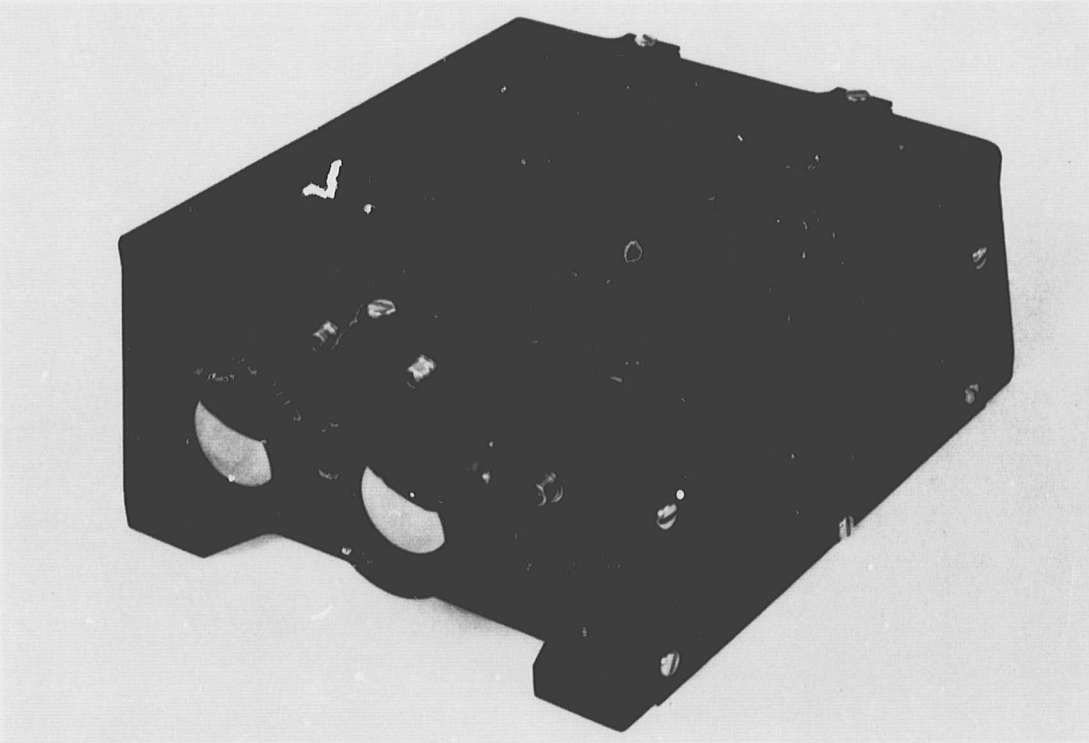

Figure 4-17. Photograph of a TIROS Operational Satellite Dual Horizon-Crossing Indicator

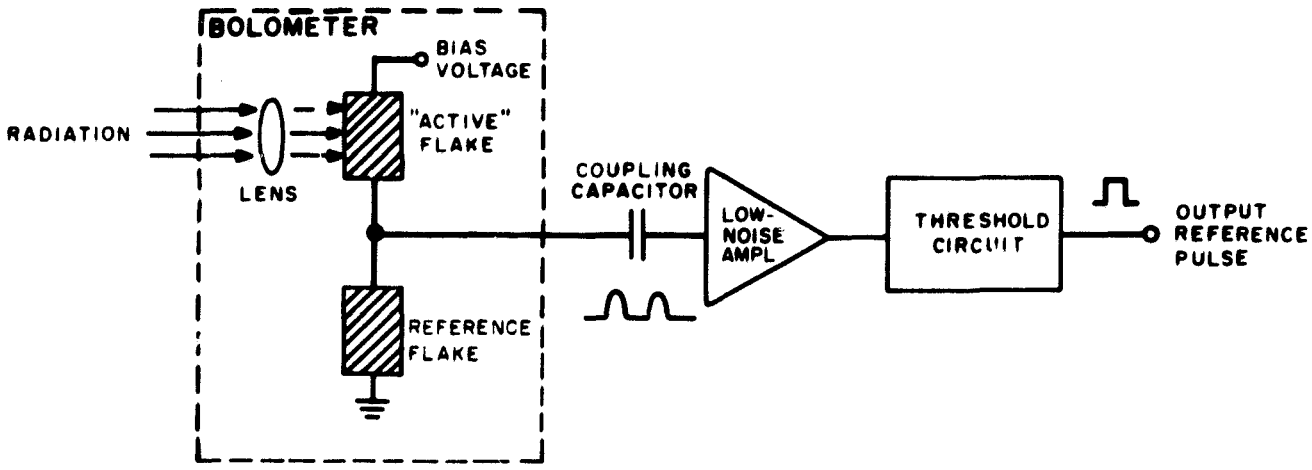

Figure 4-18. Horizon Sensor Block Diagram

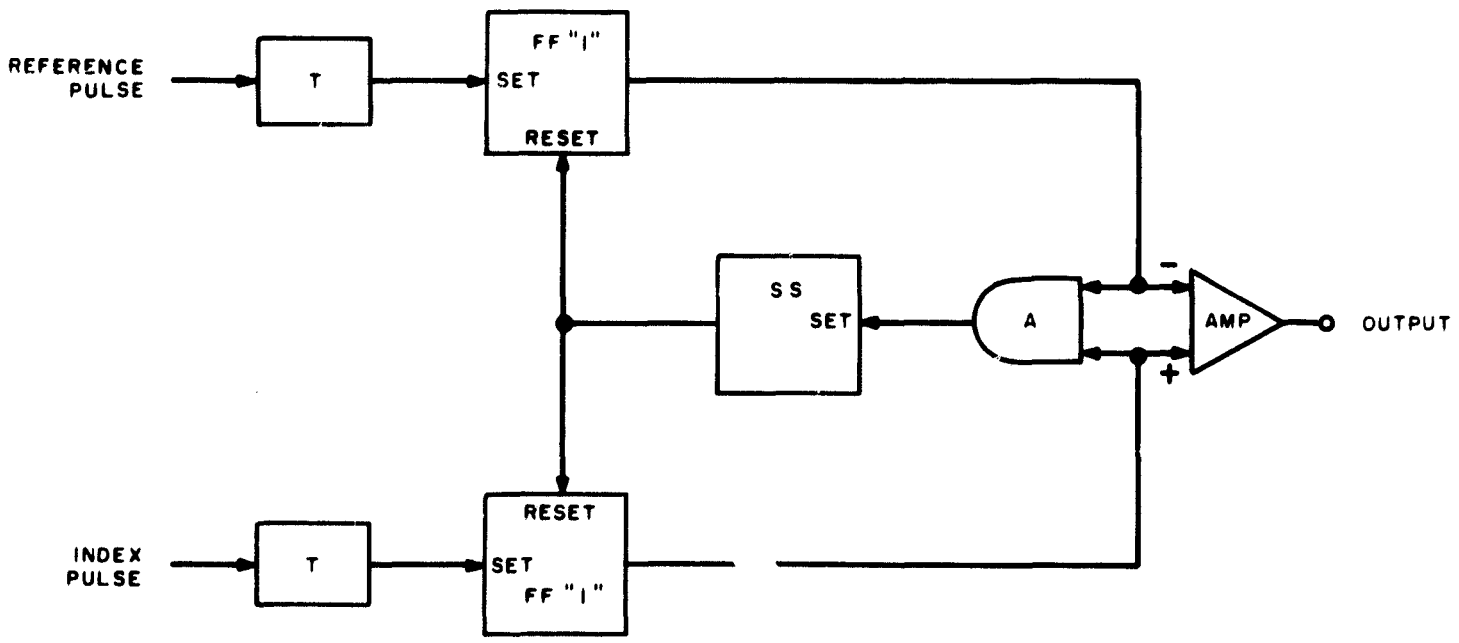

Figure 4-19. Pulse-Width Modulator

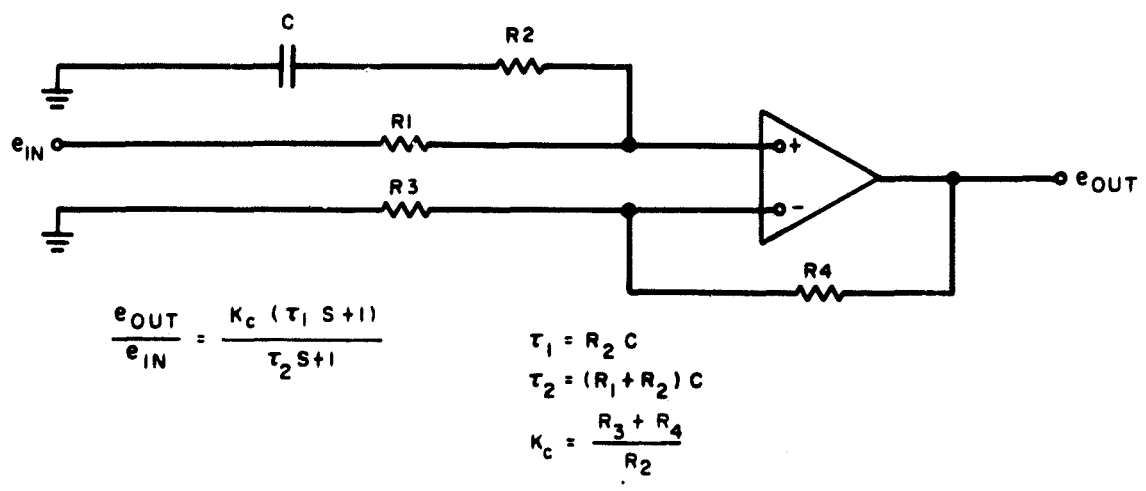

Figure 4-20. Compensation Network and Amplifier

has run extensive tests on this type motor for application to the TIROS M satellite. Experience indicates that brush wear for a five year mission can readily be accommodated by a standard type motor such as manufactured by the Inland Motor Corporation provided a proper lubrication environment is maintained. This is accomplished by sacrificial lubrication through the labyrinth seal thereby maintaining an oil vapor pressure environment. Adequate provision is made for resupplying the oil by storing it in nylason reservoirs.

4.6.4 NUTATION DAMPER

The nutation damper for the NAVOX satellite is a passive device consisting of a thin walled aluminum tube filled with a low viscosity silicone oil. It is shaped as a toroid (actually it is more rectangular with rounded corners) and mounted inside the despun canister. The plane of the damper is parallel to the spin axis. Nutational motion results when the spin axis is not colinear with the momentum vector thereby causing transverse components of angular velocity. This transverse oscillatory motion causes the liquid in the damper to move relative to the tube walls. Kinetic energy is thus converted to internal energy through the viscous drag of the fluid, causing a redistribution of the body angular rates. For stable configurations, this energy loss reduces the momentum component along the transverse axes and increases the component along the spin axis, thereby reducing the cone angle. As stated earlier the damper mounted on the despun portion satisfies the stability criteria. At very low nutation angles, small amplitude oscillations continues to excite the fluid until the fluid no longer responds inertially. The threshold is estimated as less than .01°. It can be shown that the time constant (τ) of the damper is given by

$$\tau = \frac{I_{t_{xx}} I_{t_{yy}}}{F H I_d}$$

where

$I_{t_{xx}}$, $I_{t_{yy}}$ = transverse inertias of total spacecraft

H = spacecraft momentum

I_D = inertia of the fluid about axis of symmetry normal to damper plane

F = coupling factor which is a function of damper geometry, fluid viscosity and the exciting frequency.

It has been shown by analysis and test that the optimum coupling factor for a toroidal damper is .189. For rectangular shaped units like the TOS dampers it has been tested and found to be as low as .09.

In the NAVOX application 3 pounds of silicone oil in a damper whose total weight is 5 pounds will produce a time constant of less than 3 hours.

4.7 SECONDARY PROPULSION SUBSYSTEM

4.7.1 GENERAL

A monopropellant hydrazine/Shell 405 propulsion system was selected as ideally suited for the secondary propulsion requirements of the NAVOX satellite. System selection is well supported by its ability to satisfy multi-start, rapid response, and repeatable impulse bit centroid requirements as well as by the current status of component development and flight experience. The proposed auxiliary propulsion system depicted schematically in Figure 4-21 has been sized to provide a total impulse capability of I_T=8600 lb-sec based on the velocity demands tabulated below.

Function	Velocity Increment Required ft/sec
Launch vehicle injection error correction*	250
Station acquisition	75
Station keeping (5 year life)	50
Attitude control	50
Total Velocity Increment Required	425

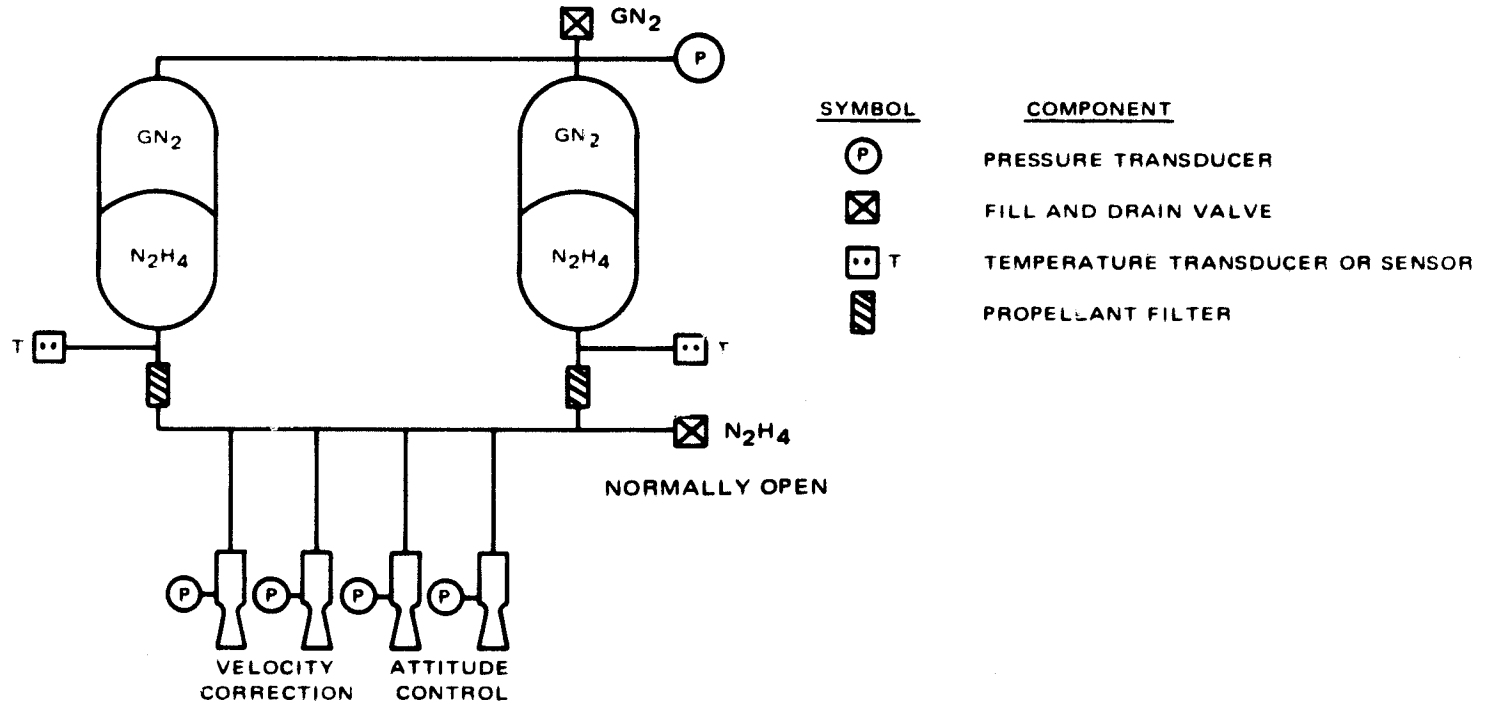

Figure 4-21. Schematic Arrangement of Hydrazine/Shell 405 Propulsion Subsystem for NAVOX

*This is a rather high allowance, bearing in mind the proposed employment of Burner II, and could provide as much as 100 ft/sec. hidden margin.

The proposed propulsion system is extremely simple. Basically it consists of a propellant feed system and four rocket engine assemblies. The feed system is composed of two interconnected cylindrical tanks, propellant fill and drain valves, pressurization connections, associated propellant lines and in-line propellant filters. Each rocket engine assembly (REA) contains a propellant valve, Shell 405 catalyst bed, decomposition chamber and expansion nozzle. A normally open squib valve is provided for each thruster to permit shutdown or isolation of any thruster from the system if the need arises. Instrumentation, such as pressure and temperature transducers to monitor the quantity of propellant remaining in the tanks, also forms part of the system. When the desired engine valve is opened, the gas forces the propellant through the manifold and into the Shell 405 catalyst bed where decomposition takes place and chamber pressure is created to produce thrust. Two of the four REA's provided are mounted axially in the spacecraft, the remaining two are mounted radially. With these thrusters the spacecraft spin axis can be corrected or the spacecraft orbital velocity changed.

NAVOX propulsion subsystem characteristics and operation are summarized in Table 4-5.

4.7.2 SUBSYSTEM COMPONENTS

State-of-the-art components are available for the NAVOX propulsion subsystem. A listing of typical components which can be used is presented in Table 4-6. All of these components have been chosen because they are either flight qualified or flight proven hardware. Thus, qualification of a propulsion subsystem utilizing these items would require a minimum of development testing. The major subsystem components are detailed in the following paragraphs.

The propulsion subsystem operates in a blowdown mode as propellant is expelled through the rocket engine during thrust actuation. The propellant tanks configured for the NAVOX propulsion system are the larger of two propellant tanks fabricated by Airtek Division of Fansteel Corporation for Hughes-JPL under the Surveyor program and are referred to as Block II Surveyor tanks. This tank is pictured on Figure 4-22. Because the propulsion system is mounted in the spinning section of the spacecraft propellant orientation and expulsion is assured. The positive expulsion device (teflon bladder-standpipe assembly) necessary for the Surveyor can be eliminated, thereby increasing the reliability of the feed system. The tanks are fabricated from 6A1-4V titanium; nominal dimensions are 10 inches diameter by 15.4 inches long, with 1000 cubic inches volume. They are designed to operate at 730 psig with a minimum burst pressure of 1038 psig. Each tank will contain approximately 22 pounds of expendables (propellant and pressurant) initially charged to a pressure of 300 psia. Tank pressure and hence engine thrust level decreases or "blows down" as propellant is utilized. The final pressure, after full propellant depletion is 126 psia, yielding a 5.0 to 2.7 pound thrust blowdown range.

TABLE 4-5. SUMMARY SPECIFICATION FOR NAVOX POSITIONING AND ORIENTATION SUBSYSTEM

OPERATION	
Blowdown propellant feed system	
Shell 405 catalyst bed in thruster decomposes the hydrazine, generating chamber pressure and thrust	
PERFORMANCE CHARACTERISTICS	
Total Impulse capability (lb-sec)	8600
Total ΔV	425
Initial tank pressure (psia)	300
Final tank pressure (psia)	126
Thrust range (lb_f)	5.0 to 2.7
Nozzle expansion ratio	50:1
Minimum Specific Impulse, (continuous/pulsing) (sec)	230/200
Thruster firing time, range (msec)	125 to 250
Reproducibility limits	±2% (pulse train of 10 or more)
PHYSICAL CHARACTERISTICS	
Propellant	Hydrazine
Pressurant	Nitrogen
Number of Rocket engine assemblies per subsystem	4
Number of propellant tanks per subsystem	2
Propellant weight (lb)	41.6
Pressurant weight (lb)	1.2
Dry weight (hardware exclusive of support structure) (lb)	14.3
Total Weight (lb)	57.1

TABLE 4-6. SUBSYSTEM COMPONENT STATUS SUMMARY

Component	Program	Source	Status
Propellant Tank			
Shell	Surveyor, Block II	Airtek	Qualified
Fill and Drain Valves			
Propellant	Apollo	J. C. Carter	Qualified
Pressurant	Apollo	Purolator	Qualified
Propellant Filter	Apollo	Wintec	Qualified
Squib Valves	Gemini	Pyrotechnics,	Qualified
Rocket Engine Assembly			
Valve	ATS-3	Walter Kidde	Qualified
Thrust Chamber	ATS-3	Hamilton Standard	Qualified
Instrumentation			
Tank Temperature transducer	Titan	Winsco	Qualified
Tank Pressure transducer	Agena	Whittaker	Qualified
Engine pressure Sensor	Minuteman	Statham	Qualified

Figure-4.22. Surveyor Program Titanium Propellant Pressure Vessels, (Block II Tank)

Figure 4-23 shows flight models of the Hamilton Standard axial and radial rocket engine assemblies which have successfully flown aboard the ATS-3, which is a spin stabilized earth synchronous spacecraft. Thus the capabilities of these units could be matched with the requirements of the NAVOX mission as both spacecraft have pulse ce centroid repeatibility and pulsed operation requirements. The thrust chamber design of the pictured REA's has the following features: a mounting flange and thermal heat barrier, six capillary tube injectors, the reactor containing a catalyst bed of Shell 405 catalyst in 20-30 mesh size pellets, and a 50:1 expansion ratio nozzle. Each of the six capillary tubes projects into the catalyst bed, and each tube is capped with a diffuser screen which serves to break up the solid stream of propellant before it comes in contact with the Shell 405 catalyst. The diffuser screens also prevent migration of the catalyst "fines" into the diffuser outlet. A cross screen is placed at a station along the axis of the reactor near the ends of the diffuser screens to mechanically retain in the catalyst in a tight pack around the diffuser. At the aft end of the catalyst bed, a perforated retaining plate, also faced with a screen, prevents exodus of the catalyst with the decomposition gas stream. The principal material of construction is Inconel 600. The thruster is thermally isolated from the propellant ON-OFF solenoid valve with a stainless steel tube stand-off. The valve is a product of the Walter Kidde Company and is a modification of a hydrogen peroxide valve successfully flown on many hydrogen peroxide reaction control systems. To date, 48 of these valves are in space on satellites such as Early Bird and Intelsat 2. The valve was modified for use with hydrazine by improving materials compatibility to hydrazine; one O-ring was changed from Viton to ethylene propylene rubber, and the shims used for controlling flow rate were changed from Mylar to stainless steel. The flow rate capability and electrical characteristics of the valve remained unchanged.

The four rocket engine assemblies are incorporated in the propulsion subsystem so as to provide complete redundancy. Normally open squib valves upsteam of each propellant valve permit shutdown or isolation of any thruster from the system if the need arises.

Other components tentatively selected are listed on Table 4-6. Selection of the J.C. Carter disconnect coupling for the propellant tank fill, drain and venting is based on the successful use of that component on the Lunar Orbiter program as well as extensive use on the Apollo program. The J.C. Carter coupling features redundant seals throughout both flight and ground halves. The halves may be connected and disconnected under pressure and flow controlled at the coupling. Safeguards are incorporated in the design so that the coupling cannot be opened in any manner dangerous to operating personnel. Spillage is zero on disconnect.

The gaseous nigrogen fill and vent coupling produced by the Aerospace Division of Purolator Corp. can be coupled and uncoupled under a flight half or ground half line pressure of 5,000 psig. Torque required to complete coupling under these pressures is about 70 in-lb. This coupling is qualified for the Apollo program and has seen extensive use on the command and service modules of the Apollo vehicle.

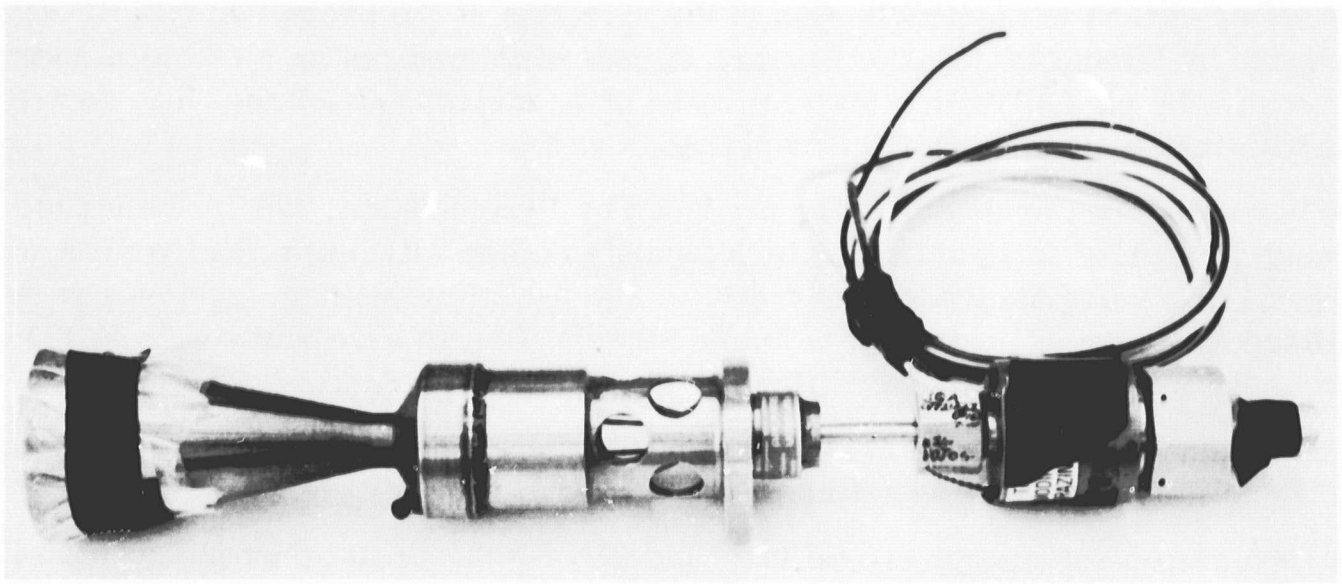

(a) Axial Hydrazine Thrust Chamber Assembly

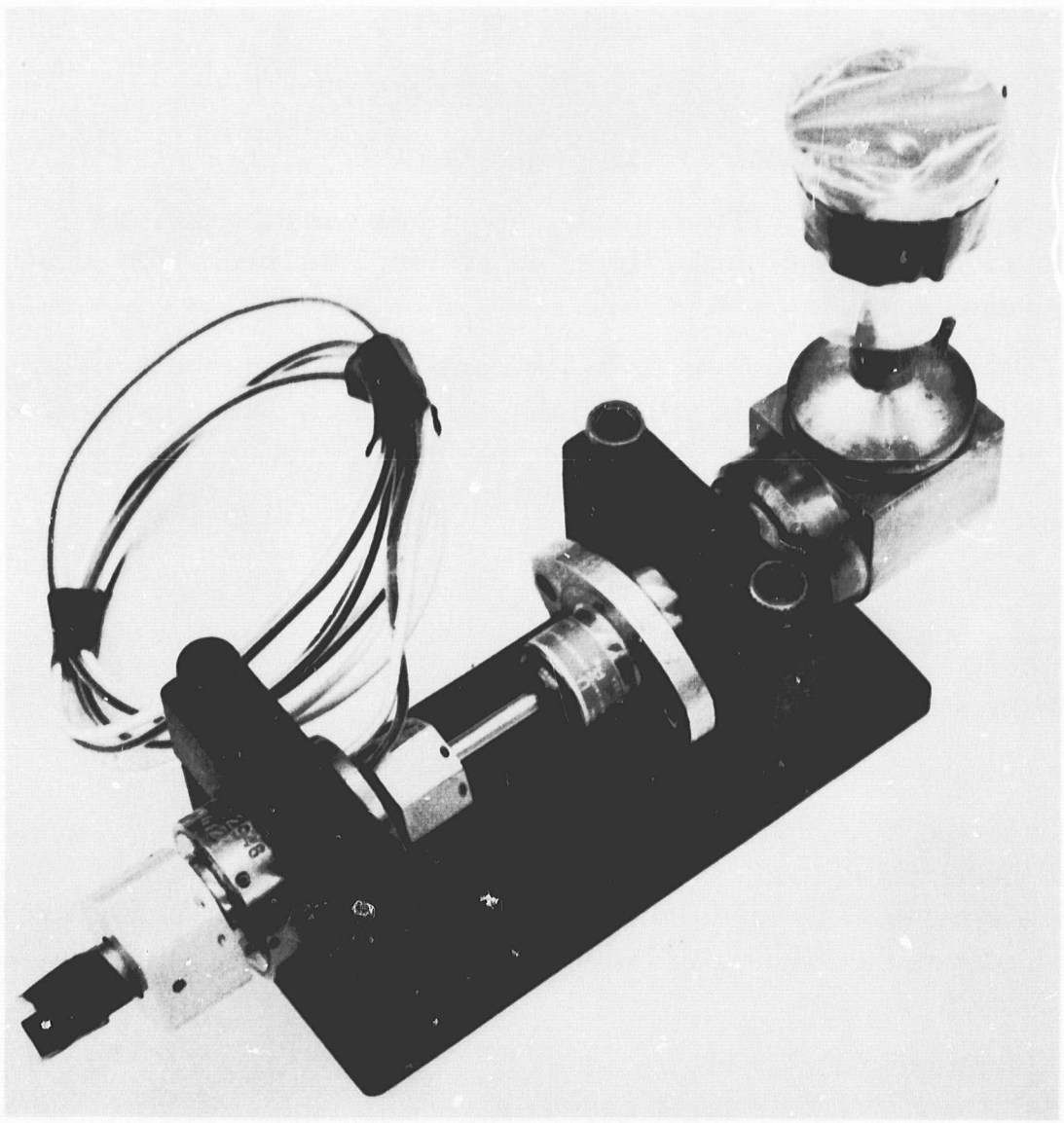

(b) Radial Hydrazine Thrust Chamber Assembly

Figure 4-23. Thrust Chamber Assemblies

The latter reason is applicable also in the selection of the propellant filter. The filter, produced by Wintec Division of Cemarc Corporation features an all welded construction with a Dutch Twill filter element rated at 18 microns absolute. It is an inline unit with tube ends for brazing or welding.

The normally open explosive valve produced by Pyrotechnics, Inc. provides straight through flow prior to shutoff, and is designed to close without producing pressure surges. The valve has redundant metal to metal sealing elements and closes in 10 milliseconds upon application of a 5 amp signal. Bridge wire resistance is 1.1 ± 0.2 ohms. This valve has been qualified for the Gemini program.

Instrumentation selection is based on required sensitivity and response characteristics as well as qualification status.

The propulsion subsystem will be installed in the spacecraft as an integrated subsystem on a module if possible, or in a minimum number of assemblies. If assembly in units is required, all mechanical joints will be welded and brazed by methods similar to those used on existing spin stabilized earth synchronous satellites to insure leak free assembly.

4.8 SATELLITE REDUNDANCY & REPLENISHMENT

4.8.1 SATELLITE LIFETIME

The NAVOX spacecraft described in this report has been the subject of reliability analysis aimed at an estimation of probable system life, and at the identification of redundancy requirements.

The reliability estimates were made at the component (black-box) level, and were based upon similar components either designed for or flown on existing spacecraft. The tables in this section were derived on this basis, and deal in turn with the

Voice Communications Subsystem	Table 4-7
Position Location Subsystem	Table 4-8
Telemetry & Command Subsystem	Table 4-9
Power Subsystem	Table 4-10
Attitude Control Subsystem, including propulsion	Table 4-11

Taking due account of redundancy, where it has been included in the basic design, the material of these tables leads to the following mean-time-to-failure "lifetimes" for the various elements of the system. The estimates have been somewhat rounded off, so that for instance the slightly differing reliabilities of the 30 watt and the 3 watt voice channels do not show.

Voice Communications -	all channels	30,000 hours
	three channels	40,000 hours
	two channels	60,000 hours
	one channel	110,000 hours
Position Location		35,000 hours
Spacecraft "bus"		25,000 hours

TABLE 4-7. VOICE COMMUNICATIONS SUBSYSTEM

Component	Failure Rate	Source and Comments
30 Watt Power Amplifier	6300×10^{-9} Failures Per Hour	The I TOS Real Time Transmitter, a 5 Watt Unit, Exhibits a Failure Rate of 5710×10^{-9} Failures per hour. Allowing an approximate 10^{-9} failure rate increase for achieving the additional power capability yields a failure rate of $\sim 6300 \times 10^{-9}$ failures/hour.
3 Watt Power Amplifier	5710×10^{-9} Failures Per Hour	
Linear Combiner	100×10^{-9} Failures Per Hour	Estimated at 100×10^{-9} Failures per hour based upon use of passive parts, non-powered and exposed to RF power only.
Filters; Bandpass, Notch, Low Pass, etc.	100×10^{-9} Failures Per Hour	Tiros M/I TOS
Mixers, Front End	115×10^{-9} Failures Per Hour	Assumes Twin Diode Mixer Configuration (balanced) in coaxial layout.
Low Noise Preamplifier	500×10^{-9} Failures Per	Three to four transistor configuration, similar to lunar orbiter transponder preamplifier operating at ~ 48 MHz.
Local Oscillators	450×10^{-9} Failures Per Hour	Approx. Four Transistor Configuration including oscillator, multiplier and isolation stage. Similar in complexity to lunar orbiter VCO with fewer outputs however.
IF Amplifiers	500×10^{-9} Failures Per Hour Each	Four to Five transistor IF strip, similar to lunar orbiter IF strip but lower in frequency.
Diplexer and Preselector	10×10^{-9} Failures Per Hour For Each	Tiros M/I TOS
Antenna	10×10^{-9} Failures Per Hour	Tiros M/I TOS
Mixers (2nd Conversion)	540×10^{-9} Failures Per Hour	Estimates Derived from Tiros M/I TOS Multiplexer circuitry equivalence.

TABLE 4-8. POSITION LOCATION SUBSYSTEM

Component	Failure Rate	Source and Comments
Transponder	$11,200 \times 10^{-9}$ Failures Per Hour	Lunar Orbiter Transponder with approximately 1200 to 1400 parts at approx. 8×10^{-9} failures per hour per part.
TWTA	2000×10^{-9} Failures Per Hour	Comsat
Filters	10×10^{-9} Failures Per Hour	Comsat (Coaxial Elements in L-Band)
Diplexer-Duplexer	20×10^{-9} Failures Per Hour	Comsat
Low Noise Pre-Amplifier	640×10^{-9} Failures Per Hour	Comsat (TDA)
Antenna	10×10^{-9} Failures Per Hour	Tiros M/I TOS

TABLE 4-9. TT&C SUBSYSTEM

Component	Failure Rate	Source and Comments
Filters	100×10^{-9} Failures Per Hour	Tiros M/I TOS
Antenna Coupler	10×10^{-9} Failures Per Hour	Tiros M/I TOS
Command Receiver	4600×10^{-9} Failures Per Hour	Tiros M/I TOS
Decoder	3380×10^{-9} Failures Per Hour	Tiros M/I TOS Decoder, Active Portion Plus a DC-DC Converter for the Decoder.
Command Distribution Unit	3380×10^{-9} Failures Per Hour	Est. same complexity as decoder.
Beacon & TM Transmitter	2700×10^{-9} Failures Per Hour	Tiros M/I TOS
TM Base Band	2700×10^{-9} Failures Per Hour	Est. 50% Tiros M/I TOS Multiplexer
TM Commutator	800×10^{-9} Failures Per Hour	Tiros M/I TOS DFC Commutator
Converters for Base Band & Commutator	100×10^{-9} Failures Per Hour Each	Tiros M/I TOS
Hybrid	100×10^{-9} Failures Per Hour	Tiros M/I TOS
Antenna	10×10^{-9} Failures Per Hour	Tiros M/I TOS

The latter entry including all the "service" items (TT&C, power, attitude control, propulsion, etc.)

It is clear from these results that small quantitative basis exists for the provision of redundancy in the voice communications and position location packages; the spacecraft itself is the limiting item. It is further of note that the critical item within the spacecraft is the despun platform (pitch) control loop, the various major subsystem lifetimes being estimated approximately as below:

Telemetry and Command	95,000 hours
Power	160,000 hours
Attitude Control	45,000 hours
Secondary Propulsion	320,000 hours

It is virtually certain that a more detailed examination of the attitude control subsystem would allow reliability to be improved via the addition of redundancy within the pitch control electronics but this has not been pursued further at this time. Given such redundancy, it is reasonable to predict a "bus" lifetime of around 35,000 hours.

With the subsystem lifetime figures as tabled, but with the postulated improvement to the attitude control subsystem, it is apparent that a rational scheme of things emerges. The loss of one voice channel out of the four per spacecraft may be regarded as a "graceful failure", albeit one that would make for operational difficulties, and the nominal "life" of the spacecraft may then be set at about 35,000 hours-this being the common lifetime both for the position location subsystem and for the spacecraft bus. Of course, the replacement life of the total vehicle ((reduced) voice block plus position location package plus spacecraft bus) is in principle less than this because of the combination of the various failure probabilities. However, the estimation of this replenishment period is complicated by the various partial failures that might occur without immediately destroying the system, and for instance the telemetry and command function could be lost for a period of several months before off-station drift or attitude deviations become intolerable.

Indeed, given spacecraft locations at 10°W and 60°W the total loss of telemetry and command (and hence of propulsion capability) would not destroy the system for at least a year. In this time, the spacecraft at 60°W could be expected to drift about 25° in longitude, while the other would remain virtually stationary, and the roll/yaw altitude would deviate by about 3°.

Deleting the Voice, the Telemetry and Command, and the Propulsion Subsystems, the remaining Position Location capability plus the supporting "bus" is characterized by an MTTF of about three years, but of course and again this is a somewhat fictitious number.

In any event, it is apparent that the various separate major blocks of the spacecraft (voice, position location, and support) are quite well matched in terms of reliability. Because of this situation no redundancy has been included within either the voice

communication or position location blocks of the basic NAVOX spacecraft described in preceding sections. However, while progressive loss of voice channels is an acceptable failure mode, the abrupt loss of position location capability is not. Furthermore, of the various spacecraft functions that might fail (secondary propulsion, power system batteries, yaw/roll sensing, etc.) very few such failures lead to immediate system loss. It is of note that the despun platform pitch control loss would be catastrophic, which re-empahsizes the need for critical examination of this function.

In these circumstances the provision of redundancy within the Position Location subsystem would be recommended in practice. Duplication of this subsystem would extend the lifetime beyond that of the basic spacecraft to such an extent that abrupt failure would become unlikely--the system wearing out in other aspects first, and being replaced. Actually, the advantages of redundancy are somewhat reduced by the need to preserve the frequency format. Thus the addition of one redundant subsystem in each spacecraft allows but one of the resulting set of four subsystems to fail, (see Figure 4-24). It will be seen that for instance failure of unit 2a can be repaired by the activation of 2b, the deactivation of 1a, and the insertion of 1b. In this manner, the frequency plan is preserved (though laterally inverted), but no further repair capability remains despite the continued existence of two "good" units in spacecraft #1.

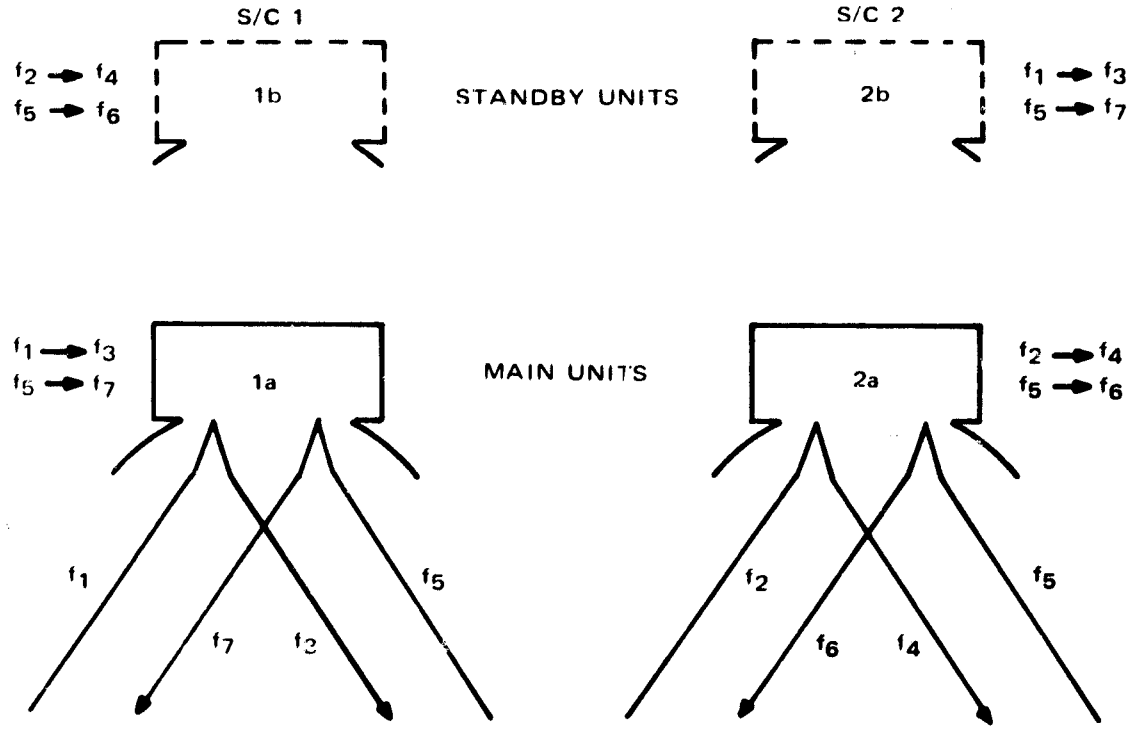

Figure 4-24. Navigation/Traffic Control Subsystem Redundancy

The weight increment for this equipment duplication above the 632 lb. baseline system is about 40 lbs. per spacecraft. There is adequate room within the equipment compartment for the extra items, viz

Forward link transponder

Backward link transponder

Forward link power amplifier

Backward link power amplifier

and the resulting total vehicle weight can be set at 672 pounds, excluding margins. With a payload of two vehicles the total booster load amounts to 1450 pounds, including adapter and shroud penalties, which is within the capability of the basic Atlas-Centaur - Burner II stack (but leaves little margin)

The conclusions of the reliability analysis may thus be briefly stated:

(1) No redundancy within the voice communications subsystem is warranted, the full and 75% capability lifetimes being estimated at 30,000 hours and 40,000 hours respectively.

(2) The reliability estimates made separately for the Position Location subsystem and for the spacecraft "bus" yield rather similar results, the lifetime being about 35,000 hours in the former case, and 25,000 hours in the latter, with this last estimate subject to straightforward improvement up to about 35,000 hours.

(3) Bearing in mind the manifold possibilities for graceful failure within the basic support subsystems of the spacecraft, and hence possible operation beyond the estimated lifetime, redundancy within the critical position location subsystem seems justified.

(4) This redundancy has not been included within the basic NAVOX design, but may be had for the addition of approximately 40 lbs of equipment.

4.8.2 REPAIR AND REPLENISHMENT

Following the discussions of the previous section, the system that is proposed will of course be subject to wear-out, and to sudden failure. Wear-out may be represented as an essentially well-behaved gradual loss of redundancy, including the loss of a fraction of the voice channel capability, and by definition provides adequate warning of the need for system replenishment. This replenishment need would generally be total, in that both spacecraft will wear out together.

The possibilities of sudden failure are more various, in that such failure can occur at any time during the system life-although more probably during the latter portion. Furthermore, by nature such failure would in general occur in one vehicle only so that full system replacement would not normally be required.

There are thus seen to be two distinct requirements, viz

(1) the requirement for total system replacement as wear-out approaches

(2) the requirement for a repair capability for random failure in a single vehicle.

Clearly, the booster demands are different in the two cases, and actually the latter case is most demanding in several ways.

For one thing, if repair of a catastrophic failure is necessary then the need will be urgent. Even with a standby booster and spacecraft the minimum repair time is likely to run into 15-30 days because of the various preparations that would be necessary. Furthermore, the situation is complicated by the specific nature of the radio frequency distribution between the two "birds."

So far as the position location equipment is concerned the frequency problem disappears if redundancy has been provided, as considered previously. If not, then "quick change" units have to be at hand to allow proper equipment to be placed on-board at launch. Similarly, with the voice channels, either two complete spare sets of equipment (or two spacecraft) have to be at hand, or previously unused frequency allocations have to be employed--otherwise pairs of channels would exist at single frequencies. This of course assumes that the spare is not held in orbit.

The employment of an orbital spare allows elimination of most of the downtime following failure, in that if a third spacecraft is placed mid-way between the two primary vehicles, then time to repair is just the time necessary to shift to station - much less than the time for a new launch. However the use of an orbital spare is a doubtful proposition, in part because of the frequency allocation problem, but more particularly because even an "inert" spacecraft is subject to wear-out and to failure in orbit. It is because of this that the (long-term) placement of orbital spares is generally unattractive, though the launch of a spare to anticipate the near-term failure of a well behaved "wearing out" vehicle is another matter.

In any event it appears that there is a possible need for a single vehicle launch in order to effect system repair following non-scheduled failure, and there are two (non-NASA) launch vehicles of reduced performance which might meet the requirement:

(1) The Atlas-Agena (with an upper stage)

(2) The Titan III B (again with an upper stage)

Neither of these vehicles comes with a shroud having sufficient diameter to meet the payload requirements. If the Atlas-Agena-0A0 shroud combination could be resurrected (using now the SLV-3A through) the shroud would be suitable but the booster would suffer considerable performance loss over the normal configuration. Indeed, using the Burner II the on-station capability is but 540 lb., and is inadequate. If the TE 364 used alone could be substituted for the Burner II stage then the capability would improve to about 700 lbs., which is somewhat marginal (particularly for the spacecraft with redundant position location equipment) but acceptable. The substitution appears possible since with a single rather than a double payload, spin stabilization during coasting is more feasible.

The Titan booster has about 300 pounds more payload capability than the Atlas, when used with Burner II, and thus has adequate performance. A "new" shroud would however be required, and would represent something of a development hurdle.

Clearly, the possibility does exist for a single spacecraft repair launch, particularly using the Atlas Agena, but with the difficulties inherent in this tactic. The cost of the booster is of course substantially below that of the Atlas-Centaur ($8.1M against $13.1M) but not so far below as to justify the use of the lesser booster for initial system installation or for complete system replacement.

On balance, the use of the Atlas-Agena (with the 0A0 shroud) does not appear favorable, principally because the only application is for the replacement of a single spacecraft - hopefully not a likely requirement given proper spacecraft design. In view of the small spacecraft population involved, and the inevitably high costs to be incurred if two types of booster are to be held in readiness, it appears to be better to provide only the Centaur vehicle. With this assumption it is necessary to accept the possibility of under-utilization of the booster in the event of a single failure or of premature replacement of the total system. As a third alternative, the full dual payload could be launched in response to a single failure, and the surplus spacecraft held as an orbital spare (subject to the solution of the voice frequency allocation difficulty).

The full treatment of the repair-replenishment problem is beyond the scope of this discussion but it is believed that the single booster route is the way to go.

4.9 DEPLOYMENT

4.9.1 BOOSTER DESCRIPTION

Based on the preliminary studies of spacecraft configurations, it was determined that the payload weight range for the multipurpose NAVOX satellite was 600 to 800 pounds. In fact the basic design presented in this report weighs 695 pounds (including 10% margin). From a brief survey of available launch vehicles in the U.S. stable of boosters it is clear that single launched satellites would require a vehicle costing about $8.5 million (e.g. Atlas-Agena - Titan IIIB/Agena). However, the SLV-3C (Atlas) / Centaur/Burner II combination could provide a simultaneous launch of two NAVOX payloads at a cost of approximately $13 million. Since the system requires a minimum of two satellites for navigation purposes, the saving in initially establishing the system amounts to $4.5 million. Replacing satellites that are inoperative however requires more planning since two must be launched at a time. As presented previously, with adequate redundancy in each satellite, a reasonable replenishment policy should be possible without report to two booster types.

The present payload capability of the SLV-3C/Centaur/Burner II with the standard Centaur shroud is about 1500 pounds. This assumes the standard propellant load of 1440 pounds in the Burner II-TE 364 rocket motor. By increasing the propellant load to 1960 pounds, the payload capability may be increased by 1807 pounds. A 6-inch increase in the cylindrical section of the rocket motor casing would accommodate this change in propellant load. Thiokol is now under contract to demonstrate the feasibility of such a modification. Table 4-12 summarizes the payload requirements and capabilities for the multiply launched NAVOX spacecraft.

TABLE 4-12. PAYLOAD SUMMARY

Element	Weight (lbs)
NAVOX S/C I (including 10% margin)	695
NAVOX S/C II (including 10% margin)	695
Burner II/SC Adapter	50
Additional Shroud (Payload Penalty)	60 (18-ft extension)
	1500
Payload Capability (1400 lb. Propellant Loss)	1500
Margin	0
Payload Capability (1960 lb. Propellant Load)	1807
Margin	307

4.9.2 INJECTION SEQUENCE

The synchronous equatorial orbit is achieved by application of a parking orbit coast mode. After suborbital burning into the parking orbit, the Centaur stage/Burner II/ Payload coast until the desired nodal (equatorial) crossing is approached. The second burn of the Centaur provides the necessary velocity change to reach the required apogee altitude for a stationary orbit (19,300 nmi). Some of the second burn impulse is used to remove a portion of the orbital inclination (in the case of the 1960-pound propellant load this amounts to a 2° change). This establishes an inclined elliptical orbit with apogee at synchronous altitude. During this transfer orbit, subsequent to separation from the Centaur, the Burner II provides attitude control for the system. At apogee the control system orients the TE 364 to make the final plane change and achieve synchronous orbit velocity. In the case of the NAVOX Satellite application where the stations are between 10° and 60° west longitude, injection will not occur until the second apogee pass to minimize the station acquisition maneuver. Figure 4-25 depicts the orbital geometry in approximate fashion.

The Atlas/Centaur/Burner II synchronous equatorial flight sequence is shown in Figure 4-26. BECO occurs at 153 seconds and SECO at 248 seconds from lift-off.

MES 1 occurs about 11 seconds after Atlas SECO; Centaur first burn (approximately four minutes) places the Centaur/Burner II/Spacecraft into parking orbit. After about 25 seconds of parking-orbit coast, the first equatorial (nodal) crossing is reached and MES 2 occurs. Centaur second burn provides the velocity required to reach the 19,300-nmi apogee altitude. A (small) perigee plane change is made during Centaur second burn. After MECO 2 the Burner II/spacecraft is separated from Centaur.

A programmed slow-roll maneuver is used during the approximately 5.25-hour Hohmann transfer to apogee, to null-out the gyro drift (1 deg/hr, 3σ) during the coast period. The Burner II GN_2 jets are commanded to roll the vehicle at a predetermined rate (approximately 10 revolutions per hour) during the coast period. The roll rate and time must

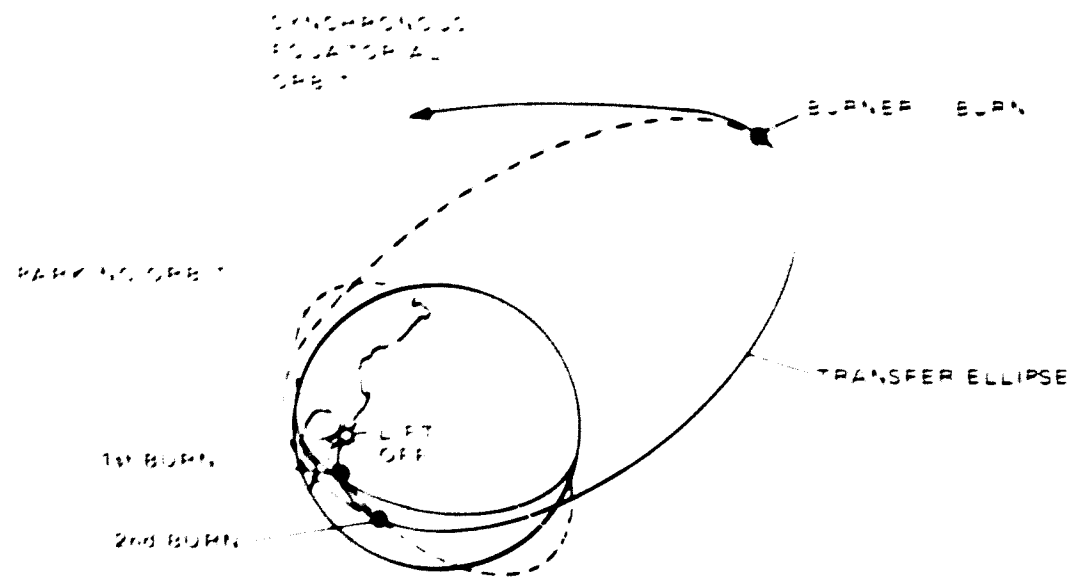

Figure 4-25. Synchronous Equatorial Orbit Achievement

result in an integral number of revolutions during each phase. During the first half of the coast period the roll is in one direction, followed by a 180° yaw maneuver and continued roll in the opposite direction. The vehicle roll during the first half of the coast period averages out most of the gyro drift error in two axes; the continued roll during the second half of the coast period eliminates drift due to the torquing and the third axis drift. The rolling maneuver also reduces potential thermal problems with the NAVOX spacecraft. This is repeated three times until the second apogee is reached.

An orientation maneuver is performed at apogee to properly align the Burner II main thrust vector, and the solid motor is ignited to provide final plane change and circularization velocity impulse. Following solid motor burnout and a short coast period, the Burner II H_2O_2 reaction control system can be used to provide final orbit-correction impulse. The spacecraft are then oriented normal to the orbit plane and spun up by the Burner II to 120 rpm. The spacecraft are then detached. The Burner II GN_2 system provides retro impulse for separation from the spacecraft.

Subsequently the two spacecraft are separated and the despun platforms released. The DPC is then enabled, locking the canister to earth to provide a nutationally stable configuration. Communications with the satellites are possible through the omni-directional (VHF) TT&C antennas. After measuring the drift rates of the satellites, and thus out-of-earth synchronism, appropriate firing plans for the secondary propulsion subsystem are prepared in the Control Center to cancel any orbit errors and to induce drifts in the correct direction to separately place the spacecraft on station. Subsequently, the induced drifts will be canceled again by the propulsion system, the antennas will be deployed, and the system ready for operation.

4.10 SPACE SEGMENT (SATELLITE AND BOOSTER) COSTS

The estimated cost for the spacecraft portion of the Nav/TC/Data/VHF voice program is $43 million. This sum includes the necessary development, and the construction of one prototype. It also includes the construction of four flight models at $4.5 million per copy and the installation--including booster cost--of one complete two-spacecraft system.

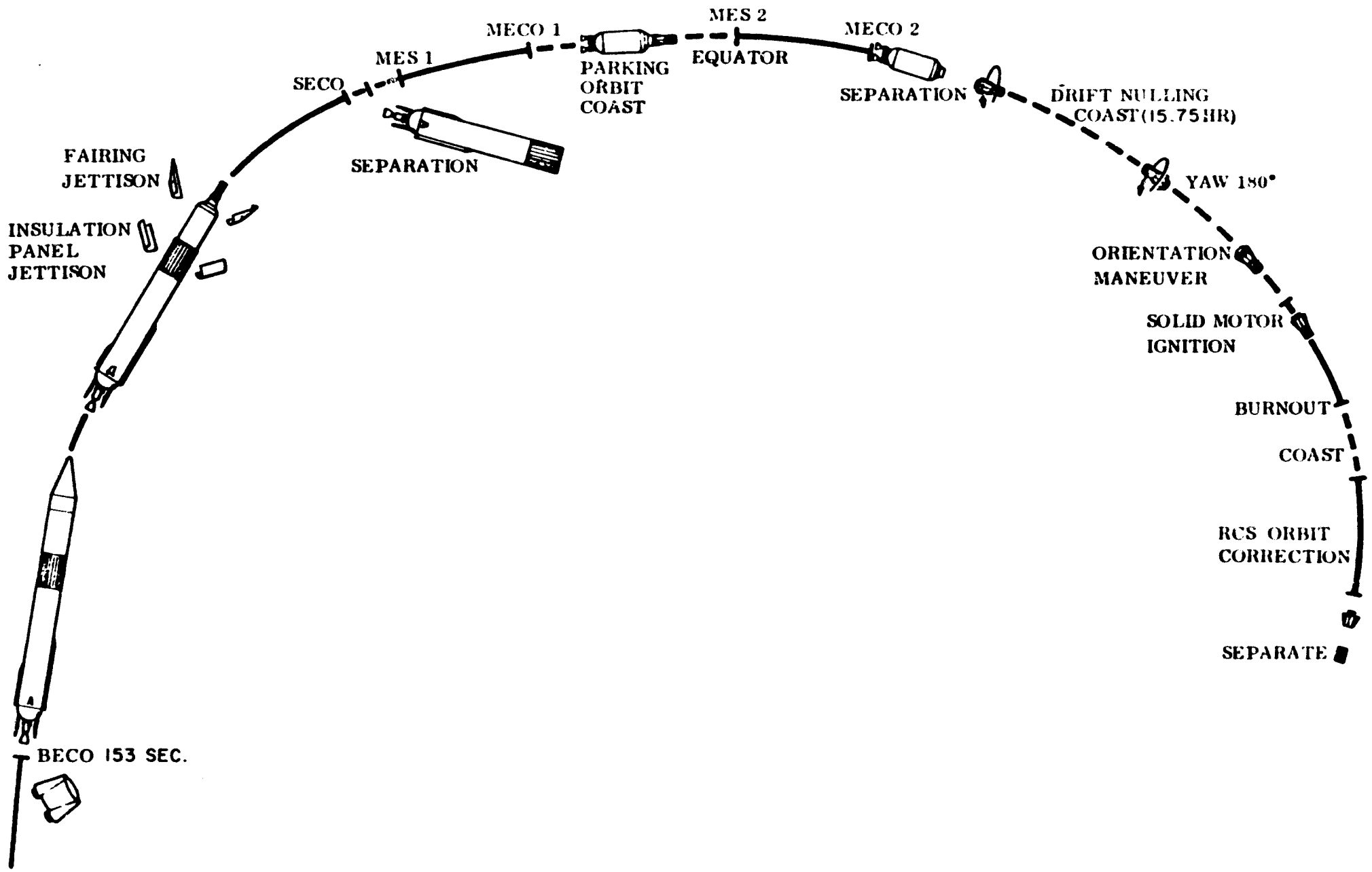

Figure 4-26. Atlas/Centaur/Burner II Flight Sequence (Synchronous Equatorial Mission)

The provision of a second booster so as to allow subsequent utilization of the flight spares would lift the total cost to $56 million.

The booster cost that is tabled ($13 million) includes recurring vehicle launch items, i.e. hardware, procurement, typical recurring mission and payload peculiar modifications, vehicle assembly, checkout, and launch support services. It also includes provision for a lengthened shroud.

The various cost items are shown in Table 4-12.

The cost assumptions that are basic to the tabled estimates may be listed:

1. Navigation/Traffic Control subsystem. Data based upon RCA Study Report "TV Network Satellite Systems" noting that two transponders are involved and adding

2. Voice Communications Subsystem. Estimate based upon this same reference, but noting that there are four VHF transponders and adding $500K for the VHF antenna.

3. Telemetry and Command. Based upon this same reference, but with added costs due to provision of redundancy.

4. Power Supply Subsystem. $4000/ft^2 of array (equivalently $400/start of life normal illumination watt), plus $5K/lb for regulation and batteries.

5. Attitude Control. Based upon experience of similar subsystems.

6. Secondary Propulsion. Based upon data derived for propulsion module proposed for TIROS M.

7. Structure and Integration. Approximately $5K/lb.

8. Testing. Based upon experience.

It is of note that the costs per "flight" pound co e out to about $11.9K for this system. TIROS currently costs about $10K/lb.

The provision of a second booster so as to allow subsequent utilization of the flight spares would lift the total cost to $56 million.

The booster cost that is tabled ($13 million) includes recurring vehicle launch items, i.e. hardware, procurement, typical recurring mission and payload peculiar modifications, vehicle assembly, checkout, and launch support sevices. It also includes provision for a lengthened shroud.

The various cost items are shown in Table 4-13.

TABLE 4-13. SYSTEM COST BREAKDOWNS FOR NAV/TC/DATA/VHF VOICE

	DEVELOPMENT	PER COPY
(1) Navigation/Traffic Control	$ 250K	$ 220K
(2) Voice Communications	2,500K	875K
(3) Telemetry & Command	250K	100K
(4) Power Supply	750K	1,250K
(5) Attitude Control	500K	150K
(6) Secondary Propulsion	500K	200K
(7) Structure & Integration	500K	380K
(8) Testing	1,000K	400K
Contingency	1,560K	895K
	Total $7,810K	$4,470K
Total Cost for R&D, One Prototype and Four Flight Models	$30,160K	
Booster Cost	$13,100K	
TOTAL INSTALLATION COST	$43M	

1. Navigation/Traffic Control subsystem. Data based upon RCA Study Report. "TV Network Satellite Systems" noting that two transponders are involved and adding $60K for the antenna.
2. Voice Communications Subsystem. Estimate based upon this same reference, but noting that there are four VHF transponders and adding $500K for the VHF antenna.
3. Telemetry and Command. Based upon this same reference, but with added costs due to provision of redundancy.
4. Power Supply Subsystem. $4000/ft^2 of array (equivalently $400/start of life normal illumination watt), plus $5K/lb for regulation and batteries.
5. Attitude Control. Based upon experience of similar subsystems.
6. Secondary Propulsion. Based upon data derived for propulsion module proposed for TIROS M.
7. Structure and Integration. Approximately $5K/lb.
8. Testing. Based upon experience.

It is of note that the costs per "flight" pound come out to about $11.9K for this system. TIROS currently costs about $10K/lb.

Section 5

SPACE SEGMENT DEFINITION (UHF VOICE)

5.1 INTRODUCTION AND SUMMARY

As a consequence of the definition of the VHF system of Section 4, it became apparent that the growth potential of this was very limited. This is so for both technical reasons and for reasons of frequency crowding in the VHF band. The provision of better than 19 dB of antenna gain at the spacecraft is difficult because of the sheer size of the consequent dish, and additionally leads of course to coverage restrictions. 3 dB can be gained by going to North Atlantic coverage only, but then what about a "world-wide" system ? It is not feasible to apply phased array techniques at these frequencies, because of problems of element size so that it is very difficult to combine broad coverage with high gain.

The VHF band is crowded, and Internationally unpopular, and the obvious "growth" choice is the UHF band, which offers prospects both of clear allocations and of possibilities for international cooperation.

The real problem (and the solution) of implementation of a UHF link lies with the antenna systems. If a nominally 0 dB user antenna is employed, in conjunction typically with an earth coverage satellite antenna, then the small physical size of the user aperture leads to very high satellite radiated power requirements. It is for this reason that relatively high gain UHF user antennas are now under consideration, on both sides of the Atlantic. The systems problem here is that if the antenna gain is raised to worthwhile levels the field of view becomes so contracted that antenna switching becomes necessary during the transoceanic passage. In aircraft this extra crew load is unwelcome.

The alternative is to place higher gain upon the space segment, but if traditional methods are followed to do this then the downward field of view very soon becomes too small.

Even the combination of some small user gain with somewhat increased spacecraft gain does not offer sufficient link improvement to make the total UHF system attractive.

However, there is a solution, and it is to use a retro-directive phased array at the spacecraft. Properly designed, this array can "see" the whole earth, and yet separately and automatically lock on, with high gain, to multiple users. At frequencies in the 1540-1660 MHz band such an array is of acceptable size and complexity.

The system that will be described in this section incorporates such an array in each of the two spacecraft and allows the provision of six FM Aviation Voice channels to 0-dB users and six FM Maritime Voice channels to 10-dB users, together with the

traffic control, navigation and data link functions previously described for the VHF (voice) system. Capabilities of this system are listed below:

SYSTEM CAPABILITIES	
Position Location:	Traffic Surveillance for aircraft. Navigation field primarily for shipping.
Data Transfer:	100 bps two-way link to aircraft, 100bps address link to shipping.
Voice Channels	Six UHF FM simplex channels to aircraft, six UHF FM simplex channels to shipping.

The all-UHF spacecraft that emerges is such as to allow launch of the total system of two vehicles aboard a single Atlas-Centaur-Burner II booster, although in order to provide a payload margin it is necessary to assume a growth version of the Burner II. The stowage of the two spacecraft within the shroud envelope is shown in Figure 5-1.

Figure 5-2 shows the deployment sequence to mission mode, and indicates the relatively straightforward nature of the spacecraft stowage arrangements. Essentially the spacecraft consists of a planar sixteen element phased array, measuring 8 feet on the side, with an outrigged solar array driven about the pitch axis to track the sun. A separate 2.3 foot diameter L-band antenna is provided for the position location/data function, and the balance of the equipment is carried in a main structure to the "rear" of the phased array. On-board propulsion is provided so as to allow injection error correction, station acquisition, and attitude trim, while basic stabilization is effected by a pitch wheel carried in the equipment compartment. An assembly of horizon sensors is carried by this wheel so as to scan the earth's disc through appropriate apertures in the antenna array, and additionally solar sensors provide solar array sun track data for on-board control of the power supply orientation.

The total spacecraft, in the deployed condition, measures about 11 feet (max.) by 22 feet, delivers an end-of-life (5 years) minimum illuminated power output of 760 watts DC, and weighs 760 pounds.

The various spacecraft subsystems are described in outline in subsequent sections, and are based where appropriate upon the analysis performed in the course of the design of the VHF system. Where the approach is radically different, recourse has been made to experience rather than to detailed design. To this extent the UHF spacecraft design constitutes a feasibility exercise, rather than the result of detailed analysis, and does require further defintion and refinement.

A blow-up of the vehicle is depicted in Figure 5-3, together with a weight and power breakdown.

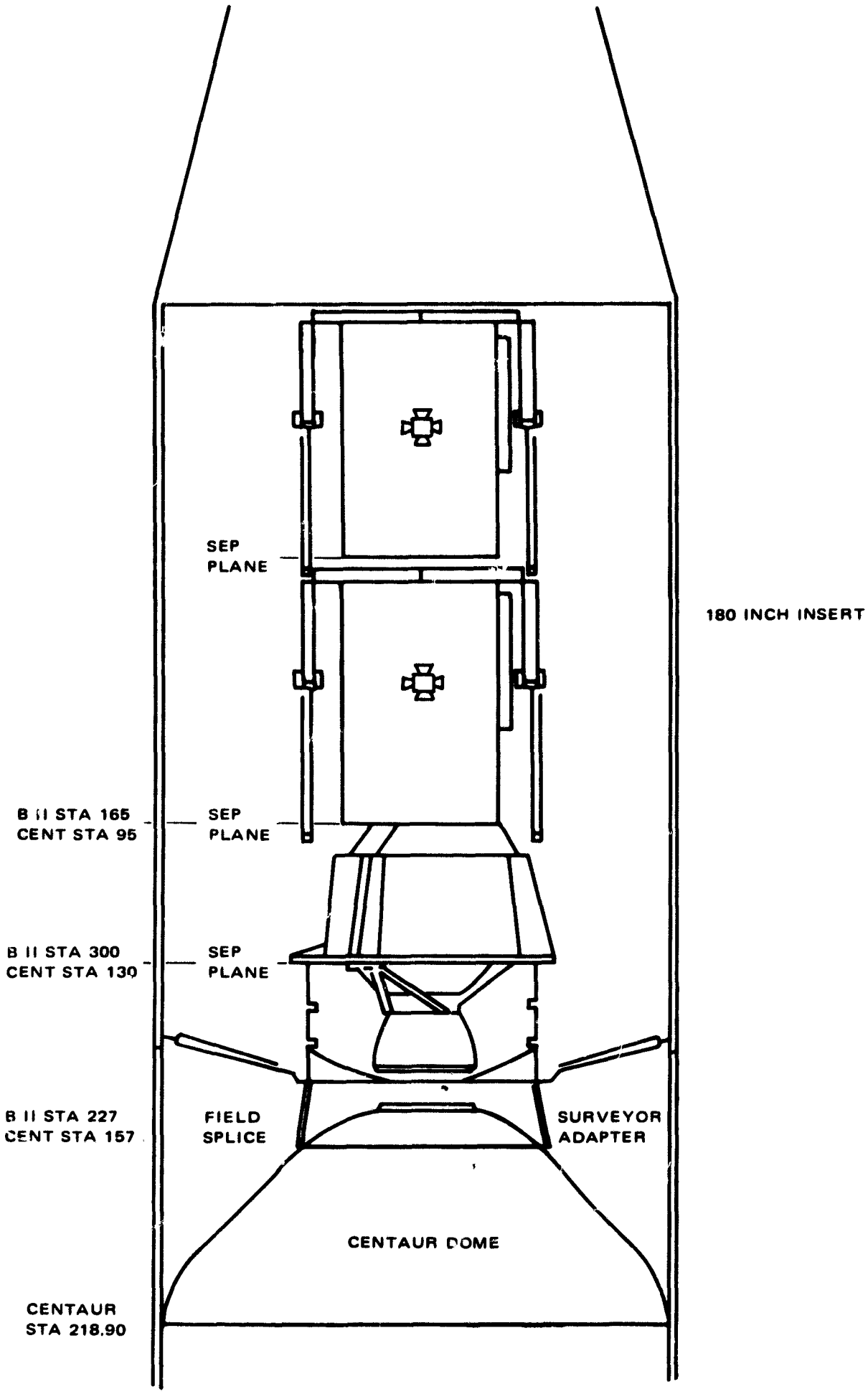

Figure 5-1. Centaur - Burner II Operational Payload

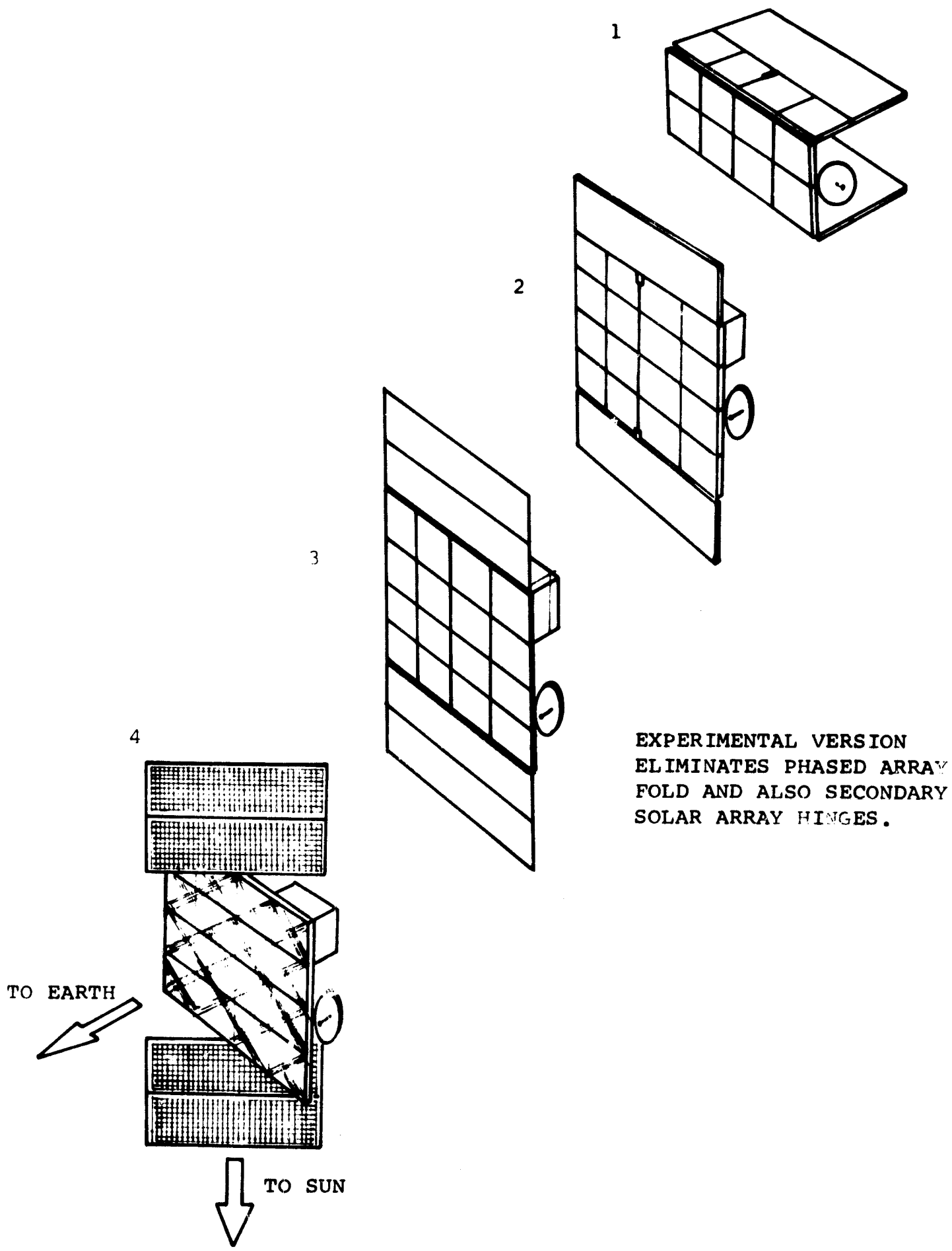

Figure 5-2. Operational Spacecraft Deployment

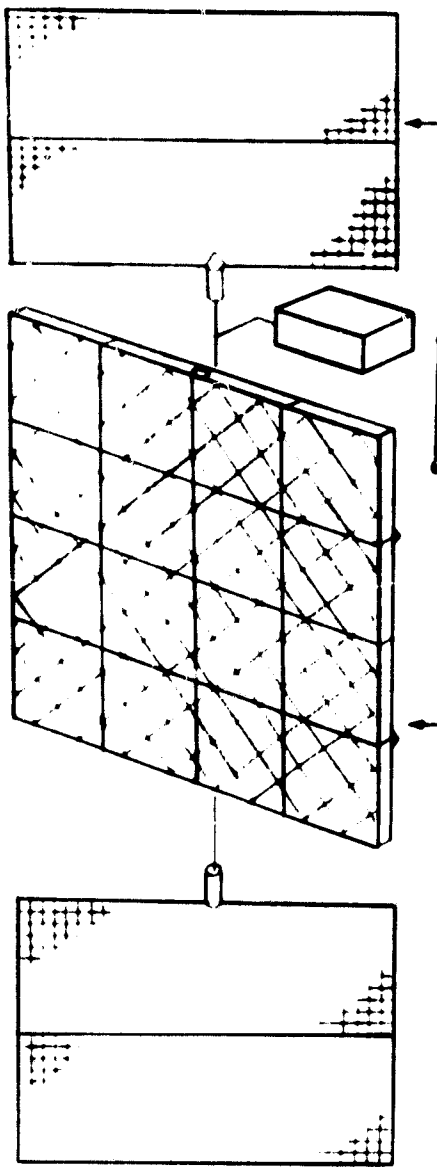

POWER SUPPLY	326 LB.	138W
HARNESS	25 LB.	–
ATTITUDE CONTROL	84 LB.	20W
STRUCTURE	85 LB.	–
TELEMETRY & COMMAND	25 LB.	14W
PROPULSION	78 LB.	–
POSITION LOCATION EQUIPMENT	44 LB.	119W
VOICE EQUIPMENT	90 LB.	464W
	757 LB.	755W

Figure 5-3. Operational Spacecraft

5.2 SPACECRAFT STRUCTURE

5.2.1 GENERAL ARRANGEMENT

The main body of the spacecraft is a tubular cage, as shown in Figure 5-3, which contains the stabilization and propulsion subsystems, the telemetry and command module, the power conditioning and storage subsystem, the navigation/traffic control block, and the central elements of the voice communications subsystem.

This main structure provides hardpoints for attachment of the Burner II assembly (in the case of the lower spacecraft) or of the lower spacecraft (in the case of the upper). Connections are also provided for attachment of the phased array/power subassembly, and (in the case of the lower vehicle) for load transfer through to the upper spacecraft.

The phased array sub-assembly of 16 array elements or antennules forms a separate structure attached to the main body and folded for launch. This assembly also carries outboard the driven and deployed solar array. Each antennule carries within a support frame the necessary arrangement of dipoles, a transmitter, a receiver, and an assembly of signal processors, one per channel. Each antennule element forms a structural "brick" in the array. Figure 5-4 shows the front and rear faces of the dipole array (measuring 24 ins. by 24 ins.) and the dipole feed system.

The two halves of the solar-array are driven to track the sun by motor assemblies mounted in the edge of the antenna array, the drives obtaining pointing information from solar sensors mounted upon the solar panels. These drive assemblies are conventionally sealed by labyrinths, and sacrificially lubricated.

The secondary propulsion subsystem, employing hydrazine as a monopropellant, is mounted within the main body so as to apply velocity corrections (upon command) through the spacecraft center of gravity as well as roll/yaw attitude trimming thrust. The attitude control momentum wheel/horizon sensor assembly is motor driven at relatively high speed, and again the motor is provided with sacrificial lubrication. The attitude information necessary to closed loop pitch control (and open loop roll/yaw control) is obtained from horizon sensors mounted upon the wheel, and operating in the same manner as those of the VHF spacecraft described previously.

5.2.2 STOWED LAUNCH CONFIGURATION

Figure 5-1 shows the UHF spacecraft (pair) mounted within the Centaur shroud, and the folding arrangements are further indicated in Figure 5-2.

The 10-foot Centaur shroud allows the employment of rather simple hinging for the phased array antenna, the spring-loaded edge rows of antennules being folded back against the spacecraft body and there retained with simple tie-downs. These latter are pyrotechnically released. The same arrangement is employed for the L-band dish serving the navigation/traffic control/data link, except that tie-down is not to the spacecraft body but rather to the rear of the fixed portion of the phased array.

The solar panels are carried by the hinged portion of the antenna array, and consequently fold down with it. The stowed array is locked so as to line up with the antennule row in the folded condition, and each solar panel is further folded once so as to remain within the required package length envelope. The solar panel drive is not articulated, since such motion is not required, and each drive incorporates DC power transfer slip rings.

The various separation devices used between the Burner II stage and the spacecraft, and between the two spacecraft, are identical to those of the VHF system—as are the interface locations themselves.

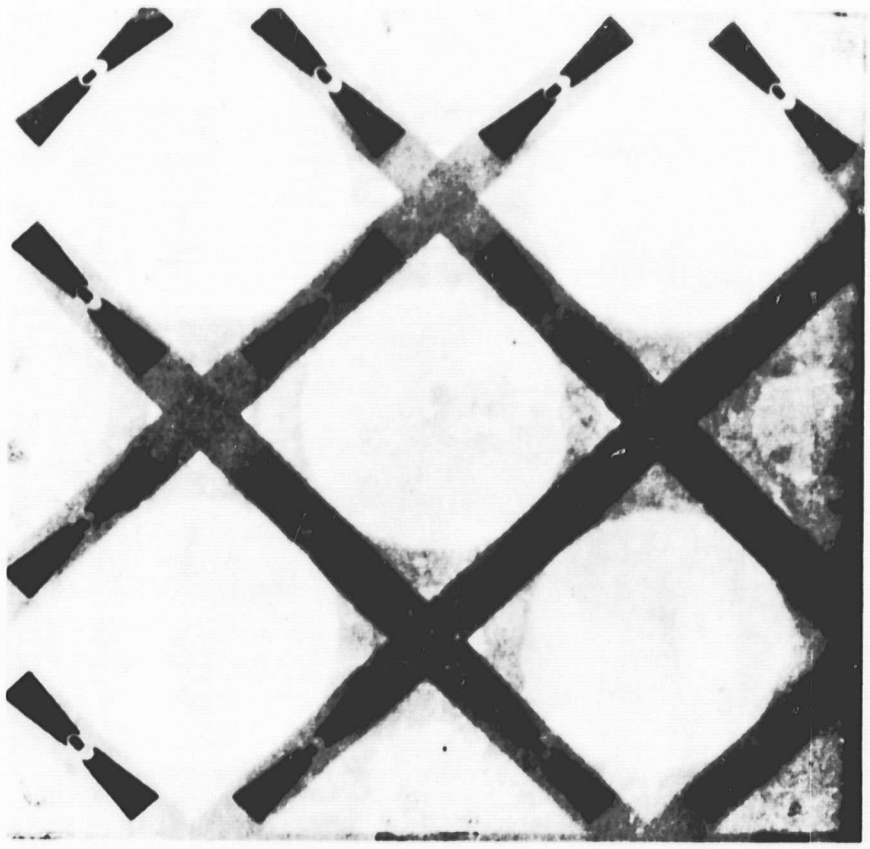

FRONT FACE

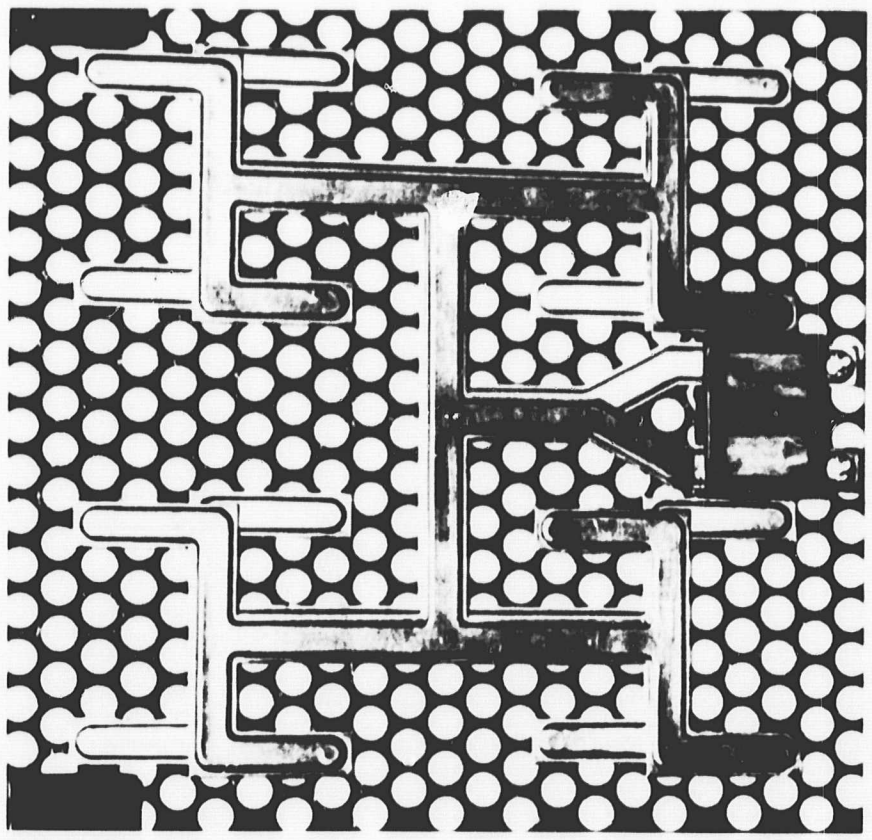

REAR FACE

Figure 5-4. Antennule

5.2.3 CONSTRUCTION

Construction follows conventional practice, the tubular framework of the main spacecraft body carrying such panelling as is necessary for thermal purposes, and for mechanical stiffening. Each of the various subsystems essentially constitutes a package, with each package designed for passive thermal control via radiation interchange.

The elements of the antenna array are formed as mechanically self-sufficient "trays" providing internal support to the internal elements of the antennule and external connection to the adjacent units. The rather high total power dissipation within the array is of small consequence as a thermal balance problem, since in effect the whole array is available as a radiator.

It is of note that the relative physical location of the separate antennules is not critical to operation of the antenna array, so that provision can be made without penalty for sensor field of view through the array, and for the solar panel drive units.

The spacecraft main body is estimated to weigh a total of 85 pounds and the connecting wiring harness to account for another 25 pounds.

5.2.4 UHF VOICE ANTENNA

The construction of this antenna has already been described in outline and is treated in detail in Section 5.3. That section describes the operation of the retrodirective phased array, and points out in detail the advantage to be obtained by use of the device—fundamentally the combination of a wide-angle search beam with high effective gain.

In mechanical terms the antenna has been seen to be relatively straightforward and current laboratory modules weigh approximately 0.3 lb/ft^2—including the sub-array of dipoles as well as the support material. The laboratory model is shown in Figure 5-5, this particular version being intended for use at $\approx$2000 MHz with somewhat greater than earth coverage and consequently measuring 1 foot on the side rather than 2 feet as in the present application.

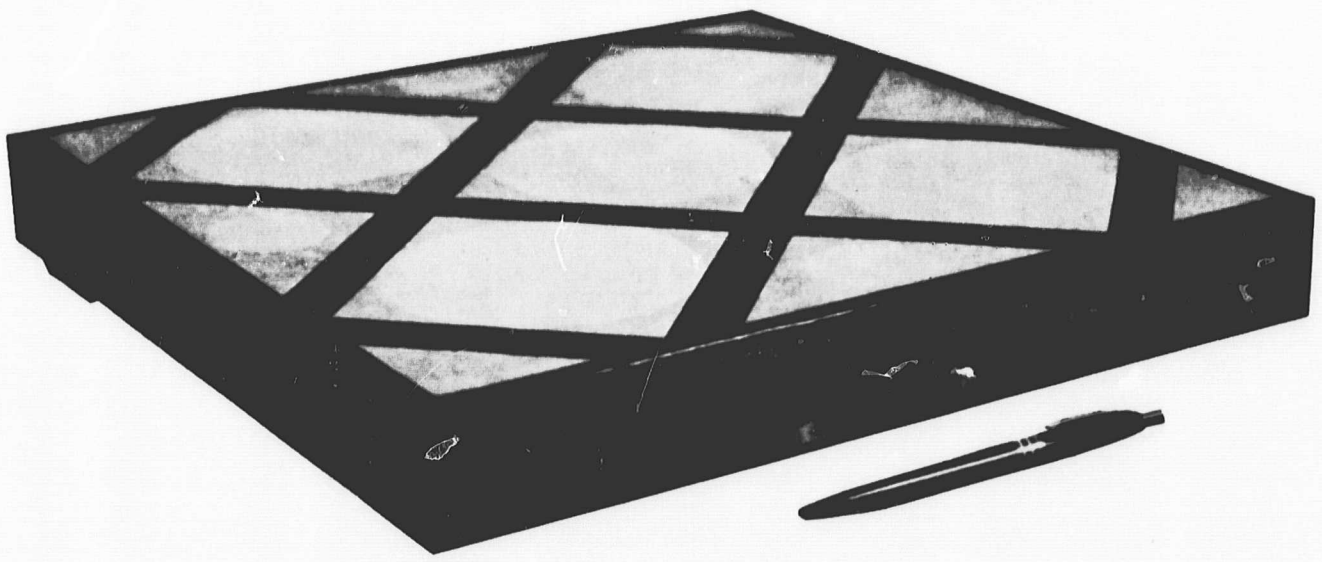

Figure 5-5. Assembled Antennule Unit

In the system described here the weight allowance for the dipole subarray has been increased to 1 lb/ft^2 in order to allow for structural items required for function in an array (including hinges, releases, springs, etc.) and the antennule weight is thus 4 pounds. The sixteen elements of the array thus amount to 64 pounds, in complete form.

5.2.5 WEIGHT ESTIMATE

The weight breakdown for the UHF spacecraft is presented below in some detail. The allowances for structure, harness, and for the voice equipment have already been mentioned and the other subsystems will be treated in turn subsequently.

Component	Weight (lb)	Power (W)	Size
Structure Subsystem			
Main body frame	60.0	-	3 ft x 3 ft x 5 ft (approx.)
Antenna support	15.0	-	-
Thermal control	10.0	-	-
Wiring harness	25.0	-	-
Subsystem	110.0	-	-
Communications			
Voice Comm. Subsystem			
Antennule Structure (16)	44.8	-	2 ft x 2 ft (approx.)
Dipole arrays (16)	19.2	-	2 ft x 2 ft
Receivers (16)	3.2	5.0	Within antennule
Signal processors (96)	9.6	24.0	Within antennule
Transmitters (16)	3.2	435.0	Within antennule
Summing & Distrib. Equipment, Acquisition Network	10.0	-	6 ins x 6 ins x 1 ft (approx.)
Subsystem	90.0	464.0	8 ft x 8 ft (array)
Position Location Subsystem			
Forward Link Transponder	8.0	10.0	7 ins x 6 ins x 10 ins
Back link Transponder	8.0	10.0	7 ins x 6 ins x 10 ins
Forward link power amp (TWTA)	10.0	66.0	5 ins x 7 ins x 14 ins

Component	Weight (lb)	Power (W)	Size
Position Location Subsystem (Continued)			
Back link power amp (TWTA)	10.0	33.0	5 ins x 7 ins x 14 ins
Antenna diplexer	5.0	-	-
Antenna	3.0	-	2.3 ft diameter
Subsystem	44.0	119.0	-
TT&C Subsystem			
VHF command recvr (2)	2.5	1.0	2 ins x 3 ins x 6 ins
Command decoder & CDU (2)	10.0	2.0	6 ins x 6 ins x 8 ins
Baseband assembly unit and modulator (1)	8.0	6.0	7 ins x 5 ins x 7 ins
VHF telemetry transmitter (2)	1.5	5.0	3 ins x 3 ins x 3 ins
Diplexer	1.0	-	-
Omni antenna	2.3	-	40 inch dipole
Subsystem	25.3	14.0	
Power Subsystem			
Solar array	84.0	-	2 x 8 ft x 6-1/2 ft.
Power regulation and charge control	26.0	13.0	9 ins x 9 ins x 12 ins
Batteries	216.0	125.0	12 ins x 12 ins x 9 ins
Array drives (2)	20.0	10.0	8 ins x 5 ins dia each
Subsystem	346.0	148.0	
Attitude Control Subsystem			
Pitch wheel	30.0	-	36 ins dia.
Wheel drive	15.0	5.0	8 ins x 6 ins dia.
Roll horizon sensors	2.0	0.5	3 ins x 3 ins x 4 ins
Pitch horizon sensor	2.0	0.5	4 ins x 7 ins x 4 ins
Pitch control electronics	8.0	4.0	5 ins x 6 ins x 5 ins
Nutation damper	5.0	-	12 ins x 72 ins
Solar sensors	2.0	-	-
Subsystem	64.0	10.0	-

Component	Weight (lb)	Power (W)	Size
Secondary Propulsion Subsystem			
Propellant tanks (2) incl. bladders	8.0	-	12 ins dia.
Pressurant bottle	2.0	-	8 ins dia.
Nitrogen pressurant	2.0	-	-
Regulation, fill & drain, transducers	5.0	-	-
Thrust chamber assemblies (12)	11.0	-	-
Support structure	10.0	-	-
Miscellaneous	1.0	-	-
Hydrazine	39.0	-	-
Subsystem	78.0	"Spike" power demands	
TOTAL VEHICLE	757 LB	755 WATTS	

5.3 COMMUNICATIONS

5.3.1 GENERAL

The communications equipment on the satellite is divided into two major subsystems:

- L-band position location transponders
- UHF voice-channel transponders

In addition, there is a telemetry and command subsystem.

The L-band position location transponders are identical to those described in detail in the description of the VHF spacecraft (Section 4.3.1). These will not be treated further here, except to note that as before there are good qualitative arguments for the inclusion of transponder redundancy- but again that this has not been included in the basic design. Further, the possibility exists for the elimination of the separate position location antenna assembly via the dual use of one of the array elements, but this has not been pursued at this time.

Six UHF voice channels (three aviation and three maritime) are provided at each spacecraft. Each of these channels is served through all sixteen elements of the array, and shares a common receiver/transmitter assembly at each element. One signal processer is provided per antennule per channel. All the voice channels lie within the 1540-1660 MHz aviation services band, and assignments were suggested in Table 1-3 of this volume. With each channel all up-link communications to the satellite are at

one frequency, and all down-link at another, so that as with the VHF system, communications between an aircraft (or a ship) and the ground terminal are in the simplex push-to-talk mode. With the high gain ascribed to the spacecraft in the locked-on condition the 3 dB ground pattern is about 2000 miles in diameter, so that even in this condition clear channel identification would not normally be a serious problem.

5.3.2 L-BAND NAVIGATION SUBSYSTEM

This is identical to that described in Section 4.3.1 of this volume.

5.3.3 UHF VOICE CHANNEL SUBSYSTEM

5.3.3.1 LINK ANALYSIS

Again, the Voice subsystem virtually "sizes" the spacecraft. Because of the relatively high space loss encountered at UHF (1540-1660 MHz in this particular application) it is necessary to take such advantage as may be gained from the fresh start offered by the proposed new service. Consequently, FM modulation with 12 dB of clipping is proposed. The desired signal-to-noise ratio has been set at 6.5 dB at the user receiver. This provides good quality reception with 75% word intelligibility, which results in essentially complete phrase intelligibility.

The analysis for the UHF FM voice link appears below in tabular form, and is based upon the selection of a 30 dB spacecraft antenna, as combining reasonably high gain with moderate coverage.

Frequency (nominally)	1560 MHz	
Path loss	188.9 dB	
Scan edge loss	3.0 dB	User normally at beam center
Polarization loss	0.3 dB	5 dB user ellipticity
Relay degradation	0.4 dB	Noise in down link
Multipath fading	0.5 dB	"Shaped" antenna
Aircraft cable loss, etc.*	1.0 dB	
Total losses	194.1 dB	
User gain	0.0 dB	
Spacecraft gain	30.0 dB	
Total link gain	-164.1 dB	
User receiver noise level	-158.2 dBW	6 dB noise figure receiver and 9.5 KHz Modulation Bandwidth
Desired S/N ratio at user**	6.5 dB	
Hence radiated power	12.4 dBW	
	17 watts	

* Preamplifier at antennas

**In 9.5 KHz Bandwidth

The reasonableness of the derived power requirement is of course totally dependent upon the 30 dB spacecraft antenna assumption. This high gain level, in combination with full earth coverage (an apparent contradiction) is only obtainable practicably in the multi-channel environment by the use of the electronically self-steered array.

5.3.3.2 RETRODIRECTIVE ARRAY

The principal advantages of using the retrodirective array may be listed:

1. The array can provide the desired coverage of the earth surface simultaneously with a high overall array gain, by means of a relatively simple arrangement. Thus, the necessary coverage is obtained by using individual array elements having this beamwidth, and the desired overall gain is achieved by using a sufficient number of elements and adding their signals in phase with each other.

2. The narrow beam (corresponding to the full array gain) is formed and steered electronically, via a transponder connected to each array element. The need for mechanical steering is completely eliminated.

3. The beam is "retrodirective" or "self-steering" in the sense that it automatically points to a user on receiving a pilot signal radiated by the latter. Thus the spacecraft does not need a separate steering system controlled by an on-board computer or by a ground station, although it can be ground commanded.

4. The same array can form multiple beams, each pointing in a different direction and having the full array gain; the only penalty is the additional circuitry required in the transponders.

Further, distinct advantages exist in terms of the details of implementation. The division of signal power into multiple transponders allows the use of solid state amplifier components. The total device is subject to graceful failure both because of the small number of common central devices and because of the independent nature of the array elements. And further, the array is insensitive to accuracy of deployment.

The retrodirective array operates as a highly directional antenna which forms a transmit and/or receive beam in the direction of an incoming pilot signal. The principle can be understood by referring to Figure 5-6(a), which shows a plane wave normally incident on a perfectly reflecting plane surface AA. Note that the phases at arbitrary points P_1, P_2, etc. are $\phi_1, \phi_2, \ldots$ for the incident wave, and $-\phi_1, -\phi_2 \ldots$ for the reflected wave. Therefore, a set of transponders located at several points along an arbitrary surface BB, and having the property of generating the phase conjugate of the incoming signal at each point, will result in a plane wave being radiated back in the direction of the incoming signal. The basic form of such a transponder is shown in Figure 5-6(b), where the received and transmitted signals have phases $\pm\phi$, the phase conjugation being accomplished by means of mixers.

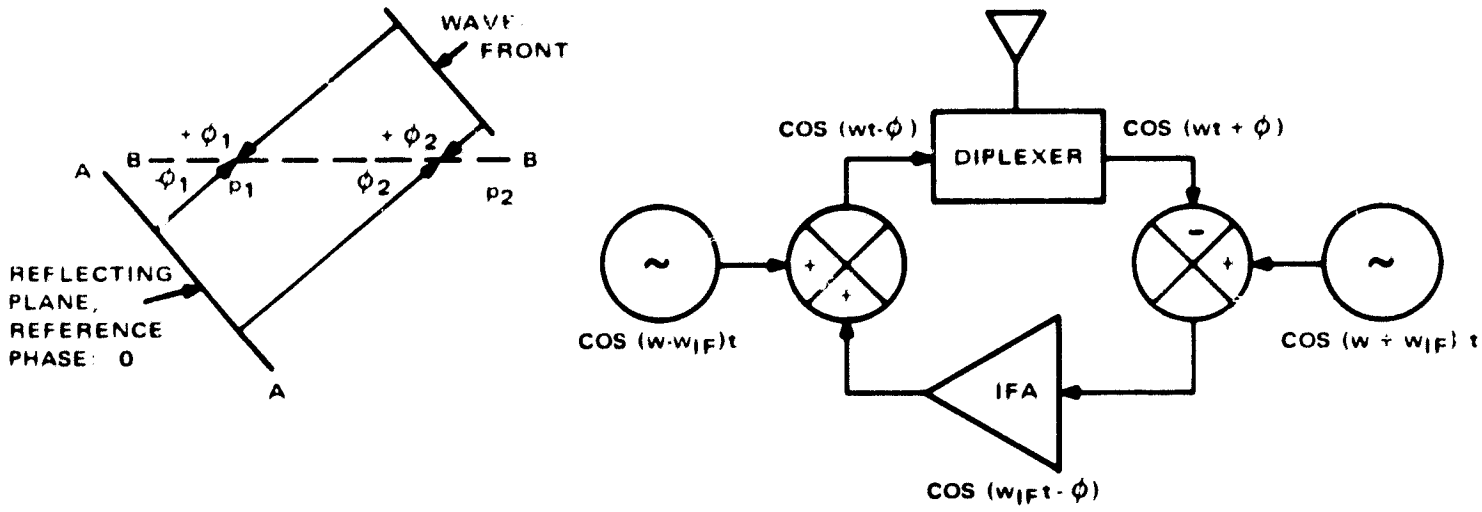

a) PHASE RELATIONSHIPS

b) SIMPLE IMPLEMENTATION OF ONE ELEMENT

Figure 5-6. Principle of Retrodirective Array

In addition to being "self-steering" as a transmitter, the retrodirective array can be also made "self-focusing" as a receiver, in the sense that the relative phases of the signals received at different array elements can be automatically adjusted in the transponder in order to achieve their addition in phase with each other, thereby enabling the array to act as a high gain antenna in the receiving mode.

Since the retrodirective property holds at a single frequency, while the incoming traffic consists of a band of frequencies and the receive and transmit frequencies are usually different, there is in general a pointing (or "squint") error between the directions of incoming and outgoing waves. This error is very small (less than 0.1 dB) for the present case because of the small traffic bandwidth (only voice channels) and the small relative difference between the proposed receive and transmit frequencies.

The basic transponder of Figure 5-6(b) must be modified with the following objectives:

- Separating the pilot signal from the traffic (voice) and improving the signal to noise ratio by appropriate filtering;
- Accommodating multiple users by duplicating certain parts of the circuitry.

Apart from the individual transponders, the overall array must have circuitry to sum the incoming traffic after it has been processed by the transponders, and to distribute the outgoing traffic (intended for transmission to users) among various transponders.

In addition, there must be provision for acquisition of the user pilot signal by the spacecraft repeater. This can be done with the minimum burden on user equipment, that is, at the same low antenna gain and at small pilot transmitter power, in spite of the large frequency uncertainty caused by user transmitter drift and doppler shift. The acquisition circuitry is described separately; it produces a "reference signal" which can be fed to each transponder in order to help in the narrowband filtering of the pilot signal (thus improving the pilot SNR) and to obtain the desired self-focusing as well as self-steering properties.

Figure 5-7 shows the block diagram for an array containing N elements. Each element consists of an antennule and a transponder. The traffic intended for transmission to users is indicated as T and that received from users is indicated as R; assuming m users, there are m distributing networks for the outgoing traffic and m summing networks for the incoming traffic. In addition, there is a single acquisition circuit which supplies the "reference signal" to each transponder.

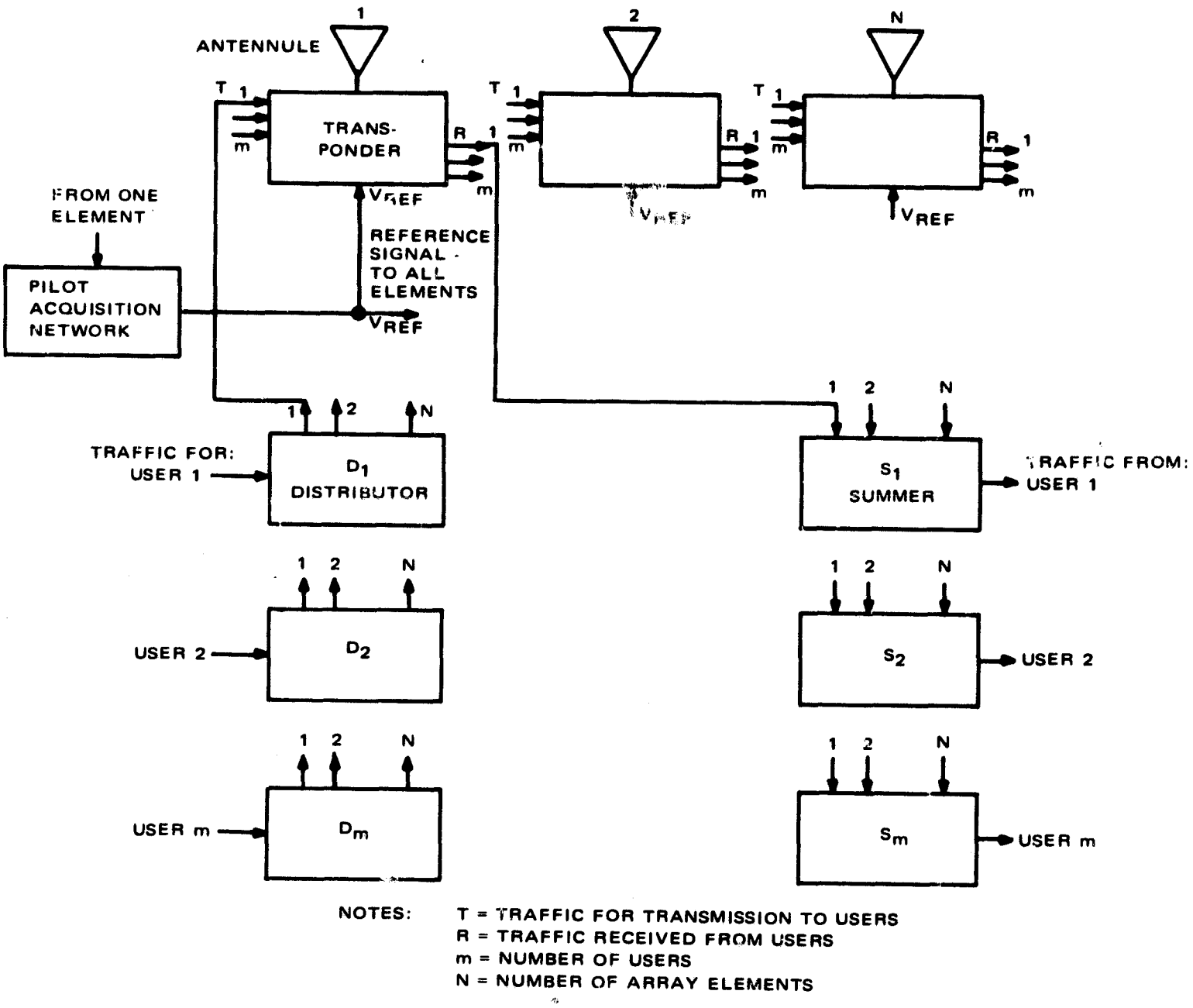

Figure 5-7. Block Diagram of an N-Element Array

Figure 5-8 shows the schematic diagram of one transponder. It is to be noted that the transponder consists of three distinct parts: the Receiver, the Signal Processor, and the Transmitter. Some of the frequencies, bandwidths and phase angles are shown in the figure. The various mixer operations can be arranged in such a manner (by using proper frequencies and selecting upper or lower sidebands) that:

(1) the IF frequencies have the desired values (shown in the diagram as 300 kHz for the first IF, and 10 kHz for the pilot and 30 kHz for the traffic for the second IF for purposes of illustration only), the values being chosen from consideration of ease of filtering and amplification;

(2) the transmitted frequency has the desired value; and

(3) the phase angle of the transmitted signal of each element is conjugate of the incoming phase angle (except for a constant phase shift common to all elements caused by the local oscillators or other circuit components), thus assuring the retrodirective property. The common phase shift does not affect this property.

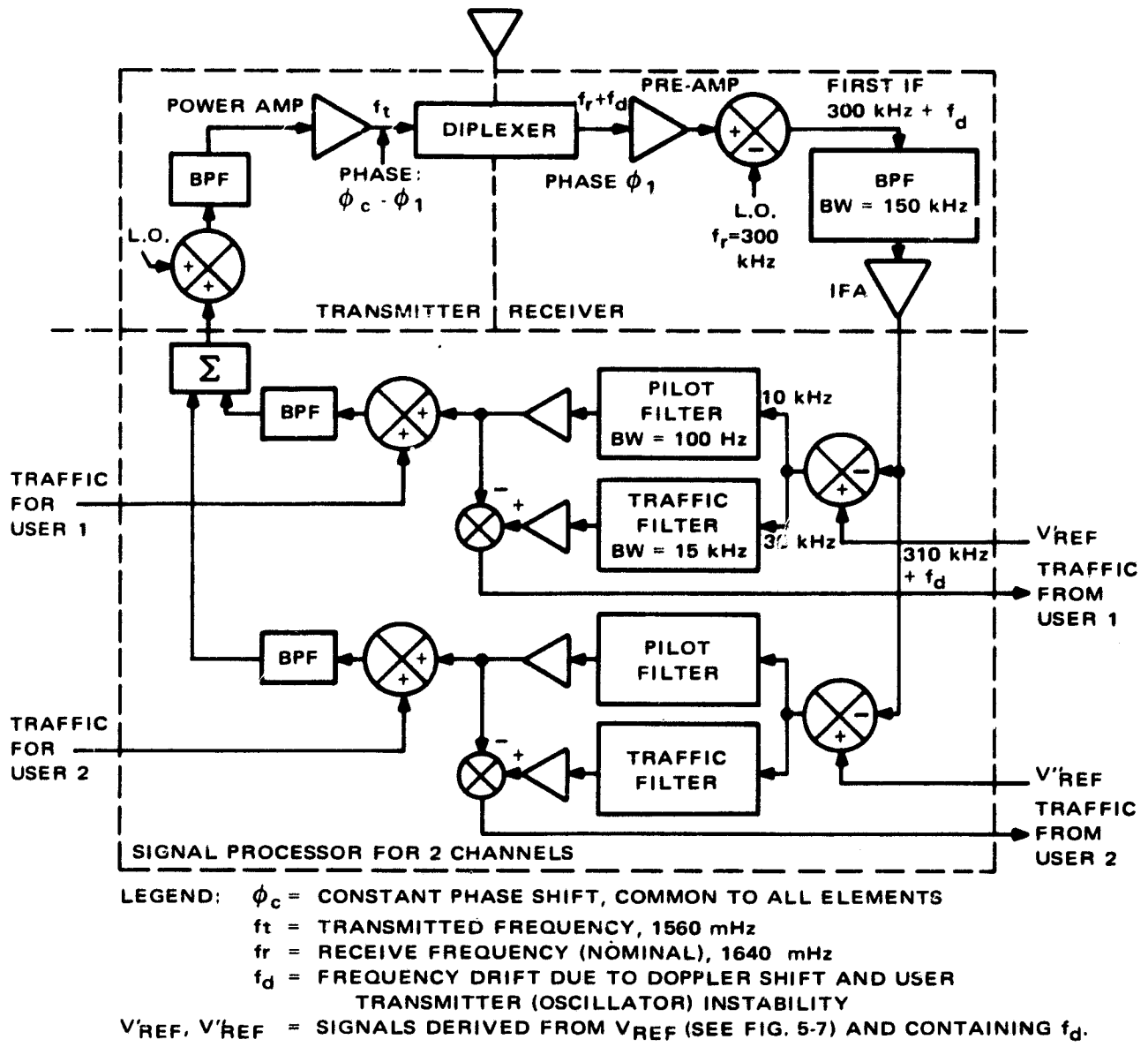

LEGEND: ϕ_c = CONSTANT PHASE SHIFT, COMMON TO ALL ELEMENTS
ft = TRANSMITTED FREQUENCY, 1560 mHz
fr = RECEIVE FREQUENCY (NOMINAL), 1640 mHz
f_d = FREQUENCY DRIFT DUE TO DOPPLER SHIFT AND USER TRANSMITTER (OSCILLATOR) INSTABILITY
V'_{REF}, V'_{REF} = SIGNALS DERIVED FROM V_{REF} (SEE FIG. 5-7) AND CONTAINING f_d.

Figure 5-8. Schematic Diagram of a Two-Channel Transponder

In recent years considerable effort has been applied to the examination of the application of phased arrays to space missions. One part of the effort has been the development at RCA of lightweight components at frequencies of 1800-2300 MHz. Considerable test data is available from breadboard models, so that it is possible to make accurate estimates of the relevant parameters for the frequencies and time-frame of interest, using state-of-the-art miniaturization techniques. Estimated values of the important transponder parameters are collected in Table 5-1 and discussed below.

TABLE 5-1. TRANSPONDER PARAMETERS

Item	Weight (lb)	Power (W)	Remarks
Receiver	0.2	0.3	--
Signal Processor	0.1	0.25	Per user channel
Transmitter	0.2	--	DC Power - 5 x RF power
Total Weight (excluding power supply):	(0.4 + 0.1 m) lb., for m user channels		
Noise figure:	3 to 5 dB, using parametric amplifier front end.		

Transponder Receiver (Preamplifier and Noise Figure) - The receiver noise figure depends on the preamplifier used in each element transponder. A comparison of micro-wave transistor, tunnel diode, and parametric amplifiers for spaceborne receivers showed that typical system noise figures for the three amplifiers are 6.4 dB, 5.5 dB and 4.6 dB. (This marked superiority of the parametric amplifier is obtained at a penalty of about 10% higher weight.) With improvements in preamplifier designs it is expected that very low noise figures—of the order of 3 dB—will be practical in the near future, while 5 dB is a conservative estimate.

The weight of the receiver section of each transponder is expected to be 0.2 lb, using micro-strip circuits and high dielectric substrate at well as large scale integration techniques. The power consumption is expected to be 0.3 W.

Transponder Signal Processor - This can be fabricated in a straight-forward manner and is expected to weight 0.1 lb per user channel, with a power consumption of 0.25 W per channel.

Transponder Transmitter, Power Amplifier - The design and construction of a minimum size and minimum weight power amplifier for the 1800 MHz band has been a major development effort at RCA, using the experience gained during the corporate-funded "Blue Chip" program. A 3-stage solid state amplifier, using two class-B stages and a final class C stage with 1 watt of RF power output has been developed. Test results show that an overall efficiency of about 20% should be possible without major additional development effort, also that output powers up to 5 watts are well within reach. The transmitter weight is estimated at 0.2 lb per element.

Antenna Element (or antennule) - An array consisting of N antenna elements or "antennules", each of gain g, has a total gain G given by G = K Ng, where K is a constant approaching unity under certain restrictions and assumptions. Thus to obtain a desired gain with the fewest elements, it is necessary to use an element which has the highest gain per unit weight for a specified beamwidth, the latter being large enough to cover the desired region on earth. After a detailed consideration of several antennule designs (e.g. disc-on-rad, helixes, yagi, multiple discs on rod, and multipole dipoles), it was found that the best performance is obtained by a "multiple dipole" arrangement. A lightweight breadboard model of such an antenna element, containing 16 dipoles, printed on a fiberglass epoxy sheet and mounted on a lightweight foam block , is shown in Figure 5-9. The dipoles can be properly fed to obtain circular polarization. The model was built and tested for 1800-2300 MHz. By scaling the results to 1540-1660 MHz, it is expected that the antennule will be a square of side 2 feet for a beamwidth of 18.6° and a gain of 18.9 dB (which is needed for full earth coverage with an allowance of ± 1/2° for attitude error).

The antennule area for partial earth coverage is inversely proportional to the square of the required beamwidth. In particular, an antennule for North Atlantic only coverage (with ± 1/2° attitude error) would have a gain of more than 25 dB.

Structure and Cables - The overall array having multiple antennules requires careful layout and manifolding. These problems have also been investigated during the DRSS study proposal and other company-funded R & D studies, and practical solutions have been found.

It is possible to go through an optimization exercise in order to size the array, trading RF power demand for array gain so as to arrive at a minimum weight system. However, in the present application the (16 element) array gain was set at 30 dB in order to lead to a reasonable antenna size (8 ft x 8 ft), and so as to keep the technical demands upon the array within bounds. It may be noted that 16 elements at 18.9 dB each lead to 30.9 dB of total gain, so that some margin exists. This gain level also leads to RF power levels almost identical to those for the VHF system once intermodulation effects have been taken into account. Intermodulation degradation is estimated to be about 1 dB for two voice channels and 2 dB for 4-6 channels. Thus these losses raise the 17 watts of the table of Section 5.3.3.1 to 26 watts for each of the three aviation voice channels within each spacecraft (and the 1.7 watts maritime channel demand to 2.6 watts for each of the three channels). It is of note that as an alternative to taking intermodulation losses a separate transmitter may be used for each channel, and the signals combined before feeding the composite signal to the antennule. This course would involve an additional weight of 0.2 lb per transmitter channel, plus a small weight for the summing network; it is also necessary to increase the ERP slightly to account for the losses in this circuit.

The 17 watts RF power requirement was, as noted, based upon "medium" quality voice. This corresponds to a 2.7 MHz baseband signal with 12 dB of clipping, and 75% word intelligibility, which requires a 15.5 dB SNR after detection. Assuming FM modulation and a phase lock receiver with a 9-dB CNR threshold, in the equivalent AM

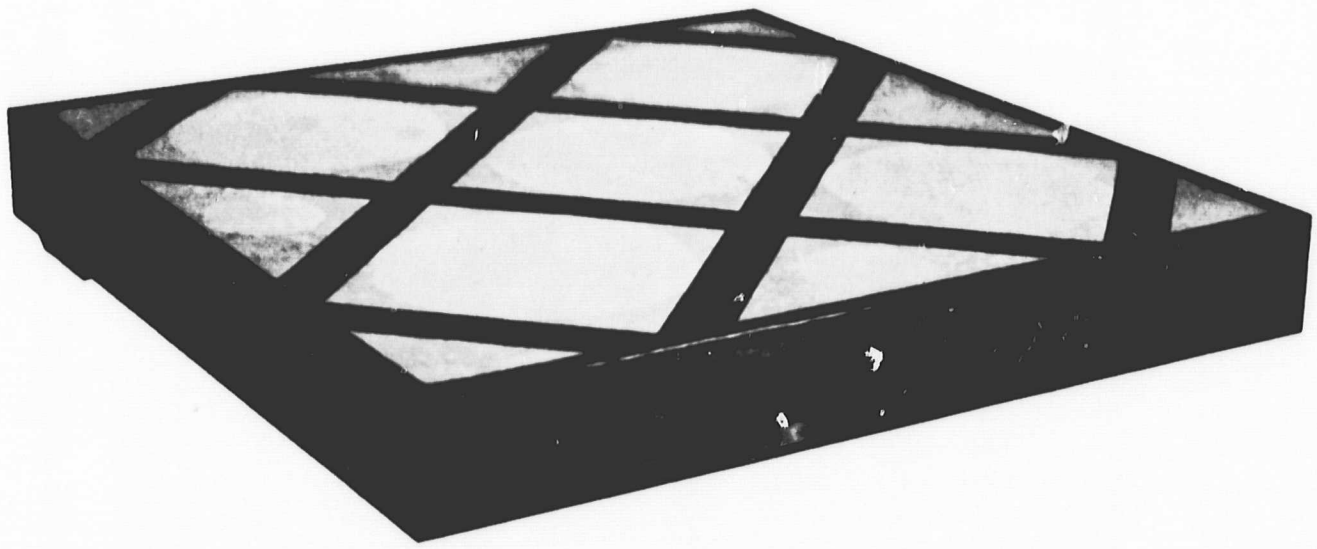

(a) Assembled unit

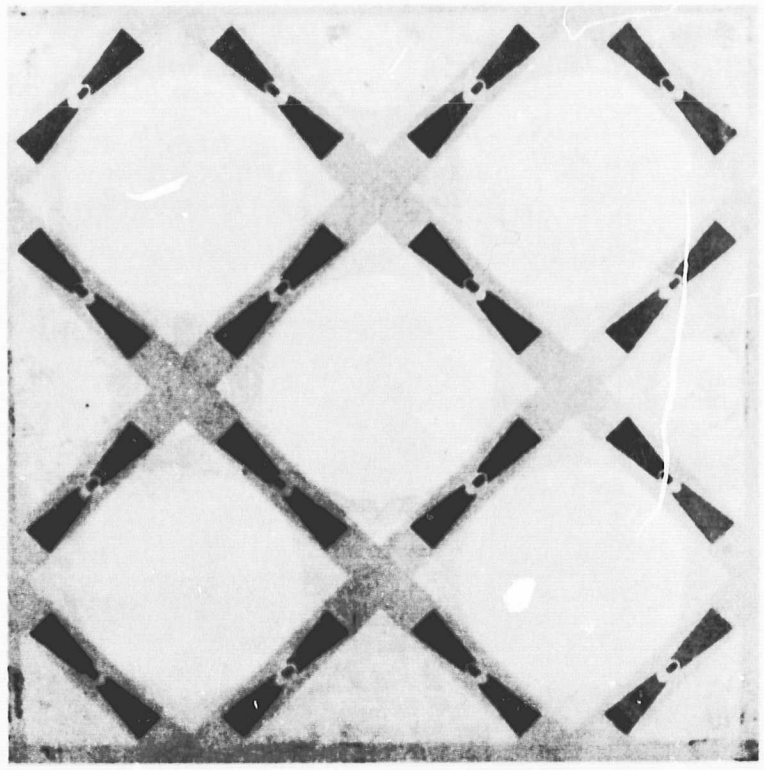

(b) Printed Dipoles

Figure 5-9. Antennule

bandwidth, this corresponds to a 6.5-dB FM threshold in 9.6 KHz bandwidth, which implies a modulation index of 0.8. Similar calculations for "High" and "Low" quality lead in total to the results presented in the tables below: the link calculation is repeated for the sake of completeness.

LINK CALCULATIONS: SPACECRAFT - USER LINK

Item		Value	Remarks
1. f, frequency, MHz		1560	
2. L_p, Path Loss, dB		-188.9	For 26,000 miles, maximum
3. L_m, Miscellaneous losses, dB		- 5.2	For one channel: add intermodulation ioss for multiple channels. Pre-amp at antenna
4. G_a, Aircraft Antenna Gain, dB		0.0	Assumed, net
5. Sum of Lines 2 thru 4, dB		-194.1	For one channel. See Line 3
6. CNR desired, dB		6.5	"Medium" quality voice channel
7. B, Noise bandwidth, dB-Hz		39.8	B = 9.6 KHz
8. N_o, Noise density, dBw/Hz		-198.0	6 dB noise figure aircraft receiver
9. N, Receiver noise, dBw		-158.2	Line 7 + Line 8
10. C, Required carrier power per channel, dBw		-151.7	Line 6 + Line 9
11. ERP required, dBw, for "Medium" quality voice	1 ch	42.4	Line 5 + Line 10
	2 ch	46.4	Includes 1 dB intermodulation loss
	4 ch	50.4	Includes 2 dB intermodulation loss

VOICE QUALITY PARAMETERS

Parameter	Value			Remarks
	High Quality	Medium Quality	Low Quality	
Degree of Clipping (dB)	0	12	30	Speaker identification is difficult with 30 dB clipping
Base bandwidth, b (kHz)	3.0	2.7	2.25	

VOICE QUALITY PARAMETERS (Continued)				
		Value		
Parameter	High Quality	Medium Quality	Low Quality	Remarks
SNR after detection, (dB)	24.0	15.5	10.0	Peak voice/RMS noise
CNR in equivalent AM bandwidth, 2b (dB)	11.0	9.0	8.0	Phase locked
Modulation index, m	1.8	0.8	0.5	To get necessary FM improvement with minimum threshold CNR
IF bandwidth, B	23.2	18	16.6	B = 2B (m + 1) + Frequency drifts
Word Intelligibility (% AS)	80	75	70	Approximate

In the system that is proposed a total of six channels per satellite is provided, three of these being 10 dB down, and the modulation loss may be held to 2 dB, as mentioned previously.

It is to be noted especially that these values correspond to 0 dB net gain and a 6 dB noise figure receiver at the aircraft, which are rather conservative estimates; the actual ERP required may be less than the values quoted. The loss budget was given previously in Section 5.3.3.1.

With regard to the user to spacecraft link, the user aircraft must have adequate power to support a voice channel as well as a pilot channel. The latter is necessary for beam formation and beam steering of the spacecraft retrodirective array. Thus the pilot signal is received by the spacecraft with an effective antenna gain corresponding to a single antennule rather than the whole array. The pilot power requirement can be kept reasonably small by appropriate narrowbanding. The voice channel has a wider bandwidth but it uses the full array gain, thus requiring a modest power.

Calculations for the pilot channel are shown in the table below, and the voice analysis is similar but for considerations of bandwidth. The array receiver noise figure is assumed to be 5 dB, and the allowance is made for the full earth temperature in computing the noise power density. With a 0 dB antenna, the aircraft needs 20 watts for a pilot channel (6 dB SNR in 1000 Hz). The quality of pilot signal (SNR and bandwidth) is important for acquisition, as discussed later.

LINK CALCULATIONS: USER - SPACECRAFT PILOT

Item	Value	Remarks
1. f, frequency, MHz	1640	
2. L_p, Path Loss, dB	-189.3	For 26,000 miles, max.
3. L_m, Misc. Losses, dB	- 6.2	For single channel
4. G_s, Spacecraft antenna gain, dB	+ 19.3	Single element
5. Sum of Lines 2 thru 4, dB	-176.2	
	Pilot	
6. CNR desired, dB	6	
7. B, Noise bandwidth, dB-Hz	30	1000 Hz for pilot (compare with 9.6 kHz for "medium" quality voice)
8. N_o, noise density, dBw/Hz	-199.0	5 dB noise figure receiver, plus earth temperature
9. N, receiver noise, dBw	-169.0	
10. C, required carrier power dBw	-163.0	
11. P_a, aircraft power required (for 0 dB antenna), dBw	13.0	
watts	20.0	

Although the net aviation user gain has been set at 0 dB, and so is undemanding, the aircraft antenna pattern is important insofar as multipath is concerned. Thus to avoid multipath fading it is necessary to reject the earth-scattered signal arriving at the aircraft, and this can be done by ensuring that the antenna pattern has a large supression in the direction of arrival of the earth-scattered signal. In view of the small size of the antenna and its location over a very large conducting surface, it is reasonable to expect that it will be well-shielded from the earth and the undesired earth-scattered signal will be adequately suppressed. (This justified a low allowance of 0.5 dB for multipath fading.)

As indicated earlier, the retrodirective property of the spacecraft array depends on the acquisition of a pilot signal by the spacecraft. A simple form of the acquisition network is shown in Figure 5-10. (Several other forms are available but will not be discussed here.) The network uses a bank of bandpass filters, each followed by an envelope detector, low pass filter, and threshold detector. The bandpass filters together cover the full range of frequency uncertainty. The presence of the pilot signal in a particular filter is detected by the corresponding threshold detector, and the logic circuit then connects the phase lock loop (PLL) to this filter. The VCO contained in the PLL sweeps over the bandwidth in order to search for and lock on to the exact frequency of the incoming pilot.

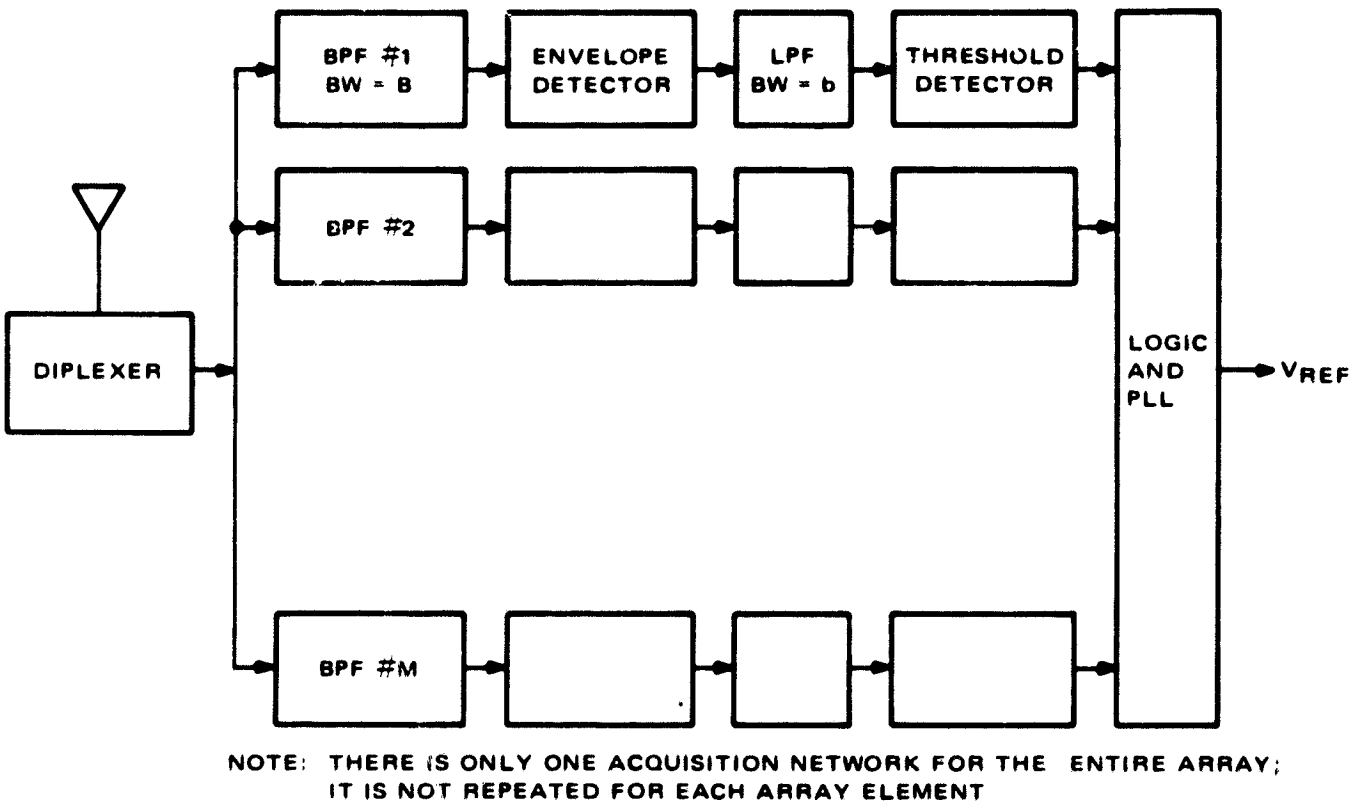

NOTE: THERE IS ONLY ONE ACQUISITION NETWORK FOR THE ENTIRE ARRAY; IT IS NOT REPEATED FOR EACH ARRAY ELEMENT

Figure 5-10. Pilot Acquisition Network

The frequency uncertainty is about 43 KHz for the present application, consisting of a Doppler shift of ±4.8 KHz for a supersonic aircraft and oscillator instability of ±16.4 KHz for a ±0.001% drift. The complexity of equipment depends on the number of filters, which is dependent upon frequency uncertainty and bandwidth. Assuming a bandwidth of 1 KHz, the circuit needs 43 filters, which is an acceptable number.

The acquisition time is the sum of the low pass filter "dwell" time (the reciprocal of the LPF bandwidth) and the PLL "search" time which is typically five times this (assuming a noise bandwidth of 2 b and a maximum search rate of $\pi/10$ times the square of the noise bandwidth). Thus the total acquisition time is 12 milliseconds for the 1 KHz example.

The pilot power requirement at the aircraft depends on the CNR desired in the band-pass filter bandwidth. A CNR of 6 dB is adequate for low probabilities of "false alarm" and "miss" during detection. As seen from the link calculations presented previously, a pilot power of 20 watts produces 6 dB CNR in 1000 Hz when the spacecraft uses low gain antenna elements for full earth coverage.

In summary, a pilot power of 20 watts in the aircraft allows acquisition of the pilot signal by the spacecraft in 12 milliseconds, if the spacecraft uses low gain antenna elements for earth coverage.

It is to be noted that the full array gain is available after acquisition, so that voice channels (with bigger bandwidths) can be maintained with modest amounts of power.

5.3.3.3 COMMON VOICE SYSTEM ELEMENTS

In addition to the items listed previously, there are a number of voice modules common to the array as a whole, and mounted to the rear of the array within the body structure. These have been indicated in function in the previous discussion and may be listed here:

Summing and distribution equipment

Acquisition network

Connections

The total common package weighs 10 lb. and has negligible power demand.

5.4 TELEMETRY, TRACKING AND COMMAND

This subsystem is identical to that described in Section 4.4 for the VHF spacecraft, except of course for the details of the antenna installations. With the VHF STADAN compatible telemetry system that is proposed a single 40 inch dipole will suffice (again) but the precise location is a matter for detailed design. In this instance the voice frequency allocations are far away from the 148 MHz/136 MHz telemetry allocations, so that signal isolation is not a problem.

In the VHF system description, the possibility was mentioned of the employment of an S-band TT&C subsystem. Such a system, based upon the Goddard Range and Range-Rate Transponder, appears to be peculiarly appropriate in this application in that it would minimize the spacecraft frequency "spread." How significant this is a matter of conjecture.

5.5 ELECTRICAL POWER SUBSYSTEM

The total power demand existing aboard the spacecraft amounts to 607 watts. This allowance covers the requirements for

Voice communications	464 watts
Position location and data link	119 watts
Telemetry and command	14 watts
Attitude control	10 watts

This demand is to be met by a solar array-battery combination, and allowing for losses in the regulation system and for (20-hour) battery charge requirements, the total (illuminated) DC power level may be set at about 750 watts. It is to be noted that the charge rate has in fact to be greater than the "20-hour" rate in order to ensure proper charging.

At this power level the selection of an oriented solar array offers considerable weight and cost advantages, relative to the alternative of a "drum" array of the type selected previously. Furthermore, the large planar and opaque antenna assembly imposes some significant constraints upon freedom of design, so that the overall result is the layout that has been described in this section.

The 750 watts net DC power level is required of the array at the end of life - set at 5 years - in the most adverse illumination angle/solar "constant" combination, and corresponds to about 104 ft^2 of conventional single axis oriented monocrystalline silicon array. With present-day techniques such an array is to be had for about 0.8 lb/ft^2, including power collection, hinging and support.

In this application the requisite array area is provided in two 8 ft x 6-1/2 ft panels, hung outboard above and below the antenna array, with each panel having a single fold so as to meet total package constraints. With the arrangement that has been described each array half is driven in "pitch" to maintain sun lock, but orbit and hence vehicle tilt is not corrected in "roll/yaw" and the illumination angle can fall to about 66 .

The regulation/charge control system proposed is essentially similar to that of the VHF vehicle, except of course that the power level that has to be handled is considerably higher. Sufficient to note that the regulation/control block weighs about 26 pounds, and consumes 13 watts of DC power.

A battery block is provided for eclipse operation, and sufficient redundancy (15%) has been included to allow for operation of four out of the six voice channels (as well as all the other functions) under eclipse conditions even with 50% cell failure. In these circumstances the depth of discharge increases from a maximum of 50% to a maximum of 67%, to the eventual detriment of the cells which can provide reliable 5-year operation only when used to the lesser discharge level. 8 W-hr/lb nickel cadmium cells are employed, as for the VHF vehicle, and the total battery pack weight is 216 pounds, with a charge demand of 125 watts. Over much of the mission of course this power provision for battery charging is far more than required—there are about 88 dark periods per year with length varying sinusoidally and the charge provision is matched to the worst times, centered around the equinoxes. This situation provides a power margin at most times, that is enhanced at any time prior to the five year point by the amount of "degradation" allowance remaining.

5.6 ATTITUDE CONTROL SUBSYSTEM

Pitch axis attitude control is provided by use of a single momentum wheel, rotating in the orbital plane, and driven so as to provide closed loop vehicle pointing control via momentum exchange. Open loop commanded yaw and roll trimming is via attitude control thrusters, provided as part of the propulsion subsystem. This attitude control system has also to provide stability during the injection phase, following booster separation, when predictably large injection errors have to be removed and the target stations in orbit acquired.

A relatively complete analysis (as was performed for the VHF vehicle) has not been undertaken in this instance, but rather the subsystem is modelled upon previous detailed studies and implementations - TIROS M specifically so far as the latter is concerned.

The mechanical details of the subsystem have already been described in outline in Section 5.1 and 5.2.1, and the principles of operation closely parallel those described for

the VHF "spinner" system — the wheel conceptually replacing the spinning body, and the despun portion becoming relatively very large. The distribution of attitude control equipment between the spinning and despun portions remains essentially the same, and the weight of the various components is listed in Section 5.2.5.

An additional requirement in this case is that for the solor array to be separately driven to track the sun. This function is performed in closed loop, and the sensing/drive components total 22 pounds. Each half of the array is driven separately, so that in the event of drive failure half power would remain available.

5.7 SECONDARY PROPULSION SUBSYSTEM

The propulsion subsystem has essentially four functions:

(1) to remove booster injection errors

(2) to allow station acquisition

(3) to allow station-maintenance (in longitude only)

(4) to serve the attitude control subsystem demands

The spacecraft weight and volume are such as to allow the launch of two such vehicles in tandem on board a single Atlas-Centaur-Burner II booster (with certain qualifications). The injection error to be expected from this booster is about 150 ft/sec at the three sigma level, and a reasonable budget for subsequent station acquisition is 75 ft/sec. Adding in station maintenance (50 ft/sec for five years) and attitude control (50 ft/sec), a total velocity demand of 325 ft/sec emerges.

This demand has been rounded up to 350 ft/sec so as to allow a margin, and the clear selection at this velocity level and in this application (noting the approximate vehicle weight) is that of a hydrazine monopropellant system—as for the VHF vehicle.

In this instance the particular form of stabilization virtually dictates that the propulsion subsystem be mounted in the despun (earth locked) portion of the vehicle.

As a consequence 12 individual thrusters are required in order to provide proper roll/yaw and velocity control, with 100% redundancy, rather than the four thrusters required in the VHF system application. Further, the feed system can now no longer employ the spin motion for propellant collection, and tank bladders are required. Separate pressurization is provided and the subsystem block diagram is shown in Figure 5-11. The subsystem components themselves are substantially the same as those described for the VHF spacecraft, with the exceptions of the use of Mariner rather than Surveyor tanks, and the addition of the components peculiar to the nitrogen bottle system. In particular, the same thrust units are employed.

Some 39 pounds of propellant are required in order to meet the subsystem demands, and the details of the weight breakdown are given in Section 5.2.5.

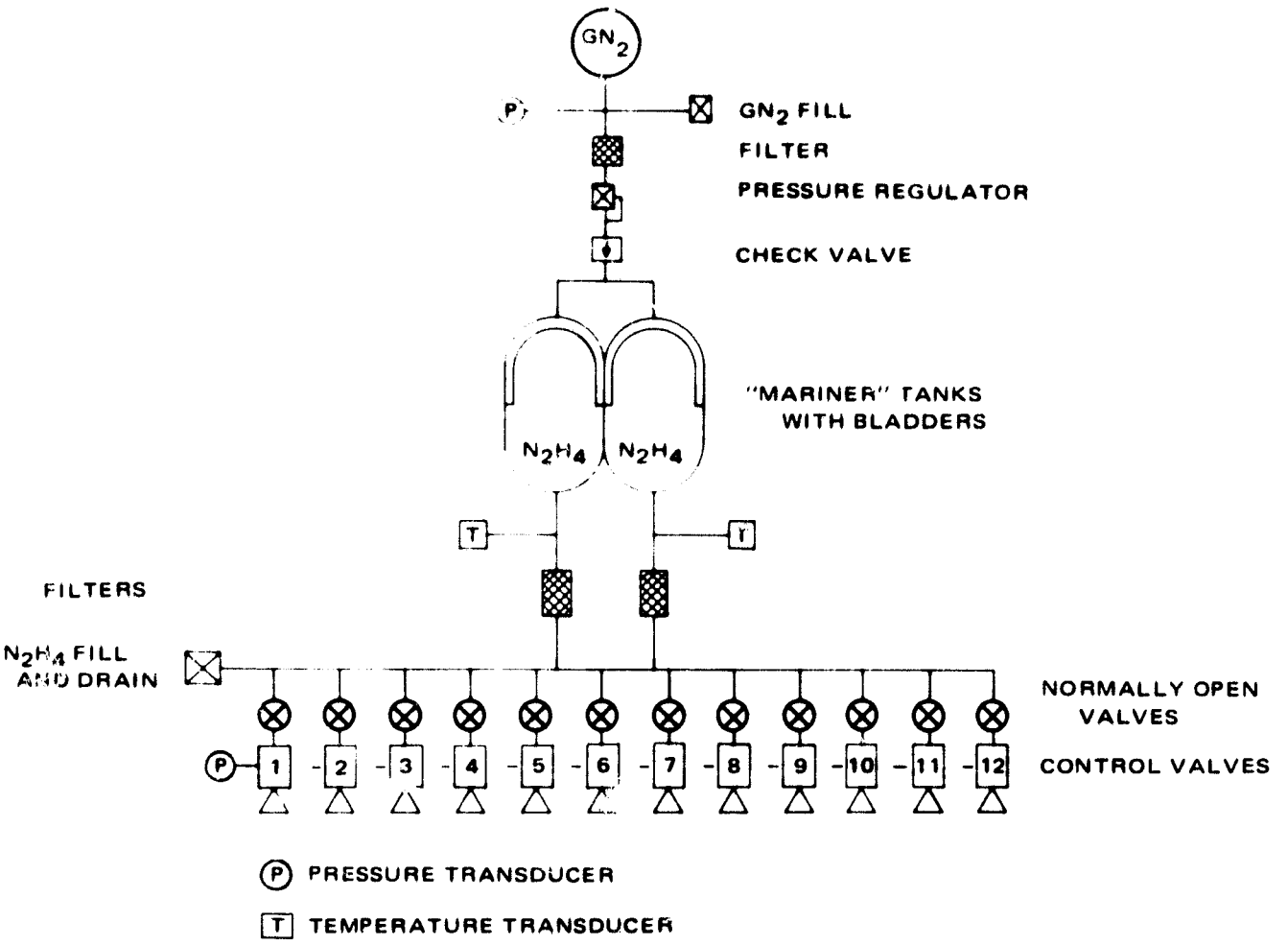

Figure 5-11. Propulsion Subsystem Schematic

5.8 SATELLITE REDUNDANCY AND REPLENISHMENT

5.8.1 SATELLITE LIFETIME

Examination of the analysis undertaken in Section 4.8 shows that much of the same data apply. Clearly, the telemetry and command, attitude control, and secondary propulsion subsystems are conceptually identical for both the VHF and UHF spacecraft, while the power supply in the latter case does suffer the complication of array orientation control. This complication is small in terms of failure probability, and has little effect on overall reliability—the drives show very low failure rate, and the drive control for sun tracking is extremely simple.

With regard to the position location function, the previous data apply exactly.

A major difference, however, does exist in the Voice subsystem. Given the retrodirective phased array with the features that have been described, the loss of elements of the array is not catastrophic (each element contributes 15/16th of the array gain and the same proportion of the RF power). The major source of voice system failure therefore has to be the common elements; the summing and distribution equipment and the acquisition network. These common functions are performed by equipment that is largely passive in operation, and is also sufficiently light as to allow for substantial and "cheap" redundancy. The conclusion is thus that the UHF voice system will be significantly more reliable than the VHF system, and that the total vehicle will correspondingly be more reliable also.

The discussion presented previously regarding the possibilities of graceful failure, and the desirability of selective redundancy (in the position location block in particular) remains applicable. However, the provision of such redundancy would undoubtedly force the employment of the stretched Burner II—this growth version is desirable any way so as to provide a performance margin.

5.8.2 REPAIR AND REPLENISHMENT

The discussion of Section 4.8.2 is applicable virtually in its entirety (although the field of "single spacecraft" boosters is narrowed solely to the Titan IIIB). On balance it appears best not to resort to different boosters for replenishment/repair and for system installation, and to use only the Atlas-Centaur-Burner II (now up-rated as discussed in Section 4.9.1).

5.9 DEPLOYMENT

5.9.1 BOOSTER DESCRIPTION

The spacecraft described in this section has an estimated weight of about 760 pounds. The addition of 10% margin (to include, for example, redundancy in the position location subsystem) lifts this to about 835 pounds so that the single launch of a two-spacecraft system requires a total (net) booster capability of 1670 pounds. With the Atlas-Centaur-Burner II stack the gross payload is subject to 50 pounds deduction for the Burner II adapter and 60 pounds deduction for the shroud "stretch" so that a gross capability for 1780 pounds is required.

The possibility for up-rating the current Burner II was discussed in Section 4.9.1. At 1960-lb propellant loading (rather than the standard 1440 lb), the total booster capability is increased from 1500 pounds to 1800 pounds and thus the UHF spacecraft can fly this booster.

5.9.2 INJECTION SEQUENCE

The injection sequence was fully described in Section 4.9.2, both for the standard and for the up-rated booster variants. Such variations as are implied by the differences in design of the UHF and VHF spacecraft occur only following spacecraft separation, and the UHF deployment sequence was shown in Figure 5-2. The basic attitude control subsystem provides stabilization during maneuver.

5.10 SPACE SEGMENT COSTS

5.10.1 SATELLITE AND BOOSTER COSTS

The cost breakdown by major subsystems of the spacecraft portion of the Nav/TC/Data/UHF Voice program is shown in Table 5-2. The total cost is estimated at $50 million. This sum allows for development, for the cost of construction of one prototype and four flight models, and for the launching of two of these. The provision of a second booster so as to allow use of all the flight vehicles would increase the total cost to $63 million.

The assumptions upon which this estimate is based are those of Section 4.10.

TABLE 5-2. SYSTEMS COSTS FOR NAV/TC/DATA/UHF VOICE SPACECRAFT

	DEVELOPMENT		PER COPY
Navigation/Traffic Control/Data Link	$ 250K		$ 220K
Voice Communications	2,500K		880K
Telemetry and Command	250K		100K
Power Supply	1,250K		1,600K
Attitude Control	750K		250K
Secondary Propulsion	500K		240K
Structure & Integration	750K		550K
Testing	1,250K		500K
Contingency	1,875K		1,085K
TOTAL	$9,375K		$5,425K
Total Cost for R&D, One Prototype Four Flight Models		$36,500K	
Booster Cost		$13,100K	
TOTAL INSTALLATION COST		$50M	

Section 6

THE GROUND SEGMENT

This section discusses the principal features of the ground segment required for the navigation and traffic control system. Most of the discussion relates to the ground Control Station. The functional requirements and corresponding block diagrams are described for two modes of operation, namely "passive" navigation and "active" traffic control. The number of control stations needed for North Atlantic coverage and Global coverage is also considered.

Two other types of ground stations are treated briefly. These are the Calibration Stations needed to determine the positions of the satellites, and the Auxiliary Stations which merely utilize the air traffic information.

Approximate cost estimates are given for the proposed ground stations, showing that they comprise a relatively minor portion of the overall system cost. Therefore, no attempt has been made to optimize the ground segment by using different configurations or conducting detailed tradeoff studies.

6.1 FUNCTIONAL DESCRIPTION OF CONTROL STATIONS

In the "passive" or navigation mode, the ground control station transmits an RF carrier which is modulated by "coarse" and "fine" tones. The signal is relayed to all users by both satellites, employing frequency-translation types of repeaters. The ground station monitors the satellite signal to obtain data on satellite status and satellite calibration; it receives no information about the users because they do not transmit any signal in the passive mode.

In the "active" or traffic control mode, the ground station wishes to know the positions of all users. This is accomplished by transmitting the navigation signals to users through one of the satellites, and requiring the users to transpond the signals back to the ground (via both satellites). Each user is identified by an address code, and systematic interrogation procedures are used to cover all users at regular intervals. In addition, provision is made for an emergency link between the ground and any user.

The ground station for the active mode requires all the equipment needed for the passive mode, plus the additional computers and hardware needed to determine and display the user positions.

It is of interest to note that the satellite equipment for the active mode differs from that of the passive mode to the extent that provision must be made to relay the signals in both forward (ground-user) and backward (user-ground) directions. The user equipment is also modified to include a transponder; moreover, the user's on-board position-fixing equipment can be eliminated, because he can receive this information from the

ground station computer via the satellite, along with the navigation tones and interrogation signals. (A discussion of the user equipment is pertinent because the satellite tracking or trilateration station consists of this equipment as discussed later.)

The "combined" mode of operation allows both passive and active modes, and requires no change in the ground station equipment compared to the active mode. (The satellite equipment is also unchanged from that for the active mode, but the user hardware must be augmented to combine the active mode transponder with the passive mode on-board position-fixing equipment.)

6.2 CONTROL STATION CONFIGURATION

6.2.1 PASSIVE MODE, CIRCULAR

As described above, the ground station transmits a modulated carrier to each of two satellites, and monitors the signal broadcast by each satellite. The configuration is shown in the block diagram of Figure 6-1. A highly stable frequency source (e.g. an atomic standard) is used to generate the coarse and fine ranging tones; it is also used to synthesize the different carrier frequencies, thus insuring phase coherence between them.

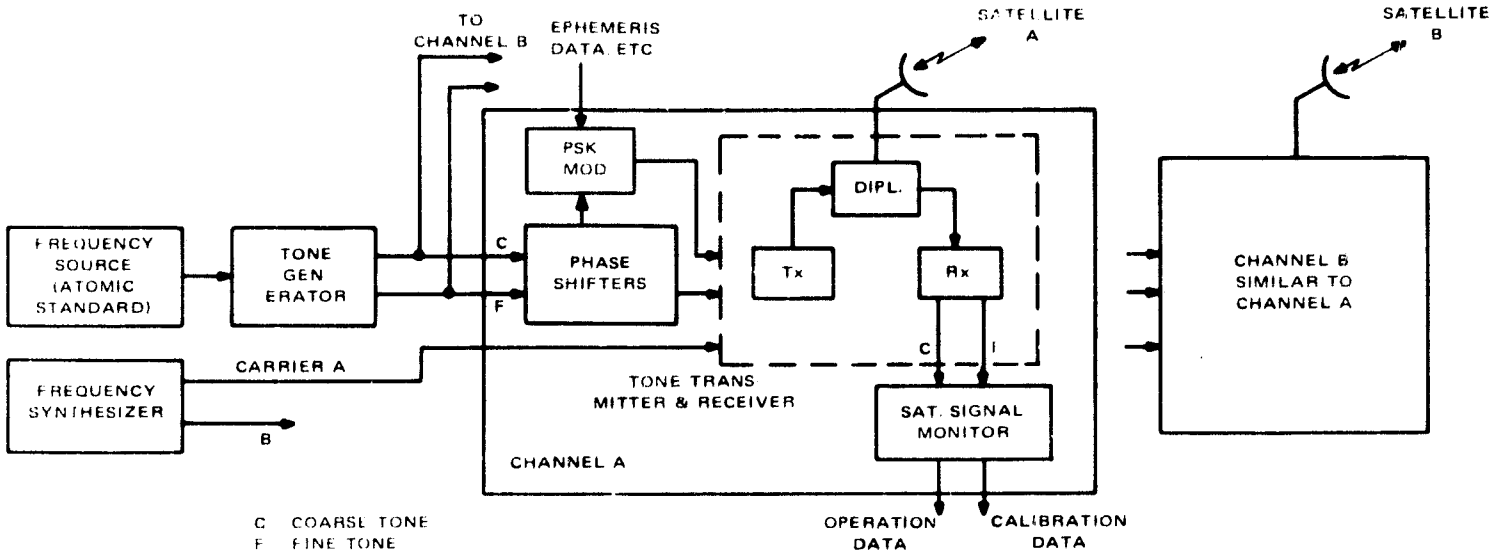

Figure 6-1. Control Station, Passive Mode, Circular Method (Two Channels)

The tones can be phase-shifted to provide synchronization with other signals, if desired. The tones are summed and used to phase modulate the carrier; the modulated carrier is amplified and applied to the diplexer, as shown in Figure 6-2.

The signal received from each satellite is demodulated as shown in Figure 6-3. The phase-angles of the coarse and fine tones provide information about the satellite positions and can be used to track the satellites in conjuction with other stations.

Important parameters of the equipment needed at the ground for passive navigation are listed in Table 6-1. It should be noted that the values indicated for transmitter power and receiver bandwidth are actually for the active mode, and are therefore more liberal than those needed for the passive mode.

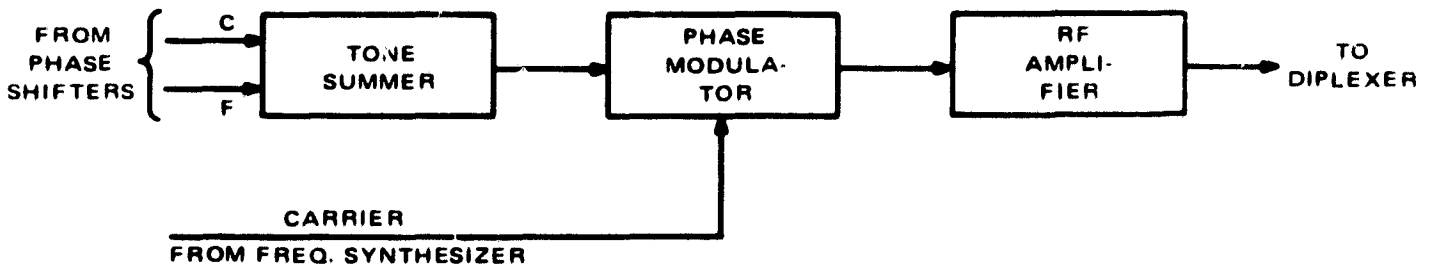

Figure 6-2. Control Station Tone Transmitter

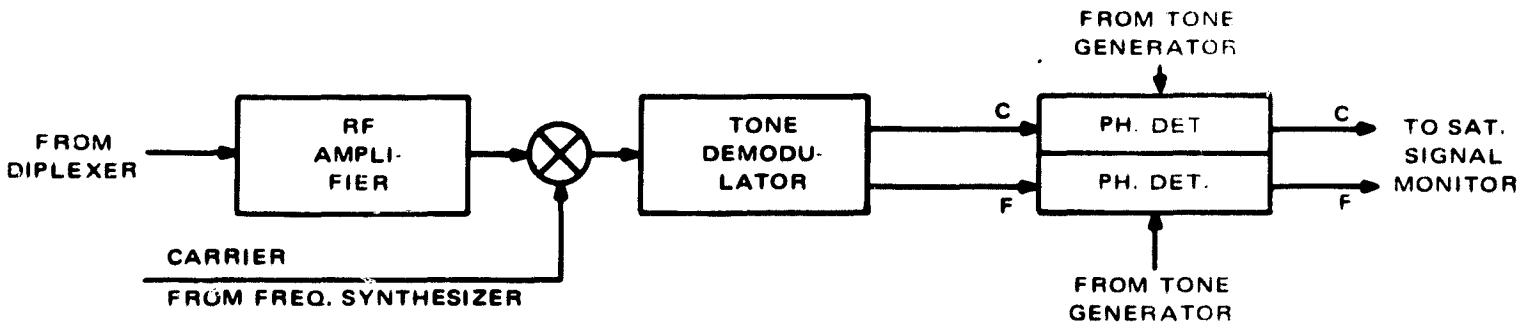

Figure 6-3. Control Station Receiver

TABLE 6-1. GROUND STATION PARAMETERS

Frequency	1600 MHz
Transmitter power	5 W
Antenna gain	37 dB
diameter	18 ft.
beamwidth	2.5 degrees
Receiver type	Multichannel, phase lock loop receiver
noise figure	5 dB
bandwidth	100 KHz per channel
Tone Source Stability	3 parts in 10^{11} (short term)
	1 part in 10^{10} (long term)

6.2.2 ACTIVE MODE

It was pointed out in the functional description that the active mode ground station requires all the passive mode equipment (to enable the user to make a position fix), plus the computers needed to determine the user position, and the equipment to display and monitor it. The resulting ground station configuration is shown in Figure 6-4.

The Control Channel of Figure 6-4 is the key to "active" mode operation. In its simplest form it contains a synchronization signal, and a coded address followed by a command for a particular user transponder to return a burst of the received tones as well as other data. This data must include user identity and altitude, and may include additional information like meteorological data. A two-way telemetry or voice link may also form a part of the control link.

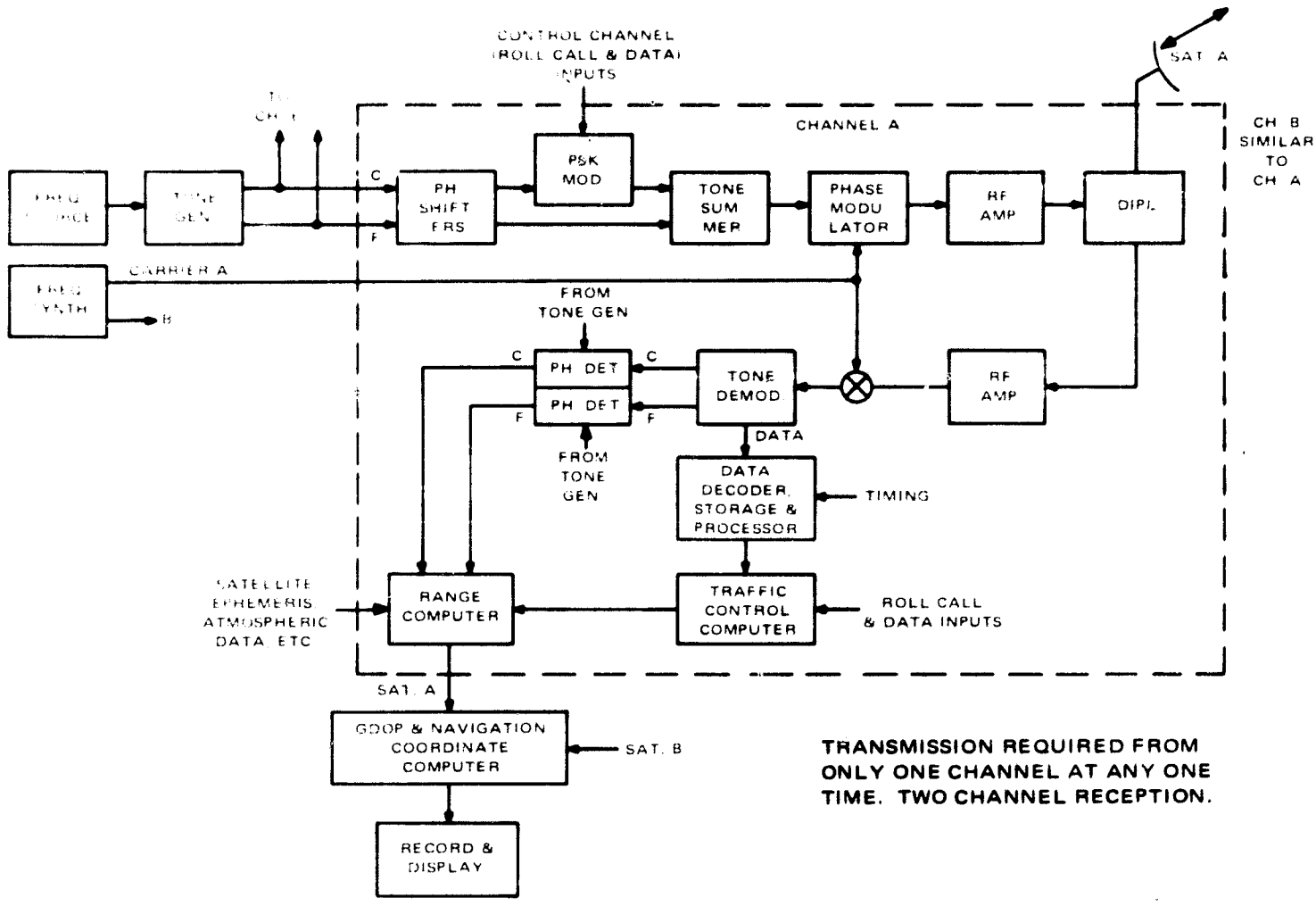

Figure 6-4. Control Station, Active Mode, Using Two Channels

The computer and display equipment must be large enough to handle the predicted traffic density, which is summarized in Table 6-2. It is expected that a small computer with a memory of about 32,000 words will suffice in the initial stages of system growth.

TABLE 6-2. PEAK TRAFFIC DENSITY FOR NORTH ATLANTIC

	1975	1980
Peak Number of Aircraft	190	225
Peak Air Traffic Fixes/Hour	1400	1800

6.2.3 COMBINED PASSIVE AND ACTIVE MODES

It was explained in the functional description that this mode requires no change in ground equipment compared with that for the active mode.

6.3 NUMBER OF CONTROL STATIONS

For North Atlantic coverage in both passive and active modes, only one ground control station is needed with two satellites in synchronous equatorial orbit. To expand the service to worldwide coverage, the system requires additional ground stations as well as satellites, and the problem of synchronization (for passive navigation) becomes more complex.

One plan for global coverage between 70°N and 70°S latitude requires 3 ground control stations (one master and two slaves with respect to time synchronization) along the equator to supply the ranging signals to six equally-spaced satellites in synchronous equatorial orbit. The number of satellites is dictated by the constraint that a user anywhere on earth must be able to see at least two satellites.

6.4 SATELLITE TRACKING OR TRILATERATION STATIONS

In addition to control stations, the ground system needs trilateration stations in order to track the satellites and determine their locations accurately. This function is an essential part of the system requirements, because the accuracy of the user's position-fix depends on the accuracy to which the satellite locations are known.

One method of implementing this station would be to have a facility with tracking, ranging and communication capabilities. The station would then determine the range of each satellite and supply this information to the control station. On the basis of such information received from several stations of known position, the control station could then compute the satellite positions.

A simpler method of implementation is to use the tracking stations simply as transponders which return the ranging signals received from the control station back to the latter, using the satellite as a relay in each direction. With this method, each "trilateration" station is simply a "user" of known position and enhanced capability - e.g., high power and antenna gain and a more sensitive receiver. No computer or display facilities are needed in the trilateration station. The ground station determines the satellite positions by computing their distances from various trilateration stations on the basis of the transponder signals.

A simplified diagram of this station is shown in Figure 6-5 and is self explanatory. At least three such stations are needed for North Atlantic coverage. The locations should be chosen to maximize the triangulation accuracy, subject to operational and logistic considerations. Figure 6-6 shows a reasonable deployment of ground stations for the North Atlantic System including the location of the trilateration stations.

For this configuration, it is convenient to have the trilateration stations located at the Ground Control (GC) sites. In Figure 6-6, GC 2 is an auxiliary control station which serves as a traffic control communications terminal for Europe.

6.5 AUXILIARY CONTROL STATIONS

These stations utilize the traffic control information generated by the control station and serve as communication terminals. Basically, an auxiliary station resembles a Ground Control Center with related display equipment. It should be able to function as a back-up control center in the event the primary GCC experiences technical difficulties. The communication link between the control station and the auxiliary station may be achieved via the satellites or other existing commercial channels. For North Atlantic coverage one auxiliary station on the West Coast of Europe (e.g. west of Paris) would suffice. For global coverage a few such stations would be needed, especially in regions where the lack of international communication facilities - or unfavorable political factors - may be the over-riding consideration.

6.6 COST OF THE GROUND SEGMENT

The ground segment consists of the control, trilateration and auxiliary stations with the functions and equipment described above. The cost estimates of various subsystems are shown in Table 6-3, leading to Nav/TC equipment costs of about $1 million for the Control Station and $30,000 for each trilateration station. An adequate display complex for the traffic control center could add $500,000 to $1 million extra to these costs.

The North Atlantic system requires a control station on the East Coast of USA, an auxiliary station in Western Europe, and three trilateration stations located as shown in Figure 6-6. The total estimated cost without displays is seen from Table 6-4 to be of the order of $4 million, of which $2.1 million is equipment and the remainder facilities.

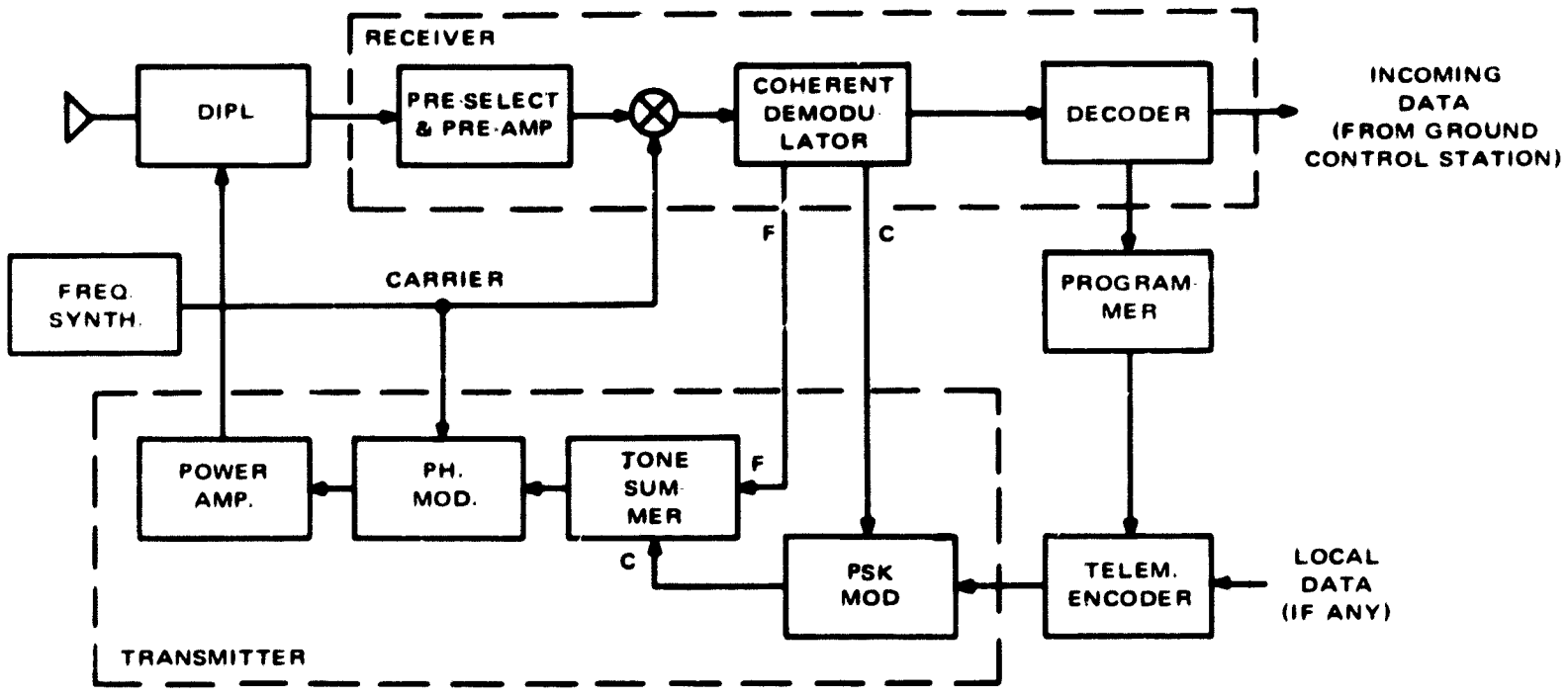

Figure 6-5. Trilateration Station

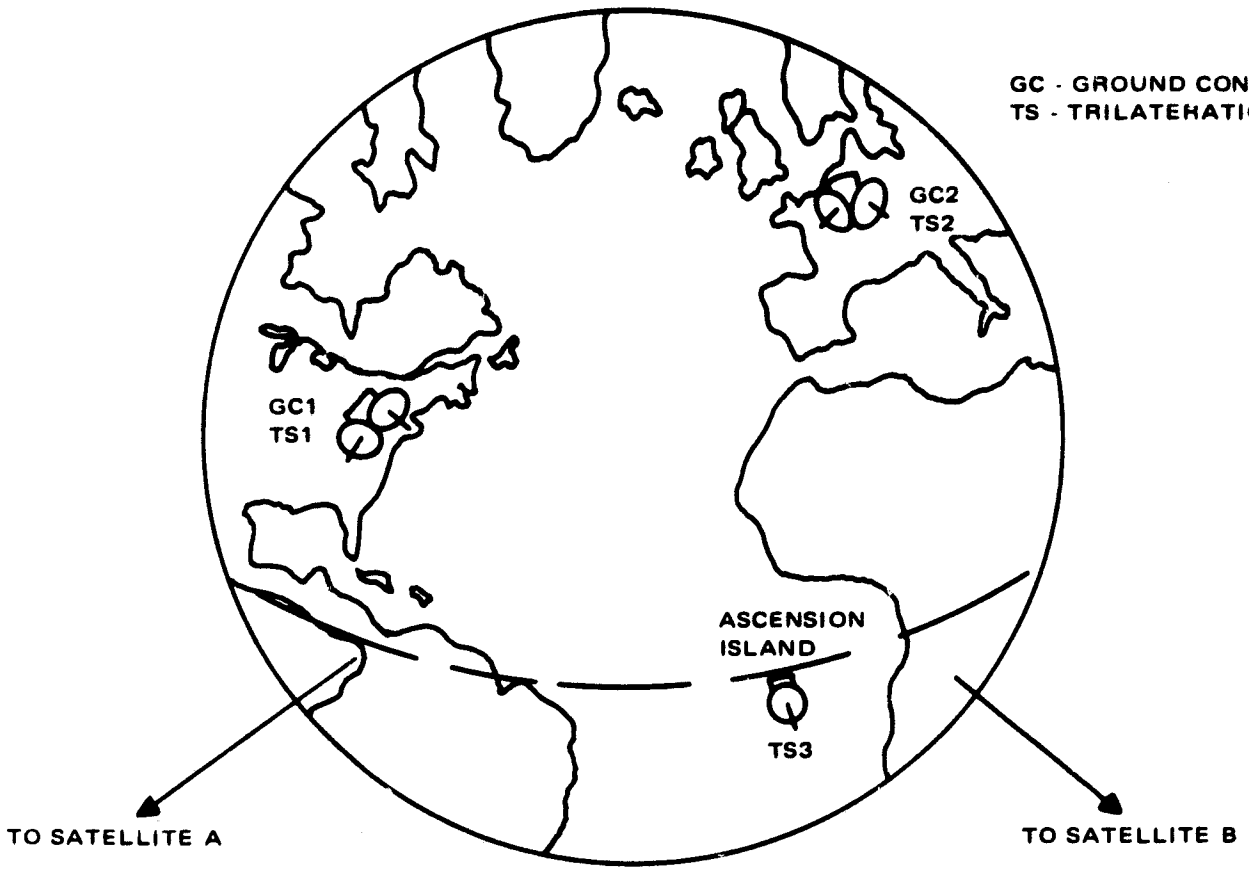

Figure 6-6. Ground System Location

TABLE 6-3. GROUND SUBSYSTEM COSTS

	Cost/Item ($ Thous.)	No. of Units Req'd	Total Cost ($ Thous.)
Control Station			
Antennas (L-band 18 ft. Dia. Parabolic)	150	2	300
Atomic Clock	15-25	1	20
Transmitter (Nav. Signals)	15-25	2	50
Receiver (Nav. Signals)	25-45	2	90
Signal Processors (Nav. Signals)	20-30	2	60
Computer Complex	200-300	1	300
Transmitter (Voice - 12 channels)	80-100	1	100
Receivers (Voice - 12 channels)	60-80	1	80
	* TOTAL		1000
Trilateration Station			
Antenna (L-band, 10 dB)	10	1	10
Transponder	20	1	20
	* TOTAL		30

* Does not include Display Complex or Building Facilities

TABLE 6-4. GROUND STATION COSTS

	No. Required	Total Cost ($ Thous.)
Ground Control Center Equip.	1	$1,000
Auxiliary Station (Backup GCC) Equipment	1	1,000
Trilateration Stations Equipment	3	100
Facilities (Buildings, etc.)		1,900
	TOTAL	$4,000

The total cost of the ground segment is found to be a small fraction of the overall system cost (including the space segment and the launch vehicles). Therefore, no effort has been made to define it more accurately or minimize it by using alternative approaches at this stage of the study. However, such an effort will be necessary for a detailed evaluation of efficient ways of utilizing the massive amounts of data generated by a Nav/TC system of this type. It is recommended that future studies apply some effort to the solution of this problem.

6.7 RF ANALYSIS FOR LINKS BETWEEN CONTROL CENTER AND SATELLITES

6.7.1 ENVIRONMENTAL AND FUNCTIONAL LIMITATIONS

The practical frequency range for earth-to-satellite communications/navigation lies between 1 GHz and 10 GHz.

The lower limit based on natural phenomena, and is determined primarily by the range error due to refraction (inversely related to the square of the frequency), the multipath, and the solar noise. The higher limit is primarily set by the atmospheric attenuation, due to oxygen, water vapor, and precipitation (rain), by precipitation (rain and snow) on the radome (if used) over the ground control center antenna, and path loss (a direct function of the square of the operating frequency).

In a previous report[1] for NASA, in which the effect of refraction error was fairly well analyzed, the results indicated an ionospheric range error of approximately 85 feet for a carrier frequency of 1.6 GHz (at an elevation angle of 10°, a total electron count of 10^{18}, and with correction assumed). The ground position error due to this range error is $3\sqrt{2} \times 85 = 360.6$ ft., under conditions of worst geometric dilution.

The ground position error at any other frequency is approximately given by the relationship

$$g = \frac{360.6}{\left(\frac{f_{GHz}}{1.6}\right)^2}$$

The minimum frequency for a ground position error of 0.1 nautical mile (607.2 feet) is thus:

$$f_{GHz} = 1.233 \text{ GHz}$$

It is apparent that multipath problems should not be a primary cause for carrier frequency selection since in general, the beamwidth of the control center antenna is around 2 to 3 degrees, while the minimum elevation angle to the satellite from that center is about 15°.

The upper frequency limit due to natural causes is determined primarily by the atmospheric attenuation A_a which consists of 3 parts, the attenuation due to gas A_g (oxygen and water vapor), the attenuation due to clouds and fog A_c, and the attenuation due to precipitation (rain) A_p. The discussion and computation of these parameters for a frequency range 4 GHz to 8 GHz is shown in Appendix 6.7-A. An abridgement of Table 4 from the same appendix is shown in Table 6-5.

---

(1) Final Report, Phase Difference Navigation Satellite Study, Dec. 1967, RCA DEP-SEER, Moorestown, N.J., Figure 6-39, p. II-6-78.

TABLE 6-5. ATMOSPHERIC ATTENUATION (A_a) AS A FUNCTION OF FREQUENCY

Frequency (GHz)	A_a (dB)
4	0.41
5	0.82
6	1.33
7	1.97
8	2.82

If the attenuation level threshold is nominally set at 2 dB then 7 GHz is the corresponding upper frequency.

In summary, the frequency limits due to natural causes are 1.2 GHz to 7.0 GHz.

6.7.2 EQUIPMENT LIMITATIONS

6.7.2.1 SATELLITE EQUIPMENT

Transmitter Output Stage - This equipment presents no apparent further restriction to the frequency range of 1.2 to 7 GHz obtained in the previous section. Feldman[2] indicates that the frequency crossover point between solid-state devices and traveling-wave tubes at an output power level of 10 watts is about 1.7 GHz (equal efficiency at 20°C, near future) with the higher frequencies being favored by the TWT. However, TWT's have shown to have good reliability in quite a few space applications so that the risk factor for the mid-1970's is quite small.

Antenna - Since the antenna size varies directly as the (RF frequency)^2, the lower limit, i.e. 1.2 GHz will set the maximum size required.

Elsewhere it is shown that a 31 inch diameter dish provides proper coverage at 1.6 GHz, so that at 1.2 GHz a 41 inch dish is required.

This is only a modest increase in size.

Receiver Noise Figure - The receiver noise figure, at 7 GHz can be maintained at 5 dB by the incorporation of a low noise tunnel-diode or parametric amplifier so that no problem is anticipated here.

---

(2) N. E. Feldman, "Communication Satellite Output Devices, Parts 1 and 2", November 1965 and December 1965, The Microwave Journal

(3) For a constant area illumination.

6.7.2.2 CONTROL CENTER EQUIPMENT

Transmitter Output Stage - The 5-watt (1 nautical mile position error) or 10-watt (0.1 nmi position error) requirement on the output power presents no critical burden over the 1.2 GHz to 7 GHz frequency range. These devices are expected to be TWT's that exist today.

Antenna - By maintaining a diameter of 18 feet as specified in the 1.6 GHz link analysis, the changes in path loss due to frequency will exactly be compensated for by the change in antenna gain as a function of frequency. Therefore, the antenna presents no serious problem.

Receiver Noise Figure - A glance at the 1.6 GHz link analysis indicates that the bulk of the system noise is that received from the satellite link and not from the control center receiver. In fact, the receiver noise figure could approach 14 dB before any increase in system would be noted. Therefore, this also presents no problem.

6.7.3 SUMMARY

In conclusion, it appears that the factors limiting the R.F. frequency range between the satellite and the control center are those that occur naturally. That is, refraction at the low frequency end and atmospheric attenuation at the high frequency end. The preferred frequency band for this link lies between 1.2 to 7 GHz.

Appendix 2.2.2.1-A

EFFECTIVE SYSTEM NOISE BANDWIDTH

Path	Location	Bandwidth (KHz)
Forward	Satellite	130
Forward	User	160
Backward	Satellite	130
Backward	Control Center	200

From Appendix 4.1.5-A in Volume II,

$$\frac{1}{B_{eq}^2} \quad \sum_{i=1}^{n} \left(\frac{1}{B_i}\right)^2$$

Where:

B_{eq} = Effective System Bandwidth (in KHz)

$B_{i's}$ = Bandwidths at the above locations (in kHz)

$$\frac{1}{B_{eq}^2} = \left(\frac{1}{130}\right)^2 + \left(\frac{1}{160}\right)^2 + \left(\frac{1}{130}\right)^2 + \left(\frac{1}{200}\right)^2$$

$$= \frac{1}{1.69 \times 10^4} + \frac{1}{2.56 \times 10^4} + \frac{1}{1.69 \times 10^4} + \frac{1}{4.0 \times 10^4}$$

$$= 2 \times 5.92 \times 10^{-5} + 3.91 \times 10^{-5} + 2.50 \times 10^{-5}$$

$$= 18.25 \times 10^{-5} = 0.1825 \times 10^{-3}$$

$$B_{eq}^2 = 54.794 \times 10^2$$

B_{eq} = 74.0 kHz.

Appendix 2.2.3.3-A

SIGNAL-TO-NOISE RATIO OF AMBIGUITY TONES

The signal-to-noise ratio S/N required to resolve a finer frequency tone in a fraction of a cycle of a coarser frequency tone of ratio m, (fine/coarse) and a specific accuracy k σ is given by:

$$\frac{\pi}{m} = \frac{K}{\sqrt{2\frac{S}{n}}}$$

i.e.,

$$\frac{S}{n} = \frac{1}{2}\left(\frac{Km}{\pi}\right)^2$$

or

$$\left(\frac{S}{n}\right)_{dB} = 20 \log \frac{Km}{\pi} - 3 \text{ dB}$$

A plot of this expression for K = 1, 2, 3 and m = 2, 4, 8, 16, 32 is shown in Figure 1. It is to be noted that the expression is no longer valid for S/n less than 7 dB (threshold).

This signal-to-noise does not include the effect of instrumentation error, θ_i. An analysis of the increase in signal to noise required over that shown in Figure 1 is given below.

The phase angle required by the ambiguity tone is:

$$\theta_a = \frac{\pi}{mK} \text{ (all constants are given above).}$$

Letting the instrumentation error be θ_i, the resulting phase angle from the two independent sources θ is given by:

$$\theta = \sqrt{\theta_a^{\,2} + \theta_i^{\,2}}$$

The increase in signal-to-noise because of the instrumentation error is:

$$\Delta\frac{S}{n} = \left(\frac{\theta}{\theta_a}\right)^2$$

$$\Delta \frac{S}{n} = 1 + \left(\frac{\theta_i}{\theta_a} \right)^2 \quad (\theta_i \text{ in radians})$$

$$\Delta \frac{S}{n} = 1 + \left(\frac{\theta_i \frac{2\pi}{360}}{\frac{\pi}{mK}} \right)^2 \quad (\theta_i \text{ in degrees})$$

$$= 1 + \left(\frac{\theta_i}{180} \, mK \right)^2$$

e.g., let $\theta_i = 3°$, m = 16 and K = 3

$$\Delta \frac{S}{n} = 1.64 = 2.1 \text{ dB}$$

A glance at Figure 1 for m = 16 and K = 3σ indicates an S/n of 20.6 dB. Therefore, the final signal to noise ratio is 20.6 + 2.1 = 22.7 dB.

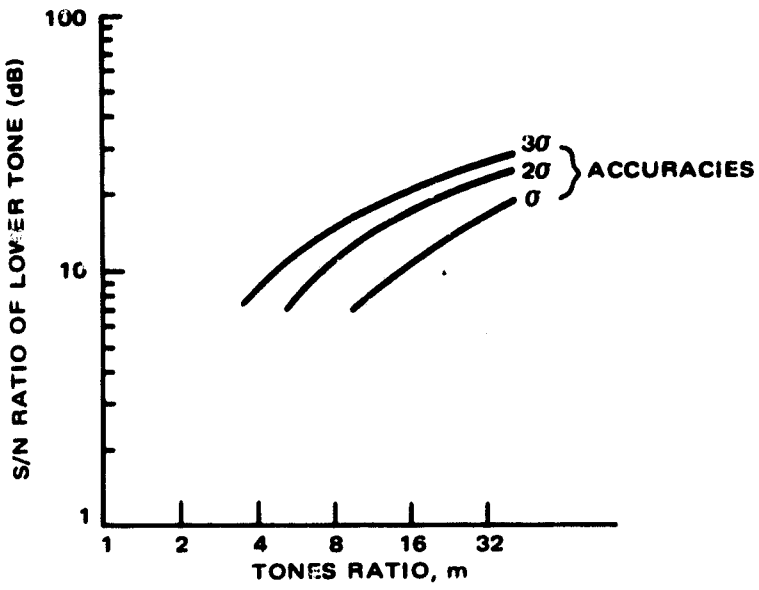

Figure 1. Signal-to-Noise of Lower Tone For Specific Tone Ratios and Accuracies

Appendix 2.2.3.3-B

MEAN TIME TO UNLOCK

From Gardner[1]

$$T_a = \frac{2}{\omega_n} e^{\left[\pi (SNR)_L\right]}$$

where:

T_a = The mean time to unlock

ω_n = The natural loop frequency

$(SNR)_L$ = The signal-to-noise ratio in the loop

But,

$\omega_n = 1.06\ B_n$ for 2nd order loops with damping factor $\zeta = 0.707$

where:

B_n = The noise bandwidth

$$\therefore T_a = \frac{2}{1.06\ B_n} e^{\left[\pi (SNR)_L\right]}$$ (See following table.)

T_a for Various noise bandwidths (B_n) and $(SNR)_L$

$(SNR)_L$ (dB)	B_n = 10 Hz	B_n = 25 Hz	B_n = 100 Hz
1	16.8 Hrs.	6.72 Hrs.	4.2 minutes
7	16.28 days	6.51 days	1.63 days
8	2.65 years	1.06 years	96.69 days
9	552.37 years	220.95 years	55.24 years
10	296,000 years	118,000 years	29,600 years
The values in the table are the respective T_a's.			

(1) F.M. Gardner, Phaselock Techniques, John Wiley & Sons, 1966, Eq. (3-18) on p. 25.

Appendix 2.2.3.3-C

MODULATION INDEX FOR 2-TONE RANGING

The rms range error corresponding to the 3/4 nmi ground range error due to the signal-to-noise is

$$\sigma_R = \frac{3/4}{3\sqrt{2}} = 0.177 \text{ nmi}$$

Now, a wavelength of an 8 kHz tone is:

$$\lambda = \frac{161,740}{8,000} = 20.217 \text{ nmi}$$

Therefore, σ_θ, the rms angular error is:

$$\sigma_\theta = \frac{2 \times \sigma_R}{\lambda} \times 360^\circ = \frac{2 \times 0.177 \times 360}{20.217}$$

$$= 0.354 \times 17.81$$

$$\sigma_\theta = 6.303^\circ$$

This σ_θ can be considered to be composed of two parts; one part the rms instrumentation error which will be assumed to be 3 degrees, and the remainder that due to the signal-to-noise $\sigma_{S/N}$,

$$\sigma_{S/N} = \sqrt{(6.303)^2 - (3)^2}$$

$$\sigma_{S/N} = 5.54^\circ = 0.0967 \text{ radian}$$

Now:

$$\sigma_{S/N} = \frac{1}{\sqrt{2\ S/N}} = 0.0967$$

therefore,

$$S/N = 53.42 = 17.3 \text{ dB}$$

Modulation Index

We see from the above analysis that the fine tone signal-to-noise ratio, $(S/N)_f = 17.3$ dB. This S/N occurs in a 1-Hz bandwidth so that $(S/N_O)_f = 17.3$ dB also. However,

the noise spectral density about the fine tone is about 2 times that about the carrier because of the turn-around of the demodulated noise at the user (See Link Analysis). Therefore, let S/N_O = 20.3 dB (N_O is same as carrier N_O).

Appendix 2.2.3.3-D shows that the coarse tone signal-to-noise density ratio, $(S/N_O)C$ = 29.5 dB. Finally, it has been shown in Appendix 2.2.3.3-B that the mean time to unlock (carrier unlock) is vanishingly small for a carrier-to-noise ratio of 7 dB or greater in a noise bandwidth of 100 hertz or less. Therefore, let the carrier to noise density ratio, C/N_O = 27.0 dB.

In tabular form we have:**

$$C/N_o = 27.0 \text{ dB} = 500$$

$$(S/N_o)_C = 29.5 \text{ dB} = 890$$

$$(S/N_o)_f = 20.3 \text{ dB} = 108$$

Now, Kronmiller* and Baghdady show that the waveform of an M-signal phase modulated carrier can be represented by:

$$e_{PM}(t) \approx C_o \cos \left[\omega_c t + \phi_c\right]$$

$$+ \sum_{i=1}^{M} C_i \left\{ \cos \left[(\omega_c + \omega_i) t + \phi_c + \phi_i \right] - \cos \left[(\omega_c - \omega_i) t + \phi_c - \phi_i \right] \right.$$

+ (smaller intermodulation terms)

where the amplitude of the spectral terms are given by;

$$C_o = \sum_{j=1}^{M} J_o (k_j)$$

$$C_i = J_1 (k_i) \left[\sum_{\substack{j=1 \\ j \neq i}}^{M} \right] J_c (k_j)$$

Therefore, the power in the carrier is C_o^2, while that in the i^{th} tone is 2 C_i^2 (includes both sidebands).

---

*"The Goddard Range and Range Rate Tracking System: Concept, Design and Performance," G. C. Kronmiller, Jr., NASA/Goddard Space Flight Center, Greenbelt, Maryland and E. J. Baghdady, ADCOM, Inc., Cambridge, Mass.

**The various signal/noise ratios stated result in a near simultaneous threshold for all, that is for a 4 db loss in signal power the carrier loop is about ready to unlock, the word-error rate is about one per message, and the ground position error increases by 10% to a value of 1.1 n. mi.

For two-tone modulation

$$C_o^2 = \left[J_o(k_1)\, J_o(k_2)\right]^2$$

and

$$2C_1^2 = 2\left[J_1(k_1)\, J_o(k_2)\right]^2$$

$$2C_2^2 = 2\left[J_1(k_2)\, J_o(k_1)\right]^2$$

Letting:

$k_1 = B_f$ = the fine-tone modulation index,

and

$k_2 = B_C$ = the coarse-tone modulation index

we have:

$$C_o^2 = \left[J_o(B_f)\, J_o(B_C)\right]^2$$

$$2C_f^2 = 2\left[J_1(B_f)\, J_o(B_C)\right]^2$$

$$2C_C^2 = 2\left[J_1(B_C)\, J_o(B_f)\right]^2$$

Now the ratio of power in the coarse tone to the power in the carrier is:

$$\frac{\left(\frac{S}{n_o}\right)_C}{\frac{C}{n_o}} = \frac{890}{500} = \frac{2C_C^2}{C_o^2} = \frac{2\, J_1^2(B_C)\, J_o^2(B_f)}{J_o^2(B_f)\, J_o^2(B_C)} = 2\,\frac{J_1^2(B_C)}{J_p^2(B_C)}$$

Therefore:

$$\frac{J_1(B_C)}{J_o(B_C)} = \sqrt{(1/2)\,(890/500)} = 0.943.$$

The smallest B with the above ratio is, $\underline{B_C = 1.40}$.

Likewise:

$$\frac{(S/n_o)_f}{\frac{C}{n_o}} = \frac{108}{500} = \frac{2C_f^2}{C_o^2} = \frac{2\,J_1^2(B_f)\,J_o^2(B_C)}{J_o^2(B_f)\,J_o^2(B_C)} = 2\,\frac{J_1^2(B_f)}{J_o^2(B_C)}$$

$$\frac{J_1(B_f)}{J_o(B_f)} = \sqrt{1/2\,\frac{108}{500}} = 0.33$$

The smallest B with the above ratio is, $B_f = 0.65$.

Power Levels of the Various Signal Components

The normalized power in the carrier component P_C is expressed by the factor C_o^2. For $B_f = 0.65$, and $B_C = 1.40$;

$$P_C = C_o^2 = \left[J_o\,(0.65\,J_o\,(1.40)\right]^2$$

$$P_C = \left[(0.8971) \times (0.5669)\right]^2$$

$$P_C = 0.259 = -5.9\ \text{dB}.$$

Similarly, the normalized power in the coarse tone P_{TC}, and that in the fine tone P_{TC}, are expressed as:

$$P_{TC} = 2C_C^2 = 2\,\left[J_1\,(1.40)\,J_o\,(0.65)\right]^2$$

$$P_{TC} = 2\,(0.5419 \times 0.8971)^2$$

$$P_{TC} = 0.473 = -3.2\ \text{dB}.$$

and;

$$P_{Tf} = 2C_f^2 = 2\,\left[J_1\,(0.65)\,J_o\,(1.40)\right]^2$$

$$P_{Tf} = 2\,(0.3081 \times 0.5669)^2$$

$$P_{Tf} = 0.061 = -12.1\ \text{dB}.$$

Summing up,

$$\left.\begin{aligned} P_C &= -5.9\ \text{dB} \\ P_{TC} &= -3.2\ \text{dB} \\ P_{Tf} &= -12.1\ \text{dB} \end{aligned}\right\}$$ with respect to the total RF power.

Appendix 2.2.3.3-D

DATA LINK BIT-ERROR PROBABILITY

Assume that all 200 bits of the message are equally important and that the message consists of 20 10-bit words with 1 bit of each word as a parity check. It is further assumed that an incorrect word (2 or more bits in error) will occur on the average, no more than once in every 10,000 messages, i.e., once every 500 hours, for a SST with 3 minutes between messages.

Let P_B = the bit error probability.

Now, the probability of any word, of a message, being in error is,

$$\binom{20}{1}\binom{10}{1} P_B = 200\, P_B,$$

(since there are 20 words per message and 10 bits per word). Now the probability of a second bit error in the specific word is,

$$\binom{9}{1} P_B = 9\, P_B$$

(since there are only 9 bits remaining after the incorrect bit).

Therefore, the incorrect word probability, P_W, is the product of the two mutually exclusive probabilities, i.e.,

$$P_W = \binom{20}{1}\binom{10}{1} P_B \times \binom{9}{1} P_B = 1800\, P_B^2 = 10^{-4}$$

$$\therefore P_B = 2.36 \times 10^{-4}.$$

If differentially coherent phase-shift keyed binary data is incorporated, then

$$P_B = 1/2\, e^{-E/N_o} = 2.36 \times 10^{-4}$$

where:

E = signal energy

N_o = one-sided noise spectral density

E/N_o = 7.65 = 8.9 dB

Since $\tau = 1/200$ bits/2 seconds $= 10^{-2}$ sec

$$\frac{E}{N_o} = \frac{S\tau}{N_o}, \text{ or } \frac{S}{N_o} = \frac{1}{\tau} \frac{E}{N_o}$$

i.e.,

$$\frac{S}{N_o} = 8.9 + 20 = 28.9 \text{ dB-Hz.}$$

However, since there is a slight loss,[1] when using realizable filters as opposed to a matched filter, e.g., 0.6 dB, the final S/N_o is 29.5 dB-Hz.

[1] M. Schwartz, Information Transmission, Modulation, and Noise, McGraw-Hill, 1959, p. 289.

Appendix 2.2.3.4-A

DIGITAL CODE MODULATION CALCULATIONS (Code, Data, Carrier, Power Division in a 5-Element Digital Ranging System)

1. Phase Modulation Indices

Foley[1] et. al. have shown that the optimum power division between a square-wave subcarrier (ranging code stream) and a sine-wave subcarrier (data subcarrier) is;

$$1) \quad \frac{P_D}{P_S} = \frac{\pi^2}{4} \frac{J_1^2(B_D)\cos^2(B_c)}{J_o^2(B_D)\sin^2(B_c)} = \underbrace{29.5 \text{ dB} - 28.8 \text{ dB} = 0.7 \text{ dB} = 1.18}_{\text{from Section 2.2.3.4.1 of this volume}}$$

While the power division between the square-wave subcarrier (ranging code stream) and the carrier is;

$$2) \quad \frac{P_S}{P_C} = \frac{8}{\pi^2} \frac{\sin^2(B_c)}{\cos^2(B_c)} = \underbrace{28.8 \text{ dB} - 27.0 \text{ dB} = 1.8 \text{ dB} = 1.52}_{\text{from Section 2.2.3.4.1 of this volume.}}$$

Examining 2), we have;

$$\tan^2(B_c) = 1.52 \frac{\pi^2}{8}$$

$$\tan B_c = 1.369$$

$$B_c = 53.7°$$

$$B_c = 0.94 \text{ radians}$$

Examining 1), we have;

$$\frac{J_1^2(B_D)}{J_o^2(B_D)} = 1.18 \times \frac{4}{\pi^2} \times 1.875$$

$$= 0.8968$$

---

(1) Thomas K. Foley, Bruce J. Gaumond, and Jackson T. Witherspoon, "Optimum Power Division for Phase-Modulated Deep-Space Communication Links", IEEE Transactions on Aerospace and Electronic Systems, VOL. AES-3, No. 3, May 1967, pp 400-409.

Thus

$$\frac{J_1 (B_D)}{J_o (B_D)} = 0.9470$$

or

$$\underline{B_D = 1.39}$$

2.0 Power in the Signal Components

a. Power in the carrier

From the reference, we have;

$$P_C = J_o^2 (B_D) \cos^2 (B_C)$$

$$= J_o^2 (1.39) \cos^2 (0.94)$$

$$P_C = (0.5723 \times 0.5898)^2$$

$$\underline{P_C = 0.114 = -9.4 \text{ dB}}$$

b. Power in the Code

$$P_S = \frac{8}{\pi^2} \frac{\sin^2 (B_C)}{\cos^2 (B_C)} J_o^2 (B_D) \cos^2 (B_C)$$

$$= \frac{8}{\pi^2} \sin^2 (0.94) J_o^2 (1.39).$$

$$\underline{P_S = 0.173 = -7.6 \text{ dB}.}$$

c. Power in the Data Subcarrier

$$P_D = \frac{2 J_1^2 (B_D)}{J_o^2 (B_D)} J_o^2 (B_D) \cos (B_C)$$

$$P_D = 2 J_1^2 (B_D) \cos (B_C)$$

$$\underline{P_D = 0.204 = -6.9 \text{ dB}.}$$

Appendix 2.2.3.6-A

SLANT RANGE ERROR DUE TO FREQUENCY OFFSETS (0.1 NMI.)

We see from Section 2.5.5 of the main text that the rms frequency error due to the user oscillator instability, the user-to-satellite 2-way doppler, and the temperature drift of the predetection bandpass filter is given as:

$$\Delta f = 2278 \text{ Hz}$$

Calling this quantity $d(\Delta f)$ and inserting it into Eq. (4) of the same section, with B = 200 kHz and Δf = 64 kHz.

$$d\phi = \frac{1}{1 + \left(\frac{\Delta f}{B/2}\right)^2} \times \frac{d(\Delta f)}{B/2}$$

$$= \frac{1}{1 + \left(\frac{64 \times 10^3}{100 \times 10^3}\right)^2} \times \frac{2278}{100 \times 10^3}$$

$$d\phi = 0.0162 \text{ radian} = 0.926°.$$

Now the wavelength of the 64 kHz tone is 2.527 nmi so that $d\phi$ represents a range error σf of 0.0064 nmi. We see from Table 2-15 of this volume that the ionospheric range error σ_I is 0.0160 nmi and the multipath range error σ is 0.0057 nmi. When the filter phase error σ_f is added to these in an rms manner the resulting ground position error is:

$$\epsilon = \sqrt{\sigma_I^2 + \sigma_M^2 + \sigma_f^2} \times 3\sqrt{2}$$

$$\epsilon = \sqrt{0.0160^2 + 0.0057^2 + 0.0065^2} \times 3\sqrt{2}$$

$$\epsilon = 0.0772 \text{ nmi}$$

The ground range error due to the signal-to-noise $\epsilon_{S/n}$, therefore is

$$\epsilon_{S/n} = \sqrt{0.100^2 - 0.0772^2}$$

$$\epsilon_{S/n} = 0.0636$$

The slant range error $\sigma_{S/n}$ to the satellite is $\frac{\epsilon_{S/n}}{3\sqrt{2}}$

$$\sigma_{S/n} = 0.0150 \text{ nmi}$$

The rms angle error σ_θ corresponding to this range error is given by:

$$\sigma_\theta = \frac{2 \times 0.0150}{2.527} \times 2\pi$$

$$\sigma_\theta = 0.0746 \text{ radian}$$

$$\sigma_\theta = 4.27^\circ$$

Allowing a 3° rms instrumentation error, the rms error due to the signal-to-noise alone becomes:

$$\sigma_{S/n} = \sqrt{4.27^2 - 3^2}$$

$$\sigma_{S/n} = 3.04^\circ$$

$$\sigma_{S/n} = 0.053 \text{ radian}$$

$$S/n = 178 = 22.5 \text{ dB}$$

Appendix 2.6.2-A

WAITING TIME CALCULATIONS

Figures 2-27, 2-28, and 2-29 in the main text of this volume were derived from the analysis given in Chapter XVII of Feller[1], Chapter 14 of Churchman[2] et al, and Chapter 23 of Goode and Machol[3].

The expected waiting time as given in reference 3 is:

$$E(W) = \frac{p^{v}\ p(o)}{(v-1)\ !\ M\ (v-p)^2}$$

where:

$$p = \frac{m}{M}$$

m = mean number of inputs per unit time

M = mean number of outputs from an occupied channel per unit time

v = number of channels

p(o) = is the probability that all channels are idle.

Furthermore:

$$p(o) = \frac{1}{\sum_{n=o}^{v-1} \frac{p^n}{n!} + \left(\frac{o^v}{v!}\right)\left[\frac{v}{(v-p)}\right]}$$

---

(1) Feller, "An Introduction to Probability Theory and Its Applications," Volume I, 2nd Edition, John Wiley & Sons, Inc., 1957.

(2) Churchman, Ackoff and Arnoff, "Introduction to Operation Research," John Wiley & Sons, Inc., 1957.

(3) Goode and Machol, "System Engineering," McGraw-Hill, 1957.

The expected waiting time for single channel operation is given in reference (3) formula (23-9) as:

$$E(W) = E(T)\ \frac{p}{1-p}$$

where:

E(T) is the mean line duration = 10 ms

Now,

$$p = \frac{m}{M} = \frac{190 \times 10 \times 9.7/3600}{\frac{1}{10^{-2}}} \quad \text{(aircraft case)}$$

$$p = \frac{1.9 \times 9.7 \times 10^{3}}{3.6 \times 10^{3} \times 10^{2}} = 5.1 \times 10^{-2}$$

$$E(W) = \frac{5.1 \times 10^{-2} \times 10^{-2}}{1 - 0.051}$$

$$E(W) = \frac{5.1 \times 10^{-4}}{0.949}$$

$E(W) = 0.54$ millisecond

Now the sync bit rate is $2 \times 6.5 \times 10^{3} = 13 \times 10^{3}$ bits/second.

$\therefore$ Number of lost sync bits = $13 \times 10^{3} \times 0.54 \times 10^{-3} = 7$ bits. Leaving 5 sync bits.

For the maritime case:

$$p = \frac{554 \times 10/360}{\frac{1}{10^{-2}}}$$

$$p = 1.53 \times 10^{-2}$$

Therefore:

$$E(W) = \frac{1.53 \times 10^{-2} \times 10^{-2}}{1 - 0.0153}$$

$$E(W) = \frac{1.53 \times 10^{-4}}{0.9847}$$

$$E(W) = 0.155 \text{ millisecond}$$

The number of sync bits lost are:

$$2 \times 6.5 \times 10^{3} \times 0.155 \times 10^{-3}$$

$$= 2.01$$

Appendix 2.7.2-A

LIMITER/DISCRIMINATOR FM DETECTION WITH BANDWIDTH TO INCLUDE DOPPLER SIGNALS

In this Appendix thresholds are determined for receiver IF bandwidths which exceed Carson's rule of $B_{if} = 2f_m (1 + m)$. This may occur for significant frequency instabilities or from a doppler frequency amounting to F.

From Skinner, it is known that (for 1 dB loss in the Noise Improvement Factor, NIF),

$$\left(\frac{C}{N_{if}}\right)_T = 5.6 \log \frac{B_{if}}{f_m} + 4.4 \tag{1}$$

also

$$\frac{S_{ms}}{N_{ms}} = 3\, m^2 \times \frac{B_{if}}{2f_m} \times \frac{C}{N_{if}} \quad \text{if} \quad \frac{C}{N_{if}} > \left(\frac{C}{N_{if}}\right)_T \tag{2}$$

At threshold for a 1 dB loss in the FM NIF

$$\left(\frac{S_{rms}}{N_{rms}}\right)_T \Bigg|_{dB} = 4.75 + (m^2)_{dB} + \left(\frac{B_{if}}{2f_m}\right)_{dB} + \left(\frac{C}{N_{if}}\right)_T \Bigg|_{dB} - 1 \tag{3}$$

and

$$B_{if} = 2 f_m (1 + m) + F \tag{4}$$

Substituting (4) in (1)

$$\left(\frac{C}{N_{if}}\right)_T = 5.6 \log \frac{(2 fm (1 + m) + F)}{f_m} + 4.4 \tag{5}$$

$$= 5.6 \log \left[2 (1 + m) + F/f_m\right] + 4.4 \tag{6}$$

Substituting (4) and (6) in (3), the output SNR at threshold is

$$\left(\frac{S}{N}\right)_T = 9.9 + 20 \log m + 15.6 \log (1 + m + F/2f_m) \tag{7}$$

Note that by definition $S_{peak} = \sqrt{2}\, S_{rms}$ Then the peak-signal-to-rms noise ratio at the output, for thresholds is

$$\left(\frac{S_p}{N}\right)_T = 12.9 + 20 \log m + 15.6 \log (1 + m + F/2f_m) \quad (8)$$

Equation 8 is solved for values of m with a value of F of 8.6 kHz and f_m of 2.7 kHz for the mission study. Table 1 shows the results and includes a value of the B_{if}/f_m ratio used in Skinner's derivation of the threshold:

or

$$B_{if}/f_m = 2\,(1 + m + F/2f_m) = 5.2 + 2\,m \quad (9)$$

It is read from Figure 1 which is based on this same B_{if}/f_m variable. Figure 1 was derived by reading Skinner's curve for those input C/Nif threshold values corresponding to a decrease of one dB below the linear relation above threshold. The one dB reference corresponds to practical equipment performance specifications.

REFERENCES - SKINNER'S ANALYSIS FOR 1dB DROP FROM LINEAR PERFORMANCE.

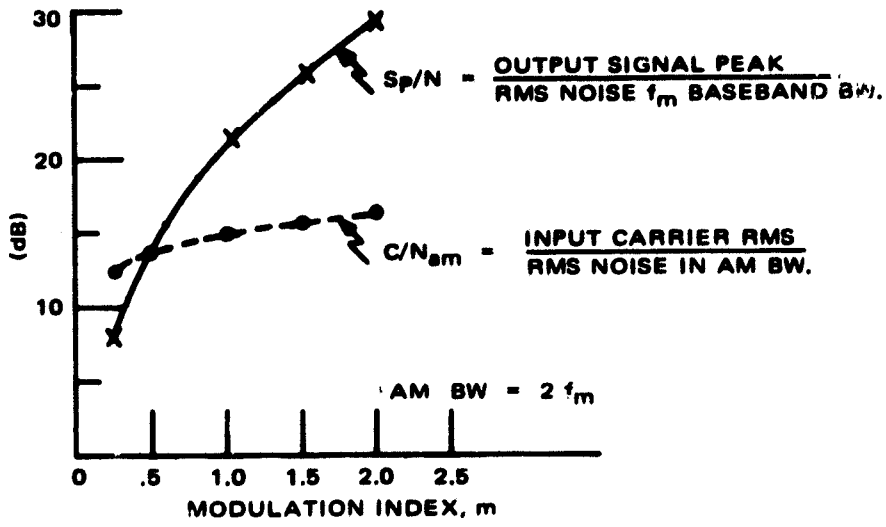

Figure 1. Lim/Disc. Performance with 8.6 KHz Total System Spurious Channel Location and 2.7 KHz Baseband Signal

Because the typical FM performance is shown as:

$$\frac{S}{N} = 3\,m^2 \quad \frac{C}{Nam}, \tag{10}$$

then compared to equation (3), in dB

$$\left(\frac{C}{Nam}\right)_T = 10 \log \frac{B_{if}}{2f_m} + \left(\frac{C}{N_{if}}\right)_T \text{ (dB)} \tag{11}$$

Using (6) for $(C/N_{if})_T$, equation (11) becomes

$$\left(\frac{C}{Nam}\right)_T = 6 + 15.6 \log \left[1 + m + F/2f_m\right] \tag{12}$$

This is also included in Table 1.

TABLE 1

M	S_p/N (dB)*	$(C/N_{am})_T$
.25	8	12.3
.5	14.1	13.7
1.0	21.1	14.8
1.5	25.5	15.6
2.0	29.5	16.4

*Peak Signal-to-rms noise ratio at output for threshold condition.

Appendix 2.7.2.3-A

PULSE POSITION MODULATION ANALYSIS

In pulse position modulation (PPM), Schwartz et al[1] develop the SNR with the variables defined as:

For PPM baseband signal,

$T \equiv$ halfwidth of raised cosine pulse

$\lambda \equiv$ peak position modulation (±)

$A \equiv$ pulse peak

$$f_b \equiv 1/T \tag{1}$$

Then the mean-square value of the PPM waveform is:

$$P_s = \frac{3\ A^2}{8\ \lambda\ f_b} \tag{2}$$

when the waveform is

$$Q(t) = \frac{A}{2}\ (1 + \cos\ \pi\ f_b t). \tag{3}$$

The SNR is derived to be: (Schwartz et al, eqn. 6-2-24)

$$\frac{S}{N} = \frac{\pi^2\ f_b\ \lambda^2\ A^2}{16\ W_o} \tag{4}$$

where

W_o = noise spectral density.

This equation can be changed into the more familiar form where λ is replaced by a frequency variable. λ may be related to f_m, the highest frequency of the modulating signal.

---

(1) M. Schwartz, W. Bennett, S. Stein, Communication Systems and Techniques, McGraw-Hill Book Co., 1966.

This relation is derived by Schwartz[2] on the basis of the minimum Nyquist sampling interval of $1/2f_m$, and the maximum allowable modulation time of $\pm 1/2$ of this sampling time. This then determines the maximum value of,

$$\lambda = 1/4f_m \tag{5}$$

Then (4) becomes

$$\frac{S}{N} = \frac{\pi^2 \quad f_b \quad A^2}{(4\ f_m)^2\ 16\ W_o} \tag{6a}$$

$$= \frac{\pi^2}{16^2} \quad \frac{f_b}{f_m^{\ 2}} \quad \frac{A^2}{W_o} \tag{6b}$$

$$= \frac{\pi^2}{16^2} \quad \frac{f_b^{\ 2}}{f_m^{\ 2}} \quad \frac{A^2}{f_b\ W_o} \tag{6c}$$

$$= \frac{\pi^2}{16^2} \quad \left(\frac{f_b}{f_m}\right)^2 \quad \frac{A^2}{N_b} \tag{7}$$

Eq. (7) shows the output SNR, S/N, in terms of the ratio of the peak power A^2 to the Noise, N_b, in the bandwidth, f_b, of the video pulse. In a gated RF waveform for the Q(t) function, the bandwidth $2f_b$ applies and a pulse amplitude A is detected with an equal level RF peak amplitude A_c with a mean-square power C of $A_c^{\ 2}/2$ so eq. (7) applies at RF as

$$\frac{S}{N} = \frac{2\pi^2}{16^2} \quad \left(\frac{f_b}{f_m}\right)^2 \quad \frac{C}{N_b} \tag{8}$$

or

$$\frac{S}{N} = 0.077 \left(\frac{f_b}{f_m}\right)^2 \quad \frac{C}{N_b} \tag{9}$$

---

[2] M. Schwartz, Information Transmission Modulation and Noise, McGraw-Hill, p. 315.

and the mean-square power of the RF pulse for the corresponding video pulse power by eqn. (2) becomes

$$P_{sc} = \frac{3}{4} \frac{P_c}{\lambda f_b} = \frac{3 f_m C}{f_b} \tag{10}$$

It is instructive to compare PPM performance with that of FM. Eqn. (6b) could be referenced to a SNR in the equivalent bandwidth of AM modulation, as is good common practice, instead of in the IF bandwidth, f_b, and the noise, N_b, as shown in eqn. (6c) and (7). Then

$$\frac{S}{N} = \frac{2\pi^2}{16^2} \quad \frac{f_b}{f_m} \quad \frac{A^2}{2 f_m W_o} \tag{11}$$

$$= \frac{2\pi^2}{16^2} \quad \frac{f_b}{f_m} \quad \frac{A^2}{N_{am}} \tag{12}$$

Then the same arguments used to derive eqn. (9) determines

$$\text{PPM:} \qquad \frac{S}{N} = 0.154 \left(\frac{f_b}{f_m}\right) \quad \frac{C}{N_{am}} \tag{13}$$

This compares with FM, using the popular expression of

$$\text{FM:} \qquad \frac{S}{N} = 3 M^2 \quad \frac{C}{N_{am}} \tag{14}$$

where

$$M \equiv \Delta F / f_m \equiv \text{peak deviation}/f_m \tag{15}$$

and for $M \geq 4$, $\Delta F = f_b/2$, so (16)

$$\frac{S}{N} = \frac{3}{4} \left(\frac{f_b}{f_m}\right)^2 \quad \frac{C}{N_{am}} \tag{17}$$

PPM Detection Threshold - Equation (7) is the baseband expression for the SNR equation which directly refers to the threshold limitation, A^2/N_b. From Black[1], for a PPM signal disturbed by noise at baseband and with a pulse occurrence defined as present when exceeding a level of $A_c/2$, the peak amplitude squared A_c^2 to the noise power in the baseband N_b must be about 18 dB to meet detection threshold conditions. This is 3 dB greater than the mean square power of a carrier cycle whic' is required of the output amplifier. Thus the maximum mean square received power to received noise ratio required will be 15 dB to meet threshold requirements. Note that the mean power defined by equation 2 is that for the pulse averaged over a sampling period λ.

The average power in the pulse is $3A^2/8$ from equation 2 by averaging over τ instead of λ, or 5.75 dB below the peak value of A^2, but the output amplifier device will need to deliver an $A^2/2$ power level.

The 18 dB peak video signal to rms noise ratio and the pulse occurrence detection level of 6 dB below A for an A/2 level means peak to rms ratios of 12 dB will cause random video pulses to occur due to noise peaks. This 12 dB increase above its rms level will occur less than 0.01 percent of the time and will thus be essentially just the start of threshold conditions. For moderate quality of voice channels of 24 dB, this actual threshold may be associated with a probability of about 0.6% that the detector slicing level is exceeded by noise, which corresponds to a 9 dB peak/rms noise ratio. Thus the 15 dB ratio derived above will be reduced to 12 dB for the carrier power/noise power ratio of the video pulse.

---

[1] H.S. Black, Modulation Theory, D. Van Nostrand Company, Inc., 1953.

Appendix 3.1-A

USER EQUIPMENT PRELIMINARY SPECIFICATIONS

1. AIR TRAFFIC CONTROL AND NAVIGATION USER EQUIPMENT SPECIFICATIONS

Air Traffic Control User Equipment Specifications - The functions of this equipment are:

(a) Acquire a CW signal that is transmitted from one of the navigation/traffic control satellites.

(b) Demodulate and decode user address and command signals.

(c) Transmit a stable phase modulated carrier.

(d) Turn around and retransmit ranging signal.

(e) Modulate transmitted signal with identification code and on board data.

The sequence of operation of this equipment is as follows:

1. The user equipment is activated and phase-locks to the received signal at the beginning of flight.
2. The user equipment continuously demodulates the received carrier (carrier is phase modulated by two ranging tones) and decodes the address and command signals that are bi-phase modulated onto the lowest frequency range-tone.
3. Upon reception of the proper address signal, the user equipment's transmitter is activated.
4. Identity and aircraft altitude data are encoded and transmitted. Transmission of this data is effected via the bi-phase modulation of the lowest frequency range tone which is momentarily used as a data subcarrier.
5. Upon completion of the data transmission, the demodulated range tones are phase modulated on to the transmitted carrier for a short period of time which is determined by an internal clock.
6. Upon completion of the range tone transmission, the user's transmitter is deactivated and the clock is recycled.

The following performance specifications are recommended for the air traffic control user equipment.

Receiver Frequency	To be designated in the 1540 MHz to 1660 MHz frequency band.
Receiver Noise Figure	3 dB maximum.

Receiver Bandwidth	200 kHz nominal.
Receiver Threshold	-135 dBm.
Frequency Search Range	±10 kHz minimum about designated receiver frequency.
Carrier Acquisition Time	10 second maximum.
Transmitter Frequency	To be designated in the 1540 MHz to 1660 MHz frequency band. The difference between the transmitter frequency and the receiver frequency will be at least 40 MHz.
Transmitter Frequency Accuracy	±0.001%.
Transmitter Power	20 Watts minimum into a VSWR of up to 1.5 at any phase.
Range Tone Frequency	The Range Tone Frequencies will be 500 Hz ±.0001% and 8 kHz ±.0001%.
Range Tone Modulation Index	The received range tone modulation indices will be 1.4 (Coarse) and 0.65 (Fine).
	Upon the receipt of a command, the user equipment will retransmit these range tones at indices that are within ±20% of the received indices.
Range Tone Phase Errors	The phase of the user equipment's retransmitted tones shall be within ±3° (bias value) of the received tones.
Data Transmission	Data will be transmitted to and from the user via a ±90° phase shift keying of the 500 Hz range tone.
Data Rate	The data rate will be 100 bits/sec.
Word Length	10 bits.
Power Consumption	The power consumption shall not exceed 40 watts when the transmitter is not active and 150 watts when the transmitter is active.
Word Error Rate	The word error rate associated with the user shall not exceed one word in 10,000 messages.

Navigation User Equipment Specifications - The functions of this equipment in airborne applications are:

(1) Acquire signals from two navigation/traffic control satellites.

(2) Measure the time difference between the arrival of satellite signals and an internal clock signal.

(3) Demodulate, decode and store satellite ephemerides data that is modulated on to one of the received signals from the satellite.

(4) Accept altitude information from an onboard altimeter.

(5) Compute the user's position based on the known satellite positions, the time delays (ranges) between the user and the satellites and the user's altitude.

The marine user navigation equipment can be simplified due to the relatively low velocity of marine vessels relative to aircraft. Thus the marine user's navigation equipment can differ from the aircraft user's navigation equipment as follows:

- The marine user can utilize a single receiver channel and time shares this channel between the two satellite signals.
- Altitude data is not required.
- Position computations can be made by hand, utilizing charts and tables, thus a computer is not essential.
- Satellite ephemerides data can also be incorporated into the tables so that a satellite to user data link is not essential.

The following performance specifications are recommended for the airborne user's navigation equipment:

Receiver Frequencies	To be designated in the 1540 MHz to 1660 MHz frequency band.
Receiver Frequency Separation	1 MHz nominal.
Receiver Noise Figure	5 dB maximum.
Receiver Threshold	-135 dBM
Frequency Search Range	±10 KHz minimum about designated center frequencies.
Acquisition Time	10 seconds maximum.
Range Tone Frequency	500 Hz and 8 KHz will modulate onto each received carrier.
Range Tone Frequency Accuracy	±2 parts in 10^{13} RMS error in received signal.

Range Tone Modulation Index	The received range tone modulation indices will be 1.4 (Coarse) and 0.65 (Fine).
User Equipment Clock Frequency Accuracy	The user's clock shall be capable of being set to an accuracy of one part in 10^{11}. The systematic drift shall not exceed a rate of one part in 10^{10} per 8 hours.
Range Bias Errors	Bias errors associated with the user's processing of the range tone shall not exceed 1000 feet.
Power Consumption	The power consumption of the user equipment shall not exceed 150 watts.

The following specifications are recommended for the marine user's navigation equipment:

Receiver Frequency	To be designated in the 1540 MHz to 1660 MHz frequency range.
Receiver Frequency Separation	1 MHz nominal.
Receiver Noise Figure	5 dB.
Frequency Search Range	±5 KHz minimum about designated center frequencies.
Acquisition Time	The acquisition time shall not exceed one second.
Sampling Rate	The user equipment shall alternately switch between the signals from the two navigation traffic control satellites. The sampling period shall be three seconds nominal.
Range Tone Frequency	500 Hz and 8 KHz will be phase modulated onto each of the received carriers.
Range Tone Frequency Accuracy	±2 parts on 10^{13} RMS error in the received signals.
Range Tone Modulation Index	The received range tone modulation indices will be 1.4 (Coarse) and 0.65 (Fine).
User Equipment Clock Frequency Accuracy	The user's clock frequency shall be capable of being set to an accuracy of 5 parts in 10^{12}.
Range Bias Error	Bias errors associated with the user's processing of the received range tones shall not exceed 1000 feet.
Power Consumption	The power consumption of the user equipment shall not exceed 125 watts.

3. VOICE COMMUNICATIONS USER EQUIPMENT SPECIFICATIONS

This section provides summary specifications for aviation and marine VHF Voice Communications transceivers and for an L-Band Voice Communications transceiver. These specifications may be used as a supplement to ARINC project paper No. 546A Draft No. 2 dated October 13, 1967 for the development of aircraft to satellite Voice Communications transceivers.

Airborne VHF Communications Transceivers - The following specifications are recommended:

Receiver Frequency Band	120 MHz to 125 MHz
Transmitter Frequency Band	130 MHz to 135 MHz
Number of Channels	Four
Type of Modulation	FM
Baseband	300 Hz to 2.25 KHz
Peak Frequency Deviation	5 KHz
Frequency Stability	0.001%
Channel Separation	25 KHz Minimum
Receiver Noise Figure	3 dB Maximum
Receiver IF Bandwidth	25 KHz Nominal
Type of IF Amplifier	Limiting
Type of Receiver Demodulator	Phase-lock Frequency Demodulator
Demodulator Loop Noise Bandwidth ($2 B_L$)	18 KHz ±10%
Loop Phase Margin	40° Minimum
Squelch Detector	Coherent Phase Lock Detector
Receiver Threshold	-116 dBm
Transmitter Power	150 Watts Nominal
Transmitter Pre-emphasis	6 dB/octave for baseband frequencies above 800 Hz.
Transmitter AGC Range	20 dB
Nominal Clipping Level	Adjustable from 0 dB to 12 dB

Marine VHF Communications Transceiver - The following specifications are recommended:

Receiver Frequency Band	156 MHz to 157 MHz
Transmitter Frequency Band	160 MHz to 162 MHz
Number of Channels	Four
Type of Modulation	FM
Baseband	300 Hz to 2.25 KHz
Peak Frequency Deviation	5 KHz
Frequency Stability	±0.001%
Channel Separation	25 KHz Minimum
Receiver Noise Figure	3 dB Maximum
Receiver IF Bandwidth	25 KHz Nominal
Type of IF Amplifier	Limiting
Type of Receiver Demodulator	Phase-lock Frequency Demodulator
Demodulator Loop Noise Bandwidth	18 KHz ±10%
Loop Phase Margin	40° Minimum
Squelch Detector	Coherent Phase-lock Detector
Receiver Threshold	-116 dBm
Transmitter Power	20 Watts Nominal
Transmitter Pre-emphasis	6 dB/octave above 800 Hz.
Transmitter AGC Range	20 dB
Nominal Clipping Level	Adjustable from 0 dB to 12 dB.

Airborne L-Band Communications Transceiver - The following specifications are recommended:

Transmit and Receiver Frequency Band	To be selected in the 1540 MHz to 1660 MHz Frequency Band
Number of Channels	Six
Type of Modulation	Frequency Modulation
Baseband	300 Hz to 2.25 KHz
Peak Frequency Deviation	5 KHz
Frequency Stability	±0.0003%

Channel Separation	50 KHz
Receiver Noise Figure	3 dB
Receiver IF Bandwidth	40 KHz Nominal
Type of IF Amplifier	Limiting
Type of Receiver Demodulator	Phase-lock frequency demodulator
Demodulator Loop Noise Bandwidth	18 KHz ±10%
Loop Phase Margin	40° Minimum
Squelch Detector	Coherent Phase-lock Detector
Receiver Threshold	-116 dBm
Receiver De-emphasis	6 dB/octave for baseband frequencies above 800 Hz.

Communications Transmitter

Transmitter Power	40 Watts
Transmitter AGC Range	20 dB
Transmitter Pre-emphasis	6 dB/octave for baseband frequencies above 800 Hz
Nominal Transmitter Clipping Level	12 dB

Pilot Transmitter

Transmitter Power	20 Watts
Transmitter Frequency	50 KHz below Communications Transmitter Frequency

Marine L-Band Communications Transceiver Specifications - The specifications for the Marine L-Band Communication transceiver equipment are identical to the aviation user equipments with the following exceptions.

The required transmitter power may be reduced through the use of a 10 dB gain antenna; a transmitter power of 4 watts is recommended for the Voice Transmitter and 2 watts for the Pilot Transmitter. In addition, the precise channel frequencies, which remain to be defined, will differ from the aviation channel frequencies to avoid conflicts.

Appendix 6.7-A

ATMOSPHERIC ATTENUATION AS A FUNCTION OF FREQUENCY

We will follow the methodology of Holzer[1] in determining the total atmospheric attenuation Aa as a function of frequency f, elevation angle θ, ray path r, and temperature-climate effects. Holzer breaks the total atmospheric attenuation Aa into three components, that due to the oxygen and water vapor (i.e., gas) Ag, that due to clouds and fog Ac, and that due to precipitation (rain) Ap.

We look at each component as a function of frequency, and assume that the upper frequency limit has been reached when Aa = 2 dB.

I. Attenuation Due to Oxygen and Water Vapor, Ag

$$Ag = A_1(f) \cdot A_2(r_1) \cdot A_3(\theta)$$

where:

Ag, $A_1(f)$, $A_2(r)$, $A_3(\theta)$ are in dB

f = the frequency (in GHz)

r_1 = the ray path (in Km)

θ = the elevation angle

$A_1(f) = 1.4 + 0.09\,f - 1.6 \exp(-2.1\,f)$

$A_2(r_1) = 1 - \exp(-0.0054\,r)$

$A_3(\theta) = \exp(-10\,\theta)$

$r_1 = 20/\sin\theta$, where 20 km is the maximum altitude for significant gaseous absorption

Let θ = 16°C the minimum elevation angle (C.C. to satellite)

The values of $A_1(f)$, $A_2(r_1)$, $A_3(\theta)$, and Ag are shown in Table 1.

---

[1] W. Holzer, "Atmospheric Attenuation in Satellite Communications," The Microwave Journal, March 1965, pp 119-125.

TABLE 1. GAS ATTENUATION Ag

Freq. (GHz)	A_1 (f) (dB)	A_2 (r) (dB)	A_3 (θ) (dB)	Ag (dB)
4	1.76	0.32	0.061	0.03
5	1.85	↓	↓	0.04
6	1.94	↓	↓	0.04
7	2.03	↓	↓	0.04
8	2.21	↓	↓	0.04

II. Attenuation Due to Clouds and Fog, Ac

$Ac = K \rho r_2$ (in dB)

where

K = attenuation coefficient ($dB/Km/gm/M^3$)

ρ = the liquid water content

$r_2 = 6/\sin\theta$, where 6 is the vertical cloud thickness in Km.

The resulting Ac with the frequency dependent parameters are shown in Table 2.

TABLE 2. CLOUD AND FOG ATTENUATION, Ac

Freq. (GHz)	K	ρ* (gm/m^3)	Ac (dB)
4	0.030	0.3	0.20
5	0.040	0.3	0.26
6	0.050	0.3	0.33
7	0.060	0.3	0.39
8	0.066	0.3	0.43

III. Attenuation Due to Precipitation (Rain), Ap

$Ap = q\ p\ r_3$ (in dB)

where:

q is a function of temperature[2], wavelength, and rainfall rate (dB/Km/mm/hr)

p is the rainfall rate (in mm/hr) assumed to be 12 mm/hr.*

2. Op Cit. See Figure 2.

*Assumed to be at Washington, D. C.

$$r_3 = E/\theta$$

where

$$E = 41.4 - 23.5 \log_{10} p$$

The resulting Ap, with the pertinent parameters are shown in Table 3.

TABLE 3. PRECIPITATION (RAIN) ATTENUATION, Ap

Freq. (GHz)	q	p (mm/hr.)	r_3	Ap (dB)
4	0.0009	12	16.04	0.18
5	0.0027	12	16.04	0.52
6	0.005	12	16.04	0.96
7	0.008	12	16.04	1.54
8	0.012	12	16.04	2.34

IV. The Total Atmospheric Attenuation Aa

This attenuation is the sum of Ag, Ac, and Ap and is shown in Table 4 as a function of frequency.

TABLE 4. ATMOSPHERIC ATTENUATION, Aa

Freq. (GHz)	Ag (dB)	Ac (dB)	Ap (dB)	Aa (dB)
4	0.03	0.20	0.18	0.41
5	0.04	0.26	0.52	0.82
6	0.04	0.33	0.96	1.33
7	0.04	0.39	1.54	1.97
8	0.05	0.43	2.34	2.82